

University of Warwick institutional repository: <http://go.warwick.ac.uk/wrap>

A Thesis Submitted for the Degree of PhD at the University of Warwick

<http://go.warwick.ac.uk/wrap/72200>

This thesis is made available online and is protected by original copyright.

Please scroll down to view the document itself.

Please refer to the repository record for this item for information to help you to cite it. Our policy information is available from the repository home page.

THE APPLICATION OF SUPERCONDUCTIVITY
TO ROTATING ELECTRICAL MACHINES

by

J.T. Hayden, BSc(Eng), DIC, MIMechE, MIEE

(Being a thesis submitted in partial fulfilment
of the requirements for the degree of Doctor of
Philosophy at the University of Warwick)

May 1973

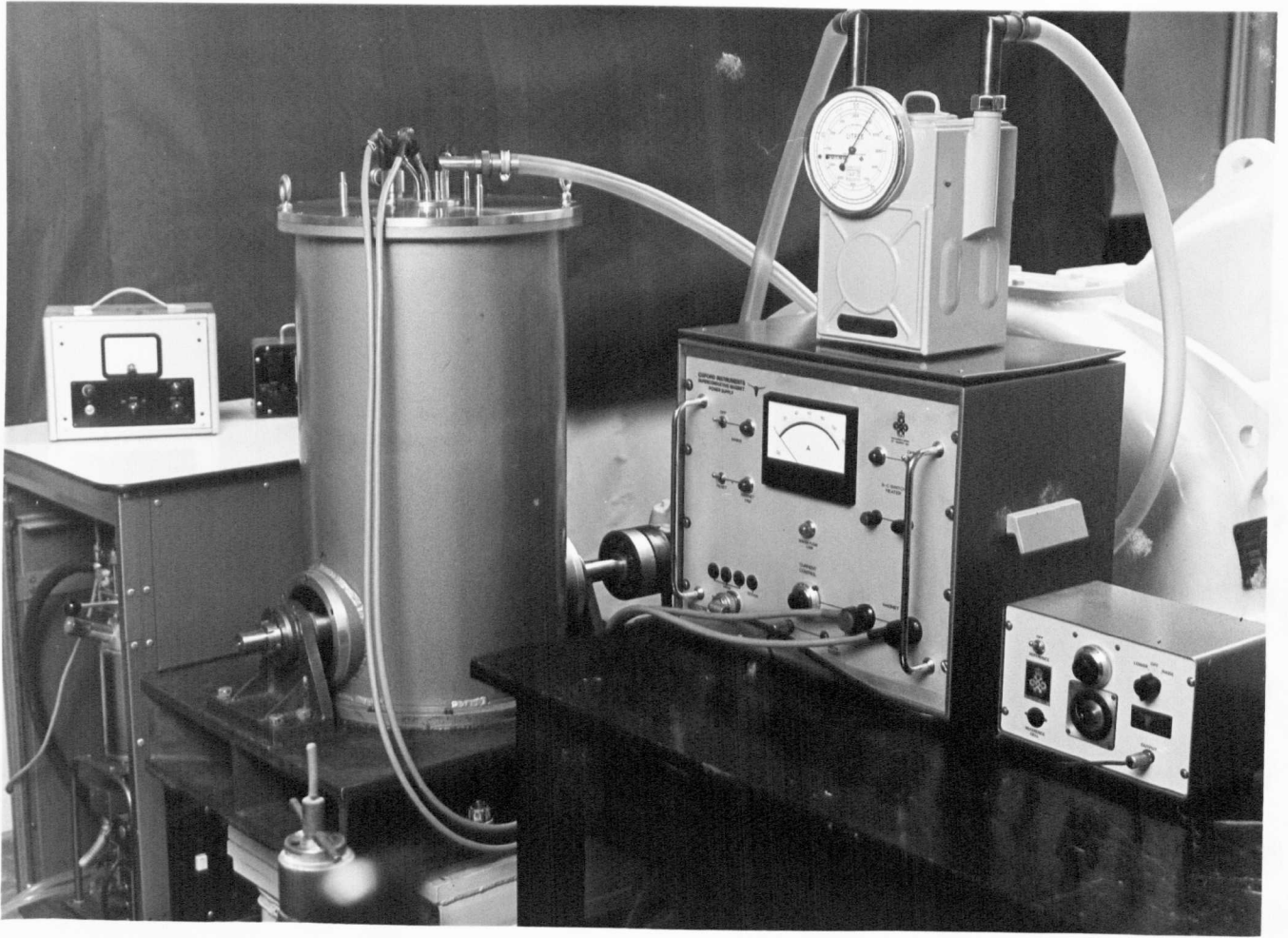
BEST COPY

AVAILABLE

Poor text in the original
thesis.

Some text bound close to
the spine.

Some images distorted



General view of Superconducting Alternator on 150 hp drive.

Abstract

After a brief review of the general properties of superconductors, the difficulties encountered in employing superconducting wires in solenoids are described, together with the measures it has been found necessary to take in order to construct coils with satisfactory performance. A comprehensive review of the attempts and proposals in the literature to employ superconductors in rotating energy converters and an appraisal of each, is then given.

The possibilities of utilizing superconducting windings in conventional types of rotating machines are then examined, and it is shown that probably only the d.c. homopolar machine, the synchronous machine and a toroidal reciprocating generator proposed by Harrowell are suitable for development with superconducting windings. The present state of development of superconducting d.c. homopolar machines is described, and the economic and market prospects for such machines assessed on the basis of the limited data available supplemented by reasonable assumptions. Design procedures for the Harrowell machine are proposed, and from these some conclusions are drawn regarding its characteristics. The prospects for superconducting synchronous generators are examined for use in large power systems and shown to be promising, but for aircraft applications it is shown there is no case for machines with ratings below 1 MVA at 400 Hz. The inadequacies of existing theories of synchronous machines to cover superconducting types are examined and proposals are put forward to modify the conventional two-axis theory for the superconducting case including parameter evaluation.

The experimental work reported covers the design, construction and testing of a 400 Hz rotating armature synchronous generator, with a rating of 50 kVA initially, but capable of being extended to 100 kVA subsequently.

Preface

This work has been carried out while I have been a non-resident, part-time student of the University of Warwick, and at the same time a full-time member of the academic staff of the Cranfield Institute of Technology.

No part of this thesis has been presented to any other institution at any time, and although I have been assisted by many people, the concept and development of the work culminating in the design, construction, analysis and testing of a laboratory superconducting synchronous generator have been my own responsibility. Acknowledgements are made in the text or by references.

The practical work has been carried out at Cranfield in the Department of Electrical and Control Engineering, and I am very grateful to Professor G.A. Whitfield, OBE, Head of Department, for his encouragement and support by way of allocation of funds and other resources to make the project possible.

One difficulty of being a non-resident, part-time student in addition to the intrusions occasioned by my full-time post, was working geographically remote from my main supervisor at Warwick. Throughout the work, and particularly at the beginning of the study, my main supervisor and mentor in superconductivity, Dr. R. G. Rhodes, has always been ready to advise, and I thank him for his counsel and interest.

The construction of a novel and intricate piece of precision machinery would not have been possible without the skill and technical assistance of the Cranfield laboratory and workshop staff, and in

particular of Mr. D. Snow and Mr. I. M. Lord.

Finally, I must acknowledge the sympathetic toleration displayed by my wife and daughters, without which it would not have been possible for me to sustain the effort required to complete this thesis.

C O N T E N T S

Frontispiece	
Abstract	
Preface	
1. Introduction and Objectives	
1.1 Background	1
1.2 Prospectus of Study	2
2. General Properties of Superconductors in Relation to Solenoids.	
2.1 Basic Characteristics	3
2.2 Type II Superconductivity	6
2.3 Flux Pinning	8
2.4 Flux Creep and Flux Flow	13
2.5 Flux Jumps and Superconducting Magnets	15
2.6 Bean's Critical State Model	17
2.7 Improvements in Bean's Critical State Model for Practical Cases.	20
2.8 Limitations of Critical State Model	22
2.9 Impressed Currents	23
2.10 Field Distribution in a Solenoid	27
2.11 The Critical State and A.C. Magnetisation	27
2.12 A.C. Losses	31
3. Superconducting Solenoids	
3.1 Experience with Early Superconducting Solenoids	37
3.2 Thermal Instabilities	39
3.3 Stability Criteria for Superconductors	43
3.4 Cryostatic Stabilisation	51
3.5 Dynamic Stabilisation	63
3.6 Adiabatic Stabilisation	68
3.7 Mechanical Strain and Vibration	69
3.8 Rapid Changes in Field and Current	71
4. Filamentary Superconductors	
4.1 Fine Filaments	77
4.2 The multifilament composite	82
4.3 Twisted multifilament composites	86
4.4 Three-component composites	94
4.5 A.C. Losses	97

5.	Possible Types of Superconducting Machine	
5.1	Possible Advantages	100
5.2	Machines utilizing properties unique to Superconductors	100
5.3	The Moving-zone Generator	101
5.4	The Atherton D.C. Machine	105
5.5	Pancake-Disc Generator	106
5.6	Current-Sheet Generator	109
5.7	Flux-Exclusion Motor	110
5.8	Frozen-Flux Motor	113
5.9	Conclusions regarding utilization of properties unique to superconductors	118
5.10	Machines utilizing the High Field Properties of superconductors	119
5.11	Homopolar Machines	122
5.12	Inductively-fed Heteropolar machines	123
5.13	Conductively-fed Heteropolar Machines	123
5.14	The Huret and Mailfert Alternator	125
5.15	Conclusions regarding utilization of high field properties	129
6.	The Harrowell Toroidal Reciprocating Generator	
6.1	Principle and Construction	131
6.2	Harrowell's Claims	132
6.3	Examination of Harrowell's Claims	133
6.4	Establishing the Leading Dimensions	136
6.5	Relative Magnitudes of Armature Forces	142
6.6	Design Procedure	145
7.	Homopolar D.C. Machines	
7.1	Types of Homopolar machines	148
7.2	The IRD Homopolar disc machine	151
7.3	Economic considerations of homopolar sectored-disc machines	157
7.4	Market prospects	161
7.5	Other superconducting homopolar machines	167
8.	Large Synchronous Machines	
8.1	Turbo-generator Development	172
8.2	Advantages of superconducting excitation windings	175
8.3	General features of superconducting turbo-generators	178
8.4	Economics and market prospects	181
8.5	Experimental machines	185

9.	Synchronous Generators for Aircraft Applications	
9.1	Aerospace and Superconducting generators	191
9.2	Preliminary studies	193
9.3	Present generators and systems for aircraft	196
9.4	Design considerations and rating limitations	202
9.5	Refrigerator weights	208
9.6	Superconducting alternator weights	210
9.7	Prospects for use in aircraft	213
10.	Laboratory Prototype	
10.1	Choice of Machine	216
10.2	Configuration	219
10.3	Ratings	220
10.4	Implications of Preliminary Cost Estimate	221
10.5	Number of Poles and Speed	223
10.6	Design Procedure	223
10.7	Leading Dimensions	225
11.	Design of Field System and Field Plotting	
11.1	Approach to field design	232
11.2	Field determination	232
11.3	Field due to symmetrical dipole coils	237
11.4	Preliminary estimates for coils	249
11.5	Final design of coils	252
11.6	Construction of coils	252
12.	Cryostat Design	
12.1	General features	257
12.2	Main construction	257
13.	Armature Design and Mechanical Features	
13.1	General features	263
13.2	Winding scheme	264
13.3	Electrical losses	268
13.4	Conductor details	273
13.5	Mechanical construction	275
13.6	Brushgear	276
14.	Electrical Performance Prediction and Testing of Prototype.	
14.1	Cooldown and Helium boil-off	279
14.2	Field plot of bore	281
14.3	Resistance and inductance measurements	282
14.4	Open-circuit characteristic	282
14.5	Load test, temperature rise and current rating	283

15.	Theoretical Analysis of Superconducting Synchronous Machines	
15.1	The two-axis lumped parameter model	292
15.2	Application to superconducting machines	294
15.3	Damper screen	295
15.4	Simplified representation	296
15.5	Operational impedances	304
15.6	Parameter evaluation	312
15.7	Effect of ferromagnetic shield	313
15.8	Effect of eddy current shield	316
16.	Conclusions and Recommendations	
16.1	Possible applications	319
16.2	The Harrowell Generator	319
16.3	D.C. Homopolar machines	320
16.4	Large synchronous machines	321
16.5	Aircraft generators	322
16.6	Experimental study	322
16.7	Synchronous machine analysis	323
16.8	General conclusions	323
	Bibliography	325
	References	326
	Appendix	337

SI Units are used throughout this thesis,

except where noted in the text. Usually

this is where values or equations are taken

from references.

1. Introduction and Objectives.

1.1 Background.

The phenomenon of superconductivity and its resistanceless state was discovered in the period when electrical machines were still in their infancy. The early visions of lossless currents being utilised in commercial engineering applications were soon dashed by the discovery that magnetic fields of less than one tenth of those employed in electrical machines would cause the superconductors known at that time to revert to the normal resistive state.

No progress in the application of superconductivity to rotating electrical machines was even contemplated for half a century until the discovery in 1961 of an intermetallic compound, Nb_3Sn , which could remain in the superconducting state in magnetic fields of several times those normally employed in commercial machines. Progress on superconducting machinery since then has been slow, and sometimes disappointing in technical achievement or economic advantage. In spite of many developments in superconductors themselves and in cryogenic technology, an economically viable and technically successful rotating electric motor or generator is not, as far as is known, in commercial operation at the present time.

Yet considerable optimism continues to be expressed that superconducting machines can be successfully developed. ^(1,2) In a survey based on the Delphi method of forecasting carried out in 1970, ⁽³⁾, the median of the opinions expressed was that there was about 60% probability of significant numbers of large superconducting d.c. machines (1000 h.p. upwards) being in commercial operation in 1980,

and about 80% probability of them being in commercial operation by 1985. Corresponding probabilities for superconducting cables were 8% in 1980 and 36% in 1985, while for power transformers the probability expressed was 3% in 1985. It is the object of this study to examine whether or not this optimism is justified, and if so, which types of rotating machines are likely to be developed and the areas of application in which they will be used.

1.2 Prospectus of Study.

For this thesis a very brief review is made of the general properties of superconductors relevant to an understanding of their possible applications in rotating electromechanical energy converters. An account of experience with superconducting solenoids and the possibilities of utilising superconductors in electrical machines is given including a consideration of the cryogenic and economic aspects. The design, construction and performance of a laboratory superconducting synchronous generator are described, and the prospects assessed for electrical machines utilising superconductors being used in the future.

2. General Properties of Superconductors
in Relation to Solenoids.

2.1 Basic Characteristics.

It is proposed to give a brief outline of the basic characteristics of superconductors in order to assist in the understanding of their application to solenoids in rotating machines. Fuller accounts can be found in the books by Lynton and Kuper listed in the bibliography and the review articles by Livingston and Schadler (4), Dew-Hughes (5), Catterall (6), and others (7, 8).

Superconductivity is primarily characterised by a total loss of electrical resistivity in a step transition as the temperature is reduced to near absolute zero. The temperature at which the transition occurs is referred to as the critical temperature, T_c , which is characteristic of the material. The highest value of T_c for an element is approximately 8K for niobium, followed by lead with a value of T_c of 7.22K and ranging down to 0.14K for iridium. The material with the highest value of T_c discovered so far is a composition of niobium, aluminium and germanium for which T_c is 20.1K.

The actual value of T_c depends very little on the particular sample on which the measurement is made, but the range of temperature over which the resistance falls to zero depends very markedly on its physical and chemical state. It varies from 10^{-3} K for a pure crystal (e.g. tin) to 10^{-1} K or more for impure or strained specimens.

The question of whether superconductivity is a state of complete absence of resistivity or one in which the resistivity has an extremely small value has been answered by several very careful and accurate experiments. In these, a current established in a superconducting

ring is found to persist without attenuation for a considerable period of time. The absence of any detectable decay over a period of many months has enabled Quinn and Ittner ⁽⁹⁾ to put an upper limit of 10^{-25} ohm-m on the resistivity of the superconductor.

It is the absence of electrical resistance in superconducting material, and consequently the absence of Joule energy dissipation, that provides the main incentive to investigate the use of superconductors in technological applications. If these applications are to be adopted on any scale, they must be not only technically superior to the alternatives, but offer economic advantages as well. Unfortunately, superconductors cannot carry arbitrarily large currents and in addition, the superconducting state can be destroyed in a specimen by the application of a magnetic field greater than a critical value H_c . H_c depends on the material and the temperature, and is zero at T_c .

There are thus three quantities with critical values which will cause a return to the normal state. These critical values are not mutually independent but are rather the extreme values of a bounding surface between the normal and superconducting states, as indicated in fig. 1. For values of current, magnetic field and temperature inside the critical surface, the material is superconducting, and normal if the combination of values is outside.

A further property which characterises superconductivity is the Meissner effect. It is found that irrespective of the previous magnetic history of a superconductor, the magnetic flux is expelled from the sample as soon as it becomes superconducting. Superconductors in which the flux is completely expelled (except for a very small

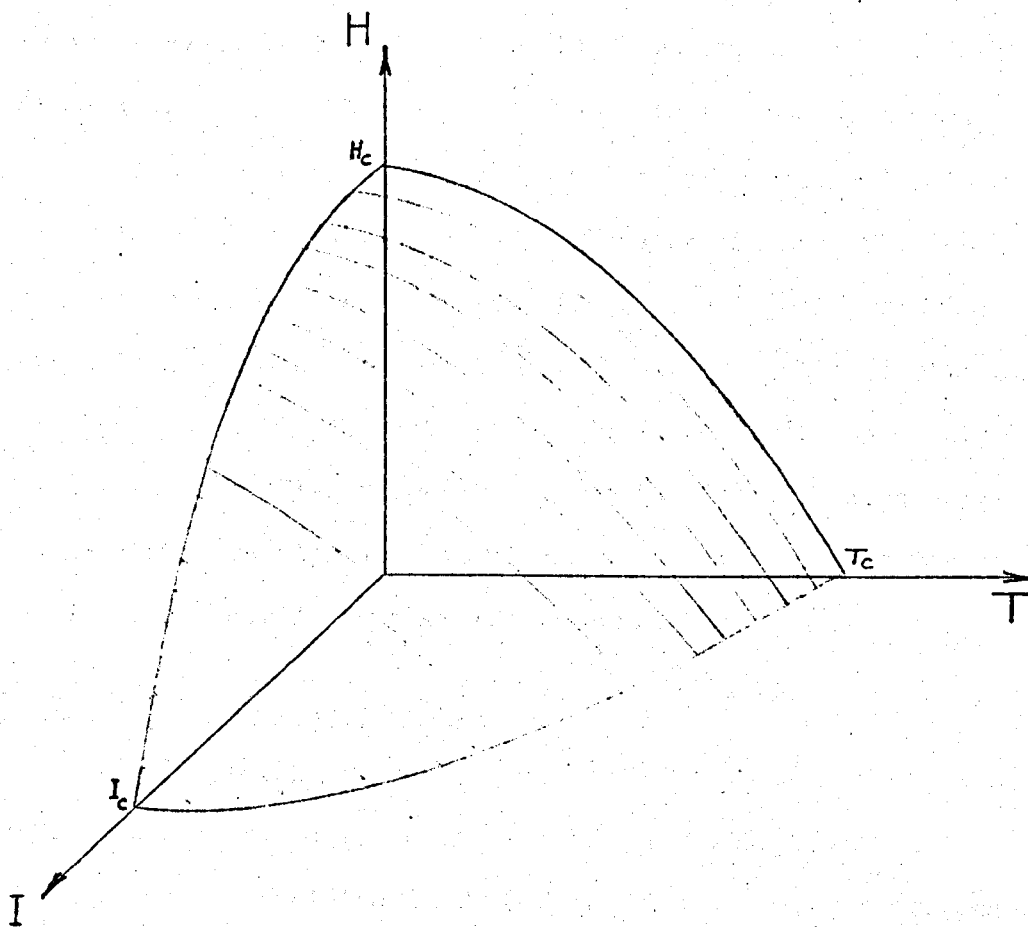


Fig.1 Relationship of critical current, field and temperature for ideal superconductor.

penetration depth at the surface) right up to H_c are referred to as type I. Other superconductors, type II, exist which behave in a similar way to type I in low fields, but at high fields the flux penetrates partially into the superconductor. In type I materials, the flux penetrates the superconductor at the critical field H_c or critical temperature T_c , and the material reverts to the normal resistive state. In type II materials, however, the flux enters in discrete amounts with a gradual change to the normal state.

Type I superconductors have low values of critical field and critical temperature, while the type II materials have very much higher values of these quantities. It is with type II, sometimes referred to as hard superconductors, which are capable of retaining their superconducting characteristics in magnetic fields of over 20T and relatively high temperatures (up to 20K) with high current densities (over 10^{10} A/m^2), that it would seem appropriate to attempt to employ commercially in electrical machines.

2.2 Type II Superconductivity.

An ideal type-II bulk superconductor with zero demagnetizing coefficient remains fully superconducting and fully diamagnetic only below a lower critical field H_{c1} ($< H_c$). Flux then begins to penetrate, and does so progressively with increasing external field, until at an upper critical field, H_{c2} penetration is complete ($H_{c2} > H_c$). Above H_{c2} the superconductor resumes the normal state. The penetration of flux into the bulk material occurs in such a way that the total free energy is minimised and a series of superconducting and normal domains are formed in the penetration layer. This is known as the mixed state.

In the mixed state, it is considered that the flux penetrates in the form of quantized flux threads (fluxoids or fluxons). Each flux thread is regarded as a line entity parallel to the external field consisting of a partly normal core and surrounded by a vortex of supercurrent. The partly normal core can be looked upon as the 'boundary' between the surrounding superconducting phase and a central line of normal phase. Each isolated flux thread carries within its core and surrounding current vortex, a single quantum of magnetic flux Φ_0 , and it has been shown ⁽¹⁰⁾ that $\Phi_0 = 2.067 \times 10^{-15}$ Wb.

At H_{c1} flux begins to penetrate abruptly until the fluxoids begin to interact on each other. Abrikosov, whose paper in 1957 ⁽¹⁰⁾ initiated the present understanding of the magnetization of type II superconductors, considered that a square lattice was that which resulted in the lowest energy, but more recent work (notably that of Matricon ⁽¹¹⁾ and Kleiner et al ⁽¹²⁾) and experimental evidence ⁽¹³⁾ shows that a triangular lattice results in the lowest energy. As the external field increases, more and more fluxoids penetrate and become more closely packed with their current vortices overlapping. This results in local forces of mutual repulsion, the resultant of which is balanced by the action of the external field. As H_{c2} is approached, the inter-fluxoid distance decreases and the flux thread cores begin to overlap until at H_{c2} the bulk of the specimen is completely normal.

For fields greater than H_{c2} , a sample should be fully normal if it is assumed that there is an infinite medium and if boundary effects are neglected. St. James and de Gennes ⁽¹⁴⁾ have shown that at a plane dielectric insulator-superconductor surface,

superconductivity is present at fields in excess of H_{c2} up to a value referred to as H_{c3} . The bulk of the material is normal, but a superconducting sheath persists in the surface regions parallel to the applied field. From the theory of Ginsburg and Landau, it has been shown that $H_{c3} = 1.695H_{c2}$. The ratio of H_{c3} to H_{c2} has often been verified (15,16), but the presence of a normal metal in place of the insulator is found to reduce H_{c3} .

2.3 Flux Pinning.

It follows from Ampere's law,

$$\bar{J} = \text{curl } \bar{H}$$

(where \bar{J} is the current density in amperes/m²), that if a current is to be carried in a superconductor there must be a non-uniform magnetic field. The uniform, triangular lattice of fluxoids inherent in the basic model of an ideal type II superconductor, would appear therefore to be incapable of carrying appreciable current. Actual materials used in magnets are known to be capable of sustaining very high current densities. The mechanism by which they can do so is attributed to "pinning" of the magnetic flux by microstructural variations such as small cavities, defects, insulating second-phase particles, dislocations, strains, etc., and thus causing a field gradient. This idea was outlined by Anderson (17), and extended by Anderson and Kim (18) to explain the results of Kim et al (19,20).

Anderson showed that "flux creep", a slow motion of fluxoids, could be explained by assuming that bundles of fluxoids were thermally activated over free energy barriers arising from the pinning effect of inhomogeneities.

As an example of the effects of pinning forces produced by inhomogeneities on the distribution of internal flux, consider a long slablike specimen in increasing longitudinal magnetic field. Once the surface barrier has been penetrated, flux threads will be driven into the specimen, but inhomogeneities will impede this motion and tend to pin the flux threads at low energy positions. An increase in external field, and a corresponding increase in driving force on a flux thread, will be necessary to move it further into the specimen.

Once the flux thread has moved into the specimen a distance appreciably greater than the penetration depth, it will no longer experience any force from the external field. It can be moved from a pinning centre by forces from neighbouring flux threads, those nearer the surface pushing it deeper and those further from the surface pushing it back towards the surface. This yields a net magnetic forward force proportional to the gradient of the flux thread density.

Kim et al consider spatial variation of the free energy to be as (a) in fig. 2. This results in pinning of flux bundles (b), the free energy of a bundle being lowest at points where the free energy in (a) is highest. When a current flows (so that the fluxoids are subjected to a Lorentz force) the free energy is effectively lowered, as in (c); if the effective height of the peaks is sufficiently low, the bundles may escape by thermal activation.

Various workers have endeavoured to evaluate the forces on a single flux thread due to neighbouring fluxoids. According to Friedel, de Gennes and Matricon ⁽²¹⁾, the force F_m per unit length

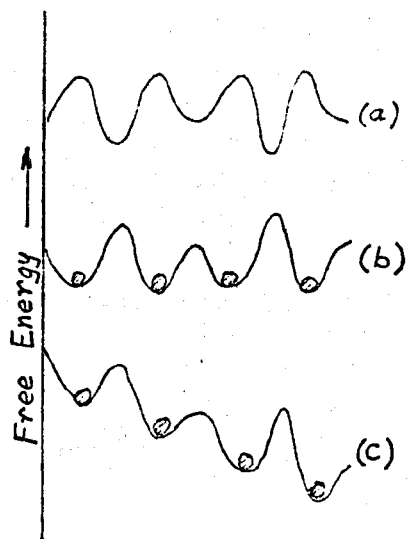


Fig. 2 Schematic diagram illustrating flux creep.

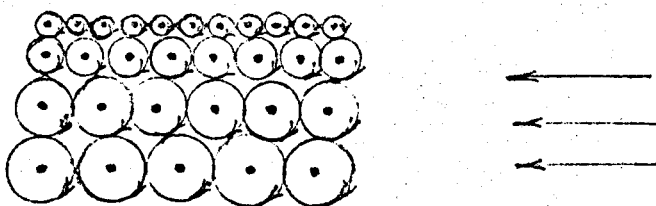


Fig. 3 Schematic illustration of current vortices being equivalent to macroscopic internal currents.

on the flux thread is given by:

$$F_m = -\frac{1}{\mu_0} \left[\frac{dH}{dB} \right]_b \frac{\partial b}{\partial x} \quad (1)$$

where x is the distance normal to the slab surface,

b is the local average internal field,

$\left[\frac{dB}{dH} \right]_b$ is the derivative of the ideal reversible E-H curve

at the value of b .

A more general form of (1) has been derived by Evetts and Campbell (22), for the driving force in a general non-equilibrium distribution of flux lines.

At zero temperature, the flux thread cannot be unpinned until the magnetic driving force overcomes the pinning force F_p caused by the defects. This defines a critical flux gradient in which $F_p = F_m$ and given by:

$$\left(\frac{\partial b}{\partial x} \right)_c = F_p \cdot \frac{1}{\mu_0} \left[\frac{dB}{dH} \right]_b \quad (2)$$

where F_p as well as $\left[\frac{dB}{dH} \right]_b$ can be a function of b . As the external field increases, flux will continue to move into the specimen until the flux gradient everywhere has decreased to just below this critical value.

Thus the magnetization of the specimen can be determined on this "critical flux gradient" concept from the flux distribution obtained from a knowledge of $(\partial b / \partial x)_c$ as a function of b , together with a boundary condition to establish b near the specimen surface.

Since the defects resist flux penetration, $-M$ will be higher in increasing fields than for a defect-free specimen. In a decreasing field, flux will try to escape against the resistance of defects, the flux gradients will be reversed and $-M$ will be less than for a defect-free specimen.

The internal macroscopic flux gradients $\partial b/\partial x$ are related to internal macroscopic currents parallel to the slab surface through Maxwell's equations by:

$$\frac{\partial b_z}{\partial x} = \mu_0 J_y \quad (3)$$

where J_y is the current density. This enables an equivalent discussion based on critical currents to replace that based on critical internal flux gradients. These internal macroscopic currents result from the superposition of the microscopic current vortices round each flux thread, and can be illustrated as in fig. 3.

From (1) and (3), $F_m = \oint_0 J_y \left[\frac{dH}{dB} \right]_b$ per flux thread per unit

length. Hence the magnetic driving force per unit volume is:

$$F_v = nF_m = bJ_y \left[\frac{dH}{dB} \right]_b \quad (4)$$

where n is the local density of flux threads. This is in the form of a macroscopic Lorentz force, except for the factor $\left[\frac{dH}{dB} \right]_b$. (17,18,21)

For high flux densities in materials used for magnet wires, $\left[\frac{dH}{dB} \right]_b$

is nearly unity, and it is satisfactory to consider the magnetic driving force as equivalent to the local macroscopic Lorentz force

and expressed as $\bar{F}_L = \bar{F}_m = \bar{J} \times \bar{B}$.

However $\left[\frac{dH}{dB}\right]_b$ departs appreciably from unity for some other superconducting materials, and for all type II superconductors $\left[\frac{dH}{dB}\right]_b$ approaches infinity as b approaches zero.

2.4 Flux Creep and Flux Flow.

At non-zero temperatures, thermal activation permits flux motion even if the magnetic force on a flux thread is less than the pinning force, (i.e. $F_m < F_p$). The Anderson model allows some flux motion, or "flux creep" (mentioned previously), even at low gradients, as the system is always slowly moving towards equilibrium. Flux creep is analogous to mechanical creep, and it has been observed experimentally (20 and 23) that once the external magnetic field has been set at a given value, the magnetic state of a specimen develops linearly with the logarithm of the time, as is characteristic of creep phenomena.

Goodman (8), in reviewing the magnetization experiments of Kim and his co-workers (and the results of other workers), quotes the average velocity V_L of the vortex lines in flux creep as being of the order of 10^{-7} to 10^{-10} m/sec. Further, in the limit of small V_L in the flux creep regime, V_L and consequently also the voltage, vary approximately exponentially with the current density. In the opposite limit of large V_L , the voltage is found to be a linear function of the current density. The flux motion occurring under this condition is referred to as flux flow, and in this case, Goodman gives a value for V_L of the order of 10^{-2} to 10^{-4} m/sec.

In flux flow, it is considered that the driving forces are opposed principally by a viscous drag acting on the vortex lines,

and from a consideration of this mechanism, the energy dissipation associated with flux flow can be estimated. Although this dissipation is quite different from ordinary ohmic dissipation, it has led to the idea of a resistivity being associated with flux flow. It has been suggested that this electrical resistance observed below H_{c2} originates in an e.m.f. induced by flux flow, but it appears that there are serious fundamental objections to this idea. It does not seem possible to explain the occurrence of steady voltages in this way, although the possibility of transient voltages is not excluded.

In more defect-free materials, a similar mechanism for explaining resistive transitions is not applicable since the flux-creep and flux-flow concepts are not relevant. However if it is supposed that a fluxoid subject to a Lorentz force and not balanced by pinning forces moves across the specimen at a rate determined by a velocity-dependent retarding force, then a voltage will be observed, as in flux creep and flux flow. This supposition is open to the same objections as in flux creep and flux flow but may account for many of the resistive properties observed.

Measurements of the voltage appearing along a specimen as a function of the current at constant temperature and magnetic field (24, 25) show that the current at which a voltage first appears is dependent on the physical condition of the sample (i.e. the density and strength of pinning centres). At high values of current, however, the voltage is linear with current and the slope $\partial V/\partial I$ (termed flux-flow resistivity ρ_f) is found to be independent of the physical condition, in accordance with the flux-flow concept. But against

this, it is found that the magnitude of the voltage is much larger than the normal electron drag mechanism would suggest.

Other loss mechanisms have been introduced by Tinkham (26) and Stephen and Bardeen (27) which give good quantitative agreement with the above measurements. Because of the vortex nature of the fluxoids, Magnus forces (analogous in hydromechanics) might be expected. There is disagreement on this, and it has not been resolved. As Goodman points out in his review, while there is little doubt that the dissipative process, of which ρ_f is a measure, is connected with the normal electron-like excitations associated with the core of each vortex line, no general microscopic theory of the field and temperature dependence of ρ_f has yet been formulated.

2.5 Flux Jumps and Superconducting Magnets.

One problem of utilizing type II superconductors in magnets is the tendency of the wire to return to the normal state in a catastrophic manner. This effect is associated with the heating resulting from discontinuous changes of the flux called "flux jumps".

Flux jumps are found to occur at reproducible values of the magnetic field (28, 29, 30); they are most common when the field gradients are steep, and this explains the prevalence of jumps at low temperatures when steep gradients are inevitable. The rate at which the magnetic field is changed can have considerable influence on the probability of a flux jump occurring. "Training" (i.e. raising and then lowering the current just before the field is raised through the 'dangerous' value) militates against flux jumps because of the reduction in steep gradient following from a re-

arrangement of the magnetic field, (31, 32).

Considerable temperature rise is associated with a flux jump, and gives support to the idea that catastrophic jumps occur when the thermal diffusivity is insufficient to carry away the heat resulting from the movement of the flux, especially as the diffusivity is likely to be unfavourable in superconducting materials used in magnets. Factors affecting diffusivity and the thermal instability resulting in a flux jump are the thermal conductivity, specific heat, normal-state resistivity, and the temperature dependence of flux motion. The energy dissipation mechanism is influenced by the nature of the pinning centres, the overall energy gap, the local flux distribution and the rate of field change. Surrounding the superconductor with a normal metal usually decreases the frequency of flux jumps, probably because the eddy currents in the normal metal protect the superconductor from high rates of field change, and the normal metal will affect the diffusion of heat from the superconductor. These aspects are considered in detail later on in Section 3.3 .

Flux jumps may be initiated by a thermal, electrical or mechanical disturbance, which gives rise initially to small flux movements, but which rapidly propagate through comparatively large volumes of the superconductor and develop into an avalanche (33). It has been shown (8) that flux jumps may move with a speed of the order of 1 to 100 m/sec. There are several indications that flux jumping is a nearly adiabatic process in which either the magnetic work done by external sources or the energy liberated by mutual annihilation of fluxoids is sufficient to heat the superconductor locally sufficiently to render it normal for the duration of the flux jump.

Another and even more serious instability occurring with solenoids should be mentioned in passing (5). It occurs when the field is reversed beyond $-H_{c1}$, when flux entering the superconductor will be attracted by the previously trapped flux of opposite sign, and annihilation will occur. The energy released thereby may be sufficient to heat the superconductor above its critical temperature (34).

Flux jumps and inhomogeneities can be detected by observation. Wertheimer and Gilchrist (35, 36) have measured the speed of flux jumps by using the Faraday rotation technique and used a high speed cine-camera to film the evolution of flux jumps with time. They demonstrate that the diffusivity depends on the flux flow resistivity, ρ_f . They show that flux jumps appear to fall in two categories: "regular" jumps with a smooth boundary associated with pure specimens, and irregular jumps having a very irregularly shaped boundary which occur exclusively in alloy samples. The flux jumps are reluctant to coalesce and new flux jumps tend to be displaced by already existing flux regions. Considerable heat is evolved during massive flux jumps evidenced by bubble formation lasting a few milliseconds near to the specimen. A redistribution of flux follows a flux jump which is presumed to be linked with thermal conduction effects. With a given sample, the flux jumps are smaller but more frequent as the temperature is lowered.

2.6 Bean's Critical State Model.

Bean (37, 38) derived a model based on the critical current concept (or critical internal flux gradients) for describing the magnetic behaviour of a type II superconductor containing defects.

The time dependence of magnetization associated with flux creep is ignored, and it is assumed that the distribution of internal flux is such that the gradient is always equal to the critical gradient. This is a quasi-equilibrium state between the magnetic forces on flux lines and the pinning forces. The current density is then the critical current density J_c . Above certain values of an applied field and transport current the critical state breaks down, the fluxoids move against the viscous forces of the pinning centres and 'flux flow' occurs.

Bean further assumed in addition to the critical flux gradient and corresponding critical current, that J_c is independent of B . The boundary condition for B at the surface chosen by Bean was to let B approach the external field. A preferable boundary value for B is B_{eq} , the internal flux density in equilibrium with the external field $\mu_0 H$, in a defect-free material. This is a poor approximation at low fields, because of surface barrier, but is probably fairly good well above H_{c1} .

Macroscopic internal fields and induced currents across the cross-section of a long slab specimen in a field parallel to it can be plotted for different values of increasing field $H > H_{c1}$. When the field is applied, the flux penetrates only to a depth determined by the strength of the pinning centres. The circulating screening currents are everywhere equal to the critical value J_c and the depth of penetration is given by:

$$\Delta = \frac{H}{J_c} = \frac{B_{eq}}{\mu_0 J_c} \quad (5)$$

Distribution of internal flux density $B(x)$ and macroscopic internal

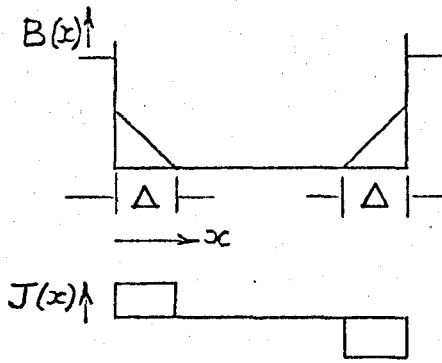


Fig. 4

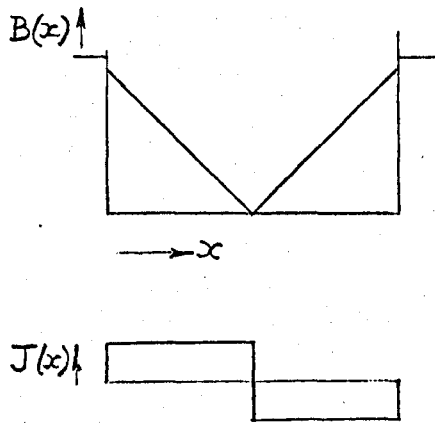


Fig. 5

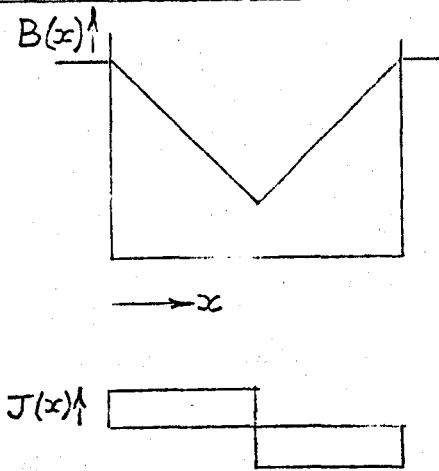


Fig. 6

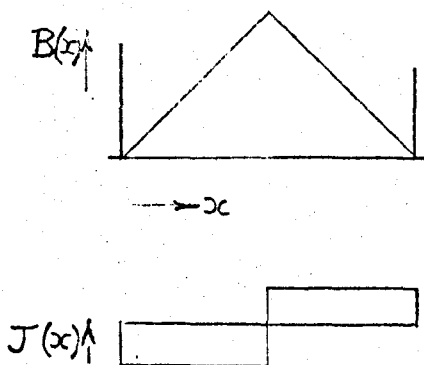


Fig. 7

current density $J(x)$ across section of imperfect type II superconductor (according to the Bean model) is as shown in fig. 4.

If the field is increased and the slab thickness and J_c are small enough, the flux can penetrate to the centre of the slab (fig. 5). J_c now flows throughout the specimen, which is now said to be in the "critical state". For any further increase in field, $B(x)$ merely moves upwards as in fig. 6.

In decreasing field, defects restrict the expulsion of flux, and flux gradients and induced macroscopic currents of the opposite sign progress inwards from the surface. On return to zero external field, the resulting distributions of the flux and current densities are shown in fig. 7.

2.7 Improvements in Bean's Critical State Model for Practical Cases.

The assumption that J_c is independent of flux density is useful for qualitative discussion, but is rarely valid in practical cases, and various empirical relationships have been established for the variation of J_c with B . For example, Kim, Hempstead and Strnad (19, 23) investigated the resistive states (i.e. energy dissipative states) of hard superconductors by cylindrical tube magnetization and equivalent resistance measurements, and found that the high-field Lorentz force could be represented by a single parameter

$$\alpha = J_c (B + B_0) \quad (6)$$

where B_0 is a constant of the material. They also measured the temperature dependence of α , and found that the persistent currents decayed as the logarithm of time. Silcox and Rollins (39) developed a model to calculate B as a function of position in a type II

superconductor utilizing the actual Lorentz force and giving

$$J_c B = \alpha. \quad (7)$$

This is equivalent to the Anderson model for fields well above H_{c1} . This relationship is followed approximately by some practical magnet materials, particularly Nb_3Sn , but usually the $\alpha = J (B + B_0)$ relation gives better results. By making certain assumptions regarding the field distribution at the surface of a non-ideal material, Friedel, de Gennes and Matricon⁽²¹⁾ develop a different expression for the magnetic force on a vortex line, but for fields well above H_{c1} , however, it reduces to the Kim-Anderson form. Irie and Yamafuji⁽⁴⁰⁾ suggest a refinement to the Silcox and Rollins expression and give $J_c = \alpha/B^{\gamma-1}$, where γ is a number which should lie in the range $1 < \gamma < 2$.

All the above expressions for the critical-current density functions assume that α is independent of field. Urban⁽⁴¹⁾ in setting out to explain some experimental results in terms of the above and similar expressions found that there were large discrepancies between the experimental and various predicted results. It appeared to him that a probable source of these discrepancies might be the implicit assumption that α is independent of field, and as a result of further investigation developed the following expression for the field-dependence of α :

$$\alpha(B) = \alpha_c (\mu_0 H_{c2} - B),$$

where α_c is a field-independent, but temperature-dependent constant. When this value for $\alpha(B)$ is inserted in equ.(6), the value of critical current is given by:

$$J_c = \alpha_c \left[(\mu_0 H_{c2} - B) / (B_0 + B) \right] \quad (8)$$

This is a functional form which vanishes at the upper critical field H_{c2} and approaches a large, finite value $\alpha_c (\mu_0 H_{c2} / B_0)$ at $B = 0$. The validity of equ.(8) has been tested empirically, but only for Nb-25%Zr for which remarkable agreement with measurements is claimed by Urban.

The critical state model can be used to predict magnetization behaviour from a known $J_c(B)$. Although it has the advantage of simplicity, it has certain limitations. Flux creep can occur at any values of J and B and thus there is no precise 'critical state'. Nevertheless, a critical state may be defined as that at which the rate of flux creep falls below a practically observable limit.

2.8 Limitations of Critical State Model.

The model referred to previously as the critical state model, is an oversimplification. Besides the assumption of J_c being independent of flux and the necessity of using an empirical relation between J_c and B for application of the model to a practical case, it also neglects factors which would cause the average depth of pinning centres to be field dependent. This may occur if the pinning centre is also superconductive but with different properties (e.g. different dependence of free energy on field) from that of the matrix, or if the pinning centre is ferromagnetic. Furthermore, simple critical state models have two further shortcomings: they ignore the role of sheath currents and they assume strictly isothermal conditions during penetration of current and flux. The role of sheath currents, while important in the behaviour of type II materials and in measurements of their magnetization characteristics, probably has

little effect on the performance of superconducting magnets. Clearly the isothermal assumption is by no means valid in many situations, and departures from isothermal conditions give rise to some of the peculiarities of superconducting magnets; this will be discussed in detail later.

Further, difficulties arise if attempts are made to apply expressions such as (6), (7) and (8) to a solenoid, since when the superconducting to normal transition takes place, only the critical current value is known and the local value of the field where the quench is initiated is not (since the precise region where the quench is initiated cannot usually be identified). There is also a certain amount of experimental evidence (42, 43) to show that the transition may be initiated by a flux jump in a region of low flux density in the solenoid regardless of the value of the field at its centre.

Although the successive penetration of flux has been considered for the Bean model only, flux penetration on any of the models for pinning proceeds through a series of local critical states which extend deeper into the material as the external field is increased. With each increase in external field, the additional flux moves through the saturated regions of pinning centres until it can be pinned by unsaturated centres.

2.9 Impressed Currents.

If the current is impressed and gives rise to the field (instead of the other way round considered hitherto), the same physical situation exists. For example, considering J_c to be independent of B , the current and field distribution for an infinite sheet of finite

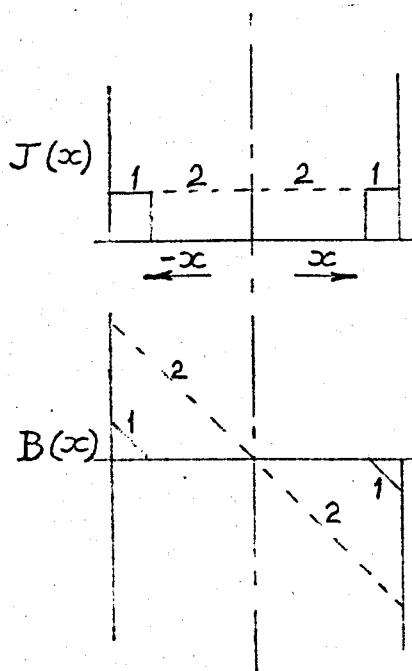


Fig. 8

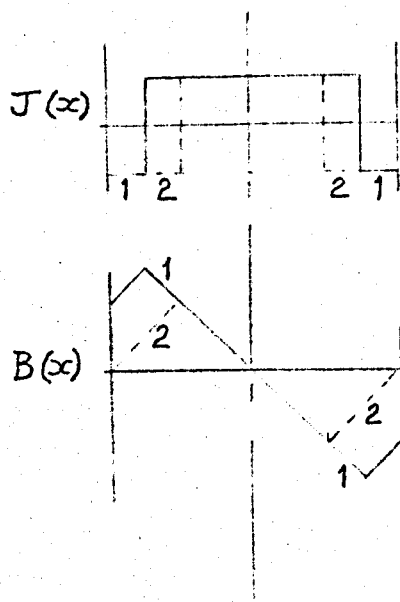


Fig. 9

thickness can be deduced in a manner similar to that used to derive current and field distributions previously. As more and more current flows in the sheet, flux and current penetration increases from both of its surfaces. At each increase, the region occupied by current consists of a distribution of local critical states. In fig. 8, any further increase in current beyond 2 would cause a transition to the normal state.

With a decrease in net transport current, a peculiar situation arises, since on the critical state model, the local value of J can only be $\pm J_c$ because the flux cannot move appreciably under less than the critical force. This means that for a decrease in net transport current, a layer of reverse current is set up at the surface; this layer of reverse current progressively extends inwards through a new series of reverse critical states as the net transport current is progressively reduced. (See fig. 9, where 1 and 2 represent the sequential values of current and flux).

It is noticed that even when the net transport current is zero, there remain circulating currents corresponding to a paramagnetic moment in the material and giving rise to a remanent field. This effect is observed in superconducting solenoids and gives rise to difficulties in the use of magnets designed to give very homogeneous fields. The effect can be reduced by the use of smaller diameter wires, but once the circulating currents are present, they can only be completely removed by heating the material above its transition temperature (and cooling in zero field).

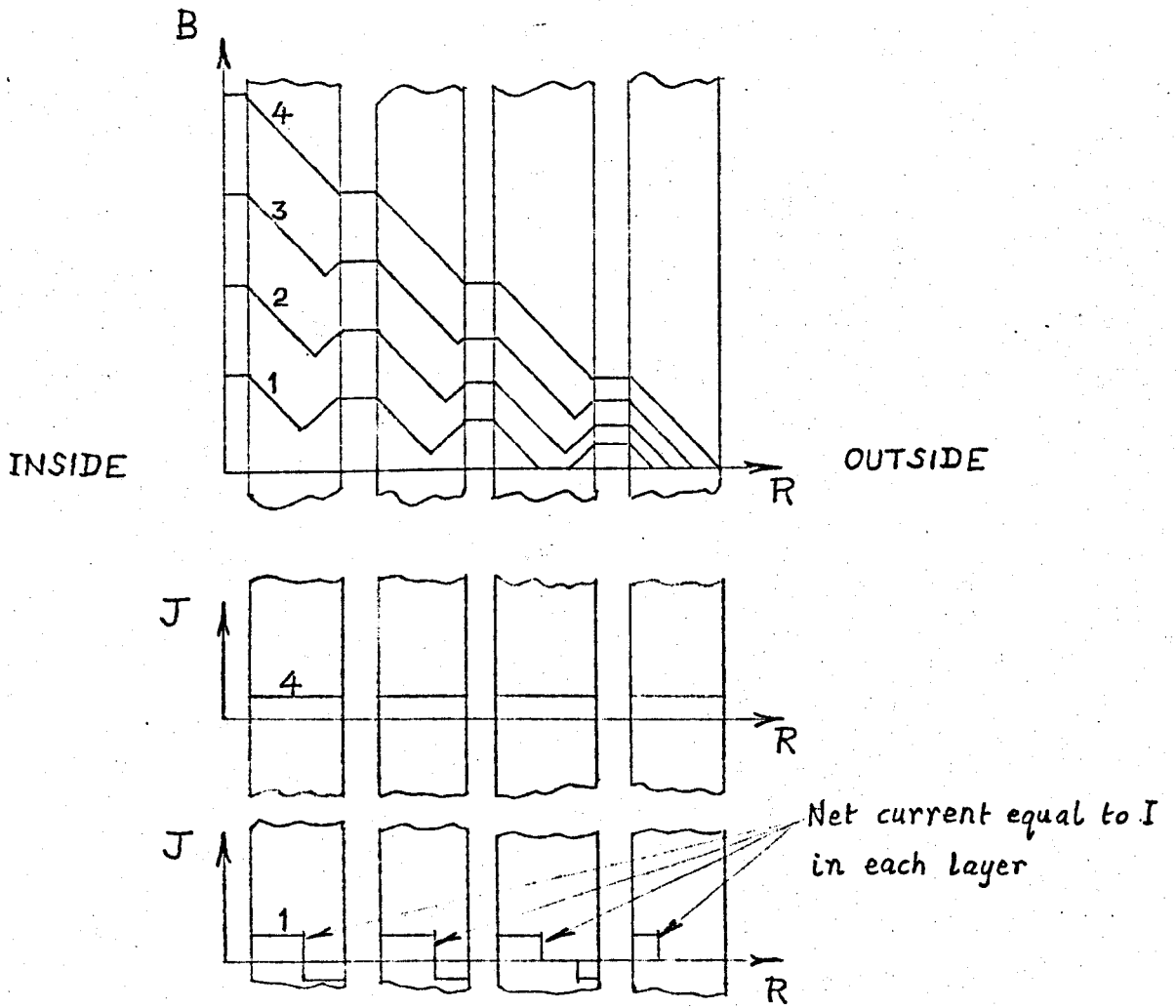


Fig. 10 Current distribution in a solenoid - current increasing.

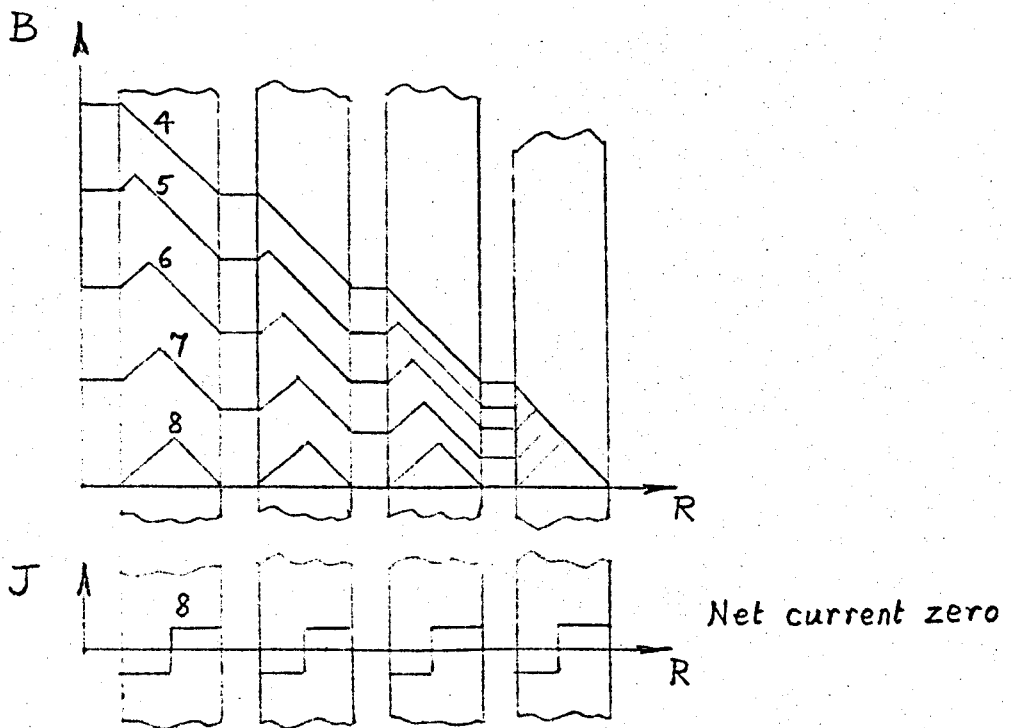


Fig. 11 Current distribution in a solenoid - current decreasing.

2.10 Field Distribution in a Solenoid.

The discussion in the previous section can be extended to the case of a long, straight, multi-layer solenoid in which, for simplicity, the total thickness of the winding space is much smaller than the radius of the solenoid so that the problem can be considered in one dimension. The assumption of the Bean model that J_c is independent of B will also be used.

The only magnetic field present is that due to the currents carried by the layers in the solenoid. If the net transport current is increased from zero up to a value corresponding to (1), (see fig. 10), the flux and current distributions will be as shown, in accordance with the critical state model. The total current in each layer is greater than the net current. Successive increases in the net transport current lead to (2) and (3) until when each layer is carrying its maximum current, (4), the coil is on the point of quenching.

If now the current is reduced in stages, the flux and current distributions will be as indicated by (5), (6), (7) in fig. 11. At (8) the net current has been reduced to zero, but the remanent paramagnetic field noted earlier is apparent.

2.11 The Critical State and A.C. Magnetisation.

The basic concept of the critical state is that the flux lines are in a quasi-equilibrium state under the influence of the pinning and Lorentz forces. If, therefore, the flux distribution changes due to an externally applied field, fluxoid motion will be resisted and energy dissipated in the process. If a complete magnetisation cycle is completed and the curve plotted, a corresponding hysteresis

effect is observed. It is the losses resulting from periodic magnetization which at present are the main obstacle to the utilisation of type II superconductors in engineering applications where they are subjected to alternating magnetisation.

The moderate success of the various versions of the critical state model has prompted several workers to apply it to alternating field conditions in order to predict the losses during a complete cycle. Among these are London (44), Bean (38), Hancox (45), Irie and Yamafuji (40), Green and Hlawiczka (47), Voigt (46), Dunn and Hlawiczka (48). As Linford points out (49), each method is based on its particular approximations but several assumptions are implicit in all forms of this use of the critical state model.

These are that:

- (a) the dynamic and static critical current densities are the same,
- (b) the response of the current-field distribution to a change in the applied field is instantaneous,
- (c) the temperature of the sample does not rise under the influence of the dissipation,
- (d) there are no flux jumps in the course of the cycle, and
- (e) the sample is homogeneous.

The validity of these assumptions is open to question, although Hart (quoted in (49)) concludes that if the slope of the electric field (E) - current density (J) curve at the point of operation,

$$\frac{\ln E}{\ln J} \gg 1$$

then assumptions (a) and (b) are valid. He calculated that the

condition was reasonably well satisfied by NbZr and excellently by Nb₃Sn.

Bean (also quoted in (49)) has predicted the temperature rise in (c) assuming J_c and the thermal conductivity K to be constant as:-

$$T_{\max} - T_{\text{bath}} = \frac{\omega H_m^4}{K J_c^2} \cdot \frac{10^{-5}}{3(4\pi)^4} \quad (\text{c.g.s. units})$$

This applies only in the lower field limit. Further consideration of temperature rises is given later, but clearly the isothermal assumption of (c) is invalid in most situations, unless a condition of thermal equilibrium can be reached.

As described earlier, the fluxoids tend to form a regular triangular array in a perfectly homogeneous specimen, but in type II superconductors of practical interest for solenoids, pinning forces are exerted on the fluxoids due to the pinning centres caused by inhomogeneities and defects in the specimen. Thus condition (e) is only approximately true, and will vary widely among specimens of similar composition. Although some of the early predictions for a.c. losses were not confirmed by subsequent measurements, nevertheless suitably modified versions of the critical state model have been used to predict a.c. losses with reasonable accuracy in well defined situations, (e.g. (48), (50) and (51)). The main difficulty in using this approach for quantitative estimates in coils and other components in superconducting machines is that the conditions are not usually well defined, and if they are, then only in a very complex manner. If the losses for a solenoid are required, they have to be computed by considering the local fields.

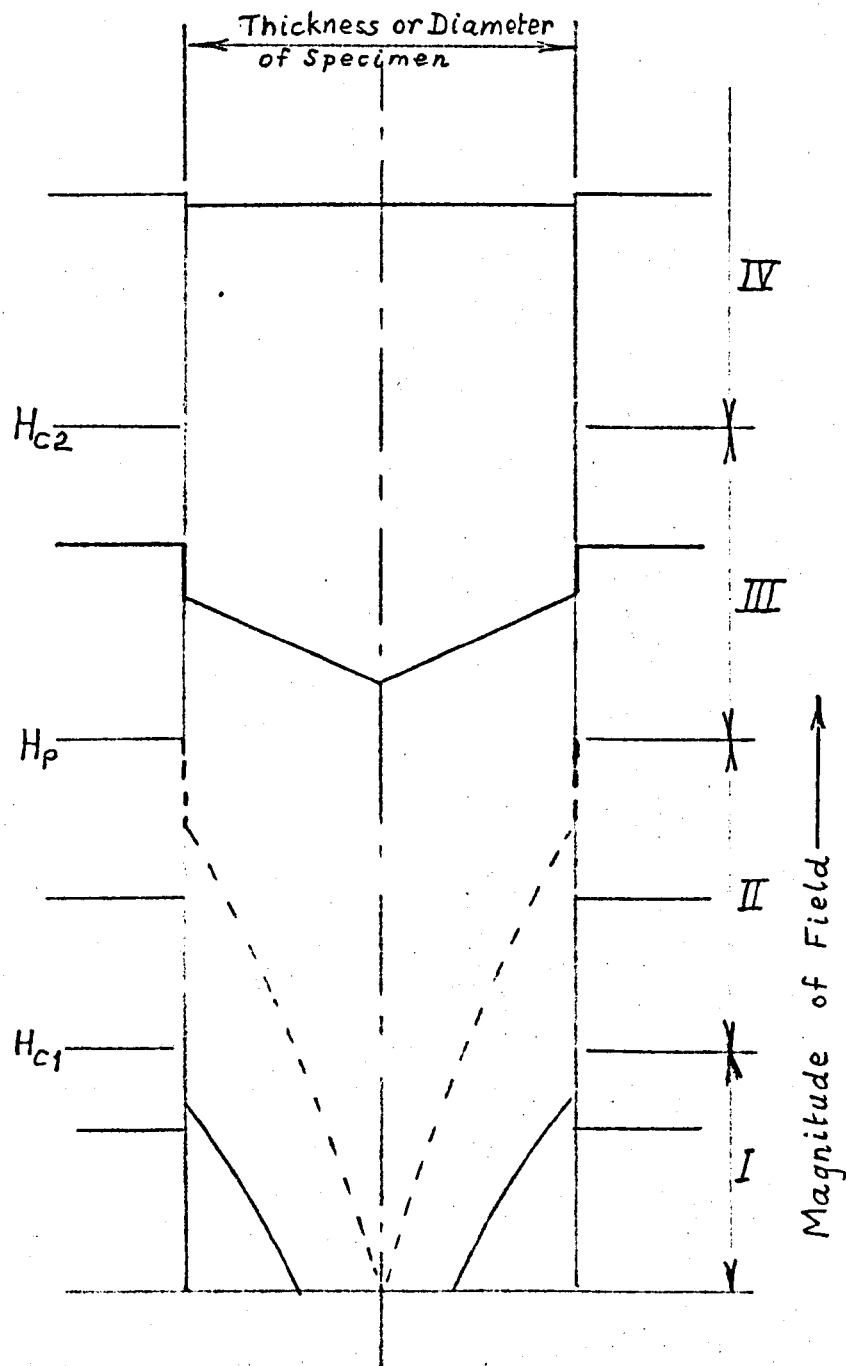


Fig. 12 Spatial variation of field inside slab or cylinder parallel to external field showing the four possible regimes.

2.12 A.C. Losses.

Various workers beginning with Kamper (52) and using a variety of methods have made measurements of a.c. losses in a number of superconducting materials of which pure Pb and Nb, and Nb alloys with Zr, Sn or Ti have been most frequently investigated. These workers include among others Rhodes et al (53), Easson et al (54,55), Slaughter et al (56), Dahl et al (57), Ulmaier and Gauster (58) and Chant et al (51).

The a.c. losses depend on the maximum value of the external field, H_e ; and its relation to other parameters. Four regimes can be distinguished:

$$\begin{array}{ll}
 \text{I} & H_e < H_{c_1} \\
 \text{II} & H_{c_1} < H_e < H_p \\
 \text{III} & H_p < H_e < H_{c_2} \\
 \text{IV} & H_{c_2} < H_e
 \end{array}$$

where H_p is the field of complete penetration, i.e. the field above which the total volume is affected by an a.c. field. These regimes are illustrated in fig. 12.

In regime I, if the superconductor is cooled below its transition temperature in zero field and subsequently a weak magnetic field is applied, the specimen remains in the Meissner state and no a.c. losses occur. However, the complete exclusion of flux except for a very surface layer (the London penetration depth $\approx 0.1 \mu\text{m}$.) does not persist as the field is increased. In type I superconductors regions of normal material appear carrying flux when the field at the surface exceeds the critical value H_c (the intermediate state). Correspondingly, in type II superconductors, flux begins to penetrate

when the field exceeds H_{c1} and the material is in the mixed state. When flux has entered a superconductor of either type in this way, losses will occur with alternating currents or fields and, even if the external field is subsequently removed, flux usually remains trapped in the specimen. Thus if a superconductor is to be used in an electrical machine in the Meissner state so that advantage can be taken of the ideally lossless characteristic, it can only be so used if precautions are observed to avoid flux trapping by cooling through its transition temperature in as low a magnetic field as possible, by operating in conditions so that the maximum field is considerably below H_c or H_{c1} , as appropriate, and by ensuring that surface irregularities do not cause local distortions of the field during operation of the machine which would cause flux trapping. Nearly always observance of these precautions would mean that such a machine would not be a viable proposition, as will be shown in Chapter 5. Even the use of relatively pure niobium, which has a value of H_{c1} higher than that of H_c or H_{c1} for any other superconductor, would mean working with fields which are *an order of magnitude* smaller than are used in conventional machines. (At 4.2K, H_{c1} for niobium is 11×10^4 A/m.)

Figure 13 shows surface a.c. loss in various niobium specimens at 4.2K as a function of the peak magnetic field, after Wipf (59). At 50 Hz and 4.2K the a.c. loss has generally been found to be less than the maximum permissible value of *nucleate boiling heat transfer of* 0.1 W/m^2 provided the amplitude of the surface field is less than approximately 6×10^4 A/m, but this is still approximately an order of magnitude smaller than the fields used in conventional machines.

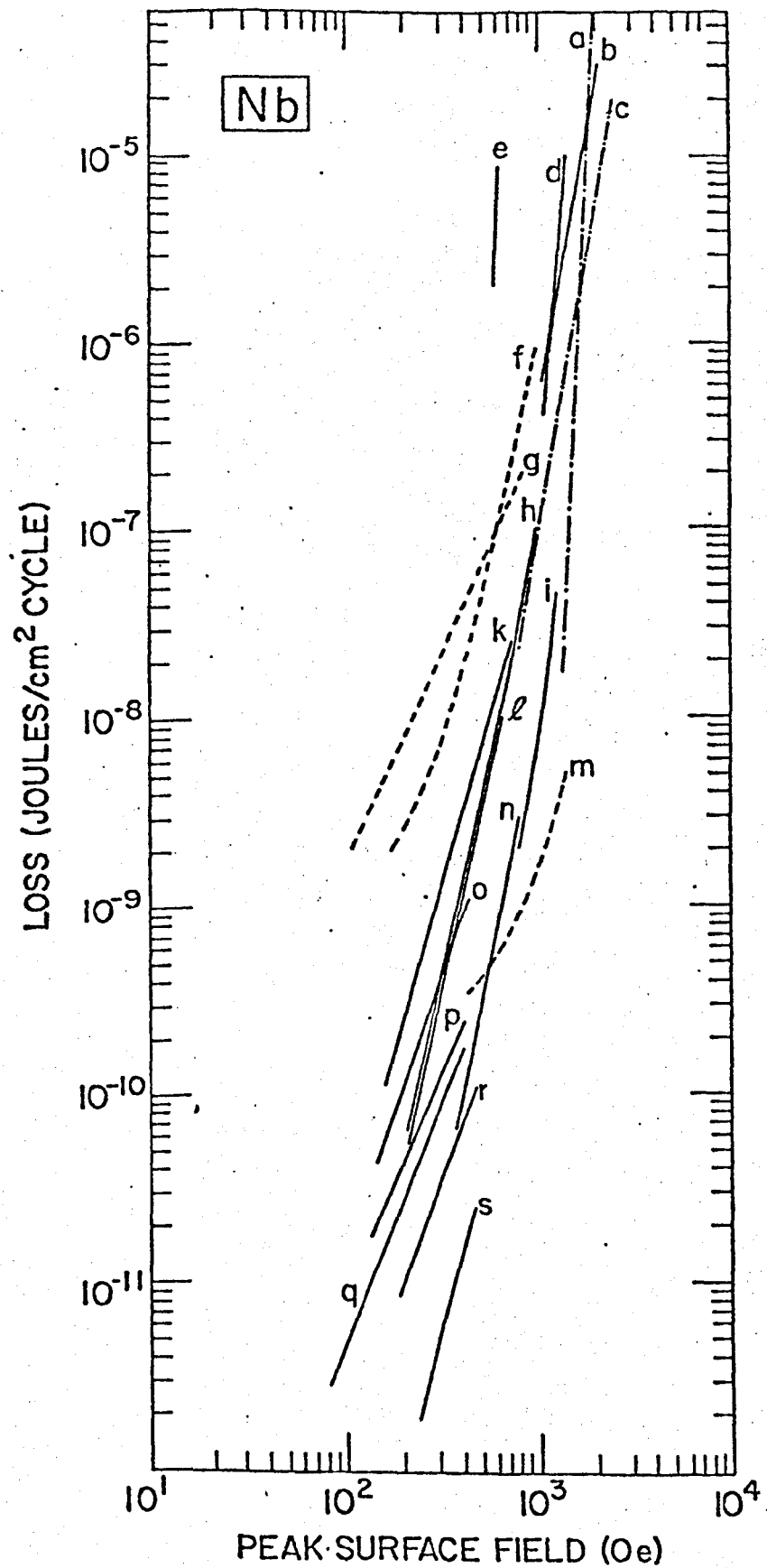


Fig. 13 Surface AC loss in various niobium specimens at 4.2K as a function of the peak magnetic field. (After Wipf)

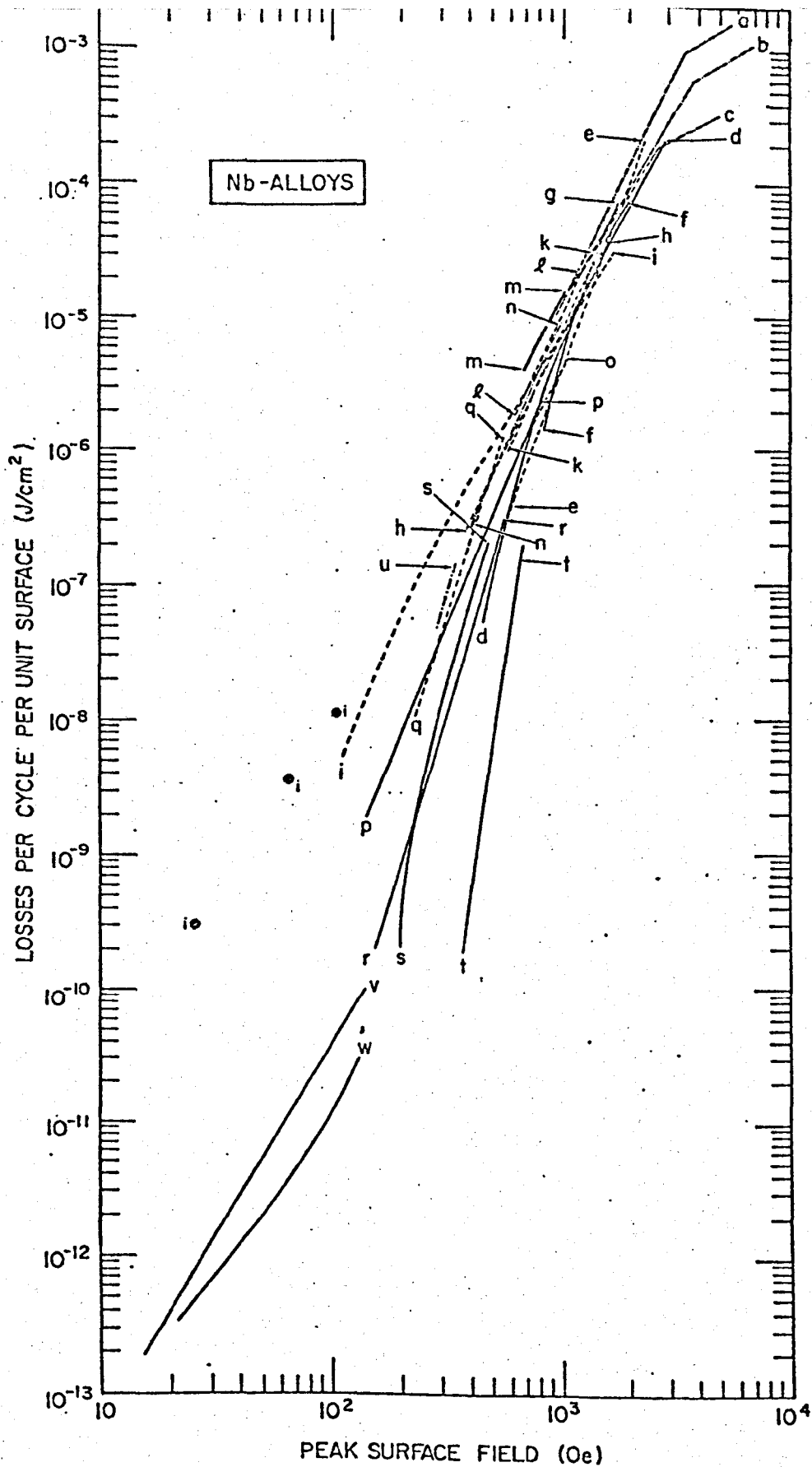


Fig. 14 AC loss per unit area per cycle for various niobium alloys. (After Wipf)

Easson and Hlawiczka have reported (55) losses of less than 0.1 W/m^2 at a surface field of $11 \times 10^4 \text{ A/m}$, but whether it would be technically feasible to produce a niobium sheathing for a machine rotor and operate it under the ideal conditions of the loss measurements is extremely doubtful.

Regime II represents that in which most of the measurements have been carried out. Figure 14 shows the results of several measurements on various niobium alloys and reviewed by Wipf (59). In an effort to relate loss measurements in regime II to a modified critical state model, Dunn and Hlawiczka (48) derived the following expression for the energy dissipation per cycle:

$$W = \frac{5 \times 10^{-7}}{12 \pi^2 J_c} (H'_m)^2 (1.5 H_{c1} + 3 \Delta H + H'_m) \quad (9)$$

(c.g.s. units)

where $H'_m = (H_m - \Delta H - H_{c1})$

J_c is the critical current density,

H_m is the field amplitude,

and ΔH is the screening effect of the surface sheath currents.

Experimental verification of equ.(9) has been provided by Linford and Rhodes (50), as do the results in fig. 14 but only in a

qualitative fashion. Taking into account the other literature

cited as well, certain generalisations can be made regarding a.c. losses in regime II:-

- (a) The losses depend on the peak field H_m to which the superconductor is subjected, and does not matter whether it is due to alternating current in the superconductor itself or to an externally applied field.

- (b) The energy loss per cycle is independent of the frequency.
- (c) The loss is independent of waveform.
- (d) To a rough approximation, the loss is proportional to H_m^3 , at the higher fields in this regime.

In regime III, the field is large enough to penetrate the entire specimen and the losses become very large, and in large specimens the heat loss per unit surface area may be sufficient to cause thermal runaway. Except possibly in the case of filamentary composites, this regime is unlikely to be of interest in engineering applications. Neither is regime IV, since the specimen will be in the normal state apart from the thin surface sheath below H_{c3} .

3. Superconducting Solenoids.

3.1 Experience with Early Superconducting Coils.

It was mainly on account of thermal instabilities and flux jumps that workers in the early 1960's had very disappointing results with superconducting coils (e.g. (60), (61), (42), (43)). Solenoids wound with type II superconducting wire, usually Nb_3Sn or Nb-Zr were not able to sustain the maximum fields and maximum currents without quenching (i.e. returning to the normal state) which could be achieved in tests on short samples of the superconducting wire when they were exposed to homogeneous transverse fields of equal strength. This effect was termed 'degradation'. (62) Until precautions were taken, the quench usually resulted in the coil being damaged in two possible ways: either a section of the coil melted, or voltage breakdown of the insulation on the wire or between turns occurred. The transition to the normal state usually commenced in a short section of the wire and was propagated through the rest of the coil by the heat generated by the current flowing in the resistive normal section. (63) If the normal zone propagated slowly, the current in the circuit would be maintained by the coil inductance for sufficient time to heat the normal zone to room temperature, or occasionally to the melting temperature of the wire. If the normal zone propagated quickly, high voltages were induced which caused insulation damage. Both types of damage were easily avoided by plating the wire (62), (63), (64) with about 0.025 mm of copper which lowered the resistance of the wire in the normal state sufficiently to prevent burn-out, and the use of improved winding

techniques and insulating materials (61) eliminated voltage breakdown.

Riemersma et al (42) attributed the initial entry to the normal state to a flux jump in which sufficient energy was released to raise a length of wire above its critical temperature thus nucleating a normal zone. Shimamoto and Ohtsuki (65), by measuring the voltages appearing at tapping points in a Nb-Zr magnet during superconducting to normal transitions demonstrated that the normal region propagates across turns, rather than along the wire. They also showed that the normal region commences at the innermost turns and propagates outwards. Another peculiarity of early superconducting coils was that however smoothly the energising current was increased, the field produced in the bore increased in a series of small abrupt steps, corresponding to small flux jumps. These were much larger at small values of field and diminished in magnitude as the field increased. Thus if an external field was first applied to an unenergised coil from another magnet, the magnitude of the flux jumps, and consequently the possibility of an early quench, were both diminished. Schrader and Kolondra (65) found that if a superconducting coil was immersed in an external field of about half the critical value before being energised, it was possible to obtain almost the full expected critical current. This led to the practice of subdividing a superconducting magnet into concentric sections each with its own power supply; the sections were energised from the outer section inwards, and by this means excessive degradation of the innermost section was avoided. (66), (67)

Apart from some coils wound with Nb_3Sn 'core wire' in which short-sample performance was obtained by Kunzler, (68), nearly all

of the early superconducting coils showed serious degradation, although coils with low space factors and with wires of small diameter seemed less prone to this effect (42). Impregnation of small sizes of coil also gave an improvement (69). Their performance could sometimes be improved by 'training' (31), that is, by repeatedly cycling the current from zero to the quenching value. Lubell and Mallick (32) have shown that training can be induced by exposing coils of unplated Nb-Zr and Nb-Ti to reverse currents or reverse fields before energizing.

In view of the importance of the thermal and magnetic environments on flux jumping, and consequently on the performance and behaviour of superconducting magnets, it is proposed to consider these in detail.

3.2 Thermal Instabilities.

It has already been pointed out in Chapter 2 that the penetration of flux into a type II superconductor is a dissipative process, and a brief review has been given of this phenomenon in connection with a.c. losses. It is now proposed to obtain an estimate of the magnitude of the dissipation in a semi-infinite slab of superconductor when it is penetrated by flux, in order to examine the factors involved in more detail and how improvements in superconducting solenoids might be achieved.

Consider a semi-infinite slab of superconductor into which flux has penetrated to a depth X , (fig. 15.) If unit area on the surface of the slab is considered, let F_s be the flux density at the surface with the flux lines parallel to the surface. Now if the flux is

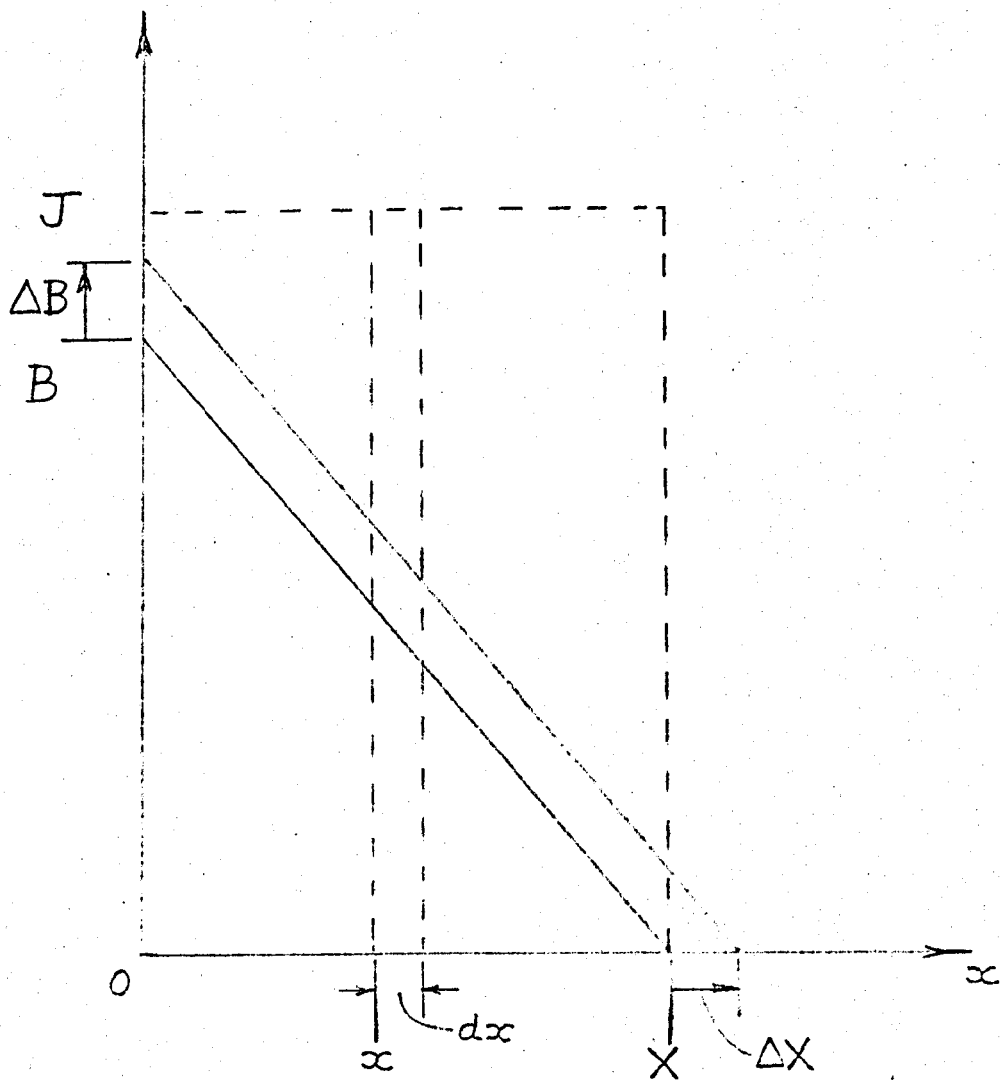


Fig. 15 Flux penetration in semi-infinite slab of superconductor.

increased by a small amount ΔB , there will be a corresponding increase in penetration by a distance ΔX . On the Bean model, the local currents are determined by the critical current density, J_c , and the flux gradient. The flux linked by every element of current in the material changes with the result that e.m.f.'s are induced in a direction tending to increase the local currents. The current, however, remains constant at its critical value, so that the work done by the induced voltages is entirely dissipated.

Consider an element dx at a depth x from the surface carrying a current of density J_c . If $B(x)$ is the flux density at x due to the field at the surface of B_s , the dissipation in the element per unit area of surface in establishing $B(x)$ is:

$$dQ = J_c dx \int_0^\infty e dt$$

$$\text{but } e = -\frac{d\Phi}{dt} = -\frac{d}{dt} \int_x^X B(x) dx$$

and corresponding to the rate at which the flux has passed dx in penetrating beyond x . Now $B(x) = B_s \left(1 - \frac{x}{X}\right)$ where X is the penetration depth given by equ.(5) and so:

$$\int_x^X B(x) dx = B_s \int_x^X \left(1 - \frac{x}{X}\right) dx$$

$$= B_s \left(\frac{1}{2}X - x + \frac{x^2}{2X}\right)$$

$$\text{Hence } dQ = J_c B_s \left(\frac{1}{2}X - x + \frac{x^2}{2X}\right) dx \quad (10)$$

and the total dissipation in the material per unit area is:

$$Q = J_c B_s \int_0^X \left(\frac{1}{2}X - x + \frac{x^2}{2X}\right) dx$$

$$= \frac{1}{6} J_c B_s X^2 \quad (11)$$

Substituting for B_s from equ. (5) gives the dissipation as:

$$Q = \frac{1}{6} \mu_0 J_c^2 X^3$$

Hence $Q = \frac{1}{6} \mu_0 I^2 X$ Joules/m² of surface (12)

or $Q = \frac{1}{6} \mu_0 I^2$ Joules/m³ of material (13)

$$= \frac{1}{6} \mu_0 H_s^2 \text{ Joules/m}^3 \text{ of material}$$

$$= \frac{B_s^2}{6\mu_0} \text{ Joules/m}^3 \text{ of material} \quad (14)$$

Thus it can be seen that for a given total current, the thicker the current-carrying region, the greater is the dissipation per unit volume of the material carrying the current. This leads to the concept of subdividing the superconductor in order, inter alia, to reduce the dissipation occurring with a change in field.

In the preceding approximate treatment, isothermal conditions were assumed and the effect of temperature on pinning strength and critical current was not considered. The penetration of flux into a hard superconductor is a dissipative process as illustrated above, and results in a rise of temperature. This in turn decreases the pinning strength and so allows further flux penetration. Flux penetration is thus a regenerative process which under certain conditions may result in a transition to the normal state, either locally or throughout the specimen. It is because of this intrinsic instability that difficulties arise in the use of hard superconductors, and why it is necessary to employ some means of stabilisation in superconducting coils.

3.3 Stability Criteria.

A precise analysis of the thermal and magnetic conditions in even a simple geometrical arrangement of superconductors is a very complex problem and would need to take into account the dependence of critical current density, thermal conductivity and specific heat on magnetic field and temperature within the superconductor, and include the heat transfer conditions at the surface and deal with the effects due to the presence of material bounding the superconductor. For practical arrangements, this has not so far been attempted in the literature, but criteria for thermal stability in simplified cases have been proposed by a number of workers including Anderson and Kim (18), Hancox (70), (71), (72), Swartz and Bean (73), (78), Irie and Yamafuji (74), Kim (75) and Wipf (76).

Hancox (70) derived two criteria for stability, one based on the Bean model and the other on that of Kim in which $J_c = \alpha / (B + B_0)$. They are both applicable to a semi-infinite slab of superconductor in which a change in surface field causes an energy dissipation, the change occurring rapidly compared with the thermal time constant of the material. This results in a local increase in temperature, and since the critical current density is temperature dependent, there will be a corresponding fall in current density expressed by Hancox in terms of a characteristic temperature, T_0 and given by:

$$T_0 = J_c \frac{\partial T}{\partial J_c} \quad (15)$$

Hancox gives the approximate criterion for stability based on the Bean model for a surface field, H_s , as:

$$H_s \leq \sqrt{8\pi C T_0} \quad (\text{c.g.s. units}) \quad (16)$$

where C is the specific heat per unit volume. Use of the Kim model yields a similar result except for a numerical constant of $\sqrt{2}$.

Swartz and Bean (73) give a more detailed analysis which leads to a similar result except for a numerical constant of $\sqrt{(\pi^2/8)}$ which is quoted by Wipf and Lubell (77).

Despite the simplicity of these approaches, they emphasise the important features of the instability. They show that the maximum field at the surface without instability is independent of the critical current density of the material, a higher critical current density resulting in a smaller penetration of the flux into the material before instability occurs. They show too, that the maximum field at the surface without instability is determined by the thermal capacity of the material C . Both of these effects have been demonstrated experimentally, e.g. by Hancox (70, 71).

In addition, these approaches show that instability results directly from the negative value of $\partial J_c / \partial T$ possessed by most hard superconductors. If $\partial J_c / \partial T$ could be made positive, inherent stability would result, (as Swartz and Bean (78) point out, and cite examples of superconductors in which this has been achieved). However, this approach is not applicable to practical materials available at present, or likely to be available in the near future.

Efforts to include the temperature dependence of both the specific heat and current density were made by Hancox (72), using computer calculations, but these did not lead to well defined stability limits. However, Hancox (72) did extend the earlier stability calculations to simple coils in which each layer of the winding is considered as a sheet of superconductor which experiences both an

increasing external magnetic field and an increasing current. It is shown that the winding is stable up to its full critical current provided:

$$JD \leq \sqrt{3C T_0/4\pi} \quad (\text{c.g.s. units}) \quad (17)$$

where J is the current density, and D is the thickness of the layer. A more ambitious, but not entirely successful attempt to predict the energy loss on magnetizing a coil, was presented by Irie and Yamafuji (74).

The practical import of thermal instabilities and degradation in small coils is illustrated by fig. 16 in which experimental results of Iwasa and Montgomery (79) have been accounted for by Hancox (72) using calculations based on equ. (16). Clearly, if the full potential of hard superconductors was to be realised in coils, efforts had to be made to overcome degradation which appeared to be due to thermal instabilities. The seriousness of this effect, which can be gauged from the results in fig. 16, lead to continued fundamental analyses of the magnetic and thermal conditions in and around the superconductor, but until the results of such work became available and their implications understood, various expedients were adopted by the more pragmatic workers, most of which advocated using large quantities of copper in the magnets. This approach certainly advanced superconducting magnet technology and will be considered in more detail later (section 3.4).

Wipf and Lubell (77) investigated the dissipation caused in solid cylinders of cold-drawn Nb-25%Zr by induced supercurrents under nearly adiabatic conditions and obtained reasonable agreement for their predictions of the field at which the first flux jump

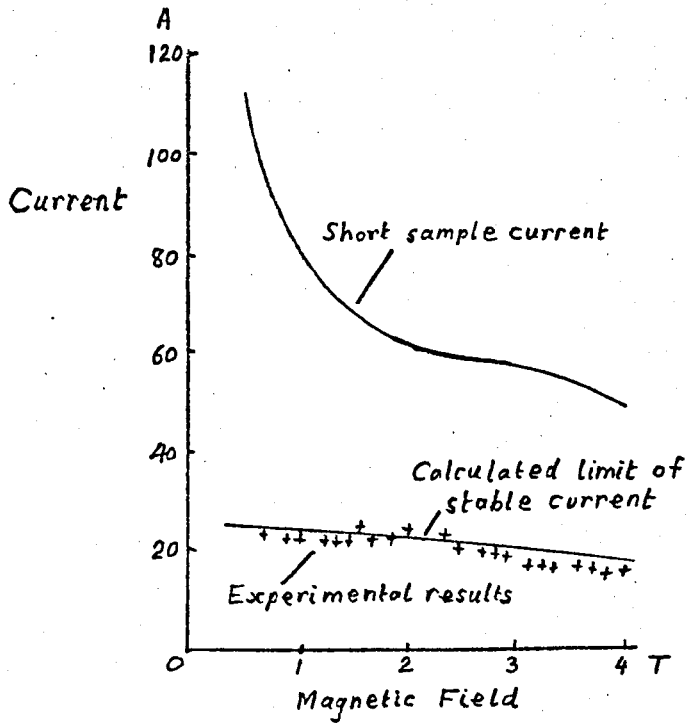


Fig. 16 Comparison of calculated degradation in a coil of 0.25 mm NbZr wire with the experimental results of Iwasa and Montgomery. (After Hancox)

occurred as a function of the time rate of increase of field, and also verification of the predicted temperature rise. Gauster and Ullmaier (80) confirmed these results and extended the calculations to solid and hollow cylinders, and claim their experiments on solid and hollow cylinders of NbZr and Nb₃Sn verify their calculations. Wipf (76) extended his previous work with Lubell, and pointed out that the limiting value of equ. 16 (or its variants), although giving the limit of stability approximately, does not in fact give the initial field at which a flux jump can take place. He identified a range of fields in which the flux lines are accelerated by Lorentz forces until thermal recovery restores the pinning forces and which he referred to as a limited instability. By using a simplified approach to the heat equation, he showed that the catastrophic stability limit or runaway could be predicted if the thermal diffusivity was known. He concentrated on non-adiabatic conditions when the magnetic diffusivity is less than the thermal diffusivity for full stability conditions, but the results for this and the other conditions cannot be expressed in any simple way and depend upon the exact nature of the magnetic disturbance that initiates an instability.

Yamafuji et al (82) derive criteria for the occurrence of flux jumps, both in the initial magnetization region and in the region of the thermal stability limit for which it is necessary to include the effects of viscous flux motion. In order to include explicitly in their theory the various quantities which are controllable experimentally and to make the solution of the thermal conduction equation tractable, they assume the temperature inside

the sample to be approximately uniform. This treatment does not permit the behaviour of flux diffusion during a flux jump to be discussed, but does enable criteria for the occurrence of flux jumps to be derived in terms of the external field and its sweeping rate. The results differ from those of Wipf (76) only by the effect of the thermal diffusivity terms and the different starting approximations.

The approximate agreement obtained by Swartz and Bean (73) with equ. (16) has already been noted. Neuringer and Shapira (83) compare their experimental results with this theory of Swartz and Bean and describe two of the salient features of the observed flux jumps; these are their repetitive occurrence at fixed intervals, and the decrease in their relative spacing when the temperature of the sample is lowered. The first of these corresponds to the conditions referred to by Wipf (76) as limited instability. Swartz and Bean develop their theory by introducing the concept of an adiabatic incremental susceptibility $d\Phi/dH$, where $d\Phi$ is the flux entering the specimen when the field is increased at the surface by dH ; they then assume that a thermal instability will result if $d\Phi/dH$ reaches infinity. They find (78) that if the external field exceeds some critical value H_{f_j} , (given by an expression similar to equ. (16)), then the isothermal critical state is not the only possible state of the superconductor, and show that the application of an infinitesimal field increment ΔH in a time short compared with the thermal diffusion time and long compared with the magnetic diffusion time can initiate an avalanching process that terminates in an adiabatic critical state. Thus they regard a flux jump as a switch

from the isothermal critical state to an adiabatic critical state in which immediately following such a jump the internal field, the induced supercurrent, and the temperature rise at each position are associated in a self-consistent way with the flux that has entered the superconductor. Fig. 17 illustrates the penetration of field in a superconductor characterised by a field-independent, bulk critical current density. The distribution due to H_s applied isothermally is given by the lowest curve. An incremental field, ΔH , also applied isothermally will cause the distribution to move to the middle curve, while the upper curve shows the further penetration if the increment in field occurs under approximate adiabatic conditions in a time short compared with that for heat diffusion.

Wipf and Lubell (77) established an alternative condition for instability at a temperature T_1 , which is followed by Swartz and Bean (78). They consider the energy dissipated in raising the field from zero to B_f , (equal to $B_f^2/8\pi$), and regard this as thermal energy which raises the temperature of the specimen from T_1 to T_u . Instability will occur if the upper critical field $H_{c2}(T_u)$ at the elevated temperature is less than the field B . Thus the conditions for instability are:

$$B_f^2(T_1)/8\pi \geq \int_{T_1}^{T_u} C(T)dT \quad (\text{c.g.s. units}) \quad (18)$$

$$\text{and } B_f(T_1) = H_{c2}(T_u) \quad (19)$$

Swartz and Bean (78) evaluate the limiting stability field for both conditions (i.e. those of equ.(16) or similar for H_{fj} , and equ.(18) for $H_f = B_f$), and their temperature dependence for the material Nb_3Sn ; the result is reproduced in fig. 18.

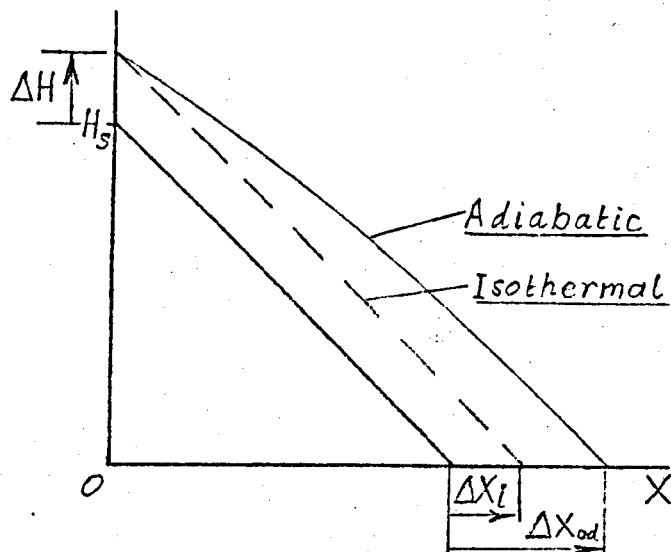


Fig. 17 Isothermal and adiabatic penetration of incremental field.

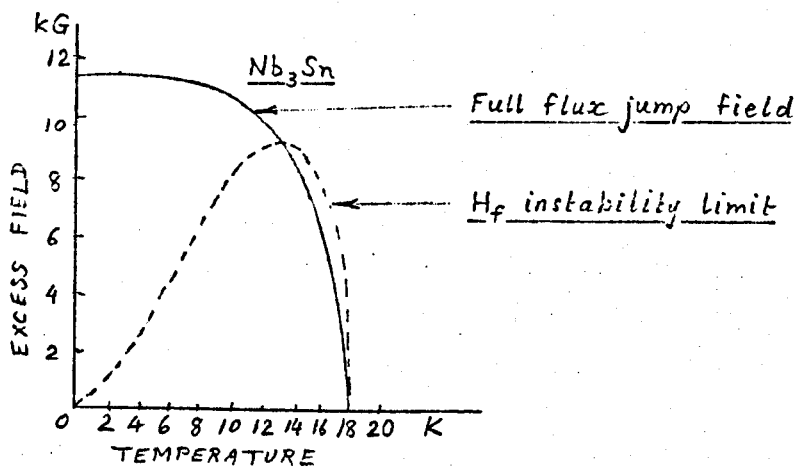


Fig. 18 Full flux jump and H_f instability limits.

3.4 Cryostatic Stabilisation.

It could be argued that historically, Kim and his fellow workers provided the first stable superconductor in 1964 by their discovery of the flux-flow phenomena because in their experimental results they demonstrate samples with a gradual transition into the resistive state (fig. 2 of reference 25). These results were achieved with low current densities and probably were dismissed from the practical point of view for this reason.

The first method to be adopted for practical magnets was due to Stekly and his fellow workers. The principle was discussed qualitatively by Kantrowitz and Stekly⁽⁸⁴⁾ and later analysed by Stekly and Zar⁽⁸⁵⁾ for the completely stable coil. The technique consists of bonding the superconductor to a normal conductor of high electrical conductivity, usually copper, and freely immersing it in liquid helium. It is sometimes referred to as cryostatic stabilisation and it operates on a simple principle: if a small section of the superconductor returns to the normal state, the transport current transfers to the copper. The heat generated in the copper is dissipated in the liquid helium bath, the dissipation being accompanied by a rise in temperature of the superconductor and copper composite. If the temperature of the composite including that of the superconductor is less than the critical temperature of the superconductor in the local ambient field strength, the current will return to the superconductor and ordinary superconducting operation will be resumed. The condition for the resumption of superconductivity in a short normal zone is that the heat generated per unit length is less than the heat trans-

ferred to the liquid helium, i.e.

$$\frac{I^2 \rho}{A} < h(T_{CH} - T_b)P \quad (20)$$

where I is the current,

ρ is the resistivity of copper or other cladding material,

A is the cross-section of the cladding material,

h is the heat-transfer coefficient,

T_{CH} is the critical temperature of the conductor in the relevant field,

T_b is the temperature of the helium bath, and

P is the wetted perimeter.

Closer examination of the stability condition given by equ. (20) shows that it is not as simple as it might appear at first sight, because it ignores certain important effects. The first is the nature of the heat transfer in boiling helium. At small temperature differences between the composite surface and the liquid, a regime of nucleate boiling exists with relatively good heat transfer taking advantage of the latent heat of vaporisation of the liquid. This persists up to a maximum value of thermal flux, or peak nucleate-boiling flux, Q_{pn} , above which an unstable regime exists with relatively lower heat transfer. With higher temperature differences complete film boiling occurs with stable conditions and relatively poor heat transfer rates. With decreasing thermal flux the process is not reversible and film boiling persists to the minimum film boiling flux, Q_{mf} , less than Q_{pn} , followed by an unstable regime and eventually the nucleate boiling regime. The precise values of heat transfer coefficient for different fluxes

and the values of Q_{pn} and Q_{mf} all depend on surface condition, orientation and the temperature of the helium bath, and therefore it will be seen that the value of h in equ. 20 must be chosen with considerable care. If I is chosen to be the critical current in the given field, I_{CH} , and h is chosen to correspond with the minimum film boiling transfer rate, then under these conditions, no matter how large the magnitude or duration of a thermal instability, superconductive operation will always be recovered for all currents up to I_{CH} . Such a composite is referred to as 'fully stabilised', or as Montgomery ⁽⁸⁶⁾ more pedantically described it, 'fully stable at the critical current'.

Other factors ignored by the Stekly criterion are any thermal or electrical resistance at the superconductor and substrate interface, any temperature gradient across the superconductor itself or across the substrate, or any thermal, magnetic or electrical transients which may occur. It assumes that all the current flows in the substrate and makes no allowance for any current still flowing in the superconductor, nor is any account taken of the temperature dependency of the normal-region resistivity. It also does not include heating due to other sources such as that due to eddy currents in the substrate.

Any composite will behave stably, however, at some level of current below its full critical value ⁽⁸⁷⁾, ⁽⁸⁸⁾. Composites designed to be used at currents less than the full critical value are referred to as 'partially stable', or preferably 'stable at partial currents'. If a current higher than the current at which the composite is fully stable is flowing and a flux jump or other

instability occurs, the normal zone will propagate down the wire. The current at which this just takes place is called the 'minimum propagating current' (87).

Several authors have presented analyses giving criteria for the minimum propagating current. Keilin, Klimenko et al (90), Williams (91), Stekly (92) (93), and Kremlev (94) use an idealisation of the heat transfer characteristic, and ignore the temperature gradient across the superconductor itself and any thermal barrier at the superconductor and cladding material interface. Tests results (e.g. those of Gauster (95, 97)) show only qualitative agreement with these theories. Other workers approached the analysis of steady-state stability by concentrating on the nucleate boiling regime (96), (97), (98), (99) and using experimentally determined data relating to the heat transfer. Kremlev et al (100) indicate the importance of the complete heat transfer characteristic, and Gauster, Efferson et al postulate an ideal composite with an electrical interconducting layer between the superconductor and the normal substrate (101) to which they apply the basic equations of ref. 85; these they extend to include flux-flow resistance of the superconductor and the non-linear heat transfer to the helium bath, but correlation of their theory with experimental results is poor.

An alternative theory for the stability conditions in a composite conductor has been propounded by El Eindari (102) which he bases on the flux flow resistance of the superconductor (24), and which allows current sharing between the substrate and the superconductor. This current sharing condition is implicit in the basic

theory of Stekly (85) leading to the stability condition of equ.(20), but is rarely explicitly mentioned. Without current sharing the current would switch suddenly from the superconductor to the substrate, and back again on return to the superconducting condition without the smooth transition which is known to occur in practice. The criterion for stability of a bare superconductor is presented in terms of a parameter involving only the constants of the superconductor and the heat transfer coefficient of the cooling medium. Evaluation of the latter parameter, of course, presents the same difficulty as for the Stekly criterion. El Bindari extends the theory to include the propagation of a resistive region and the influence of a substrate, and for a composite deduces a stability criterion similar to that of Stekly but not quite as severe. Data supporting this theory are presented by El Bindari and Bernert (103), who point out in their conclusions that 'the superconductor itself is the element to stable superconducting performance and that the substrate has a minor but important role, acting as a packaging material, and increasing the stability by increasing the cooled perimeter.' To describe the substrate as packaging material seems to be overstating the case, and ignores any damping effect it may have under transient conditions of flux movement. Since an initial assumption was that of good thermal conductivity for the substrate with negligible temperature gradient across it, it is not surprising that one conclusion is that the electrical properties of the substrate are relatively unimportant compared with its thermal properties. The model does not include the situation where external flux movement occurs, and so it is also not surprising that the

theory does not show the beneficial effects of the substrate which can accrue under these conditions. It should however be possible to extend the theory to include external flux changes and the resulting inductive voltages appearing both in the substrate and superconductor, and by this means demonstrate the damping effect of the substrate. One important aspect brought out by this work is the effect of superconductor size on stability, and that the stability of type II superconductors improves very rapidly as the diameter of individual strands is reduced.

In order to avoid the difficulty of an analytical representation of the non-linear heat transfer characteristic to boiling helium, Maddock, James and Norris (104) present a simple but comprehensive graphical scheme which shows the relevance of the various parts of the total heat transfer characteristic and which can be made to yield quantitative results. They use it to obtain in a simpler way the stability criteria already obtained by previous workers such as Stekly (93), Kremlev (94) and Gauster and Hendricks (97, 98) assuming a linear characteristic; they also use it to show the effect of surface coatings, the effect of superconductor thickness and for the construction of current-voltage relations for superconductive composites. The basis of the method is to use temperature as a variable which allows the cooling processes to be separated from the heat generation terms. Heat loss and heat generation are plotted separately as functions of superconductor surface temperature to obtain the conditions for thermal equilibrium. They show that if there are two equilibrium states, (e.g. one film boiling and one nucleate boiling), then a change from one

to the other can take place by the movement of the transition region between them along the conductor. The current for which this occurs they term the cold-end recovery current. Under certain conditions, this is the same as the minimum propagating current, but when the conditions are not applicable, the value of the latter needs closer examination and may in fact be lower than that obtained by assuming a linear heat transfer characteristic. Maddock et al also examine the effects of surface coatings and explain the surprising effect reported by Gauster and Hendricks (97), Jackson and Fruin (105), and Butler et al (106) that a surface coating of poor thermal conductivity on a composite can raise the minimum propagating current. This is of considerable practical importance in solenoids as an increase in overall current density of about 50% is suggested as being feasible. The effect of superconductor thickness is also examined, and they show that if the superconductor is moderately thick its poor thermal conductivity can lead to significant temperature gradients within it; they suggest that the stability of strands as thin as 0.25 mm diameter can be adversely affected because of this, especially if the ratio of substrate to superconductor is low.

Many successful magnet coils have been built using fully stabilised superconducting composites, but this has involved a ratio of copper area/superconductor area larger than unity, and space for adequate liquid helium circulation for high heat transfer in the event of all the current being carried by the copper. One of the first coils to use cryostatic stabilisation quoted by El Eindari (107) used 9 wires of NbZr in an OFHC copper strip with a

copper/superconductor ratio of 28:1. The rectangular section, heavy current, INI/CERL, NbTi and copper composite conductor had a copper/superconductor ratio of 8.2:1 when used in a 4.8T, 100 mm bore magnet (108). The performance of a smaller composite with 10 strands each 0.050" diameter in a copper matrix 1.9mm by 0.6 mm (giving a copper/superconductor ratio of 5.7:1) is shown in figs. 19 and 20 (after ref. 108). From these figures it will be seen that when the critical current I_c is exceeded, the excess current is carried by the copper. A further increase in current causes a slight rise in temperature due to ohmic heating which causes a slight reduction in I_c . The excess current is carried by the copper until the transition from nucleate to film boiling occurs. The temperature of the composite then exceeds the critical temperature of the superconductor and all the current is carried by the copper. On reduction of the current, it remains in the copper until the heat transfer falls below that necessary to maintain film boiling, when there is a transfer of current back to the superconductor. The current at which this occurs is the recovery current, I_r . In fig. 20a, I_c is greater than I_r which means that the composite in this field is unstable according to the Stekly criterion, whereas in fig. 20b, I_c is less than I_r and the composite is stable for all currents up to I_c . The transition from film to nucleate boiling took place with heat fluxes in the range 0.35 to 0.40 watts/cm², a value in general agreement with those quoted by Whetstone and Boom (96) and Brechna (109).

An obvious consequence of using copper for stabilisation and allowing channels for the passage of liquid helium in a winding is

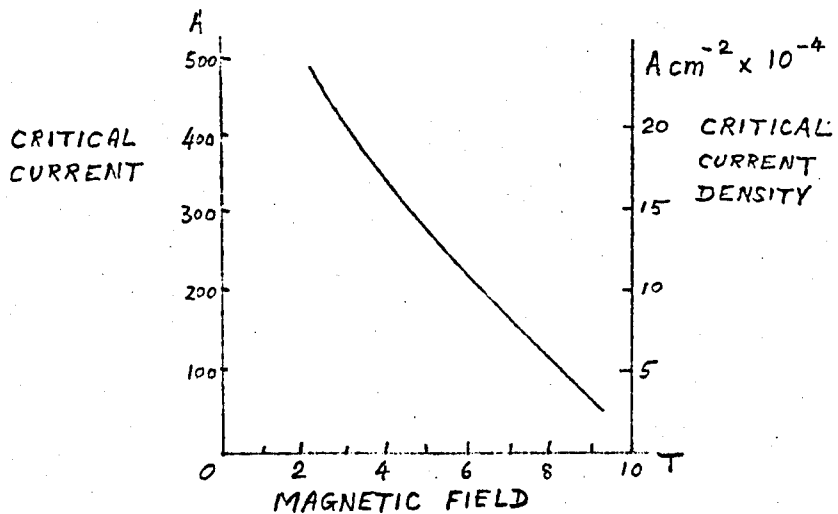


Fig. 19 Critical current of 10-strand composite.

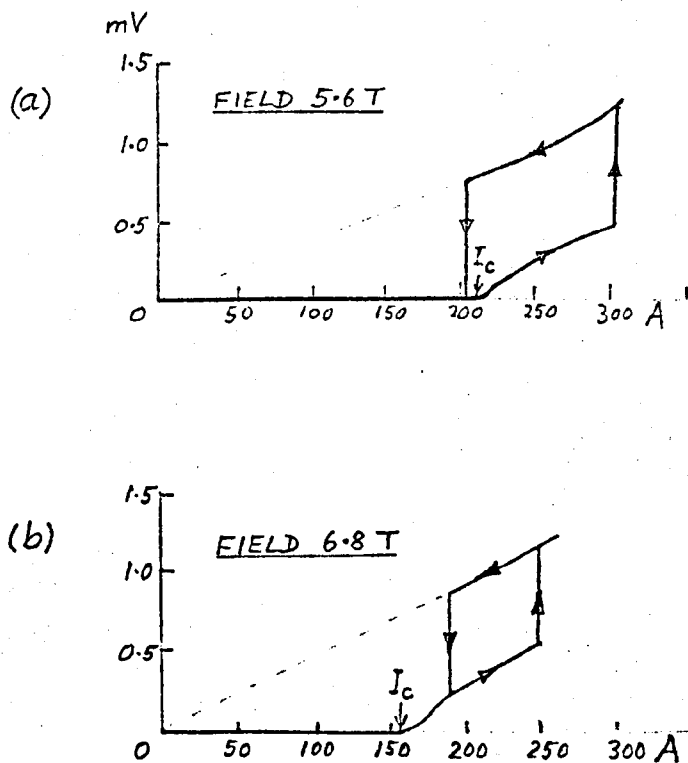


Fig. 20 Current-voltage characteristics of 10-strand composite.

that the overall current density is very much below that in the superconductor itself. Laverick (110) in 1966 reported that large stable magnets have operated at an average overall current density of 5 kA/cm^2 , and other partially stable magnets at 9 kA/cm^2 . Brechna in reviewing recent developments in the design of superconducting magnets in 1968 (109) considers that in small coils with transverse fields at the conductor of 6T, mean current densities in the composite of 50 kA/cm^2 are readily achievable, but in large coils they seldom exceed 15 kA/cm^2 ; to obtain corresponding overall current densities in the coils, allowance must be made for insulation and the helium cooling spaces, which would reduce Brechna's figure for large coils to a value in the region of that given by Laverick. Overall current densities ranging from 1 to 10 kA/cm^2 with an average of 5 kA/cm^2 for large d.c. coils were reported at the European Study Conference in 1968 (111).

Although for very large coils, full stabilisation may be considered necessary on the grounds of safety, coils designed for a lower minimum propagating current are one means of achieving a higher current density, which would reduce the size of the coils, improve the economics and enable the requirements in some applications for high field gradients to be met. Carruthers et al have considered this approach (112) and show that with normal conductor stabilization it is difficult to achieve an overall current density of much more than 15 kA/cm^2 , a value which is only slightly dependent on the current density in the superconductor.

Williams has suggested two approaches to achieving higher

overall current densities in cryostatically stabilised coils. The first (113) is to sectionalise the superconducting winding and then supply each section with a current corresponding to its local field conditions so that it gives an increased field contribution over that of a single undivided winding. This method can be used in conjunction with other methods of stabilisation, as e.g. by Montgomery and Rinderer (114). The other approach (87, 91) suggested by Williams is the use of a superconductor of high intrinsic current density stabilised at less than the short sample current, the higher overall current density being achieved at the expense of the full stabilised current. This involves reducing the ratio of copper to superconductor in the composite and operating at a relatively low value of minimum propagating current. Thus the overall diameter of the single core composite is reduced giving an increased surface-to-volume ratio but allowing more such composite to be accommodated in a given cross-sectional area of coil. Although the current carried by a single turn in the coil formed by the composite is lower, the overall current density is higher giving an improvement in field produced, or a reduction in coil size for a given duty. However, more superconductor material is used resulting in an increase of cost for a given duty. It is probably for this reason, and also the development of other stabilisation techniques, that this method of increasing current density does not appear to have been proceeded with.

Another approach to improve the current density in cryostatically stabilised coils was to endeavour to utilise the higher heat fluxes achievable below the λ -point of liquid helium. Since

the minimum propagating current of a composite in liquid helium should be equal to the current which just causes film boiling when the composite is in the normal state, any factor which increases the heat transfer rate needed to cause film boiling, should also raise the minimum propagating current and thus allow higher current densities to be used. That the minimum propagating current in a NbTi copper-clad composite increased by a factor of over 2 as the temperature was reduced from 5K to 1.8K was demonstrated by Hancox (115), but any development of this approach did not materialise because of alternative methods of stabilisation which became available, and the complication introduced by the temperature control.

Further effort to increase current densities in coils based on minimum propagating criteria and experience with such coils showed that at least in small laboratory scale magnets, such criteria were very often too conservative and lead to coils with a performance superior to that which was predicted (e.g. a high current density 9 kJ magnet reported by Montgomery and Rinderer (114)). It was thought that since propagation or recovery of a normal region in a coil is basically a transient phenomenon, this might give rise to a 'transient stability' and that it might be possible to operate coils predictably at some transient stabilised current determined by transient heat transfer conditions. This led to investigations on the transient thermal behaviour of superconductor composites under various conditions of thermal environment by Williams (91), Hale and Williams (116), Stevenson (117) and Iwasa et al (118) based on various models and sometimes using computer simulations.

Experimental work to obtain heat transfer data under transient conditions was undertaken by Smith et al (119), Iwasa and Montgomery (120) and Jackson (121). Among the conclusions drawn from this work was that interleaving the turns in a coil by materials with a high specific heat and large thermal conductivity would provide the most effective transient stabilisation. The thermal capacity of the interleaving material with its high thermal conductivity would absorb the heat associated with a small transient instability and thus prevent a significant rise in temperature. The heat must, ultimately, of course, be transferred to the liquid helium coolant. The results of this work were not generally adopted, because other contemporaneous studies lead to the concept of enthalpy stabilisation. Transient stabilisation can thus be regarded as the precursor of enthalpy stabilisation which will be discussed in the next section as an aspect of dynamic stabilisation.

3.5 Dynamic Stabilisation.

The principle of dynamic stabilisation is based on surrounding the superconductor with sufficient material of high electrical and thermal conductivities in order to control the rate of movement of flux in the superconductor and the rate at which the surface field can change, so that the resulting rate of heat generation is less than the rate at which it can be diffused through the composite so formed. In cryostatic stabilisation the technique is to obviate the consequences of a magnetothermal instability occasioning a flux jump by preventing the process of quenching which would otherwise follow a flux jump; in dynamic stabilisation the technique is to

prevent the occurrence of a flux jump in the first place. Both involve cladding the superconductor with a material of high electrical and thermal conductivity, and so in cryostatic stabilisation, additional stability is provided by the magnetic damping due to the presence of the cladding.

Chester (122) has developed a criterion for dynamic stabilisation in the case of a multilayer composite of sheets of copper each of thickness X alternating with sheets of superconductor of thickness x , the outermost layer being of copper. For a field applied parallel to the sheets, he imagines the field to suddenly increase by an amount ΔH_0 . Considering the effect on the first superconducting sheet, which will experience the greatest dissipation, the maximum rate of dissipation, Q , is given approximately by $J_c x \Delta H_0 D_m / 2X$. The magnetic diffusivity, D_m , is given by ρ/μ where ρ is the resistivity and μ the permeability of the medium, in this case copper. Since the thermal diffusivity of copper is extremely high, the rise in temperature of the superconductor above that of the copper will be of the order $Qx/(2CD_{th})$. The thermal diffusivity, D_{th} , of the superconductor is equal to k/C where k is its thermal conductivity. If the temperature of the superconductor is not to run away from that of the copper, the following condition must apply, assuming that $X/x \gg 1$:

$$H_s \leq \frac{1}{x} \cdot \frac{4X}{x} \frac{D_{th}}{D_m} \frac{C}{(\partial J_c / \partial T)} \quad (\text{c.g.s. units}) \quad (21)$$

Chester compares this with equ. (16) for adiabatic conditions and deduces that for $X/x = 6$, there is a gain as soon as x falls below approximately 0.1 mm., and H_s increases by a factor of 10 by using

sheets of superconductor 0.01 mm thick. For the case of sheets normal to the field, Chester develops a criterion for stability of the superconductor with respect to the copper, which is that:

$$x \leq \left\{ \frac{(X + x)D_{th}C}{xD_m T_o \pi} \right\}^{1/2} \quad (\text{c.g.s. units}) \quad (22)$$

This results in $x \leq 0.1$ mm for $X/x = 3$. For wires, he suggests that strands smaller than 0.05 mm diameter will be dynamically stable.

Dynamic stabilisation obviously requires excellent thermal and electrical contact between the superconductor and substrate and should have enabled higher overall current densities to be achieved in coils than with cryostatic stabilisation. However, with the development of other forms of stabilisation, dynamic stabilisation utilising thin superconductors was not used in any magnets as far as is known.

One of these developments was a form of dynamic stabilisation referred to as enthalpy stabilisation. It has already been noted that Hancox (72) has shown that the condition for a flux jump to be initiated in a semi-infinite slab of superconductor is $H_s = \sqrt{8\pi CT_o}$, or $JD = \sqrt{3CT_o/4\pi}$ approximately for a coil (eqs. (16) and (17)). If conditions are such that the thermal diffusivity is much greater than the magnetic diffusivity, then the adiabatic assumption on which these equations are based is not valid, so although a flux jump may be initiated, it may not necessarily be completed. Further, at temperatures in the region of 4K, specific heats vary very rapidly with temperature, and it may be possible

for C to increase in the course of a flux jump so that the condition for unstable behaviour (eqs. 16 or 17) is no longer satisfied. At about this point the flux jump will stop without quenching the superconductor, a process sometimes referred to as partial flux jumping. Hancox realised the practical significance of this and pointed out that partial flux jumps can occur in a magnet without quenching the transport current (72), (123). The condition for this to happen with a transition from an unstable to a stable state in a semi-infinite slab of superconductor is:

$$H_f^2 \leq 8\pi \int_T^{T_c} C dT \quad (\text{c.g.s. units}) \quad (23)$$

and corresponds to equ. (18). For a conductor of thickness D , the criterion developed by Hancox for a stable, partial flux jump under conditions in which both the external magnetic field and transport current increase is:

$$\pi D^2 \left\{ J_c^2 - J^2 + 6J^2 \ln (J_c/J) \right\} \leq 6 \int_{T_1}^{T_2} C dT \quad (\text{c.g.s. units}) \quad (24)$$

J_c is the current density which would just support the current if it flowed uniformly in the conductor; since the Bean model is assumed, this corresponds to the critical current density. T_1 and T_2 are the temperatures before and after the flux jump, and J is the average transport current density. An underlying assumption is that the thermal diffusivity across the conductor is greater than the magnetic diffusivity, so that both the temperature and the field gradient will be uniform.

Thus there are three requirements, not necessarily independent,

for enthalpy stabilisation. The first is that the superconductor size must be small enough and if necessary subdivided so that equ. (24) is complied with, and also to ensure that the energy dissipated by flux motion within the superconductor, which has a poor thermal conductivity, is averaged over the cross-section of the composite. If the diameter of the superconductor is reduced sufficiently, it becomes intrinsically stable. The second requirement is that the enthalpy of the composite conductor must be sufficient to fulfil equ. (24) throughout the relevant range of magnetic field. If with the combination of superconductor size used the enthalpy of the composite is inadequate, it can be artificially increased by adding a material of high specific heat on the outside of the composite; suitable materials would be lead, cadmium or mercury. The third requirement is to ensure that the thermal and magnetic diffusivities of the environment immediately surrounding the superconductor are suitable, and for this copper is a very appropriate material with its very high thermal and electrical conductivities.

Hancox (123) cites a composite with eighteen strands of 0.08 mm diameter niobium-titanium in a copper matrix with a copper to superconductor ratio of 1.5:1, and indicates that but for manufacturing difficulties at that time (1968), this ratio could be smaller. The copper is then electroplated with lead, and in a 3T magnet, he claims that overall current densities up to 34 kA/cm^2 are possible; values up to 100 kA/cm^2 have been suggested as feasible elsewhere (112). Magnets using enthalpy stabilisation are only partially stable, since they may be quenched by large externally

applied disturbances, but are stable against internal transients. Since no part of the winding is driven into the normal state, a high minimum propagating current is not necessary, and liquid helium cooling throughout the whole of the winding is not required. The winding can be impregnated in a suitable resin for mechanical strength and may be operated equally successfully in liquid or gaseous helium.

3.6 Adiabatic Stabilisation.

Various versions of the criterion for stability under adiabatic conditions have already been discussed. They are of the form of equ. (16), i.e. $H_S \leq \sqrt{8\pi CT_0}$, where $T_0 = J_c \frac{\partial T}{\partial J_c}$. Improvements in adiabatic stability could be thus expected from increasing C, by incorporating in the composite a material of high thermal capacity such as lead. This has already been considered in the case of enthalpy stabilisation where it is arranged that adiabatic conditions do not apply; if however the copper cladding is omitted from the composite, the thermal diffusivity will no longer be greater than the magnetic, and in order to achieve the same degree of stabilisation, much smaller sub-division of the superconductor would be required.

Reducing J_c would improve the stability under adiabatic conditions, but is unattractive from the magnet design viewpoint because of the resultant lower overall current density, although it provides an explanation for the improved stability of superconducting coils when immersed in a higher magnet field. $\partial T/\partial J_c$ has already been discussed and discarded as not being practical with present magnet materials. Improvements resulting from

metallurgical means are outside the scope of this study, but have been considered by a number of workers, e.g. by Vetrano and Boom (124), and Lange and Verges (125).

The remaining possibility to improve the stability is to reduce the thickness of the superconductor, since from equ. (17), the criterion for stability in a thin sheet of superconductor is $D \leq \sqrt{3CT_0/4\pi J_c}$. This gives typical values for NbTi below which flux jumping should not occur of about 0.08 mm for a critical current density of 300 kA/cm². Considerable analytical and experimental effort (124) has been expended on this approach which has been very successful in achieving improvements in superconducting coils enabling higher current densities to be used, and making the coil less sensitive to rapid changes in external fields and transport currents. Some difficulties are encountered in the use of composites with very fine superconducting wires, referred to as intrinsically stable or filamentary superconductors, and in view of their importance in superconducting magnet technology, will be discussed in detail in the next chapter.

3.7 Mechanical Strain and Vibration.

Beside rise in temperature above T_c , increase of external magnetic field above H_{c2} (or H_{c3}), and increase in transport current above I_c , type II superconductors are found experimentally to become normal under conditions of mechanical strain and vibration. Since these will be present in a rotating machine to some extent even in a very carefully mechanically balanced machine, it is necessary to consider the likely effects on a superconducting

coil of the presence of mechanical strain and vibration.

Mechanical strain is more of a problem with the brittle superconducting materials, such as Nb_3Sn , than with the more ductile Nb-Ti. In the former, mechanical strains can easily lead to fracture of the superconducting wire, which means complete failure of the magnet. Even in ductile materials distortions of the wire, introducing inhomogeneities in crystal structure, changes in grain size, etc., can locally modify its current carrying properties and critical fields. This may be advantageous in some cases, in that flux pinning ability may be enhanced, but this is not necessarily so.

A number of observers have found that the stability of filamentary superconducting coils may be improved if they are impregnated with various substances, such as paraffin wax, or epoxy resins (Araldite). It is thought that the chief function of such impregnation is to immobilise the coil windings. Mechanical vibration and shock, thermal contraction and expansion, and movement due to interaction of large magnetic fields and high current, all contribute to displacement of the windings. Apart from the strains induced, the positions of the current carrying wires with respect to the local magnetic field are related to the Lorentz forces acting on the lattice in the superconductors, which in turn influences the critical current.

From our own tests on small coils, it has been found that different impregnating substances have different effects, and those giving the greatest rigidity (epoxy resins) are not necessarily the best. This may be because of strains introduced by

differential thermal contractions of wire and resin. Coils impregnated with resin have been made to perform satisfactorily, but impregnation cannot necessarily be relied on as a means of improving coil stability. The impregnated coils all showed a training effect, but this was much more marked with the epoxy resins, than with the low yield fillers such as paraffin wax, ice and oil. Although for laboratory testing, such fillers may serve a useful purpose, they can hardly be regarded as suitable for regular industrial applications, and more work needs to be done with impregnating materials which are solid at room temperatures. Materials which should be investigated are epoxy resins with flexible additions, and resins with a coefficient of expansion matching that of the superconducting composite. At least one commercial organisation seems to have mastered the impregnation of superconducting coils, but is not prepared to divulge the materials used.

3.8 Rapid Changes in Field and Current.

It will be seen from Sections 3.2 and 3.3 that changes in current or in field involve energy dissipation in the superconductor, the subsequent temperature rise depending on the thermal environment of the composite. Thus rapid changes in either the magnetic field or the transport current can induce normalization at quite low levels of field and current, compared with static (slow change) tests. This property is particularly important when one is considering the use of superconductors in rotating electrical machines, because in such a system rapid changes may occur.

Reduction of Lorentz forces by the manner of winding the coil may assist in reducing the sensitivity of the superconducting wire to \dot{H} and \dot{I} . As described earlier, fluxoids may be regarded as supercurrent vortices around lines of magnetic flux penetrating the superconductor. Now consider such a vortex, centre B with peripheral velocity V_R , in the path of a transport current, velocity V_T , shown in Fig. 21, V_T being normal to the generators of the vortex cylinder. At A, the resultant velocity $V_1 = V_T + V_R$ and at C, the resultant velocity, $V_2 = V_T - V_R$.

Particles travelling along a curved path are subject to a centrifugal force normal to that path, i.e. the force exerted on a particle at A

$$F_1 = \frac{MV_1^2}{r} = \frac{M}{r} (V_T + V_R)^2$$

in the direction \vec{BA} , where r is the radius of the vortex.

At C the force exerted on a particle is:

$$F_2 = \frac{MV_2^2}{r} = \frac{M}{r} (V_T - V_R)^2 \text{ in the direction } \vec{BC}.$$

The resultant force on the whole vortex is then, to a first approximation:-

$$F_L = F_1 - F_2 = \frac{4M}{r} V_T V_R \quad (25)$$

This is effectively the Lorentz force. Now consider the case when the streamline flow is not normal to the vortex cylinder, as illustrated in Fig. 22.

The transport current may now be separated into two components

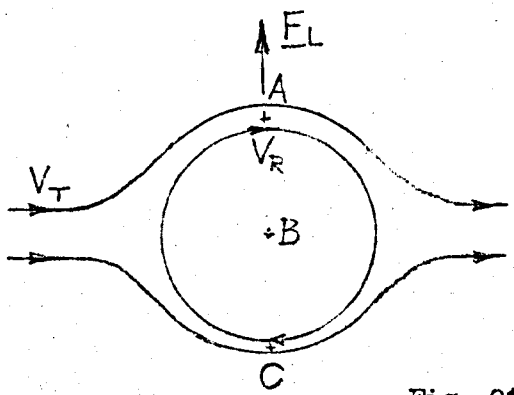


Fig. 21

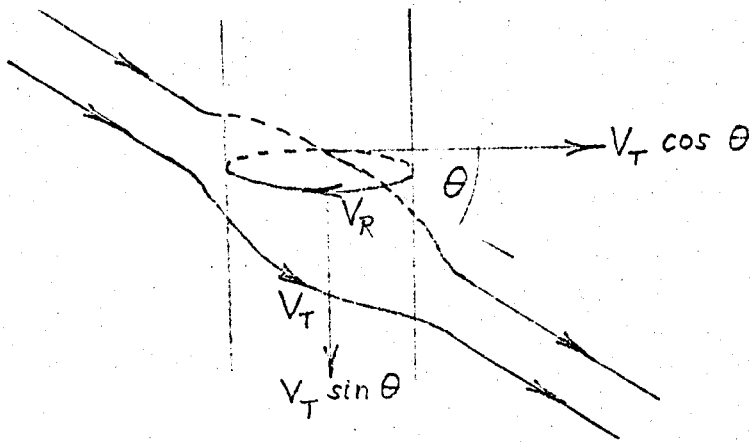
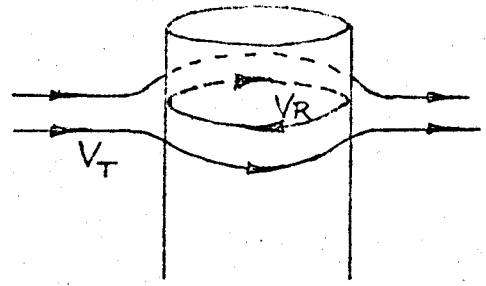


Fig. 22

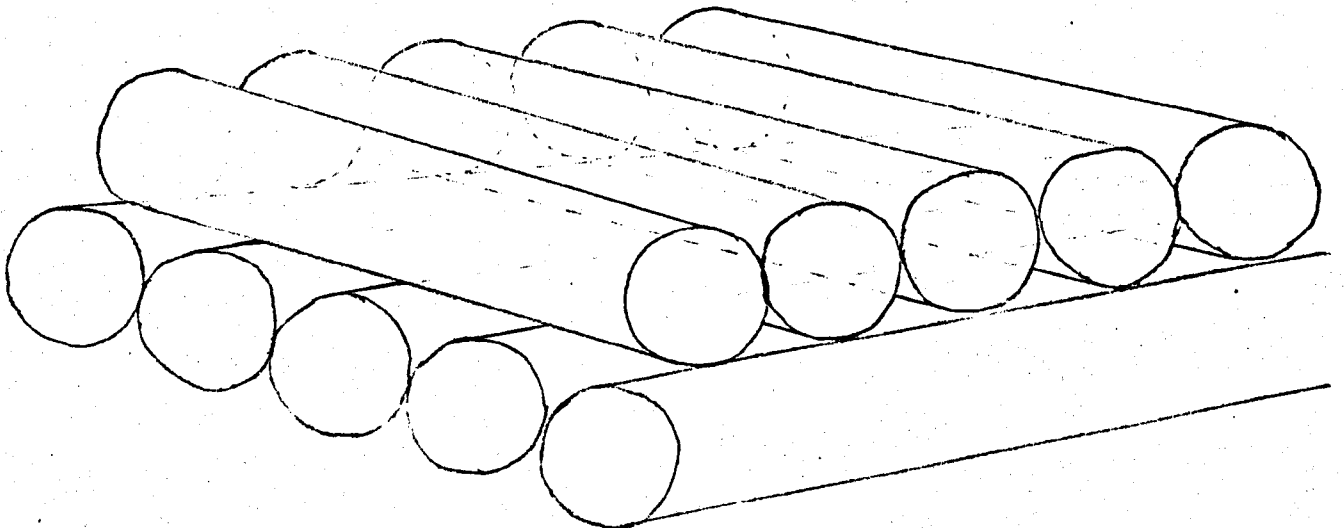


Fig. 23

with respect to the vortex. Then we have, in a direction normal to the vortex cylinder:-

$$F_{L_1} = \frac{4M}{r} V_T V_R \cos \theta \quad (26)$$

This is a minimum when $\cos \theta = 0$ i.e. when $\theta = \pi/2$, or when the transport current flow is parallel to the lines of magnetic flux. This is supported by the observations of, for example, Sekula et al (126), Heaton and Rose Innes (127) and Sugahara (128), which showed that in a longitudinal magnetic field, i.e. one parallel to the direction of current flow, the size of the transport current tolerated by the superconductor was greater than the critical current in a transverse magnetisation.

It is easy to apply a longitudinal field to a short sample of superconductor, but when the superconductor is to be the winding of the solenoid providing the magnetic field this parallelism of field and current is more difficult to arrange. It is possible that a "honeycomb" winding might approach this condition. This is a method of winding used in some early R.F. coils, and consists of winding consecutive layers of the coil so that the turns cross each other at 90° , as illustrated in fig. 23. Sekula et al (126) refer to their one-layer toroid of NbZr wire wound so that the current flow was at 45° to the radial vector as a "force-free" arrangement. The honeycomb winding of a solenoid might be a close approximation to a "force free" configuration. However, the experiment of Sekula et al does not seem to have been very successful, and the reasons for the lack of success are unclear. It may be related to the toroidal geometry of the coil. In a

honeycomb-wound coil (see Fig. 23) although the resultant magnetic field in the core of the solenoid is one parallel to the axis, within the windings each layer of turns provides a magnetic field at the adjacent layer which is parallel to the wire, and hence to the current because consecutive layers are set at right angles to each other. In a multilayer solenoid, of course, this simple picture is not really valid, but even without detailed calculations it can be seen that the layers in the depth of the windings will be acted on by virtually zero field and the other layers by fields increasing in strength towards the surface layers, but still at angles of less than 90° to the current direction. Theoretically it should be possible to calculate exactly the angle at which each layer should be set to obtain minimum values of $\underline{J} \times \underline{H}$ in all parts of the windings, thus giving the minimum value of the Lorentz forces.

Experimental work needs to be done to test this. In the first instance the effects of longitudinal and transverse fields should be compared when H and/or I are changed rapidly. Changes in H and I can be both of the transient and alternating types. If it is shown that sensitivity to \dot{H} and \dot{I} is less when H is parallel to I , experiments could proceed with stability tests on "force-free" coils. If it is found that changes in H and I induce normalisation even in a longitudinal field another approach would need to be tried. The above experiments should in the first place be performed on simple solid superconducting wire, not the filamentary form or wire protected with copper sheathing. Studies of \dot{H} -, \dot{I} - induced instabilities in the "raw" superconductor will show to what extent such instabilities are a property of the microstructure of the material.

Whether or not coils wound in this manner, even if they gave improved performance with rapid field and current changes, would be attractive for use in electrical machines is debatable, because they would result in lower current densities than in conventionally wound coils. In situations where for operational reasons or protection rapid changes might be desirable, a sacrifice of current density might be acceptable if the rates of change achievable merited it.

4. Filamentary Superconductors.

4.1 Fine Filaments.

Many of the superconducting magnets now made are wound with composite conductors comprising a large number of fine superconducting filaments embedded in a copper matrix. These multifilament composites and variations of them will now be discussed.

From the discussion of adiabatic stability in Section 3.6, it was seen that greater stability should result as the superconductor diameter is reduced. A similar deduction arose from a consideration of enthalpy stabilisation, but in this case, larger diameters can be tolerated than for the adiabatic case. In considering the acceptable diameter for filamentary superconductors, adiabatic conditions should be assumed even though there will be some heat loss. This will give pessimistic predictions, but by the same token, will increase the margin of stability achieved.

Besides enabling intrinsic stability to be achieved, filamentary superconductors also enable a higher value of critical field to be achieved. Lynton ⁽¹²⁹⁾ shows that when one of the dimensions of a superconducting specimen becomes comparable to the penetration depth, its critical magnetic field becomes much higher than that of a bulk sample of the same material at the same temperature. This follows from the basic Gorter-Casimir thermodynamic description, according to which the free energy difference per unit volume between the normal and superconducting states is:

$$g_n(o) - g_s(o) = \frac{1}{2} \mu_o H_c^2 \quad (27)$$

In an external field H_e a superconductor acquires an effective magnetisation $M(H_e)$ and becomes normal when:

$$\int_0^{H_e} M(H_e) dH_e = -\frac{1}{2} \mu_0 H_c^2 \quad (28)$$

The integral is the area under the magnetisation curve, and for any ellipsoidal specimens is satisfied when $H_e = H_c$. Actually this is true only when the penetration of the external field into the sample is neglected. Flux penetration into the sample lowers the effective magnetization and its susceptibility. The susceptibility determines the initial slope of the magnetization curve, and a lower value of susceptibility χ means that the curve has to go to a higher value of critical field in order to satisfy equ. (28). Assuming this curve remains linear with slope χ right up to a critical field H_s , then

$$\frac{H_s^2}{H_c^2} = \frac{\chi_0}{\chi}$$

where χ_0 is the susceptibility of an identical sample from which the field is entirely excluded. If λ_0 is the appropriate Pippard value for the penetration depth, and $2a$ is the sample thickness, then:

$$\text{for } a \gg \lambda_0, \quad H_s/H_c = 1 + \lambda_0/2a$$

$$\text{and for } a \ll \lambda_0, \quad H_s/H_c = \sqrt{3}\lambda_0/a.$$

Similar expressions can be derived for cylindrical and spherical samples. The resulting equations agree well with the frequently observed enhancement of the critical field in small specimens when

the appropriate Pippard value is used for the penetration depth.

Lynton (129) also shows that the field enhancement calculated from the Ginzburg-Landau theory leads to nearly identical results, the essential difference being that because of additional terms in the Ginzburg-Landau free energy expression, the penetration depth increases in the presence of an external field so that the critical field for small samples becomes even higher.

Mathematically, the raising of the critical field by decreasing the size of specimen can be expressed as follows. If $B = \mu_0 H + M$ can be written,

$$M = B - \mu_0 H = -(\mu_0 H - B)$$

and as before $\int_0^{H_c} M(H) dH = -\frac{1}{2} \mu_0 H_c^2$.

If $B \neq 0$ and $B \leq \mu_0 H$ throughout the specimen, (i.e. the specimen is not completely penetrated by magnetic flux) then

$$\int_0^{H_c} M dH = -\int_0^{H_{ci}} (\mu_0 H - B(H)) dH$$

Let $B(H) = f \mu_0 H$, $f < 1$ so that

$$\begin{aligned} \int_0^{H_c} M dH &= -\int_0^{H_{ci}} (\mu_0 H - f \mu_0 H) dH \\ &= \frac{1}{2} \mu_0 (1 - f) H_{ci}^2 \end{aligned} \quad (29)$$

This implies that complete normality will not be achieved in the specimen until $H = H_{ci}$ and $(1-f)H_{ci}^2 = H_c^2$, i.e. until

$$H_{ci} = H_c / \sqrt{1-f} \quad (30)$$

Now $(1-f) \leq 1$ (since $f \leq 1$), and since $H_{ci}/H_c = (1/(1-f))^{1/2}$, we have

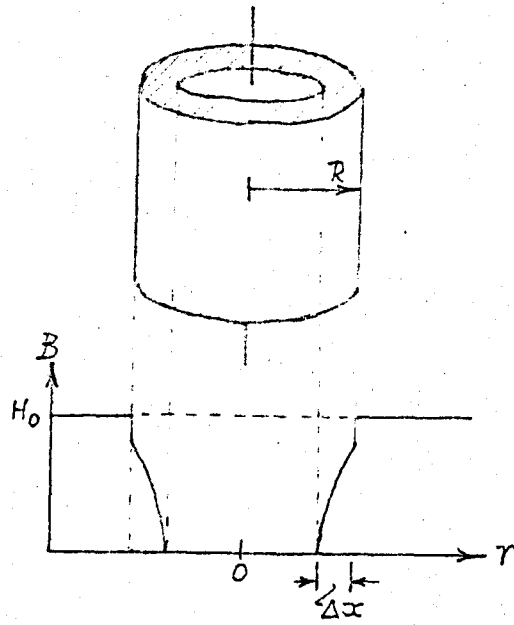


Fig. 24 Flux penetration in superconducting cylinder.

$$H_{ci} \geq H_c.$$

The meaning of the parameter f can be seen from a consideration of the Kim experiments on hollow cylinders of type II material (19) and the various versions of the critical state model described in Sections 2.6 and 2.7, also De Gennes (130), which indicate that magnetic flux penetrates a hard superconductor as shown in fig. 24.

If $\Delta x \gg R$ the flux density is nearly uniform in the sample, but if $\Delta x < R$, an estimate for f can be obtained in the following manner. If the magnetic field penetrates a cylindrical superconductor of radius R to a depth $\Delta x = \lambda$, as illustrated, the effective field inside, H_i , to a first approximation is:

$$H_i = fH_e$$

where H_e is the external field.

The flux carried by the superconductor Φ is:

$$\begin{aligned} \Phi &= B \times \text{area} \\ &= \mu_0 f' H_e \pi (R^2 - (R-\lambda)^2) \\ &= \mu_0 f' H_e \pi (2R\lambda - \lambda^2) \end{aligned}$$

where f' is the fraction by which H_e is reduced in the penetration layer by the magnetic properties of the medium. Since Φ may also be written as

$$\begin{aligned} \Phi &= \mu_0 H_i \pi R^2 \\ H_i &= \frac{f' H_e \pi (2R\lambda - \lambda^2)}{\pi R^2} \\ &= f' \frac{\lambda}{R} \left(2 - \frac{\lambda}{R}\right) H_e = f H_e \end{aligned}$$

and giving $f = f' \frac{\lambda}{R} \left(2 - \frac{\lambda}{R}\right)$. (31)

From the above argument it may be deduced that it is advantageous to use very fine filamentary superconductors in high field applications because of the higher values of critical field obtained as the conductor size is reduced. This is an additional advantage to the increased stability also obtained by reducing superconductor diameter.

The manner in which many such filaments can be disposed in a normal metal matrix to form a multifilament composite conductor will now be considered.

4.2 The Multifilament Composite.

A calculation similar to that used above for a single filament could be applied to a multifilament configuration to show the extent to which the composite conductor is utilised. Such a calculation would need to take into account the screening of the inner filaments by those in the outer layers, and would depend on the dimensions and disposition of the filaments within the matrix material. In general it would not be easy to evaluate. We are interested in the composite as a carrier of current, and since the passage of current through the filaments alters the field pattern within the composite considerably, it would be more useful to consider the current-carrying case.

For any one filament the factors which influence its ability to remain normal while carrying a current are the local magnetic field, and the product $\underline{J} \times \underline{B}$, which represents the Lorentz force. It is in the interests of maintaining the superconducting state to keep both these factors at a minimum. In particular, the local

magnetic field should not exceed the critical magnetic field of the superconducting filament. Reduction of the size of field at the filament would also reduce the Lorentz force. While a large magnetic field is required at the axis of the magnet solenoid, it would be advantageous to keep the local field at each filament as low as possible.

In a multifilament composite the calculation of the local field in all parts of the composite is quite a complicated matter. Let us first consider the simplest multifilament case, i.e. two parallel straight conductors (of infinite length) in zero external field. Let the two conductors each have a diameter b and be a distance a apart; each carries a current I , as shown in fig. 25. At the surface of conductor 2 nearest to conductor 1, the resultant field due to its own current and that in conductor 1 is:

$$\begin{aligned} H_s &= \frac{I}{2\pi b/2} - \frac{I}{2\pi(a + b/2)} \\ &= \frac{2Ia}{\pi b (2a + b)} \end{aligned}$$

(for $b \ll a$, $H_s = I/\pi b$).

The filament can remain superconducting up to a value of field, H_{ci} , so that the limiting value of field at the surface is given by:

$$H_s = H_{ci} = \frac{2Ia}{\pi b (2a + b)} \quad (32)$$

compared with $H_{ci} = I/\pi b$ for a single conductor. Thus it might appear that the current I_{2m} which can be carried in a single filament of a pair before H_{ci} is reached is greater than that in a single filament on its own, but

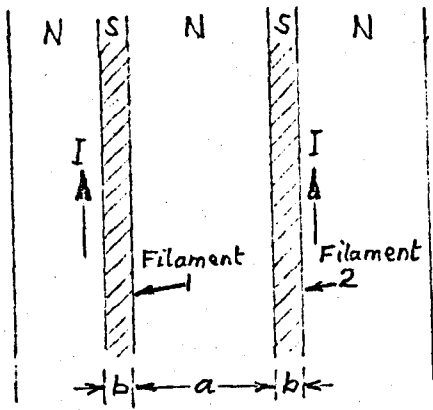


Fig. 25

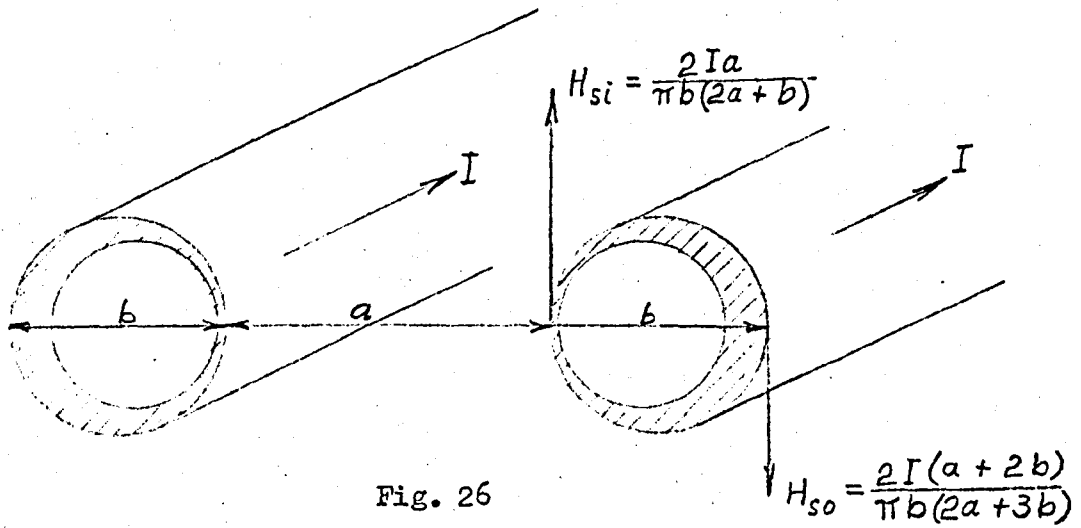


Fig. 26

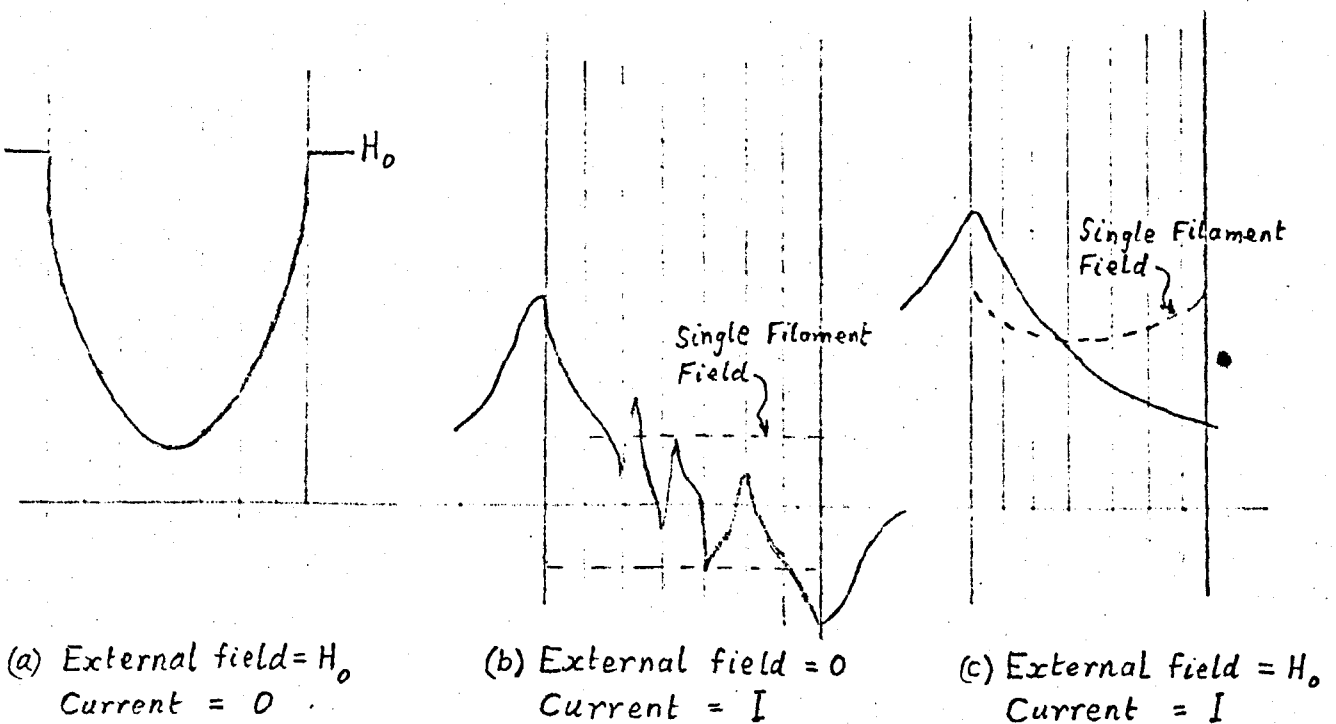


Fig. 27

this is not so because H_{ci} on the other side is reached earlier.

From this simple example it might be speculated that many filaments in a composite could be arranged in some ideal configuration to give optimum conditions for current and field within the composite. However, the matter is not so simple, and many other considerations are necessary.

When a is comparable with b , the field is not uniform at all points on the surface of the filaments: the above calculation only takes into account the field at the surfaces immediately facing each other. The matter is further complicated when b is greater than the penetration depth of the field.

Qualitatively the two-filament situation is illustrated in Fig. 26. If the fields on the inner and outer faces, H_{si} and H_{so} are unequal, the penetration of flux into the conductors is asymmetric, as indicated by the hatched areas in the diagram. As the field increases, the filament would commence to go normal from its outer face as H_{so} approaches H_{ci} , and once the normal phase is initiated the remainder of the specimen would return to the normal state. If the filaments were free to move they would converge. Without going into exact geometric field calculations, it can be seen that very complicated field patterns can be set up within a multifilament composite, especially when an external field is superimposed.

The approximate distribution of field in a multifilament composite in an external field is illustrated in Fig. 27. It can be seen from this that the Lorentz forces on one side of the composite will be much greater than on the other. The filaments subject

to greatest $\underline{J} \times \underline{B}$ will tend to become resistive, carry less current, become heated and thus place stresses on the other filaments. As some filaments become disused the field pattern will change and other filaments will become subject to large Lorentz forces. The complete normalisation of the composite would thus progress.

In an attempt to make the field distribution more uniform in multi-filament composites some authors (131, 132) have suggested transposition of conductors in a composite cable. As an approximation to transposition several investigators have tried simple twisting of the composites. (131, 133, 134, 135). The twisting does in fact appear to improve the stability of the superconductor under conditions of changing field.

The twisted composite will now be considered from three points of view. The first considers the consequences of introducing a continuous cross-over point between a pair of filaments on local magnetic fields, analogous to the cross-winding (honeycomb) of the solenoid; another considers the effect of twisting on the induced currents in the interfilament material, when H and I vary; the third considers the relative distortion of the magnetic and electric fields by the twisted and non-twisted composites.

4.3 Twisted Multifilament Composites.

In order to make the field distribution more uniform and to reduce the circulating currents in both the superconducting filaments and normal metal matrix, Smith et al (131) suggest that the filaments should be fully transposed within the matrix as in a Litz cable. The usual manufacturing processes of extru-

B

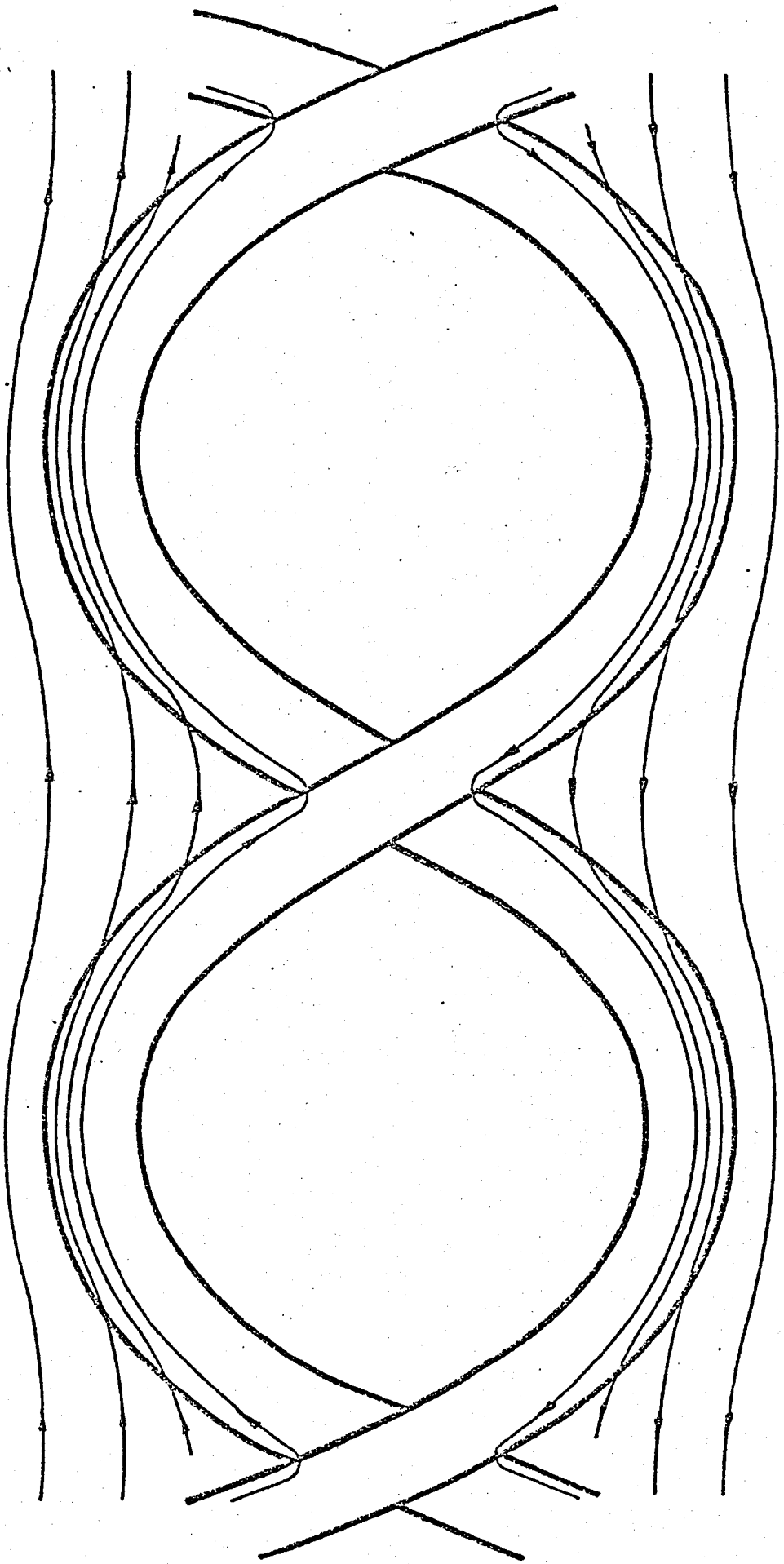
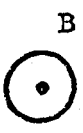


Fig. 28 Initial stage in the penetration of flux in a two filament twisted composite.

sion, rolling and drawing used for producing multifilament composites preclude full transposition of the filaments, but larger stable cables have been produced using a number of twisted composite wires in transposed arrays.

The effectiveness of twisting, although not completely efficacious as is transposition, has been described by Walters (131) using the concept of continuous cross-over points. He considers a pair of twisted filaments with an external field applied which generates screening currents as it penetrates the matrix, as indicated in fig. 28. As currents flowing in the superconductors do not decay, penetration is directed towards the regions where the filaments cross, and as further penetration occurs more of the screening currents are transferred to the filaments where they flow as equal opposing currents meeting where the filaments cross. The total screening provided at the crossing points by these currents is zero so that the flux appears to cross the filaments at these points, although since the filaments are twisted, the net flux enclosed by them is zero; thus flux does not need to cross the filaments in order to fill the composite. The behaviour of the flux lines is illustrated in fig. 29. The flow is indicated by the dashed arrows. The original flux lines (shown tagged and drawn broken in the middle) separate, and coalesce to form new flux lines and in so doing penetrate the loops formed by the twist provided the crossover points are sufficiently close together (corresponding to a maximum twist pitch).

The above description can be extended to the situation in a twisted composite containing a large number of filaments which

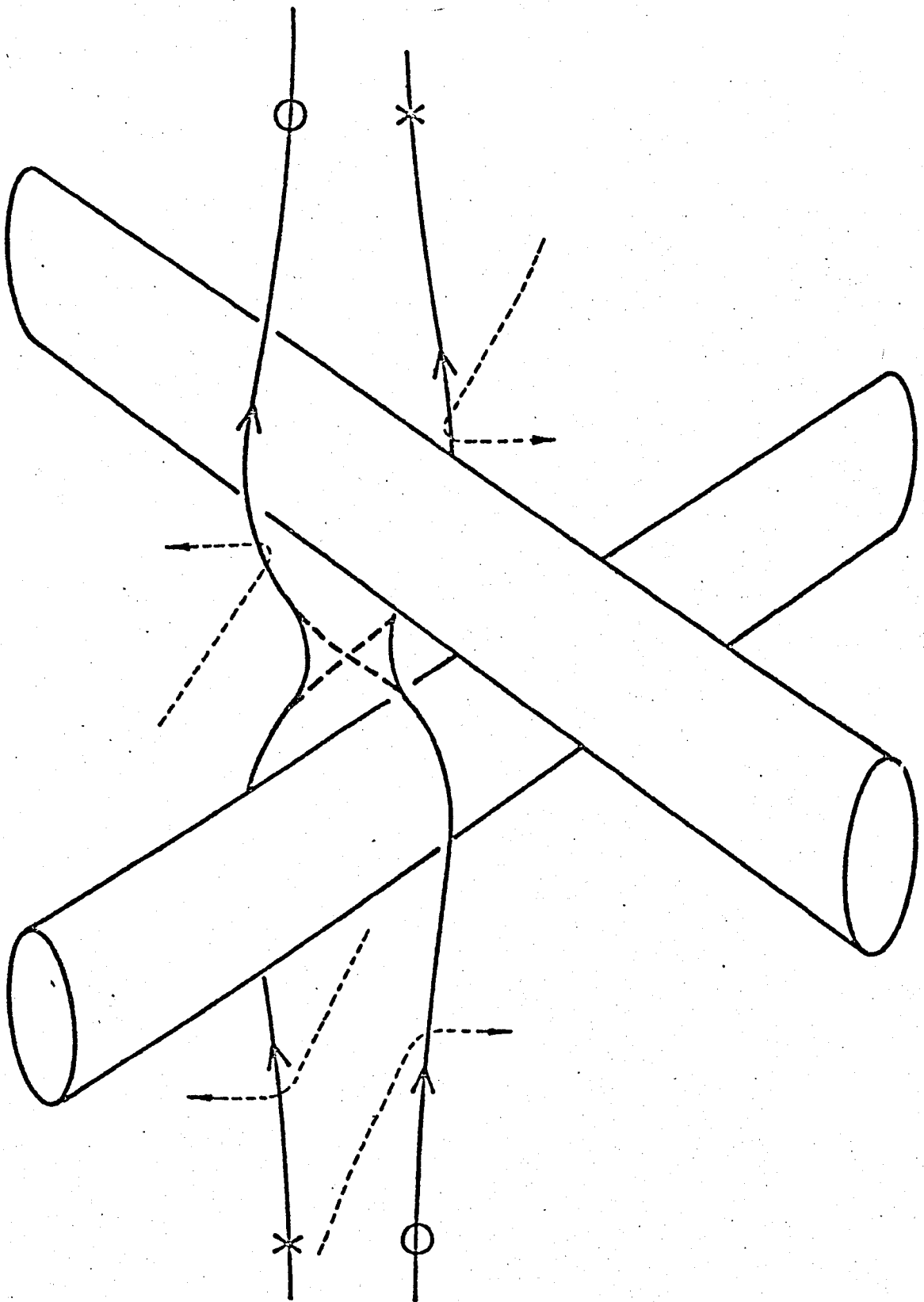


Fig. 29 Flux line behaviour in the region where the filaments cross in a two filament twisted composite.

can be regarded as the result of the superposition of a large number of crossovers similar to those described above. This would seem to be justifiable if the contribution of the currents in the rest of the filaments to the local field in a pair of filaments forming a crossover point is small compared with the applied field.

The condition for the maximum twist pitch has been developed by Wilson et al (131) by considering the induced currents in the interfilament material. The simplest case they consider is that of a composite consisting of two sheets of superconductor, each of thickness d , separated by normal metal of thickness w and resistivity ρ . The composite of length $2l$ is immersed in a magnetic field perpendicular to l and w which is increasing at the rate of \dot{B} . Suppose that a steady state has been reached and that l is just sufficient to allow all of the current in the superconducting sheets to cross the matrix, as indicated in fig. 30. This value of l is referred to as the critical length, l_c . Thus for an element dx at x we have:

$$\begin{aligned} \text{Current across AB} &= \frac{\text{Voltage across AB}}{\text{Resistance between AB}} \\ &= \frac{\dot{B} x w}{\rho w / (z dx)} \end{aligned}$$

The current in the superconductor is $J_c z d$ and equals the total current flowing across the normal material. Thus:

$$\frac{\dot{B} z}{\rho} \int_0^l x dx = J_c z d$$

$$\text{giving } l^2 = l_c^2 = 2 \rho J_c d / \dot{B} \quad (33)$$

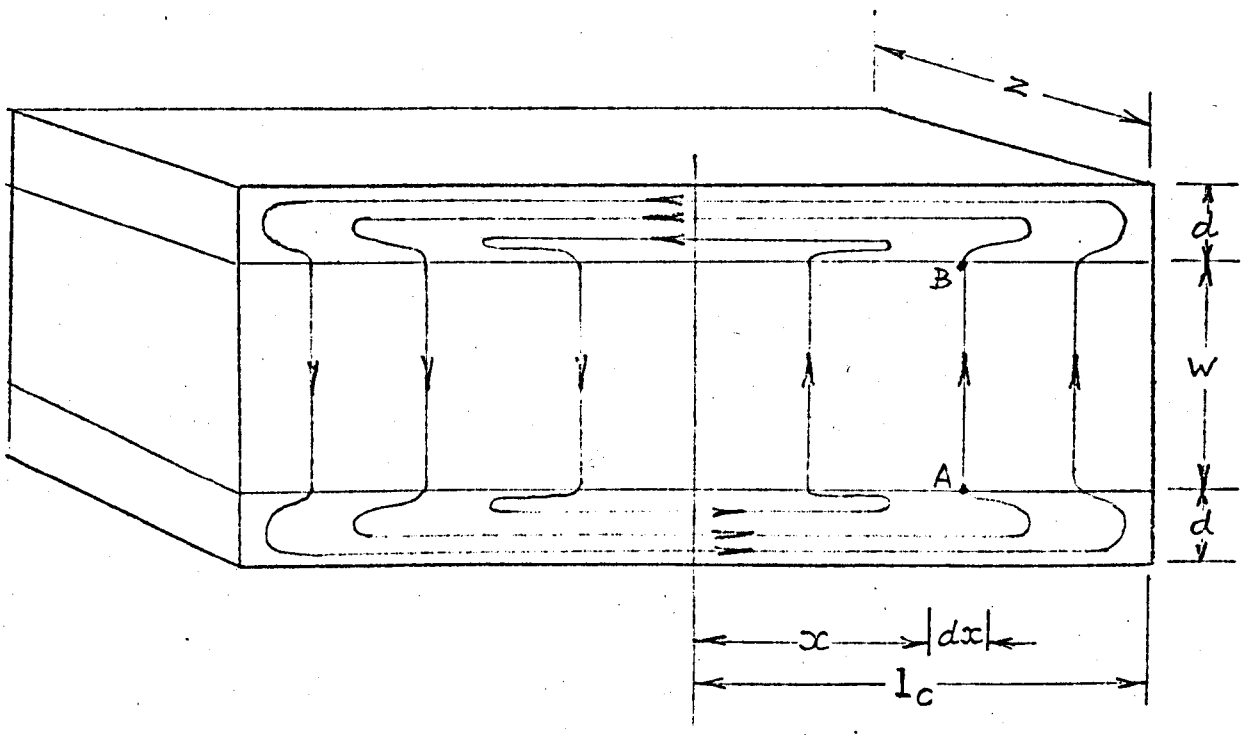


Fig. 30 Calculation of critical length for composite of two parallel superconducting slabs separated by resistive material.

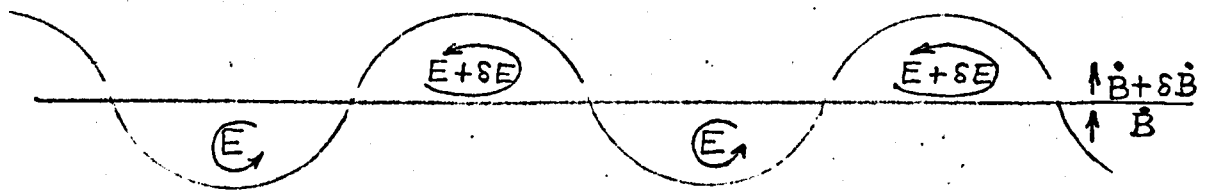


Fig. 31 Illustrating the build up of voltage in a twisted composite with imperfect decoupling of filaments in a field gradient.

As Wilson et al point out, when the superconductor is in the form of separate filaments, it is necessary to introduce an appropriate space factor, λ_1 , into the expression for l_c^2 . Also, although w cancels out in the above "Ohm's law proof", a more rigorous treatment shows that when d is not small compared with w , a further correction is necessary. This results in equ. (33) for the shortest l_c in the outer layer of a multifilament composite being replaced by ⁽⁵¹⁾⁽¹³¹⁾:

$$l_{c1} = (2w\lambda_1 J_c \rho / B)^{\frac{1}{2}} \cosh^{-1} \left(\frac{d}{2w} + 1 \right) \quad (34)$$

For values of B approximately 10^{-3} to 10^{-1} tesla/second l_c is typically in the range 0.1 - 10 metres. The significance of l_c is that for composite lengths of over $2l_c$, the current will all cross over in a distance l_c at each end of the composite and there will be no transverse currents arising from the superconductors in the normal metal. If, however, the length of composite is less than l_c , it follows from equ. (33) that only $(l/l_c)^2$ of the current will cross the matrix, and the remainder must form closed loops confined to the separate filaments. Thus by making l very much less than l_c the filaments will behave independently. This can be achieved in a long composite by twisting it about its axis with a pitch very much less than l_c . Each half wavelength of the twist will act independently and may be set to $2l$. The magnetisation currents will then behave as if the cable had been cut into sections of length $2l$. A similar expression to equ. (34) has been obtained by Morgan ⁽¹³⁴⁾ for a pair of twisted filaments with $\lambda_1 = \pi^3/16$. Moreover, he extends the discussion to multifilament composites and concludes that the various internal supercurrents

will cancel everywhere except on the surface, with the same expression for the critical length l_c as in the case of the twisted pair.

From equ. (34) it would seem desirable to make the resistivity of the matrix as high as possible, and in the limit to make it completely insulating; l_c as defined by equ. (34) is then infinite. Nevertheless some twist is still necessary since the filaments must be joined in parallel through the connections at each end of the composite unless steps are taken (as yet undevised) to prevent this happening. In a uniform field, a single twist would in principle mean that the induced voltage would be cancelled out exactly over the length, but to ensure adequate decoupling, Smith et al (131) recommend more twisting than once in this situation should it arise. This is unlikely since the requirements of adiabatic stability (or at least dynamic stability) must still be met, and this requires the presence of a low electrical resistivity material in close contact with the superconductor, although the presence of an insulating material in addition between the copper-clad filaments is a possibility.

A simple twist is not adequate for decoupling the filaments in the presence of a field gradient, as can be seen from fig. 31 which shows the build-up of voltage due to the field difference in the central and an outer (twisted) filament. In principle this can be solved by omitting the central strand, or by fully transposing all the filaments so that each follows an equivalent path. Full transposition is probably not feasible in a co-drawn composite conductor, but is possible in multi-composite cable formed from them.

The third approach to determining the criterion for the penetration of magnetic field between the individual strands so that advantage is taken of the small filament size was developed by Walters (131) using the basic properties concerning the behaviour of electric and magnetic field lines. It involves the idea of the electrical centre of a sample. This is the line separating regions of current flowing in opposite directions in a superconductor across which no flux passes and which has no electric field along its length. Although the initial treatment by Walters is of parallel untwisted slabs and deals with the transport current and external field penetration into composites, he uses a geometric adjustment which simplifies the problem considerably. Further modification enables it to be applied to a multifilament composite which eventually leads to the result of equ. (34) noted earlier.

4.4 Three-component composites.

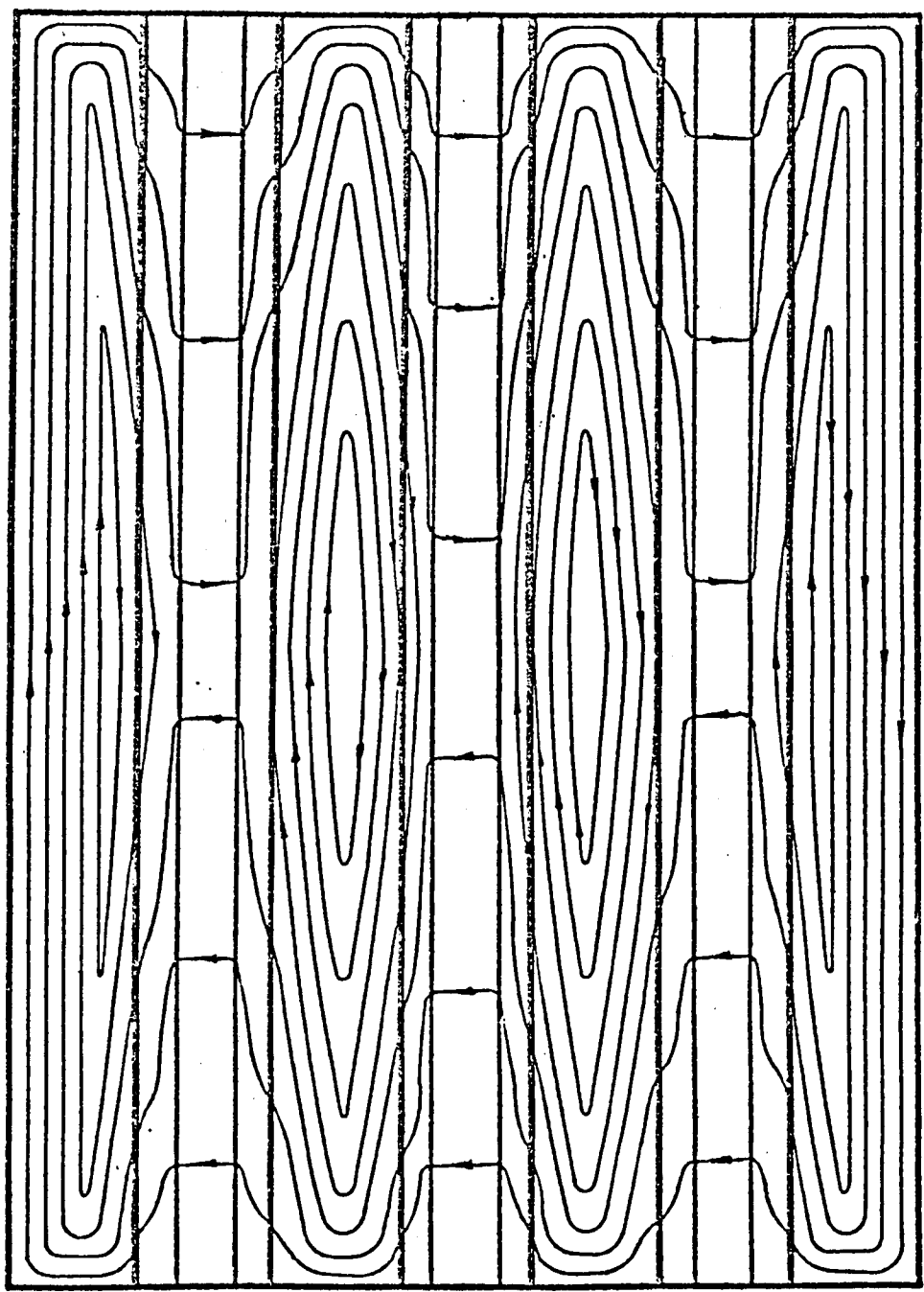
In some applications of twisted filament superconductors, e.g. in pulsed synchrotron magnets and in the field magnets of some electrical rotating machines, it is desirable to be able to change the field as rapidly as possible. Equ. (34) indicates that a matrix material with a high resistivity is desirable in order to avoid using very high rates of twist. Since cupro-nickel has a resistivity approximately 1000 times that of copper, it would be expected for a given twist pitch, that \dot{B} could be $\sqrt{(1000)}$ times as fast if cupro-nickel were used instead of copper. For pulsed magnets it is also desirable to have the filament diameter as small as possible, since when the transverse field is much larger

than the self field, the energy loss is directly proportional to this dimension.

It is important also to ensure that all of the filaments are twisted and that there is no untwisted core in the composite, as Critchlow and Zeitlin explain is possible with small twist rates. (135). In the plastic torsion of a cylindrical bar, plastic deformation first occurs at the surface. An elastoplastic boundary is formed and this moves radially inwards as the angle of twist is increased. At small angles of twist a core remains which is still in the elastic state, and when the torque is removed, this core will untwist. The data of these workers strongly suggests that at small twist rates an appreciable untwisted core is present.

The presence of a normal metal matrix in a composite immersed in a time-variant field involves further energy loss due to the eddy currents induced in the matrix. The use of a high resistivity matrix material is obviously beneficial in reducing this loss below that obtaining when a low resistivity material is used. However, the high resistivity matrix is at a severe disadvantage when stability, particularly dynamic stability, is considered. Although it may be satisfactory in very small coils intended for a.c. applications at low current densities, it is unlikely to give satisfactory performance in larger coils. In these, intended for pulsed magnets and similar applications, it is now the practice to use three-component composites employing both copper and cupronickel as materials in the matrix.

If a flat strip made up of superconductors separated by normal metals of high and low resistivities is considered to be exposed to



High ρ Low s-cr. Low High Low s-cr. Low High Low s-cr. Low High

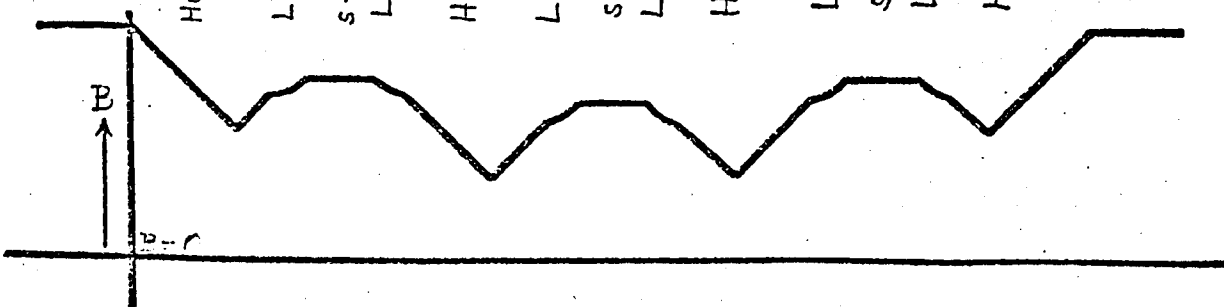


Fig. 32 Screening in a composite of superconductors and two normal metals with high and low resistivities.

a magnetic field changing at a constant rate, a screening pattern as indicated in fig. 32 will be set up. The rate of decay of screening currents is much greater in the material of high resistivity so that the flux tends to enter the composite along this path in a lengthwise direction. Penetration of the low resistivity material is mostly across the composite, so that currents in it are roughly parallel to the superconductors, as is the case in the superconductors themselves. In a given situation where the dimensions and values of resistivity are known, the relative flux diffusion times can be determined and used to calculate a weighted mean of the resistivities of the matrix materials; this value can then be inserted in equ. (34) in order to calculate the critical twist length, l_c . Usually the resistivity of the high resistance material will dominate.

4.5 A.C. Losses.

Some consideration has already been given to a.c. losses in superconductors in Section 2.12 and much of this is directly applicable to the case of filamentary superconducting composites. Experiments by McInturff (133) and Dahl et al (57) on untwisted filamentary composite superconductors in coils using either pulsed direct current or low frequency alternating current have indicated that the filaments act collectively, so that the conductor as a whole behaves essentially as a solid superconductor having approximately the same diameter as the circle which just encloses the filaments. Salmon and Catterall (132) in their experiments on composite wires show that this model is also

applicable at 50 Hz in zero magnetic field. Eastham and Rhodes (136) also confirm this finding for the self-field losses in composite wires with both untwisted and twisted filaments. Furthermore, in their consideration of the effect of transposition on the self-field losses of composites, they deduce that although for a small number of filaments, transposition within a composite would give a small decrease in self-field loss, in cases where the number of filaments exceeds 60, the loss would be increased.

In a coil carrying alternating current, the windings are subjected to an alternating transverse field which in small conductors is normally much larger than the self-field due to the current in the winding. The condition for the critical twist pitch, which if fulfilled should mean that the composite should behave as a collection of isolated filaments, has already been derived (equ. 34) and the loss measurements of Dahl et al (57) with composites subjected to transverse swept fields confirm the effectiveness of twisting multifilament composites in order to decouple the filaments. As the magnetisation of a composite is a measure of the decoupling of the filaments, Wilson and Walters have used this in their theoretical and experimental studies of a.c. losses in multifilamentary composites (131). They show that the magnetisation, M_o , and hence the a.c. loss of an adequately twisted composite, is related to the magnetisation for an untwisted composite, M_s , by:

$$\frac{M_s}{M_o} \approx \frac{2a}{d} \quad (35)$$

where a is the composite radius and d is the filament diameter. This would indicate that the a.c. loss can be reduced in a given diameter of composite wire by decreasing the filament size, provided the composite can be given a sufficiently short twist pitch. As pointed out earlier, the use of a matrix material of high resistivity increases the critical twist length, and composites with a matrix of cupro-nickel (or copper plus cupro-nickel) allow pulsed or low frequency a.c. operation of coils. At the usual industrial power frequencies (~ 50 Hz), however, the required twist pitch for an acceptably low a.c. loss becomes impractically short even with a cupro-nickel matrix. As Eastham and Rhodes ⁽¹³⁶⁾ point out, it will be necessary for these conditions to develop intrinsically stable materials in which very fine individual filaments are separated by an insulating barrier. Alternatively, transposing the individual filaments, as mentioned by Salmon and Catterall ⁽¹³²⁾, is another approach. The prospects of achieving either at present do not look very hopeful: fortunately, in most applications envisaged for superconductors in electrical machines, the superconductors will not be subjected to the high industrial frequencies, but rapid change of the field under certain conditions (e.g. short circuit in a generator) would be highly desirable.

Chant, Halse and Lorch ⁽⁵¹⁾ have measured the a.c. losses in various samples of multifilament composites. Under the conditions of their tests they show the loss in the matrix of a wire with N filaments is:

$$Q_m \approx \frac{4\pi^4}{3} 10^{-14} (N\sqrt{N}) \frac{1fH^2L^2}{\rho_w} (w + d/2) \text{ J/m cycle}$$

For their samples, this becomes $Q_m = 6.0 \times 10^{-14} fH^2L^2$; from their measurements they derive the empirical expression $Q_m = 4.9 \times 10^{-14} fH^2L^2$ which shows reasonable agreement.

5. Possible Types of Superconducting Machines.

5.1 Possible Advantages.

There is no point in developing superconductive rotating machines unless there are good reasons for doing so. The possible advantages which might be expected are:

- (a) drastic reduction in losses
- (b) reduction in weight
- (c) reduction in volume
- (d) extension of range of existing machines
- (e) reduction in first cost
- (f) lower operating costs
- (g) lower cost of foundations and buildings consequent on (b) and (c).

Of course, not all of these advantages will occur in any one application, and the extra complication and cost of the associated cryogenic plant must be taken into the consideration.

5.2 Machines Utilizing Properties Unique to Superconductors.

Before exploring the possibilities of replacing conventional windings in existing types of rotating machines by superconducting coils, it is relevant to ask whether it is possible for new types of machines to be developed which operate on novel principles utilizing properties unique to superconductors. Since rotating electromagnetic machines are basically energy converters, usually for converting mechanical to electrical energy, or vice versa, the approach should be rather to investigate methods of electro-mechanical energy conversion which employ the special or peculiar

properties of superconductors in their own right rather than to use them as substitutes for normal conductors. This approach should encourage ingenuity in the development of novel types of machines, and yet inhibit fruitless effort being expended on others which are inherently impracticable, such as motors working on the conventional induction motor principle with superconducting secondary windings.

There are three effects unique to superconductors which can be considered for utilisation in a rotating machine. These are the Meissner effect, zero resistivity and the transition between the normal and superconducting states. Several proposals have already been put forward based on one or more of these effects, and a few experimental machines have been constructed and reported in the literature. These proposals will now be examined, and general conclusions drawn on the suitability of such devices for power conversion. The general relationship between the various types is illustrated in fig.33.

5.3 The Moving-Zone Generator.

The mesh voltage equations for any circuit (including non-stationary) may be written in the form

$$\sum e = \sum iR + \sum \frac{d}{dt} (\Psi) + \sum \frac{q}{C}$$

where e and i are the voltages and current in the circuit, R is the resistivity, Ψ is the flux linkage, q is the electric charge and C the capacitance. The equations may be rewritten as

$$\sum e - \sum iR - \sum \frac{q}{C} = \sum \frac{d}{dt} (\Psi) = \frac{d}{dt} \sum \Psi \quad (36)$$

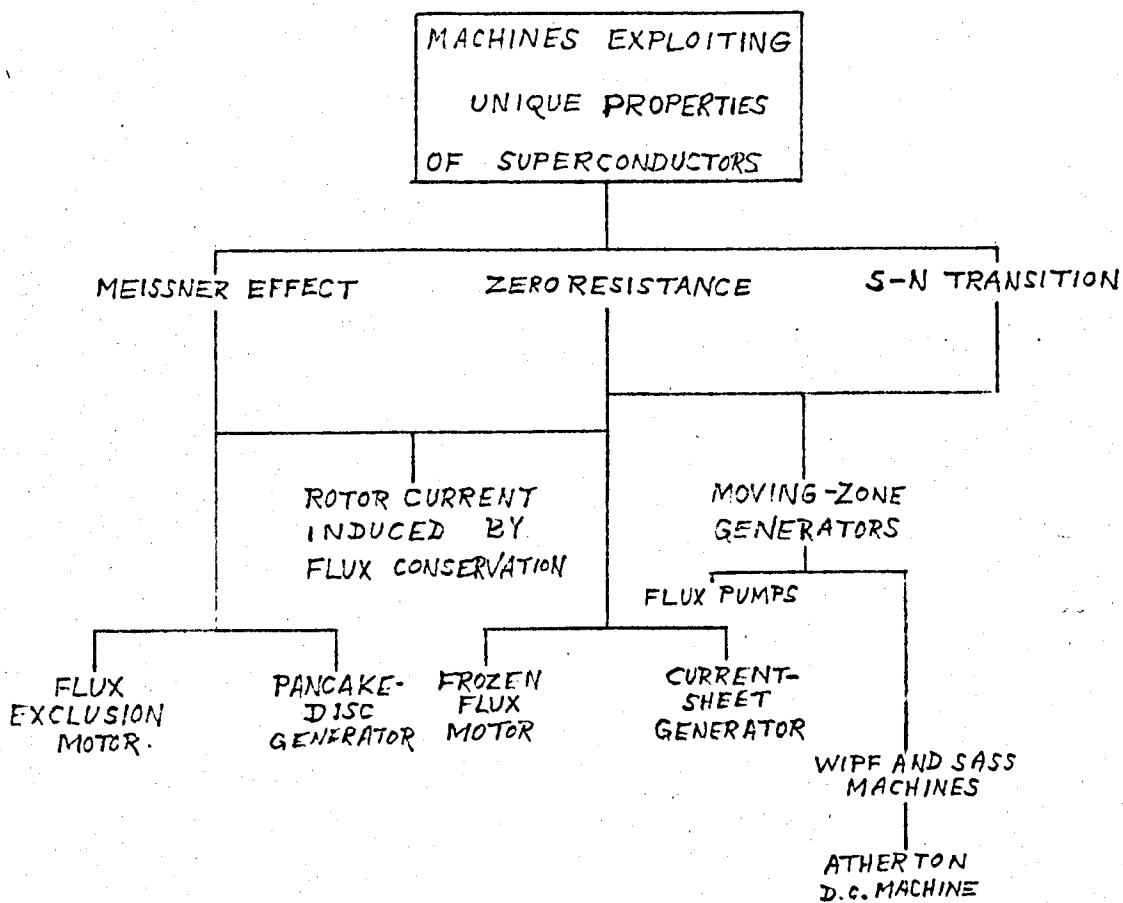


Fig. 33

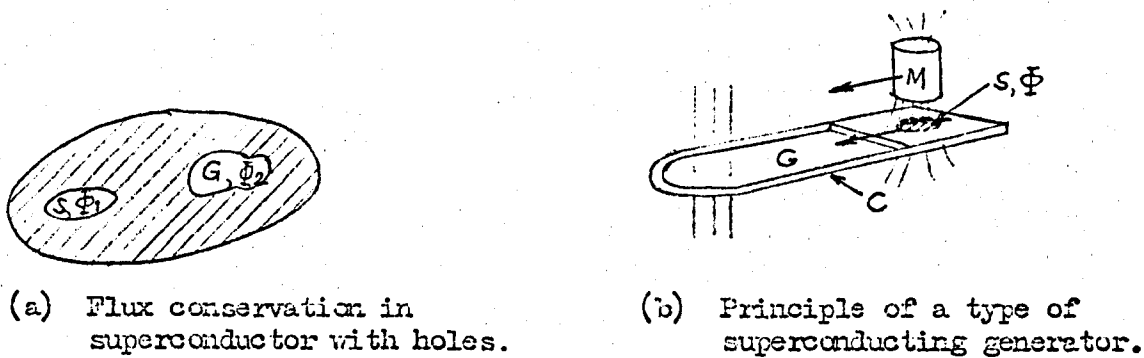


Fig. 34

In a superconducting ring, the L.H. side will be zero and thus the flux linkage within it will be conserved. As a consequence it would seem that if the superconducting ring forms part of a generator, it would never be able to increase the magnetic flux enclosed by it. This however assumes a singly-connected system in the topological sense. Providing the contour of integration is well clear of the penetration depth, it is possible in a multiply-connected system to follow various integration contours embracing the various holes in the system so that the flux to be conserved can be a multi-valued function, the module being the magnetic fluxes per hole. Volger and Admiraal (137), by clever topological arrangements, have used this concept to propose a superconducting generator.

Consider a superconductor as shown in Fig.34a with two holes S and G containing fluxes Φ_1 and Φ_2 respectively. With the condition of infinite conductivity, the condition is present which requires that the flux through a hole remains constant in time. However, a normal region in a superconductor represents a "hole" in the topological sense, and can be created in a superconductor by local heating so that the temperature of the local area is above the critical temperature, or by a magnetic field which locally raises the field above the critical value. Further if the source of heat or local field is moved across the superconductor, such a hole will follow the movement. If S is a hole formed by either of these means, it can be moved into G, and consequently the flux in G will increase to $\Phi_1 + \Phi_2$. If now G is regarded as the interior of a superconducting circuit C (see

fig. 34b) and S as the normal area created by an excitation magnet, then the total flux in G can be increased by sweeping S into G by movement of the magnet. If the magnet is then removed, the current in C must increase so that the total flux embracing C remains constant. If L is the total inductance associated with G , and if Φ is the flux increment swept into G , then the change in current in G , (δI) , is given by

$$\delta I = \frac{\Phi}{L}$$

This basic concept of Volger and Admiraal has been used by them in an experimental generator (137), although Felici anticipated their device in 1938 (138). Variants of the Volger and Admiraal machine have been reported by van Houwelingen, Admiraal and van Suchtelen (139), van Beelen (140) and van Suchtelen (141). Wipf (142) has used the idea for a generator with several plates, and Sass (143) has also developed a generator similar to the Wipf machine but with some improvements.

Generators of this type can produce very large currents, (of several thousand amperes) but with only very low voltages, (of a few tens of millivolts) (141). Further, since the current is generated in a superconductor, the practical considerations involved in transferring it to normal ambient temperature preclude such a usage. The restriction thus imposed by the heat leaks to applications at very low temperatures means that even if they were to be developed, their main application would be for energising superconducting magnets. Although they would obviate the thermal leak problems associated with leads supplying superconducting

magnets from room temperature current sources, it is unlikely that they would be used for exciting superconducting windings in other electrical machines because of the comparatively long times involved in exciting a magnet with this type of supply, and on account of the difficulties which would be associated with the control and protection of the superconducting magnet itself.

The principal objection to machines of this type arises from the fact that as the moving spot progresses across the superconductor, the local flux in the superconductor is changing relative to it, and thus sets up losses associated with a changing flux. The ensuing heat leads to reduced efficiencies of both the current generator and its dewar system. Such machines are really flux pumps, and as such, not suited for electro-mechanical energy conversion on any scale. A comprehensive review of flux pumps and current generators is given in ref. 144.

5.4 The Atherton D.C. Machine.

Atherton (145) has proposed a machine based on the moving-zone principle, but extending the ideas of Volger et al, and Wipf, and which he claims can be capable of generating large amounts of power of several megawatts. Preliminary outlines and basic dimensions for 60 MW and 500 MW d.c. generators are given in reference 145, and intended for energizing superconducting power transmission lines and in reverse as motors to drive conventional a.c. generators at the receiving end. Atherton pointed out in 1964 that these machines were not practical with the superconductor materials available then because of the impossibly high losses which would

occur due to the flux changes across the superconductors. The position regarding superconductor materials has not changed radically since then and the same conclusion anent the practicability of this type of machine is still valid.

The analysis presented by Atherton (145) would appear to be appropriate to the condition when the machine operates as a flux pump, i.e. when the output voltage is very small, but when the machine is required to generate power and deliver it to an external device, the voltage at the terminals of load is, as Atherton remarks, reflected in the superconducting loop of the machine. It seems that Atherton has overlooked the effect of this voltage on the behaviour of the machine, which is capable of generating only a limited value of this voltage. However, in view of the impracticability of the machine for the reason given earlier, it is not proposed to consider it further.

5.5 Pancake-Disc Generator.

A proposal (146, 147) to utilize the Meissner effect results in a generator producing an essentially square waveform. The rotor consists of a niobium disc rotating inside an annular field coil, Fig. 35. The rotor has slots or openings cut in it, the number depending on the number of poles required. The armature windings are mounted on each side of the disc and have a shape corresponding approximately to the openings in the disc. Due to the flux exclusion action of the rotor, all the flux produced by the field coil is forced into the openings in the disc. As the disc rotates at a constant speed, the flux threading through the openings links

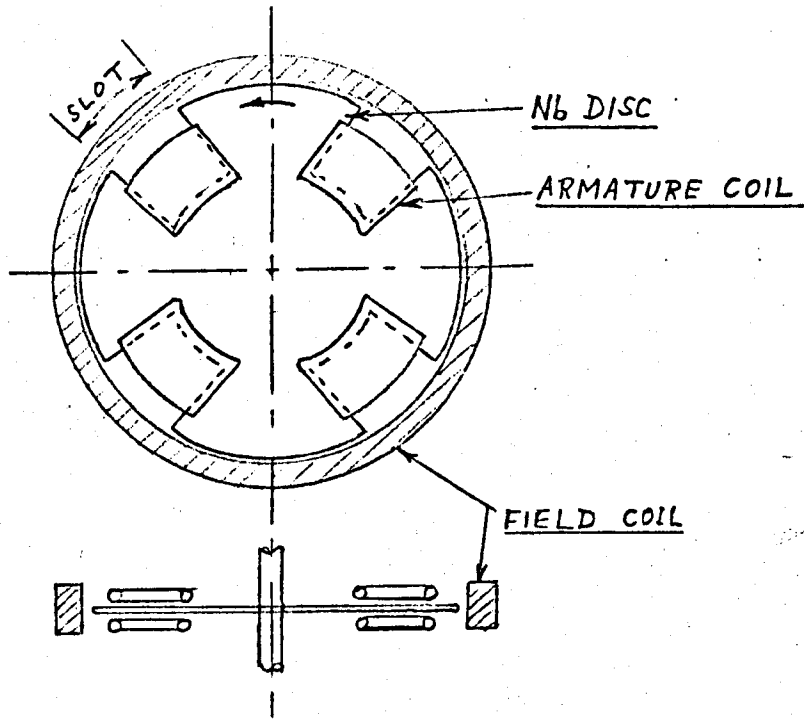


Fig.35 Pancake-Disc Generator

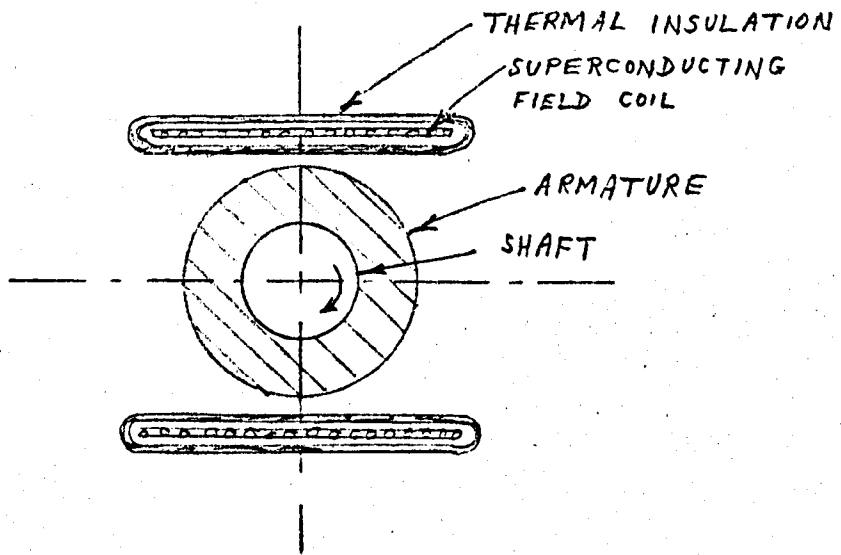


Fig.36 Current-Sheet Generator

with the armature coils and changes at an almost linear rate. Thus a constant voltage is generated during the part of the cycle the flux is increasing. The maximum linkage occurs when all the flux passing through an opening links with the corresponding armature coils, after which the flux linkage decreases uniformly, giving rise to an equal voltage of reverse polarity.

A feasibility study by Pierro and Unnewehr ⁽¹⁴⁷⁾ of a 30kW, 400 Hz aircraft generator indicated that it would have a specific weight of approximately 0.45 kg/kVA and a volume of one-tenth of that of a conventional aircraft generator. The investigation ignored the a.c. losses in the superconducting armature windings, and the heat leak and sealing of the shaft. It also ignored the heat leak along the leads to the armature windings, the windings being formed from thin-film Nb_3Sn deposited on a glass substrate operating with a current density of 90,000 A/cm². Allowance was made for the weight of the liquid helium contained in the machine, but no allowance was made for replenishing it. In view of the not inconsiderable heat inleaks which were ignored, the supply of liquid helium would last only for a few minutes.

The values quoted for specific weight and volume appear inconsistent with those for conventional generators for aircraft, where a specific weight of 0.4 kg/kVA or lower can be achieved with very little volume left unfilled. with solid material, and without the requirement for a refrigerator or liquid helium store. The pancake disc machine is thus not a viable proposition, and in any case, the non-sinusoidal waveform generated would not be acceptable for user equipment. Further, it has not been demon-

strated that such a machine would function practically, as minor flux changes in the edges of the rotor may generate sufficient heat locally for parts of the rotor to be raised above the critical temperature.

5.6 Current-Sheet Generator.

This configuration was suggested by McFee (148) and investigated by Pierro and Unnewehr (147). Although it might be argued that it does not depend entirely for its action on a property unique to superconductors (material with very low resistivity and capable of carrying large current densities would be suitable for the current sheets), it is nevertheless convenient to consider it here.

The machine is illustrated in fig. 36 and comprises two thin parallel current sheets carrying currents in opposite directions, the current sheets being formed by superconductors in order to achieve the huge current densities required by the iron-free magnetic circuit. The armature ^{of a conventional type} rotates between the current sheets and is at normal ambient temperature. By making considerable simplifying assumptions, Pierro and Unnewehr arrive at a weight-estimate for a 30 kW, 400 Hz alternator which corresponds to a specific weight of 0.55 kg/kVA. Although this is higher than for the pancake disc generator, it should be pointed out that neither includes any allowance for helium refrigeration equipment, and if the weight of this is taken into account, this conclusion may be different. Since the current sheet machine has an armature at normal ambient temperature, it does not incur the penalty of

a considerable heat leak along its shaft and armature leads, nor that due to a.c. losses in the armature, and consequently the rating of the refrigeration equipment can be considerably smaller. Thus overall the weight penalties of both types of generator may be comparable with each other if the refrigeration equipment is included in the weight estimates. Again, it is considered that the current sheet type of generator has not sufficient merit to warrant further examination.

5.7 Flux-Exclusion Motor.

Superconductors possess not only the property of zero resistance but "ideal" superconductors also exclude magnetic flux and prevent its penetration corresponding to complete diamagnetism (the Meissner effect already noted). The boundary condition imposed by the Meissner effect is that the normal component of the magnetic field vanishes at the superconducting surface which implies that the magnetic forces are normal to the surface. It thus follows that no torque can be produced on a smooth cylinder or sphere composed of ideal superconductor about its principal axis by an external magnetic field using forces set up by the Meissner effect.

Buchhold (146) and Schoch (149) have proposed a motor intended for gyro applications which depends on the Meissner effect for its operation, but avoids this difficulty. An octagonal rotor of niobium or other type I superconducting material is free to rotate on its axis. Flux from a succession of stationary coils mounted close to the rotor (see fig. 37) produces a repulsive force due to the Meissner effect. Continuous positive torque can be obtained

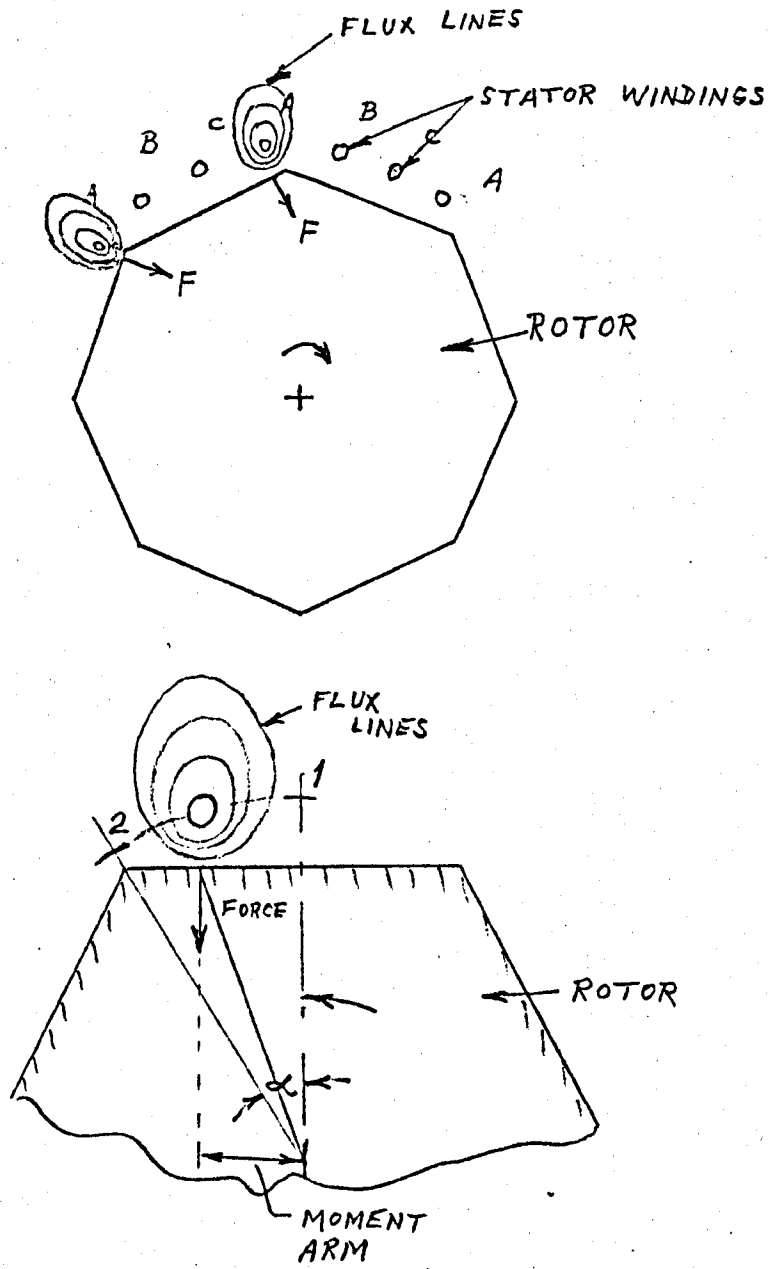


Fig. 37 Flux-exclusion Motor

from the superconducting rotor by sequential switching of the stationary coils, or by using a polyphase winding, each phase being excited in turn at the appropriate instant. Synchronisation of the pulses is controlled by rotor-position-sensing pick-offs, and both optical and inductive types have been used. The use of commutators and brushes is precluded on account of the friction and the consequent losses.

Analysis (149) of this arrangement shows that the average torque from position 1 to position 2 is equal to $\frac{1}{2}(I^2/\alpha)(L_1-L_2)$, thus indicating the importance of a maximum change in inductance in the stator windings as the rotor changes by one pole position. The torque is also proportional to the square of the coil current, but independent of speed.

Speeds up to 20,000 r.p.m. under a vacuum of 10^{-6} torr have been claimed, but no shaft output has been provided because of the formidable heat transfer and sealing problems involved. The application intended for the development was in gyros, in conjunction with superconducting magnetic bearings. The results reported in reference 149 are tentative, and no indication is given of the period over which the trial motors operated. It is claimed however, that if motor losses occur they are not of sufficient magnitude to produce a loss of super-conductivity and a resultant loss of suspension and motor torque. This is surprising since it would be expected that the movement of the flux across the face of the superconducting rotor would produce an a.c. loss of greater magnitude than could be dissipated by the residual helium gas in the vacuum space and by radiation. It is also surprising that the

repetitive switching of the superconducting stator windings did not also produce excessive a.c. losses. One can only conclude that the torque requirements of the gyro were so small that the currents and magnetic fields required were correspondingly small and the resulting a.c. losses were negligible. This is probably reasonable in a gyro system designed to have the minimal frictional resistance practically possible, but of course the a.c. loss problem would preclude the use of this type of motor in applications where larger torques are required.

5.8 Frozen-Flux Motor.

A motor operating on a different principle but requiring similar synchronization techniques to Schoch's flux exclusion motors has been built by Jones and Matthews at the University of British Columbia (150). This has three coils arranged symmetrically on the stator and supplied with three-phase alternating current to produce a rotating magnetic field. The rotor comprises one or more loops of superconductor.

The motor has two modes of operation: an induction mode and a frozen-flux mode. In the former, the flux through the rotor loop must stay constant (by the flux conservation principle) and consequently currents are induced in the loop to maintain a constant flux linkage, thus giving it a magnetic moment. Alternatively, it is possible to "freeze-in" a magnetic field in the superconducting loop, i.e. induce permanent currents in it. If such a current is present, the loop will act as a dipole, and interaction with a rotating field will produce a torque. The torque is limited by

critical current conditions in the superconducting loop.

The motor operates as a synchronous motor and therefore under normal running conditions there is no relative motion between the superconducting rotor conductors and the rotating magnetic field. Therefore a.c. losses do not arise in the rotor, unless the stator windings are unbalanced or the supply to them is unbalanced or non-sinusoidal. Under these conditions, a.c. losses may occur in the rotor due to the harmonic or contra-rotational magnetic fields.

As with the flux-exclusion motor, the stator windings have only to produce the required rotating magnetic field and therefore in principle can be normal windings, although in the very small ratings of the experimental motors constructed by Schoch, and Jones and Matthews, it was more convenient to make them superconducting providing due consideration was given to the a.c. losses occurring in them.

Before leaving this type of motor, it is apposite to investigate its method of torque production and to comment on the performance of a conventional polyphase induction motor so constructed that its rotor (or secondary) circuit resistance is zero. Some would reason (e.g. J.E.C. Williams in reference 150) that a conventional polyphase induction motor produces torque by the interaction between currents induced in the rotor circuit and the rotating field produced by the stator (or primary) windings; that the rotor currents are proportional to the difference in rotational speeds of the synchronously rotating field and the rotor (i.e. the slip); and further, the slip is proportional to rotor resistance.

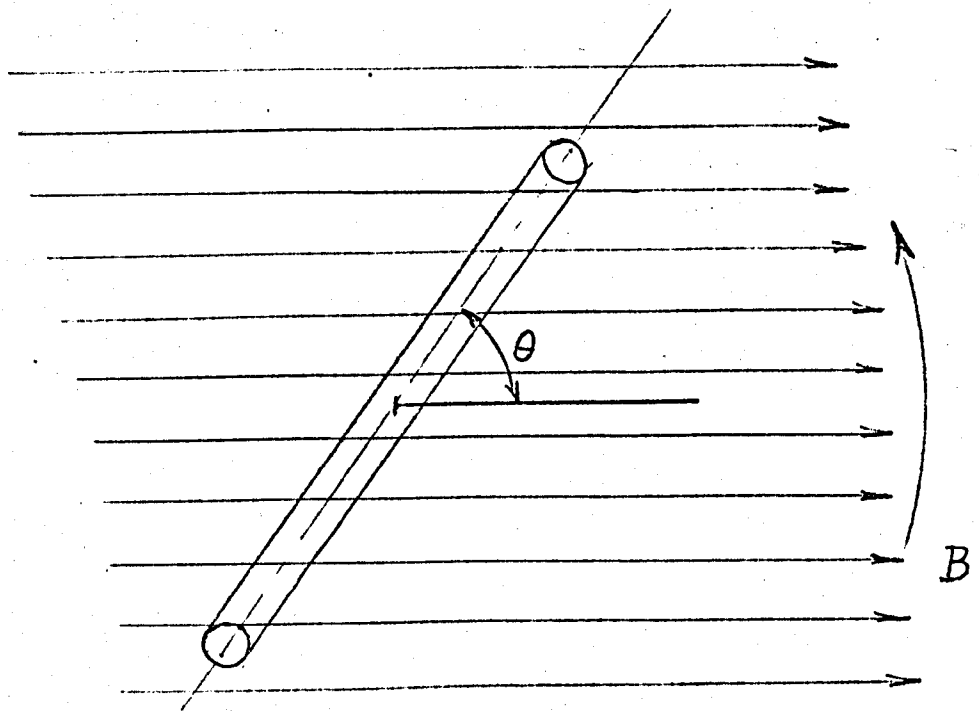


Fig. 38 Flux linkage with plane coil

Therefore, it is argued, if the rotor resistance is zero, the slip will be zero and the rotor will synchronize with the armature field rotation. This reasoning is naive and overlooks the fact that if the rotor resistance is zero, the torque produced between the rotating field and rotor currents induced by it at any speed, is also zero. This may be seen from an examination of the expression for the torque in a polyphase induction machine quoted from a standard text on electrical machines (e.g. see Bibliography 2, page 454).

$$T = K \frac{sR_2}{R_2^2 + s^2X_2^2}$$

However, this is not to say that a machine with zero rotor resistance is incapable of producing torque, but merely that the method of torque production is not due to the continuous induction of rotor currents by a rotating magnetic field. The method of torque production can be deduced as follows. Let the rotor have a plane coil with n turns of superconductor each enclosing an area A , the coil being free to rotate on its axis (see fig. 38) and forming a closed circuit of zero resistance. A uniform magnetic field of flux density B rotates at constant angular velocity past the coil. The flux linkage through the coil from the rotating field is $nAB \sin \theta$, but due to the flux linkage conservation principle, the flux linkage must remain constant. Thus a current will be induced in the coil so that the flux linkage is conserved. Let this current be i and let the inductance of each turn be L ,

$$\text{giving: } nAB \sin \theta = n^2 Li \quad (37)$$

$$\text{and } i = \frac{AB \sin \theta}{nL} \quad (38)$$

In general, i is a function of time, since θ is changing with time. The resulting torque is found from the magnetic moment of the coil, $M = nAi$, and the flux density of the applied field:

$$\begin{aligned} T &= MB \cos \theta \\ &= (A^2 B^2 / 2L) \sin 2\theta \end{aligned} \quad (39)$$

If now the coil has a frozen-in flux Φ_0 , the flux-linkage to be conserved is no longer zero, but $n\Phi_0$ and so equ. (37) becomes:

$$nAB \sin \theta = n^2 Li + n\Phi_0 \quad (40)$$

$$\text{and: } i = \frac{AB \sin \theta - \Phi_0}{nL} \quad (41)$$

$$\text{resulting in: } T = (A^2 B^2 / 2L) \sin 2\theta - (AB\Phi_0 / L) \cos \theta \quad (42)$$

Since, in general, θ is changing in time at a constant rate with respect to the coil, the mean value of torque taken over a number of complete cycles will be zero. If however θ is the constant angle between the coil and the rotating field, (i.e. the coil is rotating synchronously with the field), then equ. (42) can have non-zero values. Thus the Jones and Matthews motor must rotate at synchronous speed if it is to produce a driving torque.

The rotor of the Jones and Matthews type of motor operating primarily on the induction torque with little or no frozen-in flux would be constructed from type I superconducting material such as niobium. For a square coil of sides .02 metres and assuming a

typical value of critical field of 0.15T, the maximum torque would be less than 1×10^{-7} N-m, a very low value indeed even for a motor of these dimensions. If type II material such as niobium-titanium were to be used, appreciable flux could be frozen in (say 1T), but even so, the torque produced would probably be only of the order of 2×10^{-3} N-m. If the refrigeration requirements are included in the consideration, then it is very difficult to make a case for using either type of motor, although Jones and Matthews (150) propose its use as a positioning device in demagnetization experiments below 1K where a small mechanical movement is required without a shaft communicating with room ambient, and where the heat input must be limited to extremely low values. Few other uses can be envisaged.

5.9 Conclusions regarding utilization of Properties unique to Superconductors.

None of the machines examined so far utilizing the properties unique to superconductors is suitable for commercial development as an electromechanical energy converter. The machines employing the moving zone principle, although capable of generating very high currents, are inherently incapable of generating appreciable voltages and therefore the power involved will be small. These remarks are also applicable to the Atherton machine for the reasons discussed in Section 5.4. The pancake-disc generator and current-sheet generator cannot compete with conventional machines on a power/weight basis even if the refrigeration requirements are ignored. Although only small aircraft machines were considered in

Sections 5.5 and 5.6, they will still not be competitive as the size increases, since the power/weight ratios for both of these types of super-conducting machines and conventional types will change in a similar fashion as the size increases. This will be discussed later in Chapter 9 taking refrigeration requirements into account.

Motors employing type I superconductors must operate at flux densities considerably below those in conventional machines and will therefore produce only very low specific outputs, and the flux-exclusion motor and frozen-flux motor with type I super-conductor rotors are ruled out on this ground. Although the frozen flux machine of similar dimensions with a type II superconductor rotor should be capable of producing much larger specific outputs, it is still not worth considering. It would seem therefore that little purpose would be achieved by investigating any further the exploitation of the properties unique to superconductors in electrical machines.

5.10 Machines Utilizing the High Field Property of Superconductors.

We now turn to machines working on conventional principles of electro-mechanical energy conversion and investigate the types in which it would be feasible to employ superconducting windings, and the extent to which it would be beneficial to do so. The use of superconductors may appear to give rise to benefits because some machines would not be feasible at all without the use of super-conductors (e.g. the Harrowell reciprocating generator). This in itself is in fact no criterion, and the ultimate choice must be

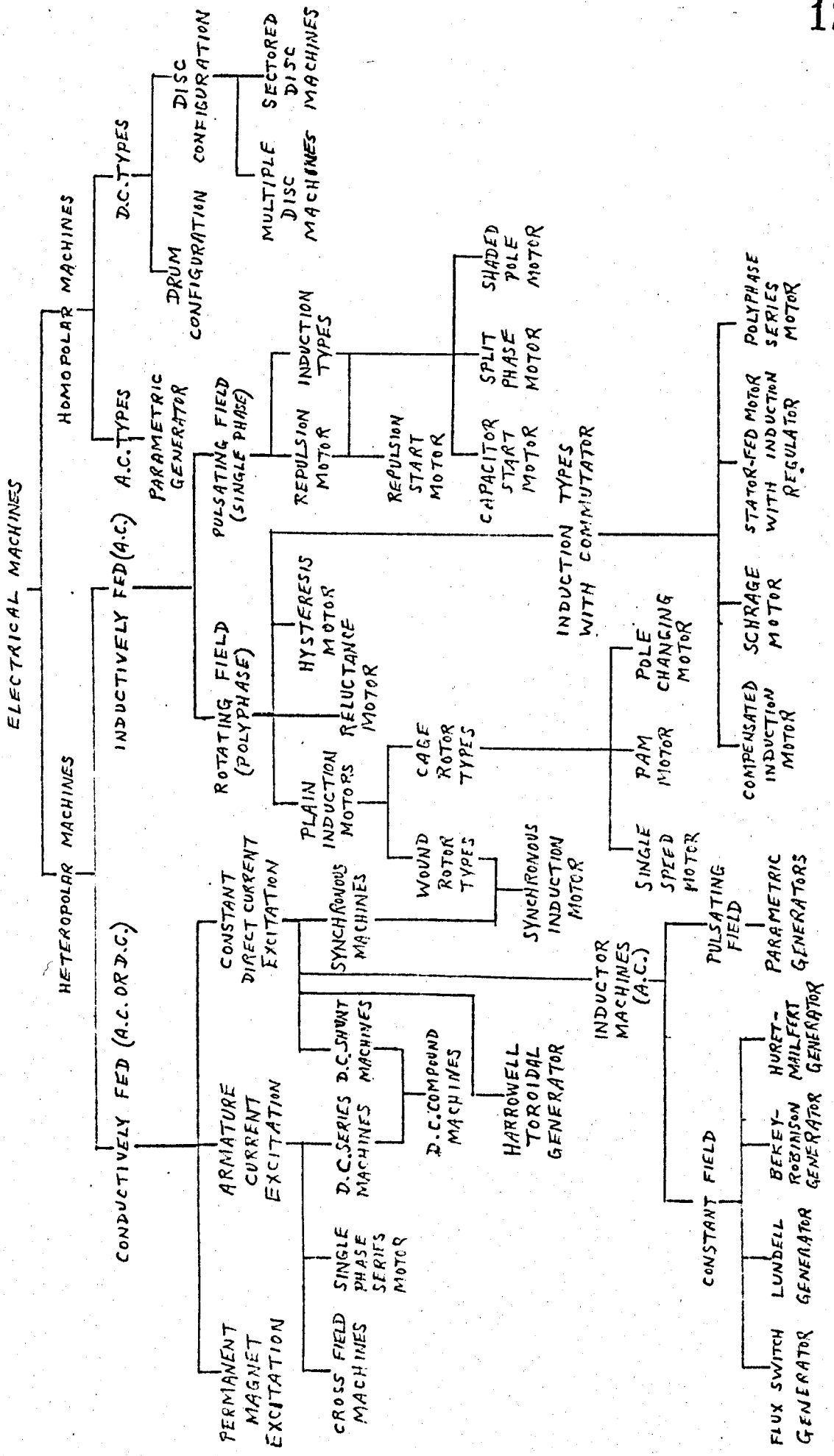


FIG. 39

based on the economics of the system of which the machine forms part. The possible advantages which may accrue from the use of superconductors have already been listed in section 5.1, and any one of these may be of sufficient importance in a given situation to make the use of superconductors worthwhile.

In general, the designer of an electrical machine is confined by three limitations: the magnetic limit, or the maximum flux density which can be produced economically in the field; the mechanical limit, or the maximum safe stress which can be allowed in the rotating parts due to the velocity of rotation; and the thermal limit determined by the current, conductor dimensions and resistivity, the allowable maximum temperature of the insulation and the heat transfer properties. By the use of superconductors which can produce very high magnetic fields in air without the necessity of using ferro-magnetic materials, it is expected that the main benefits will accrue because of the higher magnetic limit thereby gained, and to a certain extent by the higher *current loading* allowable due to the absence of iron *losses*.

It is now proposed to examine the main types of electrical machines with the object of establishing whether or not it is feasible to introduce superconducting windings in them. Figure 39 shows diagrammatically the main types of electrical machines and the relation between them. The main division is into those machines in which the magnetic poles are arranged so that adjacent poles have opposite polarities (heteropolar) and those in which adjacent poles have similar polarity (homopolar).

5.11 Homopolar Machines.

Homopolar inductor alternators operate on the principle of cyclic variation of the machine parameters, i.e. the reluctance of the magnetic circuit. Constant d.c. excitation is provided by a single stationary coil wound annularly round the shaft, and the e.m.f. is generated in stationary armature coils wound round the stator teeth by a time-variant magnetic flux, whose variation in magnitude corresponds with the reluctance variations of the magnetic circuit as the machine rotates. It is suitable for generation of alternating current at high frequencies, but has a low output power to weight ratio. The replacement of the conventional excitation coil by a superconducting winding would not be a practical engineering proposition because of the a.c. losses which would occur in the superconducting winding caused by the cyclic variations in flux. The maximum value of flux density in a parametric inductor alternator is limited by saturation in the ferromagnetic material forming the magnetic circuit and any increase above the optimum value of flux density results in a decrease of output. Thus the introduction of superconductors cannot result in improvements in output, and the only possible advantage would be the saving of the resistance loss of the field winding, which if refrigeration requirements are considered, might be more than offset by the power required to drive the refrigerator.

D.C. homopolar machines are inherently suitable for only low voltages and sometimes have suffered from the difficulty of establishing a magnetic field over a large volume in the medium of air without incurring prohibitive power losses in the field winding. This difficulty is largely removed with

superconducting windings, the use of which make the homopolar machine technically feasible for a wide range of powers and voltages, instead of it being restricted to machines intended for very heavy currents at low voltages. The economic viability of homopolar d.c. machines will be considered in detail later.

5.12 Inductively-Fed Heteropolar Machines.

Of heteropolar machines, those in which the power is transferred to the armature by electro-magnetic induction would not appear to be very attractive propositions in which to introduce superconducting windings, since such machines essentially involve single-phase or polyphase alternating currents and magnetic fields which vary in time or space with respect to the conductors, and the problem of a.c. losses in the superconductors would be of sufficient magnitude to make the machine unworkable.

5.13 Conductively-Fed Heteropolar Machines.

In conductively-fed heteropolar machines, the power is supplied to the armature either by direct connections or through a mechanical commutator. This device, the purpose of which is to reverse the direction of current in an armature conductor every time it passes from being under one pole to the next of opposite polarity, imposes severe limitations on the design of d.c. heteropolar machines (as will be explained later). The rapid reversal of current in the armature conductors takes place typically at 25 or more reversals per second, and consequently the use of superconductors in the armature is precluded on account of the a.c. losses associated with rapid current reversals.

Thermal problems also preclude their use in the armature.

The use of superconductors in the field windings is more attractive at first sight, since the field is predominantly constant in a d.c. shunt machine except for minor variations due to currents in the armature. There would, however, be considerable, if not insuperable, difficulties in providing commutating zones and interpoles (which carry armature current), and also in incorporating series windings (which are usually required) and compensating windings (which are sometimes needed) in such machines. Even if these difficulties could be overcome, the superconducting heteropolar machine would be more expensive in first cost and have a lower efficiency than the corresponding superconducting homopolar machine. The latter machine has a very simple basic configuration without commutation problems (the armature current is not reversed in the armature conductors) and therefore without the need for interpoles or compensating windings; also the field winding is not required to react the armature torque and therefore the supporting structure will be smaller in cross-section and the corresponding thermal inleaks will be much lower resulting in a higher overall efficiency. Thus the homopolar superconducting d.c. machine is to be preferred to its heteropolar superconducting counterpart.

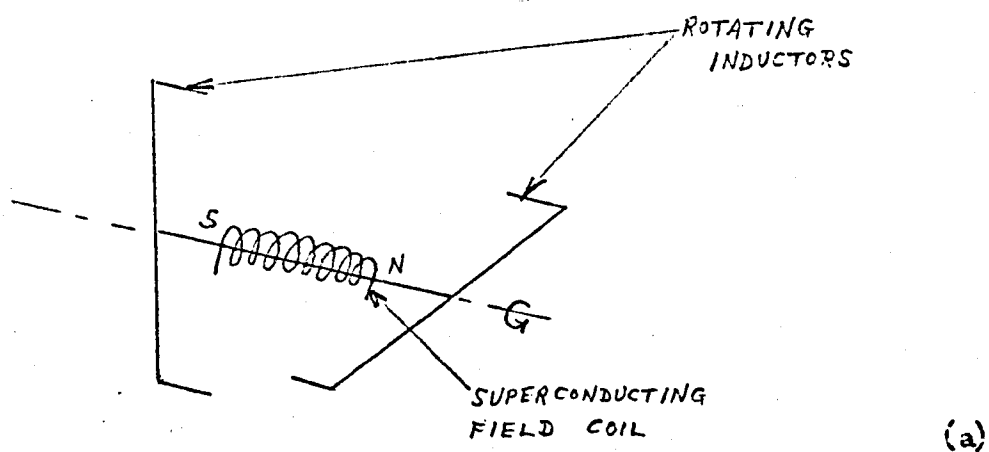
Since single-phase series motors and d.c. series and compound machines involve armature currents in their field windings, they are not practical propositions for the introduction of superconducting windings. The group of machines indicated in fig. 39 as cross-field machines and sometimes referred to as

metadynes require very small initial excitation powers and because of this, superconducting windings would not be beneficial or indeed practical in them.

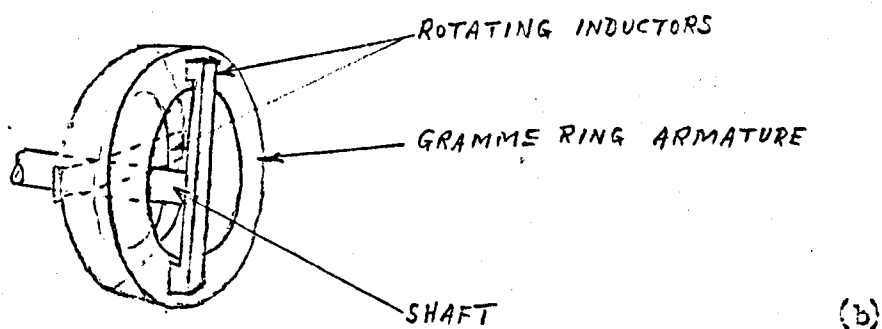
Of the heteropolar inductor machines, the pulsating field parametric types of generator need not be considered further, because of the a.c. losses which would occur in the superconductors if they were to be used in the field windings. The flux-switch, Lundell and Bekey-Robinson a.c. generators all use ferro-magnetic material (inductors) to move flux generated by stationary excitation windings past stationary armature windings. If superconducting coils were to replace the conventional excitation coils, no higher value of flux density could be used because of saturation in the inductors and the magnetic circuit would thus remain unaltered. To use superconducting windings to produce flux densities of these magnitudes in iron material would clearly be very extravagant, and so no case can be made for superconducting windings in these machines.

5.14 The Huret and Mailfert Alternator.

Huret and Mailfert proposed a type of superconducting alternator ⁽¹⁵²⁾ which in principle is similar to the Bekey-Robinson and Lundell types, but uses an armature configuration which is inferior to those machines. Basically it consists of a superconducting coil wound concentrically round the shaft which has two inductors mounted on each end of it (see fig. 40). A Gramme-ring type of armature wound on a toroidal iron core completes the magnetic circuit. The flux path can be traced out



(a)



(b)

Fig. 40 The Huret and Mailfert Alternator

- (a) Arrangement of inductors and field coil
- (b) Arrangement of inductors and Gramme ring armature.

as follows starting at the centre of the annular field coil. The flux passes along the shaft until one pair of the inductors is reached. The flux is then split into two parts radially outwards, one part following through each inductor. At the end of each of these inductors, the flux passes longitudinally backwards and across the airgap between the inductor and toroidal core, and in doing so passes some of the armature conductors. It then splits into two further parts, each part then passing circumferentially round the toroidal core for almost 90° . It then meets half the flux from the other inductor at the same pair considered originally, and these two fluxes combine and pass longitudinally past further armature conductors and across the air gap to one inductor of the second pair at the other end of the shaft. The flux then continues radially down the inductor and eventually longitudinally along the shaft to where the path commenced. Obviously, as the shaft rotates with the inductors, the flux will move past the armature conductors and so generate e.m.f.'s in them.

Thus the Huret-Mailfert machine, like the Lundell and Bekey-Robinson types, depends for its action on the presence of iron inductors to guide the flux, and therefore the magnetic limit in it is the same as in the two other types being limited by saturation in the iron circuit. However, its magnetic circuit is superior to those of both other types in that the flux has only to cross two air gaps in each complete path, whereas in the other types it has to cross four air gaps in each complete path. Besides requiring a much lower field m.m.f. for the air gaps, this arrangement results in a lower leakage flux which in turn requires even

less field m.m.f. and a lower voltage drop with load. But these advantages would exist, irrespective of whether the excitation coil is a conventional solenoid or a superconducting type, and, as has been remarked earlier, a superconducting coil in the context of iron circuits limited to less than $\sim 1.2T$ is very extravagant and is at a serious economic disadvantage. Since it is obvious that the superconducting version is not viable, it may be worth asking if a future exists for the non-superconducting version.

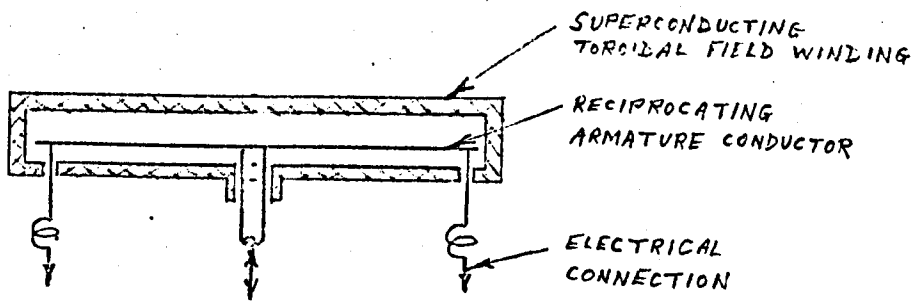
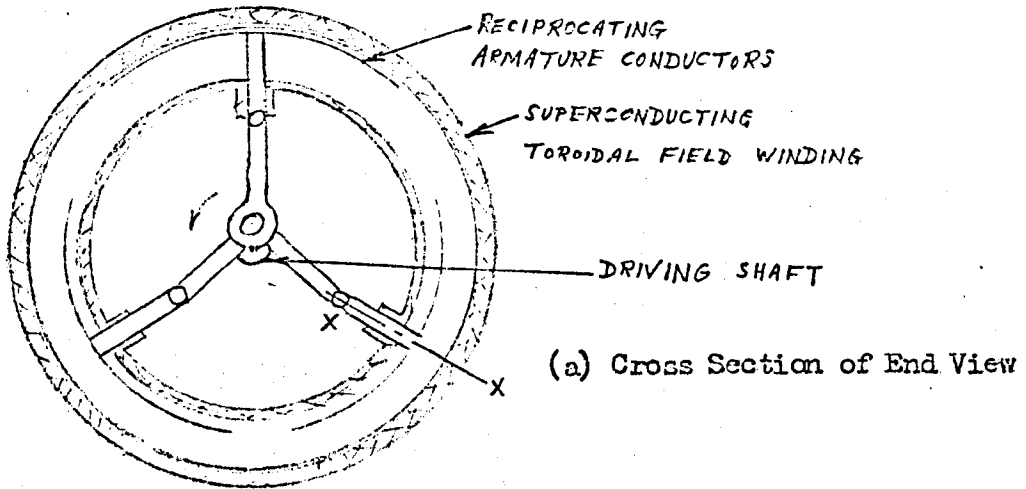
A generator without commutators, slip-rings, and particularly brushes makes considerable appeal for applications in adverse ambient conditions, and even more so if no rotating semi-conductor devices are required. The Bekey-Robinson machine is attractive for supersonic aircraft with ambient temperatures in the machine bay of $150^{\circ}C$, although its power/weight ratio may be inferior to brushless rotating rectifier generators in ratings above approximately 20 kVA. The magnetic circuit and structure weights would be approximately equal for both the Bekey-Robinson and Huret-Mailfert machines, but the armature of the latter, while being of comparable weight to that of the former, would only generate half the e.m.f. the former could produce. This is because in the Gramme ring armature as proposed by Huret and Mailfert, only one coil side in each coil at any instant is used to generate e.m.f., while in the conventional drum armature of the Bekey-Robinson machine, there are two active coil sides in each armature coil at any instant. Thus it is seen that for a given physical size of machine, the Huret-Mailfert version will only generate approximately half the power of the Bekey-Robinson type. Hence it is concluded that Huret-

Mailfert proposal has no merit which makes it worth further consideration.

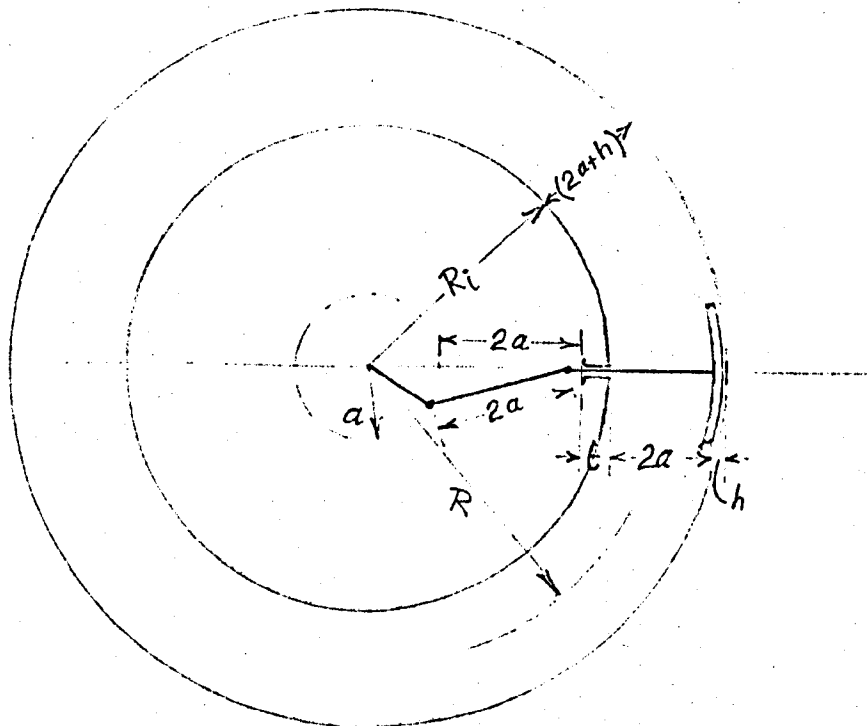
5.15 Conclusions regarding Utilization of High Field Property.

From general considerations, it is thus seen that apart from the d.c. homopolar machine, it is difficult to make even a prima facie case for the utilization of the high field property of superconductors in the electrical machines operating on conventional principles considered so far.

Of the types of machines not considered so far, only the Harrowell toroidal reciprocating generator and the synchronous machine remain. Since both are suitable for the incorporation of superconducting windings, it is proposed to examine them in detail, together with the d.c. homopolar machine, in subsequent chapters.



(b) Section on X-X



(c) Dimensions

Fig. 41 The Harrowell Toroidal Reciprocating Generator

6. The Harrowell Toroidal Reciprocating Generator.

6.1 Principle and Construction.

Harrowell has proposed (153) an ingenious generator in which the armature conductors oscillate inside a toroid. A constant magnetic field is set up by a superconducting winding in the form of a toroid, and which therefore produces practically no stray field. The armature conductors are mounted on the ends of push-rods which are radial to the axis of the toroid and are made to reciprocate by connecting rods joined to a crankshaft rotating at constant speed, as illustrated in fig. 41. In order to produce a high flux density inside the air-cored toroid, it is necessary to employ a superconducting winding for the field, but the armature conductors could be of normal conducting material, or superconducting material if the a.c. losses resulting from the armature currents could be tolerated. Electrical connections are made to each end of each reciprocating armature conductor, the conductors being joined in series by stationary interconnectors to give, within limits, any required voltage. Harrowell proposes that the interconnectors should be outside the magnetic field, but in principle they could be inside providing they are stationary. If they are inside, they would take the majority of the force reaction of the armature conductors and thus relieve the superconducting field winding of these forces. The construction and supports for it could thus be simpler, and the design of the field system would be further simplified by not having to make provision for the interconnectors to pass through the toroid walls to the outside and back again.

Also, the a.c. losses in the field superconductors would be lower because of the reduced net field resulting from the combined effects of the current in the armature conductors and inter-connectors. On the other hand, if the interconnectors occupy space inside the toroid, the maximum power output obtainable from a given toroidal volume may be reduced, because the space so occupied is not then available for power generation. However, in view of the lower stresses and simplified construction this reduction in output may not be as great as might appear at first sight. The connections between the ends of the moving armature conductors and stationary interconnectors are through flexible links, as sliding contacts would not be suitable for the large currents envisaged. Harrowell also suggests that the connections could be through springs, but gives no explanation of why they might be used instead of flexible connections. It could be that if the natural frequency of the dynamic system formed by the reciprocating conductors and springs, was made to correspond with the synchronous frequency of the electrical supply system, the forces required in the push rods, connecting rods and cranks to set up simple harmonic motion in the conductor system could be reduced considerably.

6.2 Harrowell's Claims.

Harrowell makes considerable claims ⁽¹⁵⁴⁾ for his reciprocating machine. The advantages he puts forward may be summarised as follows:

- (a) Absence of slip rings and brushes
- (b) No stray field

- (c) Better voltage regulation and system stability
- (d) Weight 0.25 of conventional machine
- (e) Approximate net cost saving of 0.4 allowing for refrigerator but not other additional costs
- (f) Stationary cryostat
- (g) Smaller length than conventional machine
- (h) No iron losses
- (i) Reduced copper losses
- (j) No a.c. losses in normal or superconducting armature conductors
- (k) Greater potential for scaling to large powers than rotary machines

Advantages for the weight and cost savings in (d) and (e) are based on design studies for 500 MW generators. The disadvantages quoted by Harrowell are:

- (a) Increased bearing losses unless driven by reciprocating prime mover.
- (b) Increased material fatigue.
- (c) Need for flexible conductors.
- (d) Radical change in design.
- (e) Increased fault current.

To these may be added the difficulty of removing the losses from the armature conductors inside the toroid to the outside.

6.3 Examination of Harrowell's Claims.

Some of Harrowell's claims of the advantages are self-evident,

such as (a), (b), (c) and (f), while (d) and (e) are plausible, but are difficult to dispute without undertaking a detailed design study. (h) is presumably based on the premise that since no iron is employed in the magnetic circuit, there will correspondingly be no iron loss; however, the push-rods carrying the conductors, although probably constructed from non-magnetic stainless steel, would nevertheless be of conducting material, and since parts of them would cut the field inside the solenoid, they would have e.m.f.'s induced in them which would give rise to eddy currents and consequently to iron losses. These could be reduced if necessary by laminating the push-rods, or completely eliminated by constructing them from carbon fibre reinforced epoxy resin. Reduced copper losses (i) would be expected because of the considerably shorter total length of the armature conductors and interconnections than would occur in a normal machine.

Because the field produced by the toroid is non-time-variant and of uniform flux density, Harrowell points out that 'by reciprocating the armature conductors, an alternating voltage is produced but, because the flux in the conductors does not change in strength or direction, no a.c. losses are produced by it in either super or normal conductors.' This statement may be questioned by pointing out that the field will not have a completely uniform flux density over the whole cross-section of the toroid, and therefore unequal e.m.f.'s will be generated at different sections of each conductor giving rise to circulating currents within the conductors and consequently a.c. losses as well. Further, since the conductors themselves will be carrying alternating current

when the generator is loaded, their apparent resistance will be higher than when carrying the same value of direct current due to the so-called skin effect. It may well be that Harrowell was only dealing with the major effects in the machine under (j), and did not intend to imply that there would be no losses due to these secondary causes. Nevertheless, in the detailed design of a machine, these would have to be taken into account and some subdivision of the conductors into parallel transposed paths would be required.

Advantage (k) claimed by Harrowell that the toroidal reciprocating machine has greater potential for scaling to large powers than the rotary (presumably the two types of rotary machines considered in the same reference ⁽¹⁵⁴⁾) is not immediately obvious. The reciprocating machine is limited by the same three considerations as for the rotating machine: magnetic, mechanical and thermal. The magnetic and thermal limits are rapidly reached in small ratings with both types of machines, so the mechanical limit remains. In rotating machines, the diameter of the rotor is increased with increasing ratings until the maximum allowable working stress induced by centrifugal action is reached, after which the length only is increased for even higher ratings. In reciprocating machines, there is no centrifugal stress in the armature, but nevertheless there are limitations due to the maximum allowable working stresses being reached. As Harrowell points out ⁽¹⁵⁴⁾, the alternating direction of the stresses in the moving parts are the worst for producing fatigue, and so, if the machine is to have an acceptable life, the stresses have to be kept below a maximum value considerably

lower than that permissible for rotary motion; a value of 40% might be anticipated. In order to explore the way various design parameters affect the alternating stresses, and to investigate the veracity of Harrowell's contention in advantage (k), a procedure for establishing the leading dimensions of a toroidal reciprocating generator will now be deduced.

6.4 Establishing the Leading Dimensions.

The position x of the armature conductors moving with simple harmonic motion is given by an expression of the form:

$$x = a \sin \omega t$$

The velocity is given by:

$$\dot{x} = a \omega \cos \omega t \quad (43)$$

and the corresponding acceleration by:

$$\ddot{x} = -a \omega^2 \sin \omega t \quad (44)$$

where a is the throw of the crank and corresponds to half

the total excursion of the conductors,

and ω is the periodicity of the supply.

It will be noted that both the total excursion of the conductors and their acceleration are independent of the dimensions of the toroid. Now the rms voltage per phase is given by:

$$E_{ph} = \frac{1}{\sqrt{2}} B \ell a \omega \quad (45)$$

where B is the mean flux density

and ℓ is the total length of the armature conductors per phase.

If J is the mean current density in the armature conductors, and

b and h their width and thickness respectively, then the total

current per phase is:

$$I_{ph} = J b h \quad (46)$$

so that the apparent power output per phase, S_{ph} , is

$$S_{ph} = E_{ph} I_{ph} = \frac{1}{\sqrt{2}} B \ell a \omega \cdot J b h$$

But $\ell b h$ is the total volume of the armature conductors per phase ($= V_c$, say), giving

$$S_{ph} = \frac{1}{\sqrt{2}} B a \omega J V_c \quad (47)$$

Now the value of B will be chosen to be as high as possible consistent with not exceeding the critical current and critical field of the superconducting coil and avoiding a transition to normality under normal operation and electrical fault conditions, ω is fixed by the frequency of the supply required and J will be determined primarily by the conductor material and the type and efficacy of the cooling inside the toroid, and also partly by the insulation thickness and similar considerations. Thus in order to minimise the volume of armature conductor material, the designer must make a , the excursion of the armature conductors, as large as possible. In fact, the designer must compromise between the quantity of armature conductor material, and the quantity of superconductor in the toroidal field coil, and do this without incurring unacceptable high stresses in the reciprocating parts.

Now the total force in the push rods required for one phase will be required to accelerate (and decelerate) the phase conductors with simple harmonic motion, to provide the mechanical power converted to electrical power and to overcome the various frictional

and aerodynamic forces set up by the rod guides and air resistance round the conductor assemblies. If the conductor supporting structure and insulation are neglected, the force required in the push rods to provide simple harmonic motion, is:

$$F_{SHM}(t) = -V_c \rho a \omega^2 \sin \omega t \quad (48)$$

where ρ is the density of the conductor material.

Alternatively, to a very coarse first approximation, the insulation and supporting structure can be considered as proportional to V_c , and ρ can then be regarded as the mean density of the reciprocating armature. Re-arranging equ. (47) and substituting V_c in equ. (48) gives:

$$F_{SHM}(t) = - \frac{\sqrt{2} S_{ph}}{B J} \rho \omega \sin \omega t \quad (49)$$

Equation (47) thus gives an approximate indication that for a machine of a given rating, the force necessary to give reciprocating motion to the armature is independent of the throw of the crank (i.e. is independent of the total excursion made by the armature).

The power input will be provided by a force acting over the total excursion distance and given by:

$$F_p(t) = B \ell i$$

where i is the instantaneous value of the armature phase current, corresponding to I , its rms value.

$$F_p(t) = \sqrt{2} B \ell I \cos (\omega t + \psi)$$

where ψ is the internal phase angle determined by the nature of the load and the internal impedance of the machine.

$$\begin{aligned}
 F_p(t) &= \sqrt{2} B \ell \frac{S_{ph}}{E_{ph}} \cos(\omega t + \Psi) \\
 &= \frac{2S_{ph}}{a\omega} \cos(\omega t + \Psi) \quad (50)
 \end{aligned}$$

substituting for E_{ph} from equ. (45). Thus from the point of view of the forces in the reciprocating parts, it is advantageous to make a , the throw of the crank, as large as possible.

The total force F_T in the push rod at its junction with the armature conductors is thus (from equs. (49) and (50))

$$F_T(t) = \sqrt{2} S_{ph} \left\{ -\frac{\rho\omega}{BJ} \sin \omega t + \frac{\sqrt{2}}{a\omega} \cos(\omega t + \Psi) \right\} \quad (51)$$

In an armature with normal conductors, the resistance, R_c , of an individual conductor of length L , thickness h and conductivity σ is given by: $R_c = L/(\sigma b h)$.

The resistance loss per conductor = $I_{ph}^2 L/(\sigma b h)$

and the loss per unit of armature surface area

$$\begin{aligned}
 &= \frac{I_{ph}^2 L}{\sigma b h} \cdot \frac{1}{2bL} \\
 &= \frac{I_{ph}}{bh} \cdot \frac{I_{ph}}{2b} \cdot \frac{1}{\sigma} \\
 &= \frac{J}{\sigma} q' \quad (\text{say})
 \end{aligned}$$

where $q' = I_{ph}/2b$. It is more convenient to write q for $2q'$ so that:

$$b = I_{ph}/q. \quad (52)$$

Thus knowing suitable values for q , b can be determined from equ. (52). At present, no data are available for either q or J , but suitable values could be obtained from tests and modified subsequently as experience is gained in the design of this type of machine.

In the case of superconducting armatures, an equivalent parameter can be deduced from which the width of the superconducting composite can be determined as a function of phase current. In both normal and superconducting armatures, the thickness of the armature conductors can be calculated from: $h = V_c / \ell b$ (53)

Turning now to a consideration of the dimensions of the toroid which for minimum length of a single turn of the superconducting wire should have a square section. On this criterion, the length of each active conductor will be equal approximately to the total conductor excursion, or $2a$. In a detailed design, allowance would have to be made for the thickness of the conductors and their insulation and supports, but these are neglected in this consideration. Thus, the number of active armature conductors per phase is given by:

$$Z_{ph} = \ell / 2a \quad (54)$$

and the length of circular arc occupied by one armature phase will be $b \times Z_{ph}$.

The circumference of the toroid, $2\pi R$, at the mean positions of the armature conductors will be three times the length of the circular arc occupied by one armature phase with due allowance to avoid mechanical interference between the ends of adjacent armature

phases in the course of their reciprocating motion. Thus:

$$2\pi R \approx 3 bZ_{ph}$$

$$\text{or } R \approx \frac{3b\ell}{4\pi a} \quad (55)$$

Now the value of R needed to accommodate the number and width of armature conductors given by equs. (52) and (54) can be expressed in terms of the crank throw a and dimensions. From inspection of fig.41,* it can be seen that:

$$R = 4a + t + h/2 \quad (56)$$

where t is the length of the push rod guide. This assumes a conventional arrangement for the crankshaft so that the little end bearing always remains outside the faces of the cranks. In a machine with a normal armature, t will be of sufficient length to pass through the inner cylindrical wall of the toroidal cryostat and also to provide a smooth sliding action between the push rod and its guide. To a first approximation, it will be assumed that $(t + h/2)$ equals a. With a superconducting armature, the push rod must provide thermal insulation as well as a smooth sliding action. A possible material might be carbon fibre reinforced plastic, but in any case, a longer push rod would be desirable in order to provide a longer thermal path. If the outside diameter of the machine is not to be increased unduly, it will probably be necessary to keep $(t + h/2)$ to about 2a or less; for the purpose in hand, a value of 2a will be assumed. Hence equ. (56) becomes:

$$\begin{array}{l} \text{For normal armature:} \\ \text{For superconducting armature:} \end{array} \quad \begin{array}{l} R = 5a \\ R = 6a \end{array} \quad \left. \vphantom{\begin{array}{l} R = 5a \\ R = 6a \end{array}} \right\} \quad (57)$$

Treating a as a variable and equating the values for R given by

equ. (55) and (57) in the two cases, enables the value of a to be estimated from the power output rating of the machine and the permissible values of the design parameters, as follows:

$$R = \frac{3b\ell}{4\pi a} = ka$$

From equ. (45), $\ell = \sqrt{2E_{ph}}/Ba\omega$ and from equ. (10) $b = I_{ph}/q$, so substitution for ℓ and b gives:

$$a^3 = \frac{3\sqrt{2E_{ph}} I_{ph}}{4\pi kB\omega q}$$

But $3E_{ph} I_{ph}$ represents the total apparent power output of the machine, S , so giving a value for the crank throw as:

$$a = \sqrt[3]{\frac{S}{2\sqrt{2}\pi kB\omega q}} \quad (58)$$

where k is a constant depending on the type of machine, and having a value of between 5 and 6.

6.5 Relative Magnitudes of Armature Forces.

At this stage, it is instructive to obtain some very approximate values for the coefficients of the sine and cosine terms in equ. (51). The following values are assumed:

$$\rho = 8000 \text{ kg/m}^3$$

$$B = 5 \text{ tesla}$$

$$J = 8 \times 10^6 \text{ A/m}^2 \text{ for non-superconducting copper armature conductors}$$

$$\text{or } J = 4 \times 10^9 \text{ A/m}^2 \text{ for stabilised superconducting niobium titanium clad with copper (mean density).}$$

The value of J for copper conductors has been deliberately chosen to be high to make the case for normal armatures as strong as possible. It must be remembered therefore that the results based

on this figure will be optimistic.

For 50 Hz Machines.

(a) Non-superconducting armature

a in m	$\rho\omega/Bj$	$\sqrt{2}/a\omega$
.01	.063	.45
.1	.063	.045
1	.063	.0045

(b) Superconducting armature

a in m	$\rho\omega/Bj$	$\sqrt{2}/a\omega$
.01	1.26×10^{-4}	4500×10^{-4}
.1	1.26×10^{-4}	450×10^{-4}
1	1.26×10^{-4}	45×10^{-4}

For 400 Hz Machines

(a) Non-superconducting armatures.

a in m	$\rho\omega/Bj$	$\sqrt{2}/a\omega$
.01	.5	.055
.1	.5	.0055
1	.5	.00055

(b) Superconducting armature

a in m	$\rho\omega/Bj$	$\sqrt{2}/a\omega$
.01	10×10^{-4}	550×10^{-4}
.1	10×10^{-4}	55×10^{-4}
1	10×10^{-4}	5.5×10^{-4}

Certain conclusions can be drawn from these figures which would help to clarify Harrowell's statement in reference (153) that it has not yet been decided whether the armature should consist of superconductors or normal conductors. Certainly for 400 Hz alternators (which would be largely for transport applications and where the saving of weight would be of considerable importance) the non-superconducting armature would not be suitable. The penalty incurred by the force for reciprocating the armature (over ten times the force providing useful output) would make such machines too heavy and expensive to be competitive with conventional types. If the armature is superconducting, the force for reciprocating the armature is insignificant compared with the useful force when the crank throw is small, and only becomes comparable with it at values of throw which would be larger than could be used in 24000 rpm machines.

With 50 Hz machines, it is obvious that the superconducting armature enables very much more effective use to be made of the material in the mechanical mechanism, than does the non-superconducting armature. With non-superconducting armatures there is

probably a limit to the maximum throw which it is advantageous to use, and it may be preferable to use an additional set of cranks and armatures in order to obtain higher ratings than to go on increasing the throw indefinitely. This deduction does not lend support to the statement claimed as an advantage by Harrowell in (k) above. The larger throws may be necessary for the higher ratings of machines, and it is here that the mechanical limit of maximum allowable working stress becomes operative.

6.6 Design Procedure.

In determining the leading dimensions of a toroidal reciprocating generator for a given voltage and output, whether with a superconducting or normal armature, the choice of the value of the crank throw a is crucial, since it is this value that determines how near the optimum criteria the resulting machine will be. A preliminary value for a could be chosen on the basis of equ. (58) and from this the magnitude of the resulting forces in the reciprocating mechanism assessed, commencing with that at the junction with the armature from equ. (51). The forces in the remainder of the mechanism (push rods, connecting rods, crank, crankshaft and big and little end bearings) can then be determined, together with the proportions and dimensions of these parts and the corresponding stresses. If the maximum stress in any part is excessive, a larger value of a must be chosen. It should be noted that since equ. (51) is a function of Ψ , the internal phase angle of the machine, it is important that the phase angle of the load be specified and that some estimate of the armature reactance/resistance ratio be available.

The design procedure is then as follows:

1. Determine a preliminary value for a from equ. (58).
2. Calculate the resulting forces in the parts of the mechanism using equ. (51) for those at the armature end of the push rods, and estimate the probable maximum stresses.
3. If the probable maximum stresses are unacceptably high, increase the value of a and repeat (2) and (3) until the stresses are acceptable.
4. Determine ℓ , the total length of armature conductor per phase, from equ. (45). A value of B , the flux density, will be needed, but a value of 5 tesla can be assumed as a conservative figure for niobium-titanium superconductor.
5. Calculate V_c , the total volume of armature conductor material per phase, from equ. (47). A value for J , the mean current density will be required based on best available estimates, and eventually on test data.
6. Calculate b , the width of the individual armature conductors, from equ. (52) for which a value of q is needed.
7. Calculate h , the thickness of the armature conductors from equ. (53).
8. Determine R , the mean radius of the toroid from equ. (56).
9. Estimate the maximum allowable length of circular arc, C , of one armature phase ($< 2\pi R/3$) making allowance to avoid mechanical interference between adjacent phases.
10. Determine number of conductors per phase, Z_{ph} , from

$$Z_{ph} = \frac{C}{b}$$

11. Determine length L of individual armature conductors from

$$L = \frac{e}{z_{ph}}$$

12. Estimate dimensions of cross-section of toroid, making allowances for clearances, connections at ends of armature conductors, thickness of armature conductors, etc. Thus:

$$\text{width of toroid (inside)} = 2a + h + \text{allowances,}$$

and:

$$\text{axial length of toroid (inside)} = L + \text{allowances.}$$

At this stage, the designer has determined the principle dimensions of the machine and can then proceed to details of the design, and to predictions of its performance characteristics.

7. Homopolar D.C. Machines

7.1 Types of Homopolar Machines.

There are two main categories of direct current machines: homopolar and heteropolar. In the former there is only one basic pole, so arranged that the active conductors move through a field of constant intensity. This category has hitherto been employed only in very rare instances because of the extremely large MMF required to establish the magnetic field; it is because superconducting coils can produce appreciable magnetic fields over large volumes in air, that homopolar d.c. machines become practicable. The voltage generated in the armature conductors is constant in magnitude, and although slip rings and brushes are required to conduct the current from the rotating to the stationary member, they are not required to act as a reversing switch. In the commonly used category of d.c. machine, the active field system consists of a number of poles arranged so that adjacent poles are of opposite polarity with the result that the e.m.f. generated in each active conductor alternates with a frequency determined by the product of the speed and the number of pairs of poles.

Various arrangements of magnet systems have been devised for homopolar machines. The simplest consists of a single coil which produces a magnetic field which is approximately parallel to the axis of the field coil, at least in the plane of coil and inside it. The armature consists of a conducting disc rotating inside the coil, and connections are made to it via brushes and sliprings

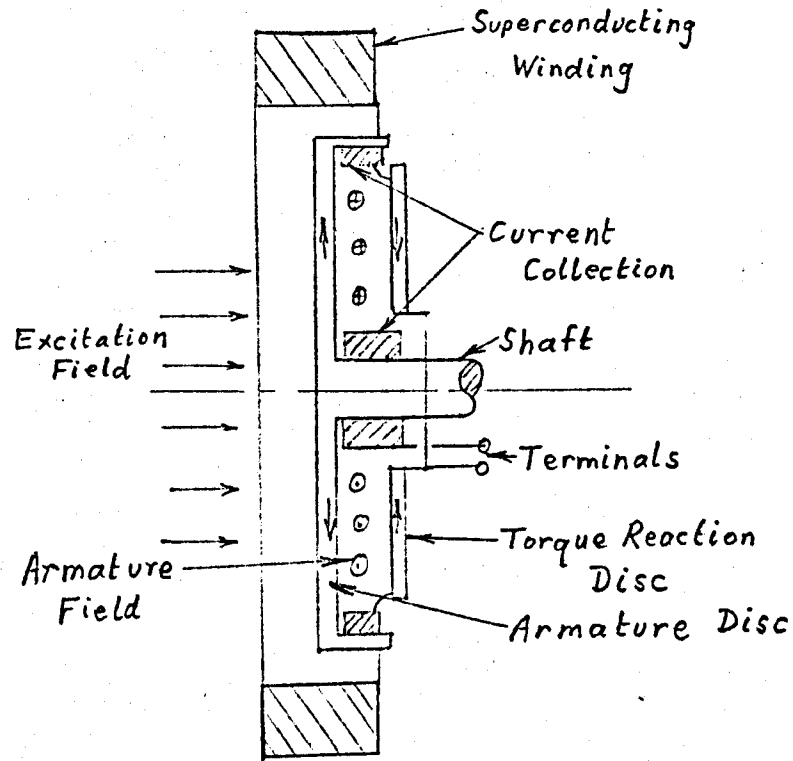


Fig. 42 (a) Arrangement of Disc Homopolar Machine

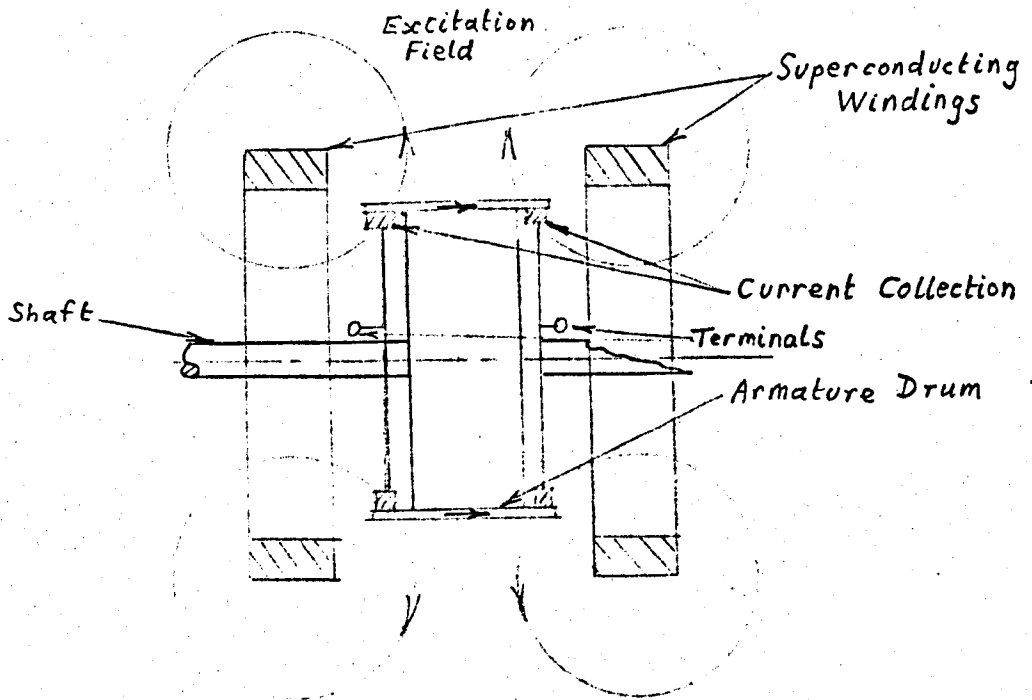


Fig. 42 (b) Arrangement of Drum Homopolar Machine

situated on the shaft and on the outer edge of the disc (fig. 42). With a non-superconducting field coil, the magnetic field which could be established was extremely low, and therefore the homopolar machine was inherently limited to very low voltage applications. For example, a homopolar disc generator with a rotor diameter of 160 mm. and rotating at 3000 r.p.m. in a field of 0.1T, a value which cannot reasonably be exceeded with a normal coil, generates an e.m.f. of 0.1V.

An alternative field arrangement can be obtained from a pair of coils carrying currents in opposite directions resulting in an approximately radial field pattern between the coils. The armature conductors are arranged axially between the two field coils, and are each connected to a slip-ring at either end. This results in an armature with a barrel or drum configuration and with the number of slip-rings equal to twice the number of active conductors. This arrangement enables the individual conductors to be connected in series, but the number is limited by the space available for the slip-rings, from each of which the full current output of the machine has to be collected. It is largely this difficulty of satisfactory collection of current combined with the inherently low voltage that has limited the use of both disc and drum types of homopolar machines to extremely rare applications where very low voltages (below 1V) and very heavy currents of several thousand amperes are required. Since the flux is constant, the iron losses are very low, but this is more than offset by the heavy losses at the slip rings. Further, until recently it proved more difficult to collect current satisfactorily from their slip

rings than from a commutator in a heteropolar machine.

7.2 The I.R.D. Homopolar Disc Machine.

The use of superconducting coils enables the flux density to be raised to values in the region of 6 to 7 teslas, but even with the addition of several discs on the shaft, the disc machine is still inherently a low voltage, high current machine. An ingenious way of increasing the voltage has been developed by I.R.D. Ltd. (155) in which the rotor disc is divided into a number of insulated sectors. Each sector generates a voltage equal to that generated by the complete disc, and thus by connecting the sectors in series by brushes, an increased voltage is obtained. In order to prevent the brushes short circuiting the output and also to avoid the sectors from being open-circuited, brushes are placed on alternate sectors. Hence the total voltage generated is equal to the voltage per sector multiplied by half the number of sectors (see fig. 43). This system merely involves the transfer of current from one set of rotor conductors or sectors to the next, the limitation to which is that the time constant of the circuit so formed is very much less than the time available for the transfer. Since the circuit has only a single turn, and there is no ferromagnetic material associated with it, the leakage inductance, and hence the time constant will be extremely low. Appleton (155) claims the values involved are well below those at which sparking at the brushes might be expected.

A disadvantage of the simple arrangement shown in fig. 43 is that a high voltage would exist between two adjacent sectors,

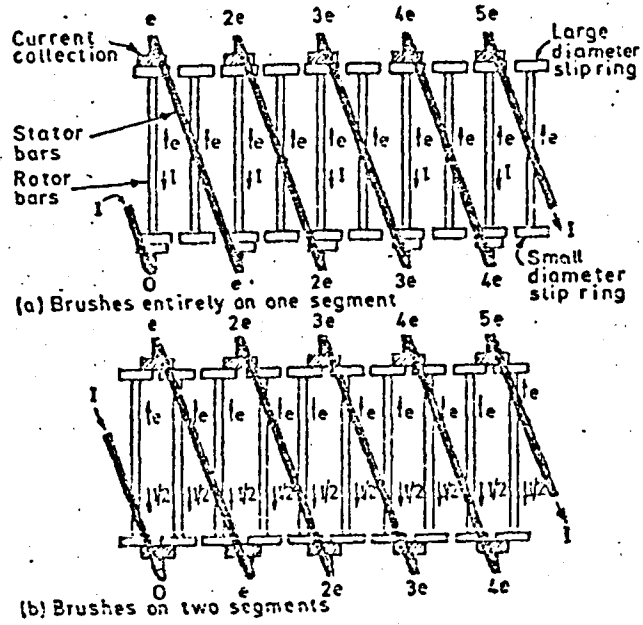


Fig. 43 Principle of Sectored Rotor

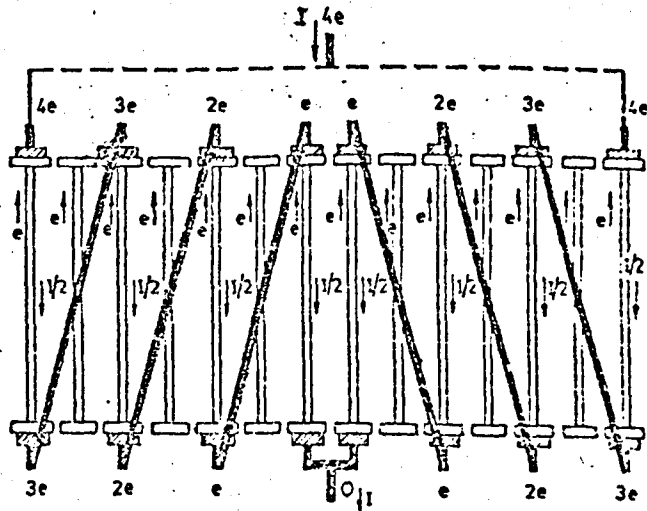


Fig. 44 Series-parallel arrangement of Sectored Rotor

which is highly undesirable since it could lead to flashover between them. Appleton has therefore introduced a series-parallel arrangement ⁽¹⁵⁵⁾ shown in fig. 44 in which the maximum voltage between any adjacent sectors is limited to that generated in one sector.

One advantage of this design is that by arranging radial conductors for the armature current between the peripheral and central brushes, and by placing them close to the armature discs, the superconducting field coil is relieved of nearly all of the reaction torque, and therefore the dewar supports can be minimal, with correspondingly small heat leaks.

This type of machine is capable of operating as a motor or generator, but is pre-eminently suited for very large ratings at high torques and low speeds, such as rolling mills, ship propulsion, and large hydraulic pumps. Appleton ⁽¹⁵⁶⁾ claims that the sectored disc machine is suitable for use as a high-voltage d.c. generator with voltages up to 30 kV and with power ratings up to 30 MW. This variety of machine would presumably operate at a much higher speed than in the motor applications just mentioned, and although the value of its voltage is low for d.c. transmission, it does open the possibility of it being applied to this application.

So far as is known, only two machines of this type have been constructed to date, both by the International Research and Development Co. Ltd. at Newcastle-on-Tyne. The prototype machine ⁽¹⁵⁷⁾ produced a power of 50 hp at a speed of 200 r.p.m. The field coil was wound from a composite niobium-zirconium fully stabilised conductor with a copper matrix. The coil had 2000 turns,

carried a current of 200 A and produced a field of approximately 3T at the outside of the double disc armature which had a radius of 15 inches. The brushes were of a conventional type with a high copper content (86%).

The other machine built by I.R.D. ⁽¹⁵⁵⁾ with support from the N.R.D.C. was a 3,250 hp, 200 r.p.m. motor which was tested under industrial conditions by driving a cooling water pump at the new Fawley power station of the C.E.G.B. It was intended to be a direct substitute for a conventional a.c. motor running at 900 r.p.m. through a 4½:1 reduction gearbox. The superconducting motor drove the pump through a 1:1 gearbox to take up the difference in heights between the motor shaft and pump shaft.

The 3,250 h.p. I.R.D. motor used a fully stabilised niobium-titanium/copper composite superconducting field winding weighing 5¼ tons and costing £60,000. The mean current density in the five strands of superconductor in the composite was 3,000 A/cm², and the field current of 725 A was obtained from a thyristor supply. The mean diameter of the coil was 101 inches with a motor bore of 88 inches. The flux density in the bore was approximately 4 tesla. The magnet, when it was cooled down, took three weeks to do so. The field was unloaded rapidly into a dumping resistor with a maximum voltage of 300 V; the field inductance was 55 henrys.

The helium refrigerator cost has been quoted ⁽¹⁵⁶⁾ as £40,000 and it would have a capacity to liquefy 30 litres of helium per hour; its input power was 80 kW. The losses in the cryostat were estimated at 25 W at 4.4 K, plus 100 W at 70 K to cool the heat shield and 300 W to cool the leads from ambient to 60 K.

Gaseous helium at 70 K was used to cool the heat shield, and no liquid nitrogen was employed.

Efforts are being made to avoid the use of liquid helium and investigations are in hand at I.R.D. to use niobium tin cooled by helium vapour. Also, by the judicious use of iron it might be possible to increase the permeance of the magnetic circuit in order to reduce the m.m.f. required thus enabling economies to be made in the amount of superconductor required. This was one conclusion drawn from the 50 h.p. motor project.

The armature voltage was 430V and full load current was 5800 A. This supply was taken from a 6-phase unfiltered thyristor/diode rectifier. The rotor was water-cooled and the overall motor efficiency was thought to be about 95% on full load.

It should be noted that I.R.D. has done considerable work on current collection and brushes, and has produced several novel and ingenious developments, besides the use of carbon fibres. It was originally intended ⁽¹⁵⁶⁾ to use silver-plated carbon fibre brushes, but as far as can be determined, the motor at Fawley employed graphite brushes with a high copper content. Strong objections have been raised by various speakers at conferences (e.g. at that reported in ref. 1) against carbon fibre brushes, mainly on the grounds of very high costs, debris and high wear rates. Since carbon fibre brushes were not employed in the Fawley motor, it is inferred that there is some truth in these objections, in spite of claims by Appleton ⁽¹⁵⁶⁾ that the new brushes have a life of 10,000 hours at a current density of 320 A/in² and a peripheral speed of 10,000 f.p.m. Clearly some further work and independent testing

is required in order to resolve the opposing claims.

For larger machines at low speeds, say above 5 MW, there may be advantages in employing the drum-type of homopolar machine because of limitations on the maximum practical diameter of the disc-type rotor and the voltage per sector which can be generated.

That the 3,250 h.p. Fawley motor was a useful exercise in which considerable expertise and valuable experience were gained, is undisputed. Whether or not it was an unqualified success, or indeed whether it can be regarded as an engineering success at all, is questionable. It has been reported (158, 159) that the helium refrigeration system gave considerable trouble, and perhaps its manufacturer would have been prepared to have expended more development effort in producing more reliable equipment if a higher price had been paid for the refrigeration system. It was also reported (158) that the rotor overheated badly on load, and in fact full load was sustained for only a few minutes. In any case, the motor was not put in service for 12 to 18 months as originally envisaged, presumably because it failed to convince the C.E.G.B. that it met the specification for the duty intended. At least, it demonstrated the technical feasibility of a large homopolar machine employing a superconducting field winding. Whether or not it is worthwhile proceeding with the development of such machines, is a matter of economics and available markets. It is proposed to examine the former aspect in more detail and to mention the latter in the light of any conclusions drawn from the economic considerations.

7.3 Economic Considerations of Homopolar Sectored-Disc Machines.

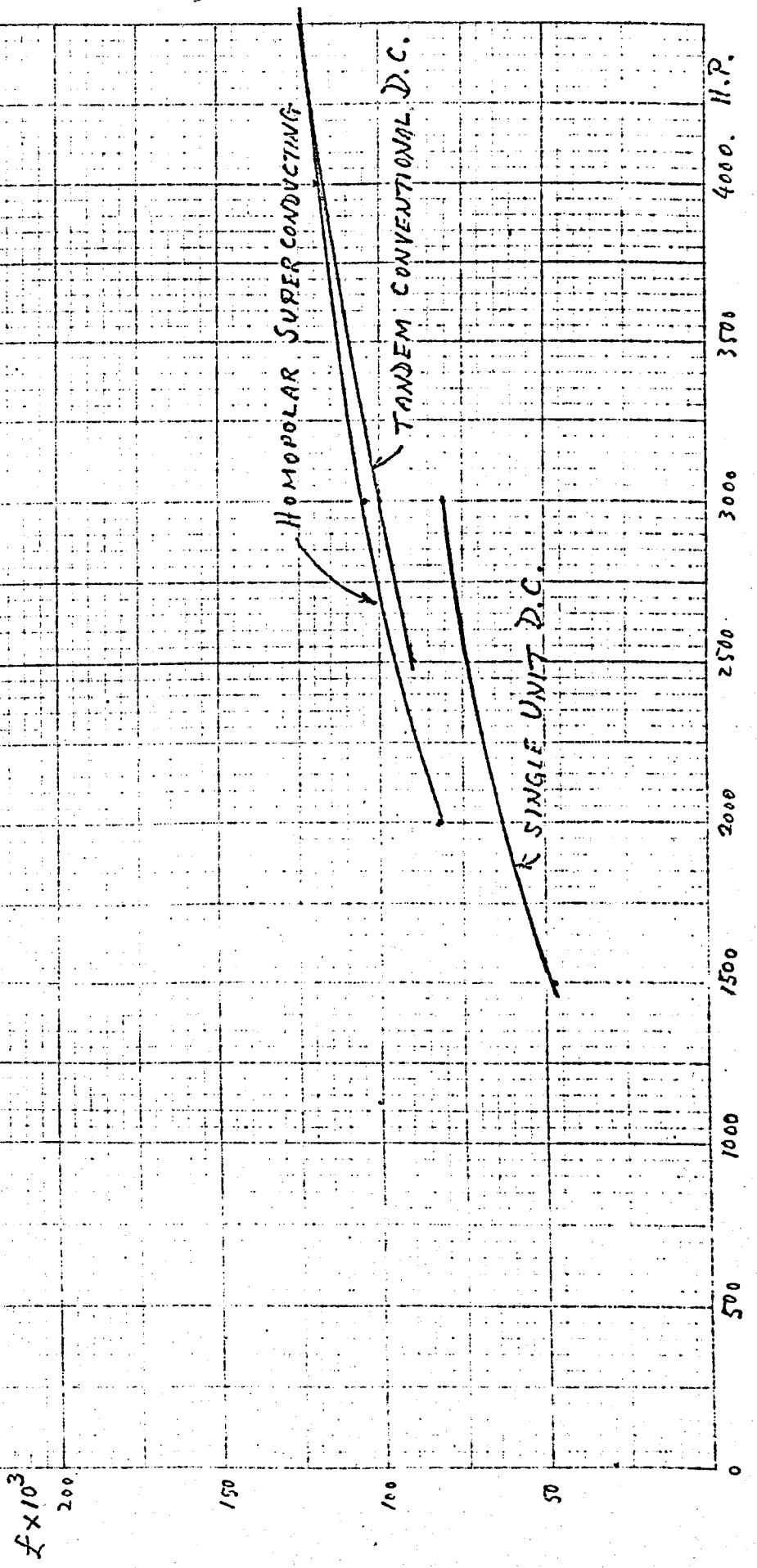
The economic breakeven point between conventional and homopolar sectored-disc d.c. superconducting machines has been quoted (111, 156, 160) as being at about 3000 h.p. and 200 r.p.m. Above this rating it is claimed that the superconducting motor with the necessary refrigeration plant would be cheaper than the conventional machine. It would also be about 1/6 of the weight (111), which in some applications would be an important consideration. In comparative studies between large conventional variable-speed machines and superconducting machines, several important other factors must also be borne in mind. As with most comparisons, this type is only strictly valid when considered on a system basis. The lower weight of the superconducting machine enables considerable savings to be made in foundations and basic structure. It will probably have a higher efficiency; various estimates have been quoted from 1% higher at 3000 h.p. (156) to 3% higher 8000 h.p. In some installations, particularly low speed, as for example in marine propulsions, it may be possible to omit the step-down gearbox required by the conventional machine. Superconductor material costs are remaining constant in terms of monetary values (161) and therefore falling in real values; helium refrigerator costs are falling rapidly, while conventional machine costs are rising. All these factors would point to the economic break-even point for capital cost becoming lower than the 1968 figures already quoted, were it not for an important factor not yet mentioned. There needs to be a considerable drop in the estimated capital cost of the superconducting machine in ratings below 3000 h.p., as the I.R.D.

comparison is based on the conventional machine consisting of a pair of half-rating machines running in tandem. The 3000 h.p. rating can be considered as the limiting power for transition from a single machine to a tandem-pair based on conservative design; there is thus a discontinuity in the cost/power curve at around this rating which means that the superconducting type must show a reduction greater than this if it is to be at a capital cost advantage below 3000 h.p.

The question to be asked is whether or not the break-even rating for the I.R.D. machine is realistic. The price of a 3000 h.p., 200 r.p.m. tandem-pair conventional machine would be between £100,000 and £105,000 (162). Taking the quoted costs of the refrigerator and the superconducting material together for the I.R.D., 3,250 h.p. motor gives £100,000 to which must be added the cost of the cryostat and vacuum equipment, sectored rotor, brush gear, water cooling arrangements, supporting structure and bearings. Clearly the direct material and labour costs with the factory on-costs will make the cost of this prototype machine considerably in excess of that of its conventional counterpart. Development costs have been entirely neglected in this consideration, but even so, it is perhaps unfair to compare the cost of the prototype machine with that of conventional types. It is therefore necessary to extrapolate for anticipated future costs if a satisfactory comparison is to be made, and to exclude development costs completely.

For large d.c. machines (162), material, including purchasing and handling on-costs, accounts for between 40% and 50% of the

FIG. 45 - COSTS OF 200 R.P.M. MACHINES



price, and labour with direct workshop on-costs (such as workshop buildings, cranes, tools etc.) for between 20% and 25%, the lower material percentage cost usually being associated with the higher labour cost, and vice versa. Testing accounts for 5%, and the balance of approximately 25% to 30% covers drawing office and estimating, fixed overheads and profit. This breakdown is applicable to single-armature machines, tandem-pair armature machines of comparable rating (where this is feasible) being approximately $12\frac{1}{2}\%$ more expensive. Conjectural designs were prepared for conventional 200 r.p.m. d.c. machines of ratings from 1500 h.p. to 4000 h.p. and the cost of the basic materials estimated for them. Using the above cost breakdown percentages and making reasonable assumptions regarding the variation in manufacturing on-costs with size, prices for these machines were estimated. Necessarily, these estimates will not be very accurate, but they do give a fair basis for comparison with the corresponding superconducting machines. For these a similar procedure was followed in arriving at a comparable price for the machine alone. Superconductor costs were obtained from references 109, 155 and 161 and a mean value of £2 per A-km was used. Refrigeration costs were obtained by estimating the heat leaks into the cryostat, and using cost data from reference 109. The results are plotted in fig. 45 from which it will be observed that the cost curves for the tandem-pair conventional machines and the superconducting machines intersect at a very acute angle, and since the accuracy of both curves is not very high, it would be unrealistic to draw too definite conclusions from them. It can be inferred however that the break-even point for capital

cost is not well defined, but it is certainly not below the transition rating from a single conventional machine to a tandem-pair. It is also apparent that it is desirable for much more accurate cost assessment studies involving detailed designs to be carried out, but such studies are beyond the scope of the present work and would need to quantify such items as the comparative reliability of both types of machines including sub-systems such as refrigeration. Although large d.c. superconducting machines would not appear at present to offer a large margin, or possibly even none, in respect of capital cost, yet the prognosis is good if the present trends in superconductor and helium refrigerator prices continue. Appleton⁽¹¹¹⁾ considers that if superconductor costs could be reduced to £1½ per A-km and refrigeration prices could be reduced by 20%, the prospects for d.c. motors would look good. Although the first condition may now obtain, (since Goodman⁽¹⁶³⁾ gives a price of £1.3 per A-km at 4 tesla), the second has not been achieved and until it is, the main cost benefit seems to arise, not from reduced capital costs of the actual machine, but rather in terms of the economic advantages accruing from lower losses, and smaller and lighter machines.

7.4 Market Prospects.

The commercial prospects for superconducting sectored-rotor d.c. machines must be viewed in the context of the market for electrical machines as a whole. The production of a.c. motors manufactured in the U.K. from 1967 onwards has remained approximately constant at about £40m. per annum and the production of

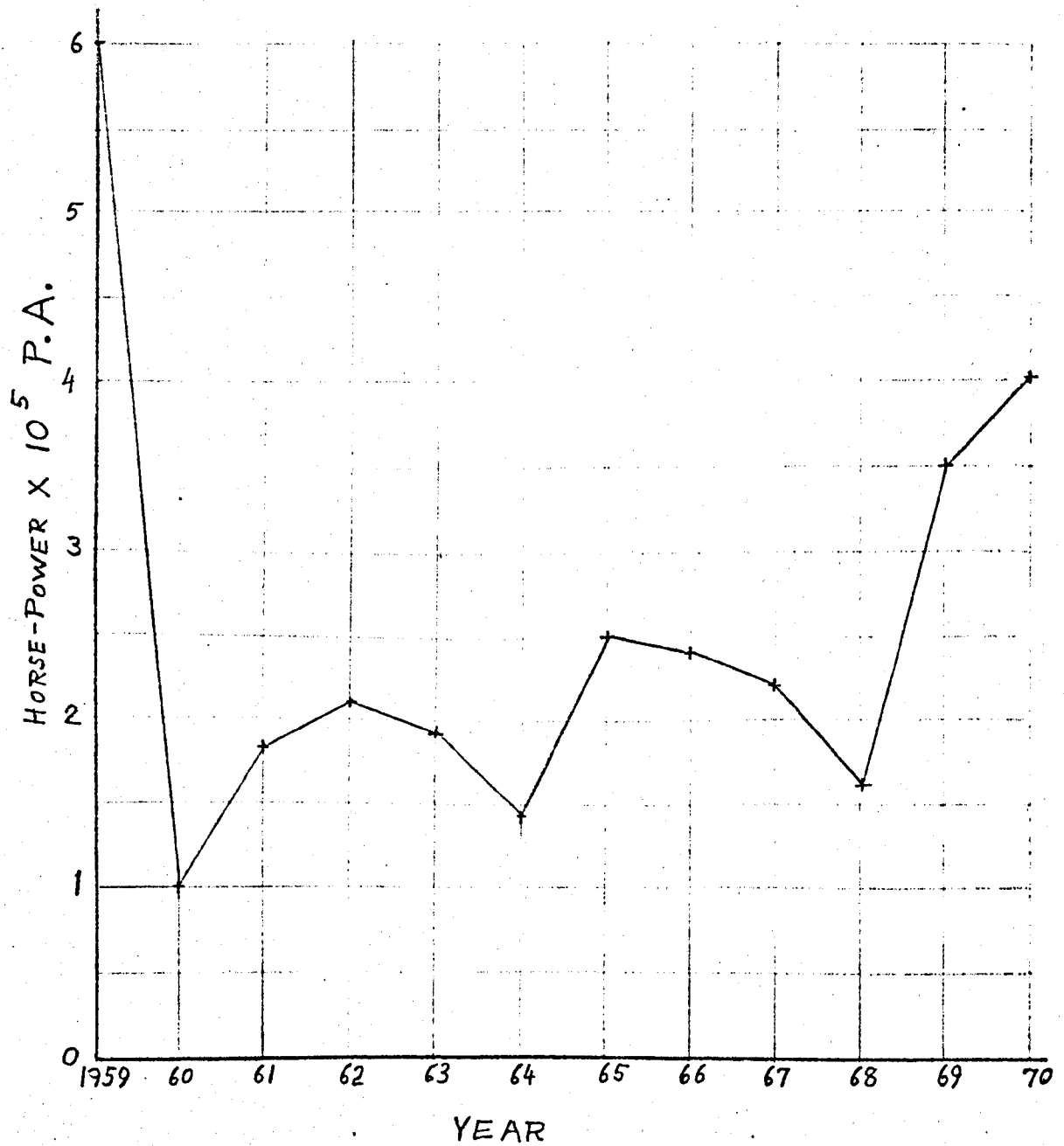


Fig. 47 Annual Production of D.C. Machines over 1,000 H.P.

a.c. generators (excluding turbo-generators) has also remained constant but at about £8m per annum. The production of d.c. machines below 1000 h.p. fell steadily for a number of years and was £12m in 1967 and £9m in 1968; there was an increase in 1969 but the rate of production has remained at approximately the 1968 level subsequently. These values are taken from the relevant Business Monitors published by the Board of Trade, (now the Department of Trade and Industry).

In the case of d.c. machines over 1,000 h.p., corresponding production figures are not published by D.T.I., but Appleton (155) quotes the value of such motors sold in the U.K. in 1965 as £5.4m. Although apart from this one figure, annual values have not been available, it did prove possible to obtain the annual U.K. production of the motors over 1000 h.p. since 1959 in terms of aggregate horse power (164). These are shown in fig. 47. Unfortunately figures after 1969 are not available because the organisation responsible for producing them was disbanded in 1969.

The remarkable feature of the graph in fig. 47 is the dramatic fall in production from the reasonably constant level prior to 1959 of 600,000 h.p., to 100,000 h.p. in 1960. Production has remained low, although rising slowly, ever since, and reached approximately half the 1959 level by the end of 1969. The other feature, common also to Continental manufacturers, has been the way production followed a four-year cycle.

The main consequence of the very depleted market for large d.c. machines has been that prices for them have been based on marginal costing. It has not been possible to carry out a thorough

survey of prices during the period since 1959, but from such evidence as is available (164) it seems that all machines in this category are being sold at 80% or below of the price based on normal costing procedure incorporating the proper proportion of fixed costs. In a few cases, the price has been as low as 55% of that arrived at by normal costing.

This position needs to be understood in relation to superconducting machines, since unless price comparisons are made on the same basis for both superconducting and conventional types as in section 7.3, the true competitive commercial position of the former with respect to the latter will not be correctly assessed. Because this point has been missed by some who have been critical of estimates quoted by I.R.D., they have concluded that "break-even" points are not as low as the I.R.D. quoted estimates, and then they have further concluded that prospects for large superconducting d.c. machines are not as favourable as in fact they may be. Whether a worthwhile market for large d.c. machines exists at present or will do so in the future, or whether such a market can be created are separate questions.

The general depression of the market for all d.c. machines is probably largely due to a contraction in some industries such as coal-mining, rationalisation and automation in steel-making, coal and mineral mining (overseas) and similar industries, improved techniques requiring smaller motors, the changeover from d.c. to a.c. in ship supplies, the cost reduction in silicon diodes and the development of the thyristor. The declining market resulted in prices of d.c. machines of all sizes falling. For example,

statistics (163) supplied by a large industrial organisation which purchases large numbers of electric motors show that the average price of d.c. motors fell by 31% between 1958 and 1963, while the average price of a.c. motors fell by only 3½% in the same period. Although these figures are not up to date, it is believed that they are still indicative of the relative profitability of manufacturing both types of motors.

The development of low frequency a.c. supplies from thyristor inverters in very large powers in the megawatt range has made variable-speed drives employing non-commutator a.c. motors a practical possibility combined with economic viability. An example of such a drive (165) is a 6 MW synchronous motor driving a cement kiln in Belgium. The motor has a speed range of 8 to 19 r.p.m., and the complete installation has given satisfactory service since 1970. The existence of such drives diminishes the prospects for d.c. superconducting machines, but assuming that the latter can be developed successfully, applications for motors of this type could be considered where:-

- (a) Very low speeds and high torques are required, (e.g. marine propulsion, mine winders, submarine motors) particularly where low weight and compactness are desirable.
- (b) Powers above, say 3000 h.p., where a wide range of speed control is required, (e.g. steel mills: reversing, multiple stand).
- (c) Motors of a few hundred horse power, where very rapid response to speed control is required and where the much smaller rotor mass and armature inductance enable this to be achieved.
(e.g. continuous multiple sequence strip and plate mills,

aluminium foil mills, paper mill drives).

- (d) High current, very low voltage d.c. supplies are required to be converted to a.c. supplies (e.g. at the receiving end of a d.c. superconducting cable).
- (e) High voltage, d.c. supplies require conversion to a.c. (e.g. at the receiving end of a conventional d.c. link).

Applications for generators of this type exist where:-

- (a) High current, low voltage d.c. supplies are required, (e.g. marine propulsion, electrolytic zinc extraction, refining of copper, vacuum arc furnaces, aluminium smelters, electro-deposition and electrophoresis, etc.). The superconducting machine may score on grounds of efficiency, ease of control and fast response, compactness and weight over other supplies such as conventional generators, and diodes and thyristors. The latter may generate prohibitive harmonics in the a.c. supply, which could be avoided with a motor-generator set.
- (b) High current, low voltage d.c. supplies accurately controlled and free from ripple, (e.g. magnets for physics research).
- (c) Large d.c. power supplies are required in industrial complexes, (such as chemical plants, dockyards, factory areas, electro-chemical plant for production of chlorine, hydrogen, oxygen, etc.) and where possibly large quantities of heat at comparatively low temperatures are also required. Such complexes may justify a "total heat" scheme with local electrical generation.
- (d) Traction and rapid transit system supplies are required characterised by low voltage, high current and regeneration, (i.e. feeding back to the supply).

Thus viewing the market situation as a whole, in spite of an impressive list of possible applications, it would not appear to be a prudent commercial exercise to undertake the development of d.c. homopolar machines as a private venture because:-

- (a) of the contracting market for d.c. machines with ratings over 1000 h.p.,
- (b) prices for large d.c. machines are based on marginal costing,
- (c) alternative drives employing a.c. machines and thyristor supplies are being successfully marketed,
- (d) of the smallness of the market in relation to the cost of individual units,
- (e) of lack of sufficient capital cost advantage above 3000 h.p. at 200 r.p.m., and higher capital cost below this rating.

As far as is known, the only machines of this type under construction at the present time in the U.K. are a generator and a motor for a marine propulsion system sponsored by the Ministry of Defence (Navy) (159). Mole et al report (167) that a number of developments are under way in France, Japan and the United States on superconducting homopolar machines for various applications, but principally ship propulsion.

7.5 Other Superconducting Homopolar Machines.

It is generally recognised that in order to fully utilize the magnetic flux developed by superconducting magnets in homopolar machines, very high density current collection systems are required; (see, for example, Appleton in refs. 155 and 159). Other considera-

tions for the current collection system are low voltage drop, ability to operate at a high slip-ring velocity, and low wear rates with low friction. This has led to the use of the high copper content graphite brushes and to development of the silver-plated carbon fibre brushes already noted. A variation of the solid brush material has been proposed by Yamamoto (166) who planned to use silver graphite brushes in a superconducting homopolar generator with multiple armature discs of 1.2m diameter.

The alternative method of current collection in homopolar machines of both non-superconducting and superconducting types has been achieved using liquid metal collection systems, and as Mole et al remark (167), non-superconducting machines employing this method have been built for a number of years. They have utilized simple centrifugally fed collectors and jets with mercury and sodium-potassium as the liquid metals. Only limited information is available regarding operating experience with these machines, but it would be reasonable to assume that since none of them has been used extensively for commercial application, there are economic problems which prevent commercial exploitation.

The very high fields present in superconducting homopolar machines cause severe losses in the liquid metal current collection zones, and recently designs of homopolar machines have been evolved specifically to reduce the flux densities in these zones (167).

Extensive studies have been conducted at Laboratoire Central des Industries Electriques (L.C.I.E.) to determine the most suitable liquid metal for use in superconducting homopolar

machines (168). The choice of liquid metal lies between sodium-potassium, indium-mercury, gallium-indium, and gallium-indium-tin, and all of these are hazardous in one way or another. Sodium is highly reactive in the presence of moisture, mercury is toxic and unacceptable in many locations, while gallium is slightly toxic and highly corrosive. Systems using these materials must be carefully designed to prevent leakage, and to exclude oxygen. The most commonly used liquid metal is NaK and normally a nitrogen blanket is employed with it.

It appears that under certain flow conditions, probably non-laminar, these materials produce non-negligible quantities of scale or amorphous powder. These particles of powder are troublesome, since they take the place of the liquid alloy and interfere with the current collection. The solution proposed by Robert (168) is to exclude the basic causes of the problem, i.e. impurities and absorption of gases. Thus it is necessary to use very pure alloys or metals and to prevent exposure to absorbable gas atmospheres. As a result of the extensive investigations at L.C.I.E., mercury-indium was selected for use in the homopolar machine. Gallium-indium was rejected because black powder was generated in the closed system.

The homopolar machine eventually developed by L.C.I.E. (169) is a 60 kW motor with a novel flooded rotor. This represents a significant development in that all the space between the rotor and stator is filled with liquid metal and the sides of the rotating and stationary discs are insulated. The basic configuration of the flooded rotor concept is illustrated in fig. 48,

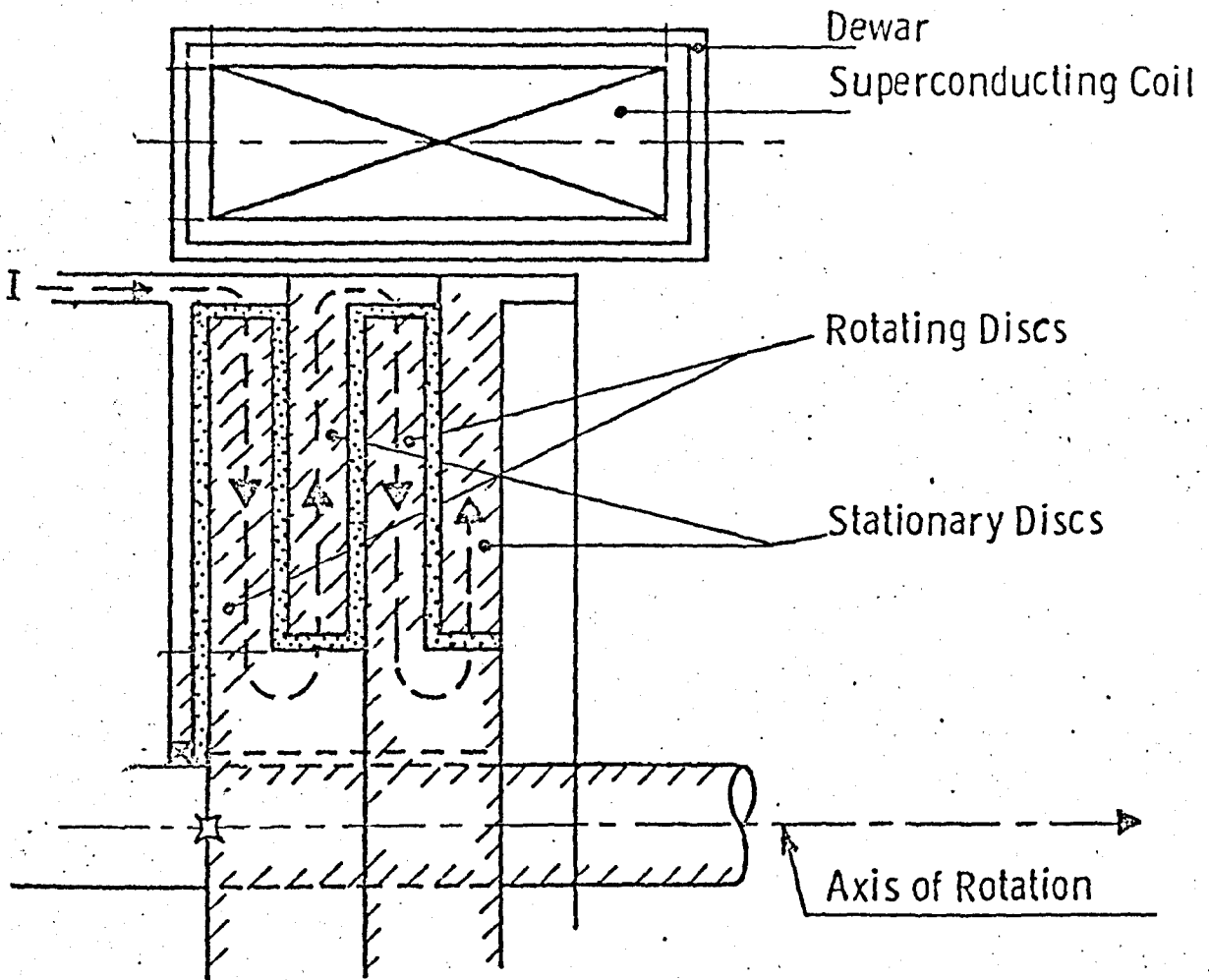
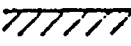


Fig. 48 Flooded-rotor Homopolar Machine

Insulated Surface 
 Liquid Metal 
 Armature Current 

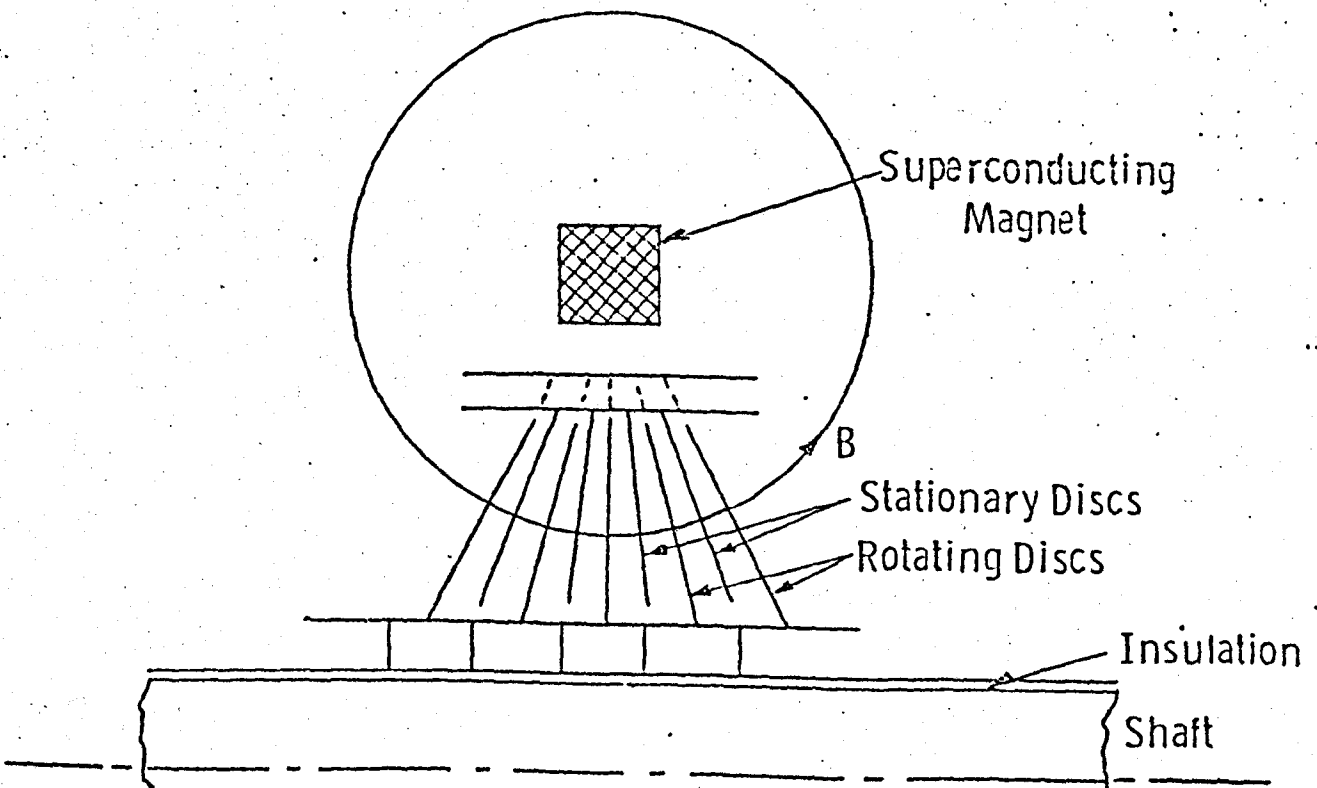


Fig. 49 Basic arrangement of L.C.I.E. Motor

while the basic arrangement of the L.C.I.E. motor is presented in fig. 49. It has five rotor discs insulated from each other and interleaved with the stationary discs. All of the discs are set at angles such that the magnetic flux is perpendicular to each disc in the system.

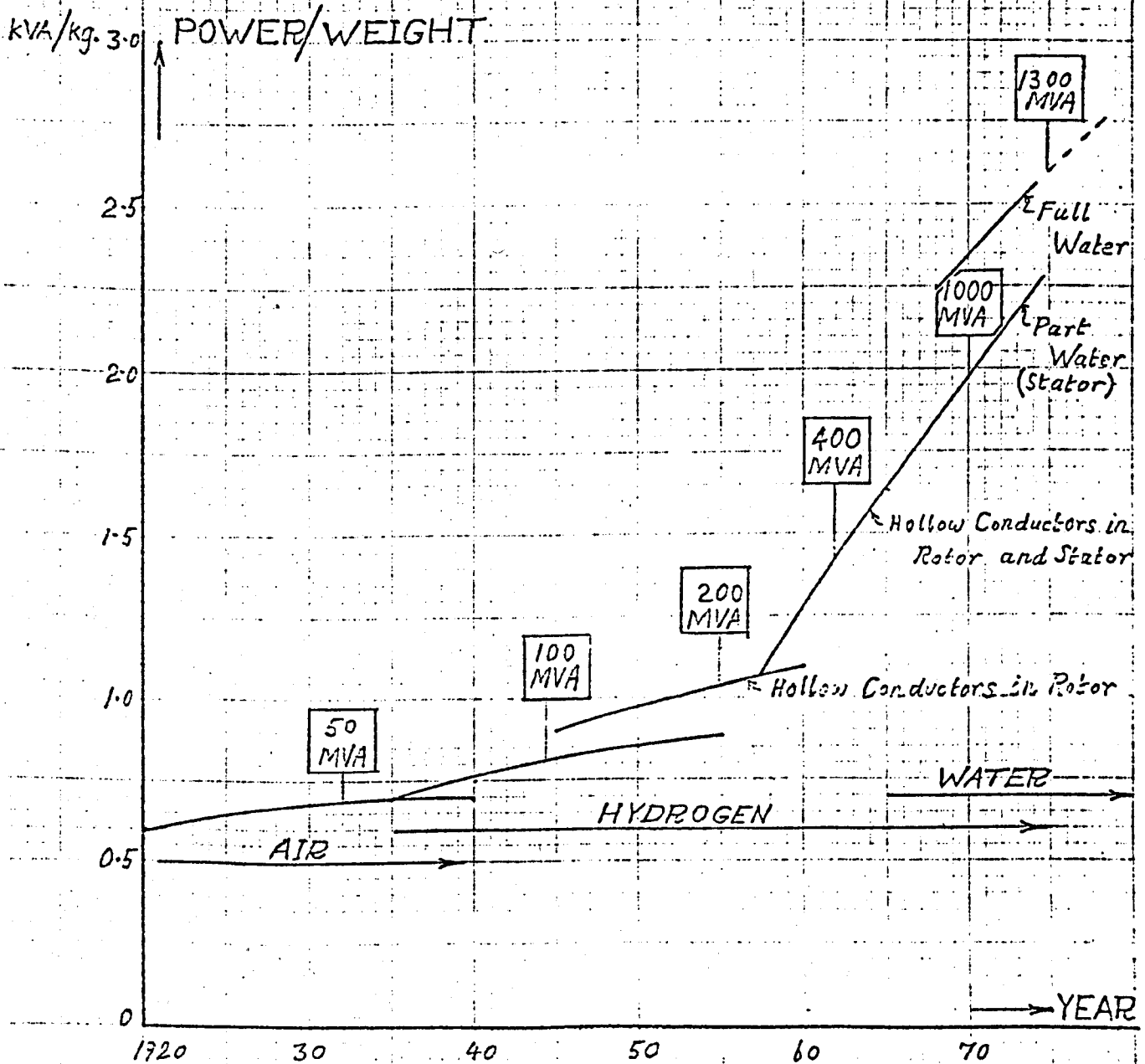
The machine, while not without its problems, has been tested successfully and produced 56.5 kW at 600 r.p.m. with an efficiency of 82%. The viscous losses on the sides of the discs are proportional to the cube of the disc velocity ⁽¹⁶⁷⁾ and are very severe at high speeds. This concept of the machine is therefore limited to low speeds and small diameters.

8. Large Synchronous Machines.

8.1 Turbo-Generator Development.

The demand for electrical power doubles approximately every ten years in the U.K., and in order to meet this demand the aggregate generating capacity must be increased by a corresponding amount. The ratings of the generators installed to meet the increased demand have also increased at approximately the same rate. With the trend towards bigger and bigger units, it is to be expected that turbo-generator designers should be considering methods of raising the limit of the maximum rating for which it is possible to design a single unit. The limit to the largest rating that can be successfully designed is imposed by magnetic, thermal and mechanical stress considerations. Improvements in materials have contributed to make machines with larger ratings possible (170, 172) but the main contribution has been due to improved methods of cooling. These have resulted in more effective use being made of the generator material, and hence in greater power being obtained per unit weight. This development is summarised in fig. 50 where power output per unit weight is plotted against year of manufacture. Also shown is the maximum rating which can be achieved with each type of cooling. The largest unit generators ordered to date are 1,300 MW, and these must be approaching the maximum practical rating which can be achieved without some further radical development in electrical machine technology (172). From the survey given by Arnold in reference 170, of predictions for the requirements of maximum

FIG. 50 - TURBO-GENERATOR DEVELOPMENT IN TERMS OF POWER PER UNIT WEIGHT AND MAXIMUM RATINGS FOR EACH TYPE OF COOLING.



generator ratings, it seems clear that 2000 MW sets ~~could~~ be required by 1980, and that ratings of 3000 MW will eventually be required. As Arnold states in his survey, at present interest is concentrated largely on single-unit generators; generators in tandem will not be an economic proposition as long as it is possible to build unit generators of the required output.

The use of larger sizes for turbo-generators results in units which are more economic. Furthermore the capital costs of building new power stations are reduced by using larger units. The C.E.G.B. claims ⁽¹⁷¹⁾ that due to the use of larger units, for the five-year period, 1960 - 65, its power station capital costs fell by 20% in spite of a 30% rise in price levels of building materials and labour, and this trend has continued.

Unless the policy to use larger and larger generating units is reversed, new developments must be evolved which will enable these higher ratings to be achieved. The use of refrigerants, such as freon, for cooling the rotor can be envisaged as a possibility, with resultant lower resistance of the field winding and consequent reduced field losses and higher efficiency. The next logical step might be the use of a cryogenic cooling medium, such as liquid nitrogen, for the rotor, with further reduction in resistance and improvement in efficiency, although the power required for the refrigerator would offset these to some extent. Both of these types of cooling media could also be used in the stator and further advantages gained.

The logical conclusion to this approach is, of course, superconductivity, at least for the field winding. Whether superconducting stator armature windings will be advantageous or not, depends on the development of a suitable superconductor. As Appleton points out (155), to achieve the present efficiency of a 500 MW turbo-generator, the a.c. losses in a superconducting armature winding would have to be limited to about 5 kW because of the refrigerator power required. This limit is probably orders of magnitude away from the present performance of superconductors at power frequencies. Thus the application of superconductors is limited to the field winding, a view shared by a number of other investigators including Mole (1), Sabrie (174), Woodson et al (178) and Lorch (1).

8.2 Advantages of Superconducting Excitation Windings.

Besides the attraction of extending the maximum ratings of the largest machines which it is possible to manufacture thereby gaining further economic advantage from the resulting unit ratings, superconducting field windings are attractive in smaller ratings of turbo-generators as well. A number of studies have been published from various laboratories where the advantages likely to accrue from the use of superconducting turbo-generators in power generation systems have been investigated. These include Thullen and Smith (173), Sabrie (174), Mole, Haller and Litz (175), Stekly and Woodson (176), Smith, Kirtley, Thullen and Woodson (177) and Woodson et al (178). There is considerable overlapping of material in these and similar reports, but the main potential

advantages relative to the conventional machines can be summarised as follows:

- (a) Lower weight and volume. Superconducting field windings enable higher flux densities to be employed, and the absence of magnetic iron provides increased volume for active armature conductors; it also reduces the insulation requirements since each conductor need not be insulated for the full phase voltage to earth, but only for the voltage between turns, providing the overall insulation requirements to earth are met. To a first approximation, the flux density can be increased by a factor of 2 and the specific current loading by a factor of 2, thus enabling up to about 4 times as much power to be anticipated from a given frame size.
- (b) Reduced costs. The stator constructional materials are conventional and less are required. *If*, the ferromagnetic core is absent, the expensive and labour intensive process of stacking the laminations is eliminated. Superconductor and refrigerator costs at the large ratings required are modest in relation to the other costs. Further economies result from the smaller foundations and buildings required, and also from easier shipment and reduced site erection expenses.
- (c) Higher terminal voltage. The simplified stator insulation arrangements should allow higher terminal voltages to be used with lower currents and with consequent savings in the unit transformer.

- (d) Higher efficiency. More effective use of space reduces stator copper losses and the absence of the ferro-magnetic core eliminates iron losses. Reduction in size reduces windage losses. The superconducting field requires almost negligible excitation power, but this is partly offset by the refrigeration power required.
- (e) Improved electrical characteristics. The synchronous impedance of a superconducting generator will be very low so that in effect there is no steady-state stability limit and it can be operated at its full MVA rating under-excited down to zero power factor.

Although the rotor inertia is considerably lower, it is possible to reduce the transient reactance also. This, combined with the lower synchronous reactance giving a smaller rotor angle, results in improved transient stability under large changes in load or under electrical system fault conditions.

Another electrical advantage is the effect of the thermal shield which acts as a damper (or amortisseur) winding, and reduces the effect of unbalanced loading by reducing negative sequence currents.

- (f) Improved mechanical characteristics. For a given rating, the rotor will be shorter and have significantly higher critical speeds and hence less tendency to develop vibration problems.

8.3 General Features of Superconducting Turbo-Generators.

A synchronous machine has three main windings: an alternating current armature winding, a direct current excitation field winding and a damper winding interposed between the armature and field windings. When a generator supplies current to a load, the current in the armature sets up a flux wave in the air gap which rotates at synchronous speed and interacts with the flux produced by the field current to give electromagnetic torque. Mechanical driving torque must then be applied from a prime mover to sustain rotation.

A superconducting synchronous generator has the same general features and winding arrangement as a conventional machine, but considerable changes in the design details are required in order to achieve a practical machine arrangement. A re-appraisal of the basic configuration for large turbo-generators has been undertaken by a number of designers (173 - 178), and invariably a rotating field system is favoured. The problems of constructing and cooling a rotating vacuum-insulated cryostat and current leads for the superconducting field winding are considered to be less severe than the construction of a reinforced plastic rotor with embedded conductors and a high voltage, very high current, three-phase current collection system. Such a system would be very large, require considerably maintenance and would be very costly. There is also agreement that the field should rotate inside an annular armature, since this configuration requires less superconductor, a smaller and simpler dewar, a smaller shield system and allows more space for the armature and a simpler construction than if the

armature is inside a rotating dewar.

The armature winding on the stator is constructed without a ferromagnetic core or teeth, and this requires the use of transposed finely stranded conductors to reduce eddy current losses in the conductors. This is treated in detail in Chapter 13.

The superconducting field winding must obviously be supported on a low temperature structure and maintained at a temperature close to that of liquid helium. Thermal leakage from ambient into the low temperature zone and, in particular, thermal leakage along the leads between the slip-rings and field winding, will require special attention so that it is reduced as much as possible. A helium transfer system is required to convey liquid helium from the stationary member to the rotor dewar and back to the stationary member. It is also necessary to isolate the superconducting winding from non-synchronous alternating fields originating from the armature currents. These will arise primarily from the unbalanced currents in the three phases, or from asymmetric placing of the windings in relation to each other. A high conductivity shield placed between the armature and field windings and rotating with the latter should be capable of attenuating most of these fields, but the design of the shield needs careful consideration. This shield also performs the function of the damper winding in a conventional machine, and will have considerable influence on the sub-transient characteristics of the machine. The location of the damper shield in relation to the vacuum complicates the issue. A system with the damper shield in the vacuum will require shaft vacuum seals, the development of which is certainly non-trivial,

and the use of helium exhaust from the field winding to cool the damper shield. The location of the damper shield outside the vacuum will require the shield to be much thicker because of its higher resistivity at the higher temperature outside the vacuum and will require cooling to remove the eddy current losses in it. This latter configuration will consist of two separate structures one of which will contract and expand in relation to the other. A compromise solution might be the use of a liquid nitrogen cooled shield, but this would involve the transfer of liquid nitrogen to the rotor. The choice of damper shield location may largely depend on the particular requirements of the individual machine. Considerable theoretical analysis is required to determine the performance and characteristics of damper shields which will subsequently require experimental verification.

Another significant problem relates to the effect of the rotating magnetic field inducing currents and forces on adjacent objects, and the reactions of these on the rotor possibly causing dynamic instability. Two methods of keeping the rotating field within the confines of the machine have been proposed (175); one method is to use a thick laminated iron screen on the outside of the armature, while the other is to utilise a solid cylinder of high conductivity around the armature in which eddy currents are induced. The iron screen reduces the reluctance of the machine magnetic path, improves the magnetic coupling between field and stator windings, and allows minimum active rotor length. The alternative eddy current screen attenuates the rotating field, and thus the superconducting field winding will tend to be

demagnetised; because of this and the inferior electromagnetic coupling between the windings, a larger superconducting field winding is required than in the iron screen version. The iron screen machine will be more efficient than the eddy current screen version, the difference being due to the eddy current losses in the latter. The weight of the iron screen machine, according to Mole et al (175) will be about one-third of that of the corresponding conventional machine, but the eddy current screen machine may be only one-tenth of its weight. Again considerable detailed examination of the two methods is required, and the ultimate choice may well depend on the application for which the machine is intended. The theoretical aspects of these two methods of screening will be considered in Chapter 15.

8.4 Economics and Market Prospects.

The pricing and marketing of large turbo-generators and other heavy electrical equipment is currently presenting considerable difficulties in the whole of the Western world. In the U.K. this has become a political issue. The implementation of the Richardson Report on Britain's key heavy electric plant industry would have given manufacturers a better deal in home markets but could have backfired badly on exports. The problem is that with the trend towards bigger and bigger single generating units, the need for long term planning becomes essential if manufacturing capacity is to be kept fully employed, and yet able to meet

the demands made upon it. It is fortunate for the British turbo-generator manufacturers that they managed to secure considerable export orders during the lull in ordering by the C.E.G.B. At the end of July, 1969, the total capacity of generating plant being built for overseas customers amounted to 16,000 MW, compared with 11,770 MW of home business in hand. The increased demand for generating plant in North America and the lack of manufacturing capacity by North American manufacturers, coupled with competitive prices and deliveries from British manufacturers, has enabled the disastrous position which would otherwise have occurred in the U.K. to be avoided. Some co-ordinated policy is needed and likely to be forthcoming in the U.K., but for proper long-term economic efficiency to be achieved, this planning needs to be extended on an international basis. According to "The Times", "Returns are so modest that there are few who would contemplate trying to break in to the market now, and some of those who find themselves in it through tradition would happily get out of it if they could cut their losses".

Nevertheless, the U.K. is a major manufacturer of turbo-generators in the Western World. According to the 1968 O.E.C.D. survey of electric power equipment, the delivery of generators for steam turbines from the U.K. in 1966 was 40 generators aggregating 9,855 MW, (out of 19,507 MW, 170 generators, for all O.E.C.D. countries). In 1967, the U.K. delivered 10,687 MW, (50 generators) out of 22,351 MW., (170 generators) for all O.E.C.D. countries. To these figures must be added the deliveries of generators for hydraulic and gas turbines, viz. 286 MW (27

generators) for gas turbines and 265 MW (5 generators) for hydraulic turbines delivered by the U.K. in 1966, with 349 MW (40 generators) for gas turbines and 115 MW (4 generators) for hydraulic turbines in 1967. The total deliveries for all O.E.C.D. countries for 1966 and 1967 were, respectively, 798 MW (63 generators) and 1397 MW (108 generators) for gas turbines, and 6,269 MW (113 generators) and 6,756 MW (139 generators) for hydraulic turbines.

The O.E.C.D. survey also showed that the U.K. produces the majority of generators with ratings in excess of 300 MW. (7,100 MW out of an O.E.C.D. total of 8,740 MW in 1966, and 8,520 MW out of 13,386 MW in 1967). Later O.E.C.D. surveys show similar production figures for the U.K. in relation to other European manufacturing countries.

Prices for turbo-generators are difficult to obtain, but collating such figures as are available from a number of different sources, and making allowances for items other than the generator where these have been included in an overall price, it has been possible to gauge some indication of prices.

Approximate prices for generators driven by steam turbines, (generator only but including excitation system) fall from £4/kVA for ratings in the region of 250 MVA to £3/kVA in the region of 500 MVA, and to £2.5/kVA in the region of 800 MVA. No effort has been made to speculate on the possible prices of superconducting generators in this thesis, because as Mole remarked ⁽¹⁾, an economic assessment on paper is tediously detailed, very arguable and at present more or less unreliable. Lorch ⁽¹⁾ however has conducted an economic study for a machine in which a conventional stator and

conventional flux densities are used and in which the rotor has a superconducting winding; he suggests that a capitalised advantage of £0.83m for a 1000 MW alternator seemed reasonable. In a study carried out at M.I.T. (178), Woodson et al demonstrate at least in theory, that by the use of superconducting field windings, the decreasing prices per kVA can continue to be realised for turbo-generators with ratings up to and beyond 5,000 MVA. No composite overall figures are given for prices in terms of cost per kVA rating, but the indications of the data presented are that the weight/kVA rating, losses/kVA rating, superconductor cost/kVA rating and refrigerator input power/kVA rating all fall off as the generator rating increases, and that this form of technology can supply economically the turbo-generators needed by the power industry for a good many years to come.

Because of the small financial returns on turbo-generator manufacture in the U.K. due to haphazard placing of orders, it would seem most unlikely that U.K. manufacturers would be prepared or able to finance the development of superconducting generators. In view of the leading position of the U.K. in turbo-generator manufacture in Europe, particularly in the larger ratings, and the need for a large industry for it to be commercially viable, it would appear desirable for a U.K. national or E.E.C. international policy to be formulated, and development of high powered superconducting turbo-generators put in hand with Government finance, (either direct or indirect) or with C.E.G.B. funding. The alternative seems to be to allow the U.K. industry to be eclipsed by overseas manufacturers, whose prices are very

uncompetitive compared with those of the U.K. manufacturers. In the long term, in the national U.K. interest, it would seem highly desirable to undertake such a development programme, since all the indications are that superconducting generators will be technically feasible and probably economically attractive. At least the group of utilities in the U.S. represented by the Edison Electrical Institute (E.E.I.) considers superconducting turbo-generators to be potentially advantageous, in that they have initiated and are financing a development project to this end, known as the E.E.I. Research Project on Superconductors in Large Synchronous Machines (179).

8.5 Experimental Machines.

The first synchronous machine to be operated with a superconducting field winding was constructed by Stekly, Woodson et al (180) in 1965. It was an iron-free machine and no attempt was made to optimise any of its parameters. It consisted of a stationary 4-pole field winding of Formvar-insulated copper-plated Nb-Zr wire which had a critical current of 28A. No effort was made to design a special dewar and a typical laboratory type was used. This resulted in a field at the armature of an average value of 1.2T, a value not very different from that in a conventional machine although the maximum value on the axis of the field coils was 6T. The armature had a conventional 3-phase winding and was rotated with its axis vertical on the outside of the dewar containing the field winding. The machine was rotated at speeds up to 12,000 r.p.m. and generated a maximum steady power of 8 kW. This machine

demonstrated the basic feasibility of employing a superconducting field winding in a synchronous generator, and although repeated switching and unbalanced loading did not quench the field winding, this cannot be regarded as a conclusive test because of the very loose magnetic coupling between the armature and field winding.

The second generator to be reported (181) was that of Oberhauser and Kinner at the Dynatech Corporation. The design objectives were very ambitious: power, 50 kW; rotational speed, 24,000 r.p.m.; voltage, 1,000 V.r.m.s.; superconducting armature and field for low-weight, low-volume aerospace applications. The maximum power generated by this machine was only 6.1 kW in low-speed tests at 6,000 r.p.m., this value of power being only 72% of that expected at this speed. The machine experienced trouble in two respects: some of the armature phases were insufficiently cooled from which it is inferred that they were not superconducting; and secondly, problems were encountered in balancing the relatively long and slender shaft. Oberhauser and Kinner state that the first critical speed was 10,500 r.p.m. and because the buildup of shaft vibration was so swift, the operating range was restricted to less than 10,000 r.p.m. in order to avoid causing major damage to the machine before acquiring any data. It seems reasonable to infer that major damage did occur when an attempt was made to go through the first critical speed to achieve rated speed. As far as can be determined from the published literature, this has been the only attempt to build a synchronous generator with a superconducting armature as well as a superconducting field.

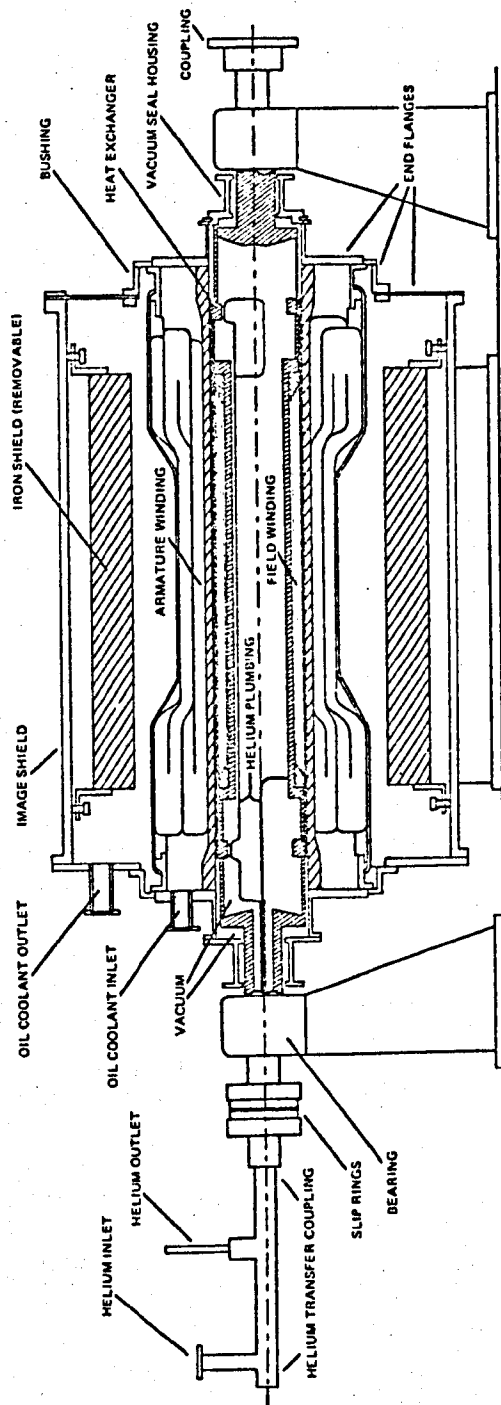


Fig. 51 M.I.T. 2 MVA Superconducting Alternator

A major effort on the study of superconducting synchronous machines has been carried on at the Massachusetts Institute of Technology (MIT) under the E.E.I. programme on large superconducting synchronous machines (179). The first experimental machine of this project produced 45 kVA in June, 1969 (177). The main feature of this machine was that it had a rotating superconducting field cooled by liquid helium (173). Although the rated power of 80 kVA was not achieved, this machine demonstrated that at least on a small scale, liquid helium can be contained within a cryogenic vessel, run up from rest and rotated at 3,600 r.p.m. Secondly, it demonstrated that the superconducting winding is not adversely affected by rotation.

The design philosophy, overall configuration and leading dimensions for the second MIT machine were finalised at the end of 1969. The objectives of this machine are to test features which are likely to be suitable for application to machines of the 1,000 MVA class. It is not a scale model, but rather an attempt to develop and evaluate suitable design and construction techniques with a small size machine. It was decided to make the rating of the machine as large as possible within the facilities available at MIT, and this has resulted in a machine rated at 2 MVA, 60 Hz, 3,600 r.p.m. The machine is described in detail in reference 177, and a cross-sectional view is given in fig. 51. The results of the initial cooldown and tests on this machine are awaited with interest.

A 5 MVA synchronous generator is under construction at the Westinghouse Electric Corporation (183). Although it was started

considerably after the MIT 2 MVA machine, it was probably completed before it and testing with it should have commenced. Both machines have iron screens, but different rotor constructions.

Another 5 MVA generator is being constructed by the Westinghouse Electric Corporation (167); this time the machine is intended for airborne use, rather than as a test vehicle for large synchronous generator development. This machine has a continuous rating of 1 MVA, 5 kV, 400 Hz, at 12,000 r.p.m. and a 10 second rating of 5 MVA. Only the rotor has been constructed to date, but test data on it are not yet published. The helium transfer system from the stationary storage system to the rotating field has been operated at 12,000 r.p.m. for over 40 hours, and helium transfer has been accomplished under these conditions with an efficiency greater than 85%. It is proposed to use a cryogenic storage system weighing 300 lb. for the machine and not to employ a closed cycle helium refrigerator system. The overall machine weight excluding the storage system is estimated to be 800 lb. A conventional generator of proven reliability and with several years in operational service weighs 2,600 lb. with a continuous rating of 5 MVA. Against this performance and weight, the superconducting design is not particularly promising especially when the helium cooling arrangement is considered.

It is understood from reference 176, that superconducting machines have been built at the University of Paris (96.5 watts), by AVCO (no details available), Fort Eelvoir (16 kVA, 400 Hz)

and the Dresden Institute for Solid State Physics (21 kVA, 50 Hz).
It has not been found possible to obtain further details of these
machines.

9. Synchronous Generators for Aircraft Applications.

9.1 Aerospace and Superconducting Generators.

About a decade ago, when high field superconductors began to be available, it was thought that their application in electrical machines would result in considerable economies in weight and volume. It was natural, therefore, that the early investigators should consider developing superconducting machines for situations where the saving of weight, and to a lesser extent of volume, were of primary importance, that is, in aerospace. Rockets and space vehicles were using liquid propellants, including liquid hydrogen, and a cold environment was required for certain low-noise electronic and microwave equipment, and although temperatures lower than that of liquid hydrogen were needed for superconductivity, a very cold environment for some equipment was already in use and the basic cryogenic technology already established. Aerospace is also where there is comparatively little prejudice against innovation where this is shown to be of advantage.

In aircraft in the early 1960's, cryogenic liquids, e.g. liquid nitrogen were beginning to be used and in military aircraft the problem of accommodating the increased electronic equipment and the larger demands for electric power were becoming acute. Several studies were undertaken to investigate the possibilities of meeting these demands and Smith (184), Pierro and Unnewehr (147), Stekly and Woodson (185), Mueller (186) and Woodson, Stekly and Halas (187) published their findings. They were generally optimistic and predicted that the weight of a 400 Hz superconducting generator

would be approximately an order of magnitude less than that of the corresponding conventional machine, the weight of the auxiliaries (such as pumps and blowers for conventional machines, and refrigerators for super-conducting machines) not being included. Stekly and Woodson (185) give an outline design for a 1000 kVA turboalternator system comprising a gas turbine, superconducting alternator with an ambient temperature armature and a refrigerator; this system had an estimated specific weight of 0.84 kg./kW which indicated that it could be competitive with a conventional auxiliary power unit. Mueller (186) supposed that an intermediate heat shield at liquid hydrogen temperature would be used, and with this supposition and optimistic values for refrigerator power requirements, deduced that the weight of a 100 kW generator and refrigeration system would be 10 kg, giving a remarkably low specific weight of 0.19 kg/kW. In the later paper of Woodson, Stekly and Halas (187), design formulae were presented for power output, terminal voltage and current and machine reactances in terms of machine size, configuration, overall current density of the field winding and heat transfer from the armature. These formulae were then used to calculate the performance, specific weight and volume as a function of power output for a 400 Hz alternator having a simple air-cooled armature optimised for minimum volume. Their results showed a significant gain in compactness over conventional alternators at power levels above about 100 kW. It is not clear why the armature was optimised for minimum volume rather than for minimum weight or why the consideration was restricted to air cooled armatures, as at that time (1966), oil-cooled armatures

were usual in aircraft alternators. No consideration of the weight of the refrigeration requirements was included. At first sight it would seem that the conclusion of this later paper is at variance with that of the earlier (185), but the earlier paper considered the problem in general terms while the later took into account some practical considerations such as dewar wall thicknesses. These considerations become of less significance as the dimensions increase, and in fact, as the power of the machine increases, the original conclusion that the superconducting machine was approximately one-tenth of the weight of a conventional could be deduced from the results of the later paper (187) at powers of about 1,000 kW and above. Although the design formulae (187) are useful, the method of their application by these authors does not yield very useful results as a basis of assessing the merits of superconducting alternators over conventional types. From the point of view of the aircraft constructor, the data must be presented in terms of the overall system required for electrical generation, and not merely for a component of that system.

9.2 Preliminary Studies.

Our own preliminary studies in this area were given in a paper presented at the Conference on a.c. properties of superconductors and their applications, organised by the Institute of Physics and Physical Society in 1968 (183). In this paper it was pointed out that in the design stage of a civil airliner, the saving of weight is of utmost importance, as operators assess the profitability of a particular aircraft type, *ceteris paribus*, on

its freight and passenger carrying capacity. The revenue earning potential of an aircraft gives a quantitative indication of the importance of weight saving in the design stage, but whether this potential is realised by the aircraft when it is in service is entirely another matter. For an aircraft like the Boeing 707 or VC 10 the potential revenue earning capacity is at least £100 per annum per lb. of payload. The corresponding figure for the Concorde based on such financial data as were available in 1968 was taken as £200 per annum per lb. of payload ⁽¹⁸⁹⁾ and it was pointed out that if the total generator weight could be reduced from 320 lb. to 160 lb., the potential revenue earning capacity over a ten year life of the aircraft would be increased by £320,000. It was argued then that superconducting generators including their associated cryogenic cooling systems offered the possibility of achieving this saving in weight. Possible configurations for these generators were considered and it was anticipated that the main difficulties, besides the maintenance of the cryogenic environment, would be those associated with the control of the output voltage and the behaviour under conditions of sudden load changes, unbalanced loading and short circuits.

In an endeavour to test the feasibility of halving generator system weight, a preliminary design was prepared by the author ⁽¹⁸⁸⁾ for a 50 kVA, 400 Hz alternator with a four-pole superconducting field. It was estimated to have a weight of 3.6 kg which seemed very promising until the weight of the refrigerator needed to maintain the cryogenic environment for the superconductors was considered. It was supposed that liquid nitrogen was going to

be used in the aircraft in any case (e.g. for crew support after evaporation with liquid oxygen) and would be available for cooling intermediate thermal radiation shields in the alternator. Even with the use of this additional cryogen, the total weight of the combined alternator and 77K to 4.2K helium refrigerator was estimated to be 16.6 kg, and this was probably an optimistic figure. The weight of the refrigerator was a very disappointing feature of this preliminary study, but it emphasised the need for the continued development of small, lightweight, reliable helium refrigerators if the potential weight-saving of superconducting generators was to be realised in any way at all.

As an alternative to using an airborne refrigerator, the use of stored liquid helium was considered. In this case, the weight of the liquid helium and storage dewar brought the overall weight of the 50 kVA generator unit to approximately 14 kg for a 6-hour flight. The stored helium system might be acceptable for civil operation, but would be unsuitable for military aircraft. The specific weights were 0.33 kg/kVA with the refrigerator, and 0.28 kg/kVA with stored liquid helium, both systems requiring in addition a further cryogen for cooling the thermal radiation shields. These specific weights were of the right order of magnitude to indicate that it should be possible to achieve the 50% reduction in generator weight set as an initial target. There were many uncertainties, mainly concerned with the cryogenics and availability of small lightweight helium refrigerators, but it was felt that the results of this preliminary study were sufficiently promising to justify proceeding with the construction of a laboratory 400 Hz

superconducting synchronous generator. A certain amount of experience had been gained at Cranfield at this stage with the installation of a laboratory for superconductivity experiments, together with expertise in winding superconducting magnets, cryogenic instrumentation and the handling of liquid helium.

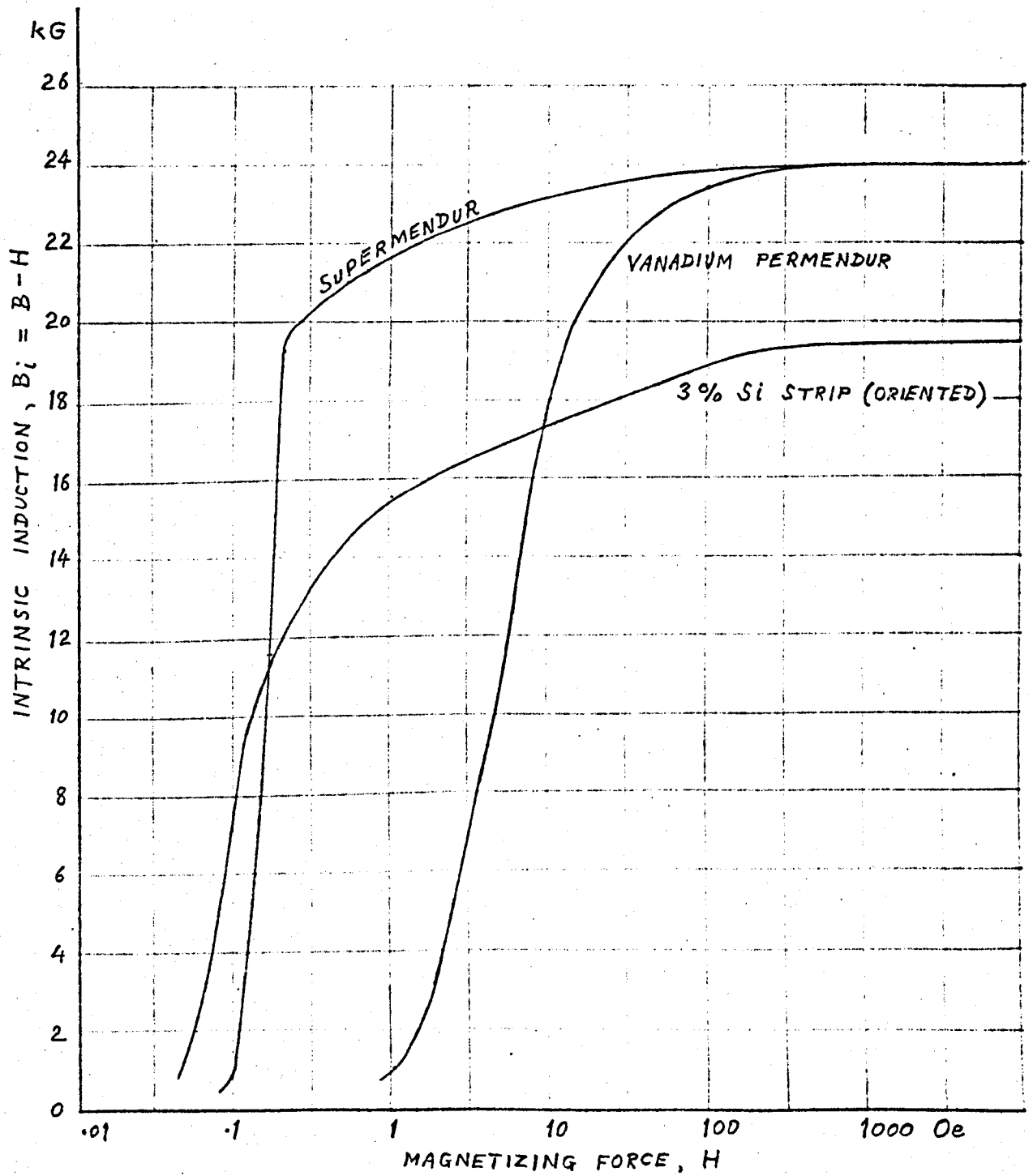
It must be admitted in retrospect that certain aspects of our preliminary studies, and also of those of some other workers reviewed in Section 9.1, were naive, mainly because the role of the iron circuit particularly in a small machine was overlooked. Further, developments in conventional generators for aircraft were not anticipated, and progress with small lightweight helium refrigerators has been disappointingly slow. As will be developed in the next section, the case for superconducting generators in civil aircraft including Concorde, has receded since 1968, and is now not tenable.

9.3 Present Generators and Systems for Aircraft.

It is now proposed to examine the specific weights, performance characteristics and general features of conventional alternators (that is, those without superconducting windings) available at present for aircraft, and then to consider the extent to which improvements on these figures might be expected from the use of superconductors, together with any penalties which may be incurred.

Considerable advances have been made recently in the design of brushless alternators, both of the rotating rectifier and Bekey-Robinson types. These may be summarised as being due to design

FIG. 52 - MAGNETIZATION CURVES



optimisation by computer as proposed by Khan and Reece (190) and others, improved cooling methods and the use of magnetic materials with higher saturation values such as the 50% cobalt alloys. These are available commercially under the trade names of Hyperco 50 and Permendur 49. The magnetisation curve for typical samples is given in fig. 52 together with that of 3% silicon steel for comparison. The 50% cobalt steels allow maximum flux densities in the region of 2.2 to 2.4 T to be used in present generators for aircraft. The use of these steels has involved the generator manufacturers in a quantitative study of notch sensitivity and saturation density characteristics for various heat-treatment cycles.

The main improvement in cooling has been the development of the oil-spray cooling method. In this, the working fluid of the constant-speed-drive unit (csd) is fed by a charge pump located inside the csd into a duct in the ac generator frame. The working fluid, which is a synthetic turbine oil, is transferred from the generator frame into the hollow shaft where some is diverted through metering orifices to lubricate the bearings. The remainder passes through either holes or a calibrated weir under the action of centrifugal force to impinge on the rotor windings and stationary armature windings thereby cooling them. The hot oil drains into a sump where it is returned to the hydraulic system by a scavenge pump located in the csd.

Further decreases in weight have come about by improved insulating materials, such as polyimide enamel and glass tapes impregnated with ptfе, and suitable for operation at temperatures of 250 - 290°C. Usually somewhat lower temperatures are maintained

on oil-washed surfaces to prevent accelerated degradation of the cooling oil.

TABLE 1

Weights of Rotax Oil-Spray-Cooled AC Generators

Type No.	Output Rating kVA	Weight kg.	Specific Weight kg./kVA
AE 2136	15/22 20/30	7.3 8.2	.483 .410
AE 2130	40/60	14.5 (hev 15.9)	.360 (.40)
AE 2129	60/90	17.7	.295
AE 2134	120/160	26.0	.216
Concorde	63/98	19.0	.302
Design only	750	300	.40

hev = high efficiency version

As a result of these advances, a range of conventional alternators with oil spray cooling has been produced by a British manufacturer with weights given in Table 1 and figures 53 and 54. Doubtless manufacturers in other countries produce comparable machines. The largest machine in this range at present available can generate 160 kVA continuously and weighs 26 kg. If allowance is made for the weight of the cooling oil and for external heat exchange, the total weight penalty is 31 kg. As basis of comparison

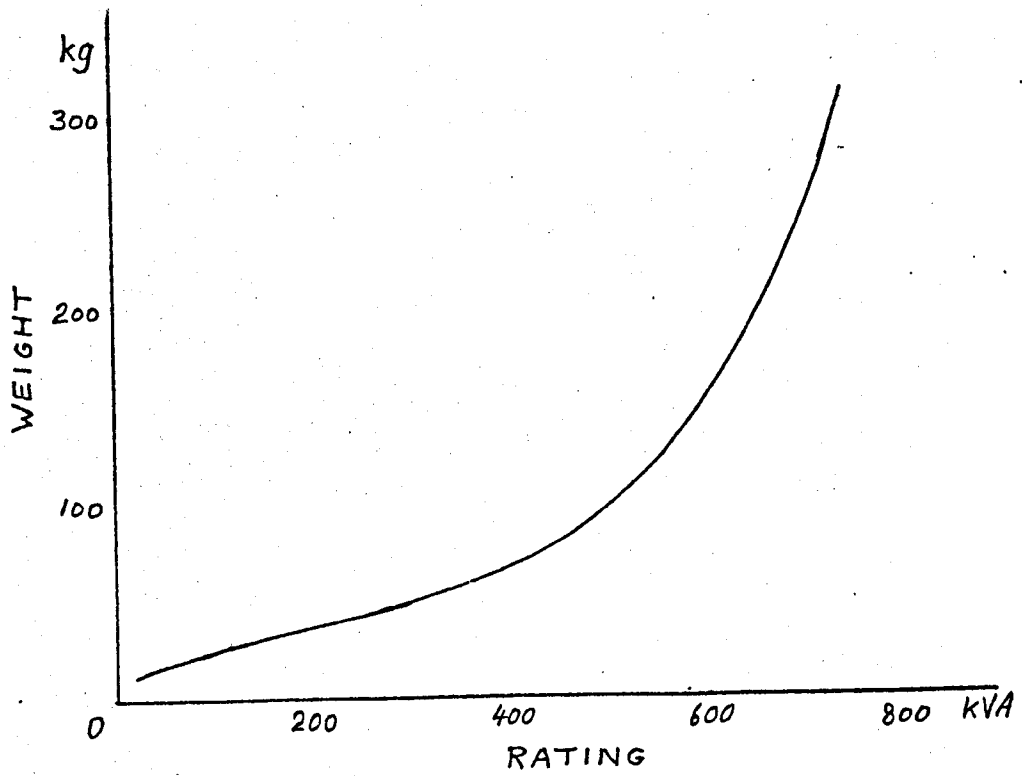


Fig. 53 Weights of Oil-spray Cooled Generators

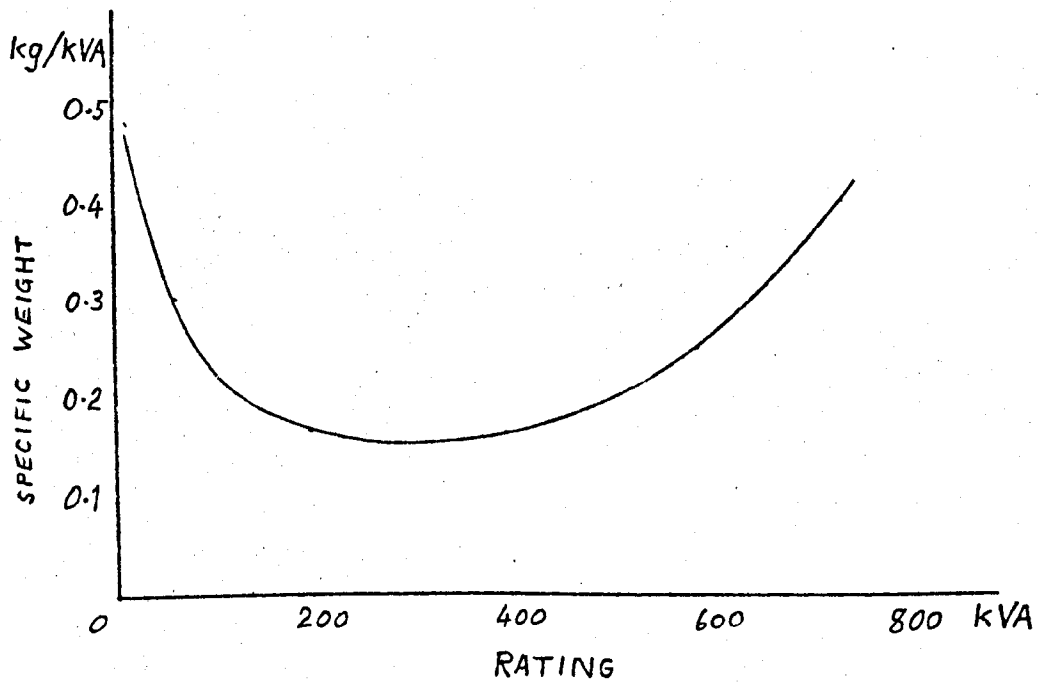


Fig. 54 Specific Weights of Oil-spray Cooled Generators

a specific weight of approximately 0.3 kg/kVA may be taken as typical for present conventional alternator systems up to 500 kVA per machine. Above this rating, spray cooling becomes less efficacious because of the difficulty of removing heat from the inside of the solid parts of the machine to the spray-cooled surfaces, with the result that the specific weight begins to rise steeply. At these higher ratings resort must then be made to more conventional methods of cooling, in order to prevent the steep rise in specific weight as the rating increases but the possibility of employing freon (191) or even liquid nitrogen cooling should not be overlooked. The former is attractive since a refrigeration system is already available in most aircraft and the additional cooling load would represent only a small increase in weight. The use of liquid nitrogen for this purpose would almost certainly involve separate liquefaction plant and would not be attractive on this account; if cryogenic liquid fuel (e.g. hydrogen) were employed this objection might not exist.

An explanation of the "slash" rating given in Table I, column 2 is required. Certifying authorities such as the Air Registration Board and the Federal Aviation Agency require aircraft generators to be capable of supplying 150% full load for 5 minutes to allow the pilot time to shed load manually in the event of one generator failing out of three running in parallel with full load on each. The thermal time constant of oil-spray cooled generators is much less than 5 minutes for normal ratings, and so the generators are capable of supplying the 150% overload condition continuously without a further rise in temperature. Thus the first number

before the slash indicates the normal recognised rating, while the number after the slash indicates the maximum power the generator can supply continuously.

A specific weight of approximately 0.3 kg/kVA is probably still not the best that can be achieved with existing materials and techniques, and further improvements in specific weight might well be anticipated for the future. At first sight it would seem that superconductivity is a phenomenon which, at least for larger ratings, may allow savings in generator weights to be made, and indeed for aircraft electrical systems requiring powers of a few megawatts, its use should be considered, but at smaller ratings it is unlikely to be competitive. Before discussing the extent to which superconducting alternators appear to be capable of meeting aircraft requirements, the constraints imposed by the electrical systems themselves should be noted. The reduction in specific weight achieved with the recent advances in design of conventional alternators has been accompanied by corresponding reductions in the impedance parameters. Typical per unit values applicable to present conventional machines are:

Direct-axis synchronous impedance	1.8 - 2.0
Direct-axis transient reactance	0.4 - 0.5
Direct-axis sub-transient reactance	0.15- 0.17
Quadrature-axis synchronous impedance	1.0
Quadrature-axis sub-transient reactance	0.25

These low values are already causing difficulties to some electrical system designers (e.g. 192, 193), and in one or two cases

have provoked the suggestion that external reactors should be incorporated to lower the fault levels available. Although it would be inappropriate to generalise and to quote limiting values for the per unit impedance parameters, it is probably correct to regard the values quoted above as approaching those which most designers of electrical systems for aircraft general services would regard as being the limit, any appreciable reduction being unacceptable. One problem which arises with higher fault currents is the greater duty imposed on protective switchgear which in turn may demand the introduction of special techniques such as air-blown circuit breakers, or the use of an arc-quenching medium such as sulphur hexafluoride. The prevention of large overvoltages during normal switching and during fault clearance will be much more difficult under these conditions, and their prevention will be all the more important to obviate the production of corona discharges which may occur at altitudes above 50,000 feet at voltages above 300V. Thus the consequences of the extremely low values of the impedance parameters which are characteristic of superconducting alternators must be assessed in the context of the complete electrical system. On the other hand, where large pulsed loads or cycloconverters are involved, the very low values of the impedance parameters would give the superconducting machine advantages over the conventional types.

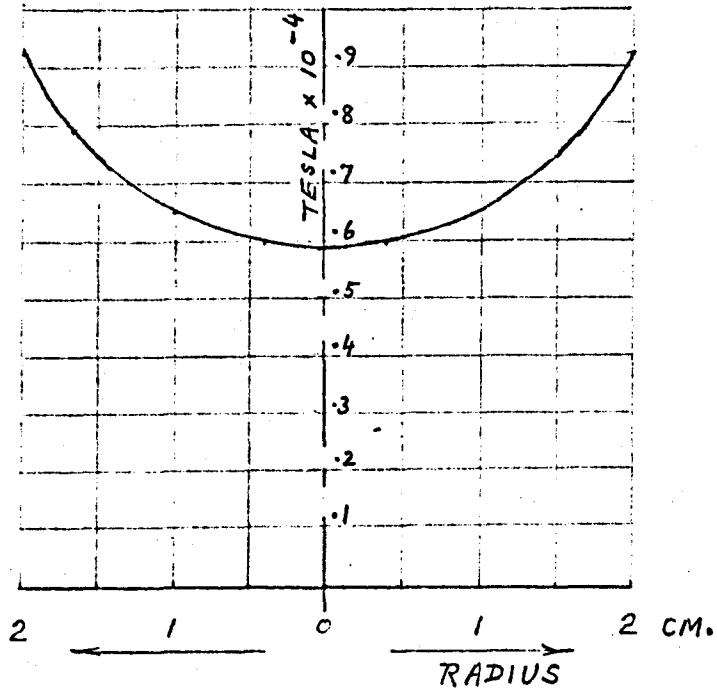
9.4 Design Considerations and Rating Limitations.

In a conventional machine with a ferromagnetic core, the flux density at the armature is largely determined by the magnetic

properties of the iron at the boundaries of the air gap. In a superconducting machine without an iron core the magnetic field is determined by the maximum value of field experienced by any part of the superconducting field winding, since if this field exceeds the critical value appropriate to the current and thermal conditions existing in the wire, a transition to the normal state will occur. A consequence of these facts is that the underlying philosophy and design procedure must be different for each type of machine. In the superconducting type (in which it is assumed that only the field is superconducting, for reasons already discussed), the field and current density are no longer independent variables subject only to the constraints of stress or, more usually, cooling but are also related by the characteristics of the superconductor. As will be discussed later in Chapter 11, the field at the centre of a solenoid, H_0 , can be expressed in terms of an entirely geometry-dependent function $F(\alpha, \beta)$ and the effective uniform current density, $j\lambda$, as:

$$H_0 = j\lambda a_1 F(\alpha, \beta)$$

where a_1 is the bore of the coil. Actually the field at the centre of the coil is of little interest to the designer, except for the convenience of calculation. The fields of interest are those at the inside turn on the central plane of the coil, which is the maximum field experienced by the superconductor, and the field at the armature which will usually be beyond the end of the coil. The calculation of these fields will be given later, but fig. 55 shows the form of the field distribution across the central plane of a



$\alpha = 2$
 $\beta = 0.35$
 RADIUS OF COIL
 = 2 cm.

Fig. 55 Flux distribution per ampere-turn across the central plane of a solenoid.

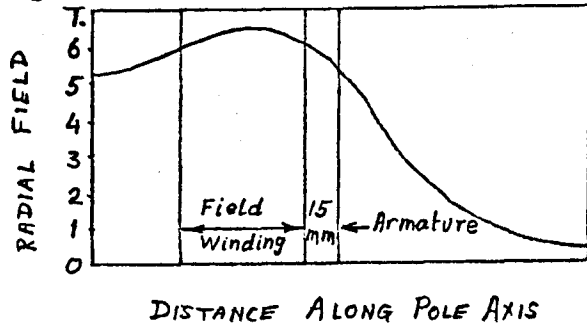


Fig. 56 Field along the axis of a dipole for a machine.

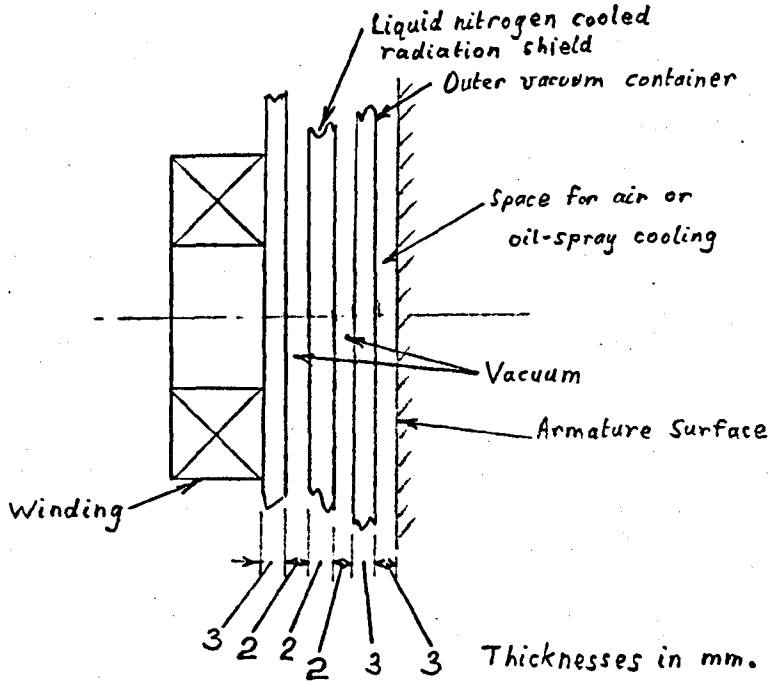


Fig. 57 Cryostat wall construction.

coil, and fig. 56 the field along the axis of a pair of coaxial coils, normalised in terms of the bore of the coil. Although circular coils will not necessarily be used as field coils, the field distribution due to rectangular coils will be approximately of the same form.

One of the underlying assumptions in the preliminary design mentioned was that the maximum flux density at the armature conductors would be 5T; another was that no iron would be used. In fact, it would be difficult to develop a field of 5T at the armature of a machine of small rating with niobium-titanium superconductors at 4.2K. Figure 56 shows the field along the axis in terms of normalised lengths of a pair of superconducting windings with uniform current density and might be used as a trial proposal for the field in a superconducting machine. If the medium is air, the shape of the flux profile is entirely dependent on the geometry of the coil and the distribution of the current it is carrying. However, the distance between the end face of the winding and the outside surface of the armature has a minimum value which cannot be reduced for practical reasons (fig. 57) such as obtaining sufficient support for the superconducting windings, allowing adequate circulation of liquid helium round them and maintaining sufficient thermal insulation. It is considered that 15 mm is the smallest distance which it is practical to use, and if this value is taken, it can be used to determine the scale of the flux profile in terms of actual lengths. It will be seen from fig. 56 that the flux profile has a small gradient inside the winding which increases somewhat in the region beyond the end of the winding.

At some further distance from the end of the winding, the flux density falls off very rapidly. (With a thick circular solenoid the field in this region falls off as the inverse cube of the distance from the centre of the solenoid). If advantage is to be taken of the principle property of a superconducting winding (i.e. its ability to produce very high flux densities in air), then the armature winding must be closer to the field winding than the region in which the approximate inverse cube drop occurs. Of course, the proportions of the winding dimensions influence the shape of the flux profile along the axis of the winding, but there are limits to which the winding proportions can be altered, on account of the quantity of superconductor used and the profile of the flux density round the periphery of the armature. In a conventional alternator, the proportions of the iron dimensions (pole arc/pole pitch ratio and variation in the length of air gap) can be used, amongst other methods, to control the flux profile in the air gap so that the waveform of the generated voltage is sinusoidal. This method is not available in a superconducting machine without an iron core, and adjustment of the winding proportions and limited current grading are used instead, thus restricting the choice of winding proportions if a reasonably sinusoidal output voltage is to be generated.

These considerations with others can be used to make an estimate of the minimum flux per pole and subsequently the minimum rating of alternator for which it is likely to be advantageous at all to use superconductors. These values are estimated to be approximately .005 Webers and 200 kVA respectively, based on a specific electric

loading of 140,000 ampere-conductors per metre of armature periphery. As ratings of machines below this value are attempted, the flux density at the armature reduces very rapidly to that obtaining in a conventional machine (even though the maximum flux density and current in the winding remain the same). Under these circumstances, the only advantage of using a superconducting field winding is that it allows a higher specific electric loading to be used in the armature than that in a conventional machine due to the absence of iron round the conductors, but this is more than offset by the environmental requirements of the superconductor. From trial designs, we find that weights of 400 Hz alternators below 200 kVA show very little reduction in weight below that of the 200 kVA machine, and we conclude that this probably represents the minimum rating for which it is practical to introduce superconducting windings. This is not to say, however, that a superconducting machine with its associated cryogenic equipment at this rating is lighter than its conventional counterpart.

9.5 Refrigerator Weights.

The weights of superconducting alternators on their own and in the larger ratings can be estimated with a moderate degree of accuracy, but the same cannot be said in regard of cryogenic refrigerators. Nevertheless, since the weight of the refrigerator is likely to be between 2 and 4 times the weight of the alternator on its own at ratings above 500 kVA, it is important to make some estimate of reasonable accuracy. Unfortunately, small lightweight refrigerators for 4K and suitable for use in conjunction with air-

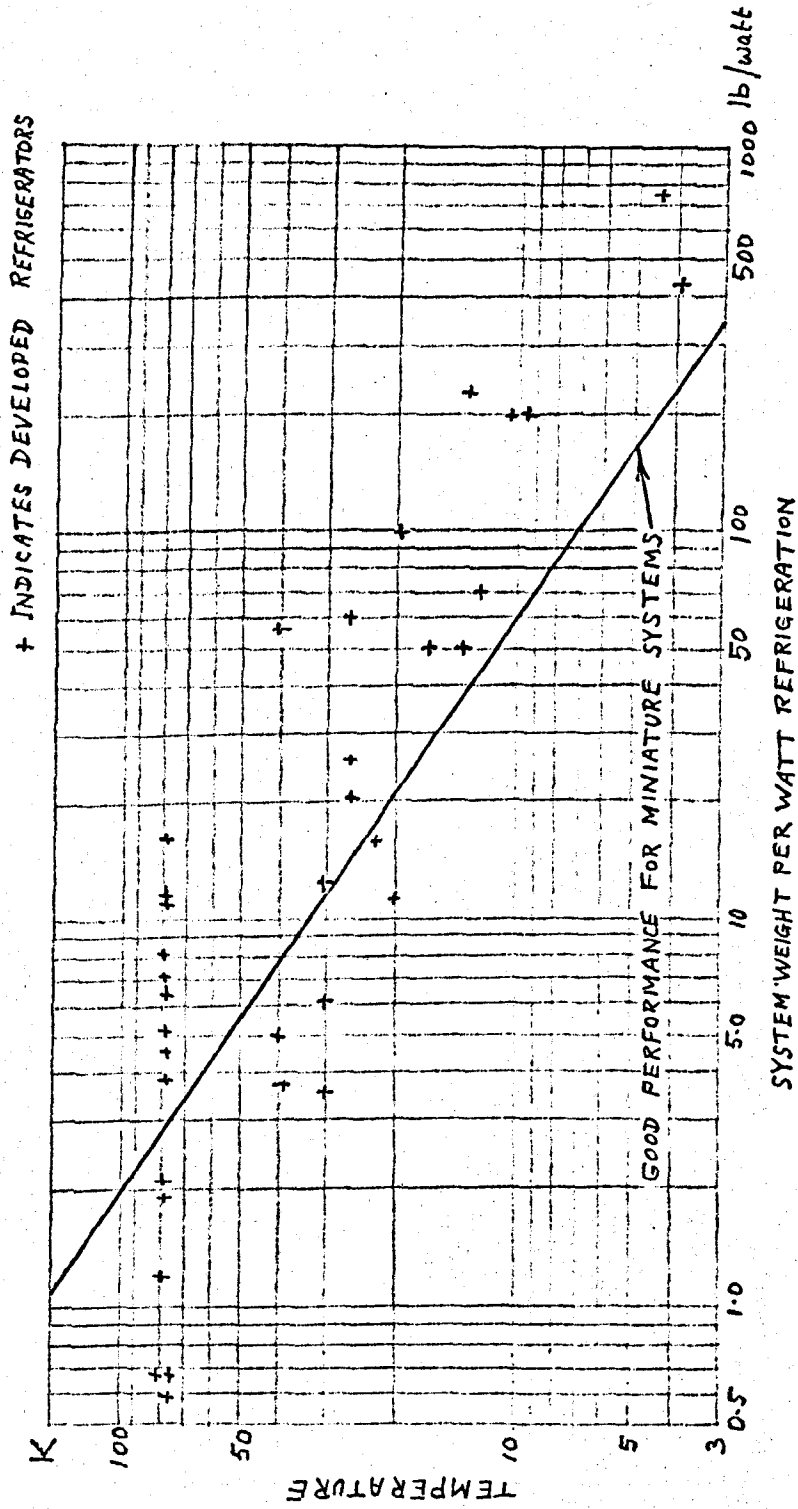


Fig. 58 System Weight per Watt of Net Refrigeration as a Function of Refrigeration Temperature. (After Daunt and Goree, ref. 194)

borne alternators do not seem to be in a very advanced stage of development. Daunt and Goree (194) carried out a survey of miniature cryogenic refrigerators in which their primary objective was to visit all the U.S. companies building miniature refrigerators and most European companies as well. They also investigated developmental refrigerators and components and attempted to ascertain the near-future trends in the miniature refrigerator industry. Figure 58 is taken from their report (194) and gives an estimate of "good performance for miniature systems", from which it will be noted that although several commercial products exceed this performance for temperatures above 20K, none do so for a temperature of 4.2K. In spite of this, and in order to allow for development in due course, the "good performance" criterion was used for the weight estimates of 4.2K to 77K refrigerators quoted subsequently.

It was found that the heat leaks into the alternators were prohibitive unless intermediate cooled thermal radiation shields were used. It has been assumed therefore that liquid nitrogen will already be in the aircraft and available for this purpose and will not therefore incur any further weight penalty.

9.6 Superconducting Alternator Weights.

As has already been discussed, it is considered that a rating of approximately 200 kVA represents the smallest size of 400 Hz superconducting alternator which it is practical to build and below which only insignificant reductions in weight can be achieved. As ratings are increased above this value, the specific weight falls rapidly to 0.33 kg/kVA at 1 MVA and further to 0.25 at 4 MVA. These

figures are based on weight estimates of 4-pole, rotating field alternators with liquid nitrogen cooled radiation shields and include estimates for the 4.2K to 77K refrigerator to remove the net heat leak. The refrigerator weight was taken as 97 kg/watt of refrigeration. Other sources of heat inleaks are along the shaft and along the leads to the field winding. The results are summarised in Table II and figs. 59 and 60, and were submitted to the NATO/AGARD Conference on Aircraft Auxiliary Power Systems (195).

TABLE II

Rating, MVA	0.5	1	2	3	4
Heat inleak to dewar, watts	1.78	2.55	4.06	5.57	7.08
Refrigerator weight, kg.	175	248	395	540	685
Alternator weight, kg.	50	80	160	240	320
Combined weight, kg	225	328	555	780	1005
Specific weight, kg/kVA	0.45	0.33	0.28	0.26	0.25

Although machines designed with two poles were lighter than those designed with four, the difference was not very great, and it was thought that at the lower speed of the 4-pole machine, stressing and other problems would not be so severe and because of this, the 4-pole machines were used in the above weight estimates.

The absence of ferromagnetic teeth enables extra copper to be used in its place and permits a much higher specific electric loading to be used. A figure of 100,000 ampere-conductors per metre was used which is approximately 2.0 times that in a conventional aircraft

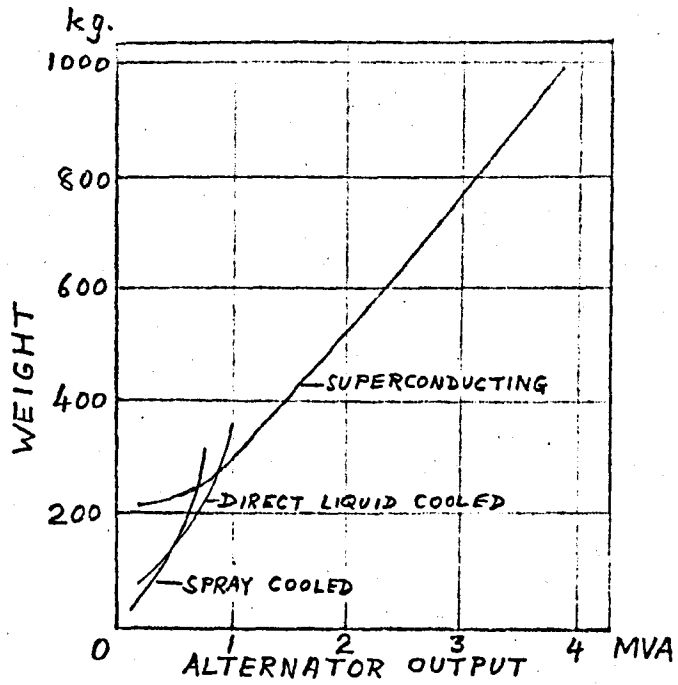


Fig. 59 Superconducting Alternator Weights

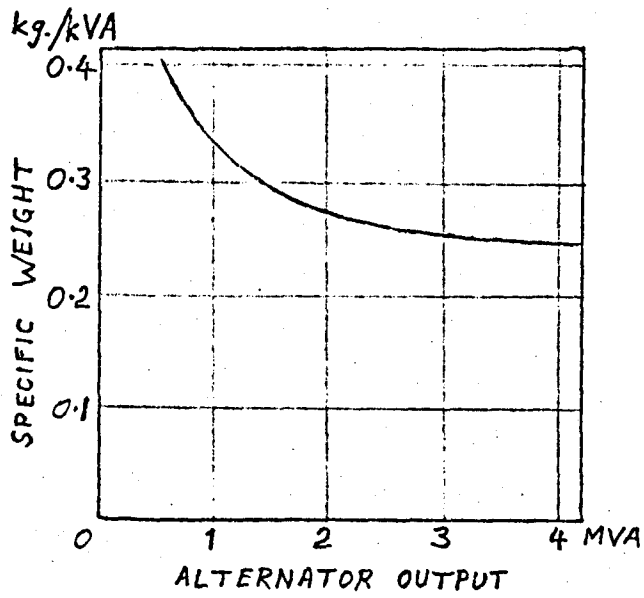


Fig. 60 Specific Weights of Superconducting Alternators

machine, in which there are iron losses to be dissipated in addition to the copper losses. The armature conductors need to be stranded and transposed to avoid circulating currents between the strands. A nitrogen-cooled electrothermal shield isolates the superconductors from rapid time variant fields produced by armature currents (such as those produced by negative sequence currents) and thus they do not contribute to the heat generation in the liquid helium part of the cryostat.

There are considerable uncertainties in the above estimates, and they are probably on the pessimistic side. Further development is necessary in order to obtain reliable and accurate data, and with further development, the range in which superconducting alternators become attractive may be extended considerably.

9.7 Prospects for Use in Aircraft.

With the present state of development of superconductors and the anticipated feasible future development of lightweight helium refrigerators, the prospects for superconducting alternators in aircraft may be summarised as follows:-

- (a) The recent developments in conventional oil-spray-cooled alternators for 400 Hz outputs enable them to have specific weights below those of superconducting machines (making allowance for 4.2K to 77K refrigeration) for ratings up to 500 kVA. Since generators in civil airliners have ratings in the range 40-90 kVA, there is no prospect of them being of the superconducting type unless some very radical development takes place. For military aircraft applications, and similar situations where

larger powers are required with minimum weight, the prospects are not so bleak.

- (b) Between 500 kVA and 1 MVA the superconducting machine becomes more competitive, although direct liquid cooled machines would probably be marginally lighter.
- (c) Above 1 MVA, the superconducting machine would be lighter than a conventional type, the weight advantage increasing as the rating increases.
- (d) Unless liquid nitrogen is already on board and available for cooling thermal radiation shields, superconducting generators are unlikely to be competitive even at ratings above 1 MVA.
- (e) The predominant weight, and that which is known with the least certainty, is that of the 4.2K to 77K refrigerator. This aspect could well be the major influence on the prospects for superconducting machines in aircraft, and emphasizes the need for the continued development of small, reliable, light-weight helium refrigerators with ratings up to approximately 8 to 10 watts.
- (f) The use of stored liquid helium is not a viable alternative to the use of a refrigerator in a military aircraft.
- (g) Since the weight of a 400 Hz alternator with a rating below 200 kVA will show an insignificant reduction in total weight below that of a 200 kVA machine, this rating probably represents the lower limit of alternator rating at which it is practicable to introduce superconducting windings.
- (h) Superconducting alternators have very low internal impedance which may make them unacceptable for supplying systems for

general aircraft services without special measures being necessary.

- (i) Conversely, the low values of internal impedances would make superconducting alternators very suitable for supplying pulse loads and cycloconverters, and also impose less stringent demands on the excitation control system.
- (j) Several important problems require further development before superconducting alternators are a practical proposition. These include dewars rotating at high speed, couplings for introducing cryogens for stationary to rotating members, and brushless excitation systems (or brushes and sliprings capable of operating satisfactorily in the aerospace environment).
- (k) Superconducting alternators present some problems from the operational aspect and lack the instant readiness of conventional machines which do not require to be cooled down to extremely low temperatures before they can be excited and loaded.

Superconducting generators are in their infancy and new developments in superconductor technology (such as niobium-tin in filamentary form) or in cryogenic engineering (such as the use of supercritical helium for superconductor cooling, or the utilisation of liquid hydrogen for radiation shields if it were already on board as a fuel) would make present estimates for superconducting alternators out of date, and greatly improve the prospects for the use of such machines in aircraft.

10. Laboratory Prototype

10.1 Choice of Machine.

In the preceding five chapters, various types of machines capable of converting mechanical energy from a rotating shaft into electrical energy, or vice versa, have been considered but only three types show any possibility of viable exploitation in commercial applications. In seeking to demonstrate the practicability of superconducting windings in rotating energy converters, and in order to verify some of the predictions based on theoretical considerations in terms of experimental evidence, it was obvious that a machine should be constructed and that if the results were to be of any value beyond merely an academic pursuit, then the choice should be one of the types with some prospects of commercial usage.

The homopolar d.c. machine is simple in concept and has been demonstrated in principle by a large scale model (155). Although it is not without its problems, the machine operates on principles now well understood and the success of future models depends on engineering the components to function satisfactorily. As the superconducting magnet did not give trouble as such, as far as is known, presumably the manufacturers do not need to do any basic work in this area, and now have sufficient data in order to be able to design the armature, current collection apparatus and refrigerator to give a satisfactory performance in future models. It was, therefore, considered that the scope for research on the homopolar d.c. machine, particularly in ratings in which it would be practical to work with the resources available to the author, was very limited

and so it was decided not to undertake a practical study on this type of machine.

The choice was thus between the toroidal reciprocating machine and the rotating synchronous machine. The former is an intriguing device and worthy of a practical study, but in view of its very novel principle of operation, it is less likely to be accepted by operators than the synchronous machine with a superconducting field winding. If and when the latter is in operation and confidence in superconducting windings in machines is established, then the additional novelty of reciprocating conductors might be accepted as well. It was felt therefore, as the short-term prospects of acceptance for the synchronous machine were better than those for the toroidal reciprocating type, that effort should be concentrated on the former. Furthermore, since the practical study was finance limited to about £4,000 initially for the machine construction, it seemed that the prospects of being able to construct a rotating synchronous machine within this sum were more favourable than those for the reciprocating type. The major expense in either machine would be the superconducting material, and it would be easier to start with small coils and limited fields in a synchronous machine and to extend them at a later date, if more money should become available, than to do so with the reciprocating type. It was, therefore, decided to construct a machine of the synchronous type, with the main objective of investigating its electrical performance. No effort was made, therefore, to optimise its volume or weight. In fact, so that constructional changes could be made in components which affect the transient performance, certain parts were arranged

to be de-mountable which involved an increase in overall dimensions.

The general feasibility of a machine of the type proposed for the experimental study has already been demonstrated by Stekly et al (180), using an improvised arrangement of a NbZr copper plated wire coil mounted inside a typical laboratory-type helium dewar with a 3-phase, air-cooled cylindrical copper wire-wound armature mounted over the finger and rotating about a vertical axis. No attention was paid in this machine to the effect of a damper screen between the field and armature.

The machine reported by Oberhauser and Kinner (181) used NbSn but with a field of only 1 tesla at the armature conductors. This machine was intended to generate 50 kW, a considerable advance over the machine of Stekly et al which generated 8 kW successfully. The success of this larger and subsequent machine is in considerable doubt, as it appears to have been abandoned and in need of repair.

It was considered that the machine to be constructed should be a synchronous superconducting generator with a facility for investigating the effects of the damper screen on the terminal performance (although this aspect might not be fully pursued in this investigation), to utilise NbTi for the field winding and to operate the field winding as close to its critical field value as would be expedient. Also, since the armature would be free from ferromagnetic material, it would be desirable to examine the effect of as high a magnetic field as possible on the losses in the armature conductors and the necessity for sub-dividing and transposing them. Further, since at the beginning of the experimental study it was thought that the present generators used in aircraft could be made

lighter in a superconducting form, then the experimental study should be directed towards this type of machine. Another factor influencing this choice was the availability of test equipment and drive motors for aircraft-type generators and supplies.

10.2 Configuration.

From the point of view of electrical performance, it would make very little difference whether the armature or field were rotated. Since rotation of the field would involve problems concerned with the fluid behaviour of liquid helium in a rotating cryostat, not to mention those associated with the construction of the dewar itself, it was decided to construct the machine with the field stationary and the armature rotating.

In order to simplify the armature construction, it was decided to rotate the armature inside the field system with the armature shaft horizontal. With this configuration, the field coils would be farther apart physically, and therefore the stresses between them would be lower than if the armature were on the outside of the field system. As there was no advantage to be gained, as discussed earlier in Chapter 9, in making the armature superconducting, it would be constructed from normal conductors with slip rings and brushes to collect the power generated. The cryostat would have a horizontal cylindrical cavity at room temperature inside which the armature would be mounted and in which the magnetic field would be generated. The cryostat would have a liquid helium reservoir and have intermediate heat shields cooled with liquid nitrogen to reduce thermal radiation from the outside ambient in order to

minimise the boil-off of the liquid helium. Vacuum thermal insulation would be used.

10.3 Ratings.

Originally it was the intention to construct a generator of a power rating comparable with that of aircraft generators currently in use, i.e. in the range 40 to 60 kVA. However from the discussion in Chapter 9, it can be seen that the physical size of a 200 kVA superconducting generator designed for aircraft use is only slightly greater than that of say, a 50 kVA superconducting machine; also, since another objective was to investigate the effect of high magnetic fields on the armature and its losses, it would be necessary for the field coils to be large enough to produce a field of, say 5T, at the armature conductors and not just at the centre of the field coils. Thus a field system with dimensions required from an aircraft generator of 200 kVA rating was decided on for the laboratory prototype. In this machine, however, the maximum allowable temperature rise in the armature would be considerably below that used in current aircraft generators (i.e. 290°C with polyimide or PTFE impregnated glass tape) because of the synthetic resins it was proposed to use in the armature construction. Also, the highly effective cooling used in aircraft machines would be very difficult to arrange with the limited facilities available in this respect at Cranfield, and even if it were available, it would not enhance the value of the results. Thus the very high specific electric loadings used in aircraft machines would not be attempted in the design of the laboratory machine, and consequently it was thought

that a rating in the region of 100 kVA would be appropriate as a target. This rating would also coincide with the largest drive system available to rotate the generator at the required speed. This drive system is a Ward Leonard set capable of providing 150 h.p. (112 kW) at any speed between 2,500 and 12,000 r.p.m.

The voltage and frequency decided on were the standard aircraft supply values of 208V, 400 Hz, 3 phase.

10.4 Implications of Preliminary Cost Estimate.

Having decided on the target ratings for the laboratory prototype of 100 kVA, 208V, 400 Hz, 3 phase, we then found from a preliminary cost estimate that these values were incompatible with a cost of £4,000. We, therefore, decided that because much of the value to be gained from this machine depended to a certain extent on its rating ultimately not being less than the values quoted, to proceed in two stages. The first was to design the machine for the ratings quoted and to proceed with its construction on this basis as far as possible. The two exceptions would be the armature winding and the field coils. The size of the first stage field coils would be determined by the money available, and it seemed that this would be sufficient to provide coils capable of producing approximately 2-3T at the armature conductors; the armature winding would be designed to operate in this field and generate 208V at 400 Hz on open circuit and with a reduced value of full-load current. The second stage would consist of adding another set of field coils on the outside of the first field coils, and re-designing the armature to generate the same voltage but with full load current correspon-

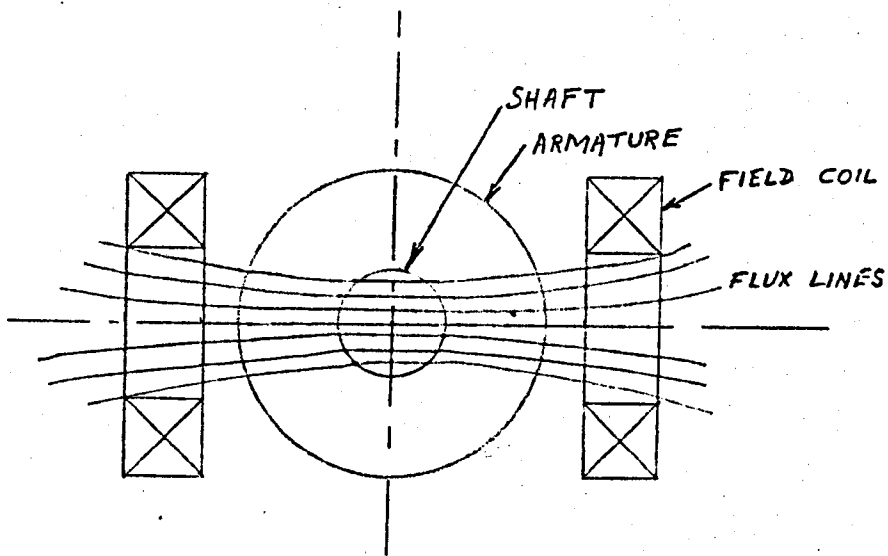


Fig. 61 Two-pole Field Pattern Across Shaft

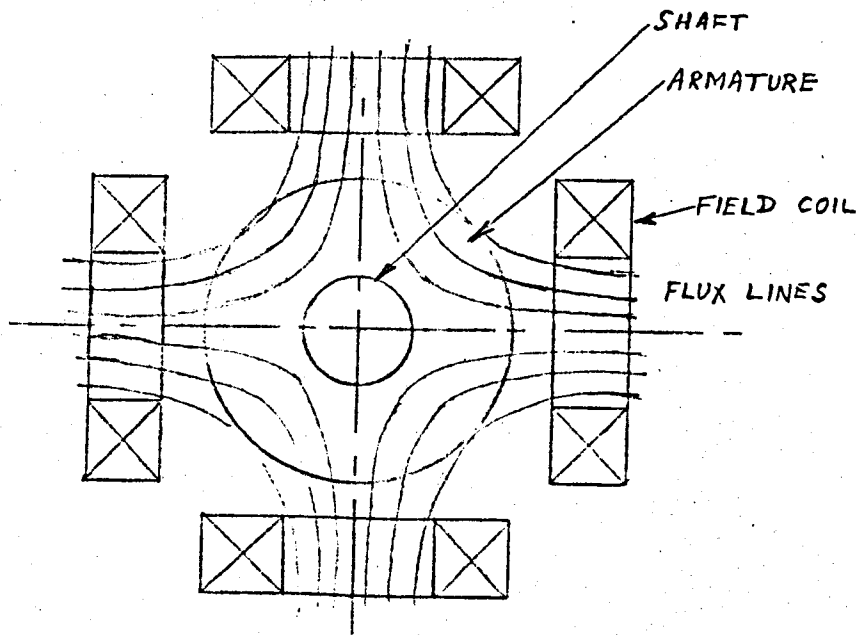


Fig. 62 Four-pole Field Pattern

ding to the full rated value of 100 kVA. The extra cost of the second phase would be in the region of £4,000, and it is unlikely that this funding will be available in time for this study. Nevertheless the basic machine should provide some useful results and be available for further work after the completion of this thesis.

10.5 Number of Poles and Speed.

The rating of 100 kVA already proposed was on the assumption that the machine would have four poles. In fact there was very little choice in the matter since a two-pole machine is ruled out unless a non-conducting (electrical) shaft is used. The field in a two-pole machine would pass straight across the shaft as indicated in fig. 61, and therefore if it is an electrical conductor, eddy currents would be set up as the shaft rotated resulting in large losses and heating of the shaft, bearing in mind the very large field and speed (24,000 r.p.m.) involved. With any other number of poles, the field on the axis is zero and the shaft rotates in a region of comparatively very low field as shown in fig. 62. Since a number of poles greater than four would have meant a larger machine, both in physical dimensions and power rating, the obvious choice was four.

With a four-pole synchronous machine, the speed is fixed at 12,000 r.p.m. in order to generate 400 Hz. This speed meant also that the machine could be coupled directly to the 150 h.p. drive motor.

10.6 Design Procedure.

The procedure adopted for the design of the laboratory prototype falls into three distinct stages. The first two are closely

linked and can be referred to as the "determination of the leading dimensions" and "detail design". The third is the prediction of the performance of the machine carried out after the detail design has been completed.

By determination of the leading dimensions is meant primarily the establishing of the armature dimensions. Once these dimensions are established, the rest of the dimensions follow and can be regarded as the secondary part of this stage of the design. Normally the determination of the leading dimensions involves an optimisation process to achieve the specified design objective, such as minimum weight, maximum efficiency or minimum cost. In the laboratory prototype, most of the latitude available to other designers for optimisation has been forfeited because of a decision taken on ground of expediency and the workshop facilities available. This was the decision to use plane circular coils in the superconducting field windings. Although coils with straight sides and with the ends formed round a cylinder have been successfully constructed by commercial organisations, they have nearly always used superconducting composites of much larger cross-sections which therefore give much stiffer constructions with less liability for individual conductors to move than the composite wire which it was anticipated would be used in the laboratory prototype. We felt confident in our ability to construct plane circular superconducting coils successfully, and wished to avoid any unnecessary dubious constructional features of the machine. This form of coil also enables them to be acquired in stages.

Of course, the design process and the determination of the

leading dimensions may depend on some parts of the detail design. But the detail design cannot be proceeded with until the leading dimensions are established, so the design procedure is in some sense an iterative process, with the initial values of a number of elements in the detail design being represented by assumed or nominal values followed by subsequent and final values as more and more of the design is established.

It should be pointed out that the account given here does not necessarily present the actual chronological sequence of the design of the prototype as there was trial designing, re-thinking, clarification of ideas, testing and re-working. Apart from these aspects, the important features of the design process are presented.

10.7 Leading Dimensions.

Besides using superconducting windings to produce the magnetic field, the other novel feature of this machine is that no ferromagnetic material is used in the magnetic circuit. A consequence of these features is that the established design procedures for conventional synchronous machines (e.g. Bibliography (2) or (12)) are only partly applicable in this case. The total magnetic loading and the total electrical loading are still meaningful since they are basic quantities unrelated to the constructional features of the machine, and so, since the apparent power rating per phase per

$$\text{rev/sec is } S/n_s = k \times 2 p \Phi \times Z I_c \quad (59)$$

$$\text{or } S/n_s = k \times \text{Total magnetic loading} \times \text{Total electric loading,}$$

where $k = (\text{form factor of voltage wave}) \times (\text{Distribution factor of winding}) \times (\text{coil-span factor of winding})$

p = no. of pole pairs

Φ = flux per pole

Z = no. of armature conductors in series per phase

I_c = current in each conductor

In a conventional machine, the active materials are a conductor (usually copper) and a ferromagnetic compound with an iron base and the extent to which they are utilized is determined by the specific electric loading and the specific magnetic loading respectively. The designer chooses appropriate values for these quantities based on his experience and the particular circumstances of the individual design. In a superconducting machine of the type being considered, the active materials are a conductor and a superconductor, and although the extent to which the former is utilized can be expressed in terms of a specific electric loading, the use of a specific magnetic loading is not strictly appropriate for the latter. This is because the limitation is due to conditions at individual turns in the field winding such as the local temperature, field and current which are almost independent of conditions at the armature, while in the conventional machine the limitation is saturation of the iron in the teeth which is directly related to the flux density in the air gap. Furthermore, the use of iron means that the magnetic field boundaries are reasonably well defined and at any cross-section, the flux density can be regarded as constant in the initial stages of the design. These factors are not applicable in a superconducting machine and consequently the concept of specific magnetic loading as a starting point is not as useful in

the design of superconducting machines as for conventional types. Nevertheless, the designer needs some preliminary value on which to base his first estimate for the armature dimensions and a value of the average flux density at the armature radius over the area of the field coil can be estimated approximately and taken as a guide for this purpose. It may need considerable correction when details of the field system have been finalised.

Before a preliminary estimate for the average flux density can be made, it is necessary to consider the superconducting winding itself. This is particularly necessary in machines of small dimensions since the difference in flux density at the central inside turns and at the armature may be considerable, but in large machines where this difference may be quite small and with design experience, it will be possible probably to assume a reasonable value for the mean flux density. The value of maximum flux density at the winding cannot, of course, be selected without reference to the current in the superconductor composite and the relation between its critical field and current. The use of IMI filamentary 'Niomax-FM' intrinsically-stable niobium-titanium alloy superconducting wire composite was an obvious choice. It is readily available in three standardised sizes each containing 61 filaments of niobium-titanium in a high-purity copper matrix with a copper/superconductor ratio of 1.35:1 by volume. Relevant nominal dimensions are given Table III and typical short-sample critical currents are given in fig. 63. The overall critical current density varies only slightly with size and is therefore indicated in a single curve in fig. 63. The current density given is for the cross-section of the wire including the niobium-

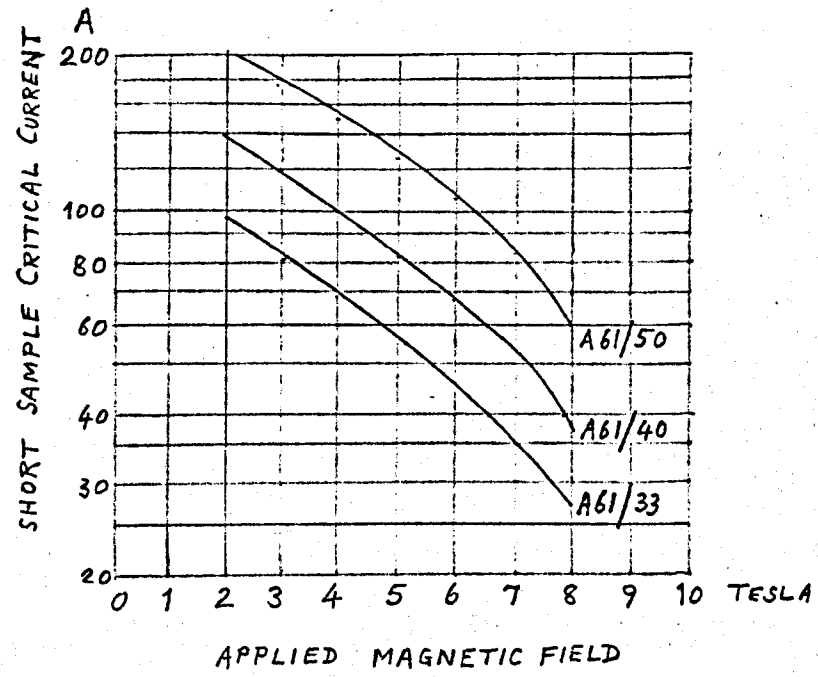


Fig. 63 Typical Short-sample Critical Currents of NIOMAX FM A61

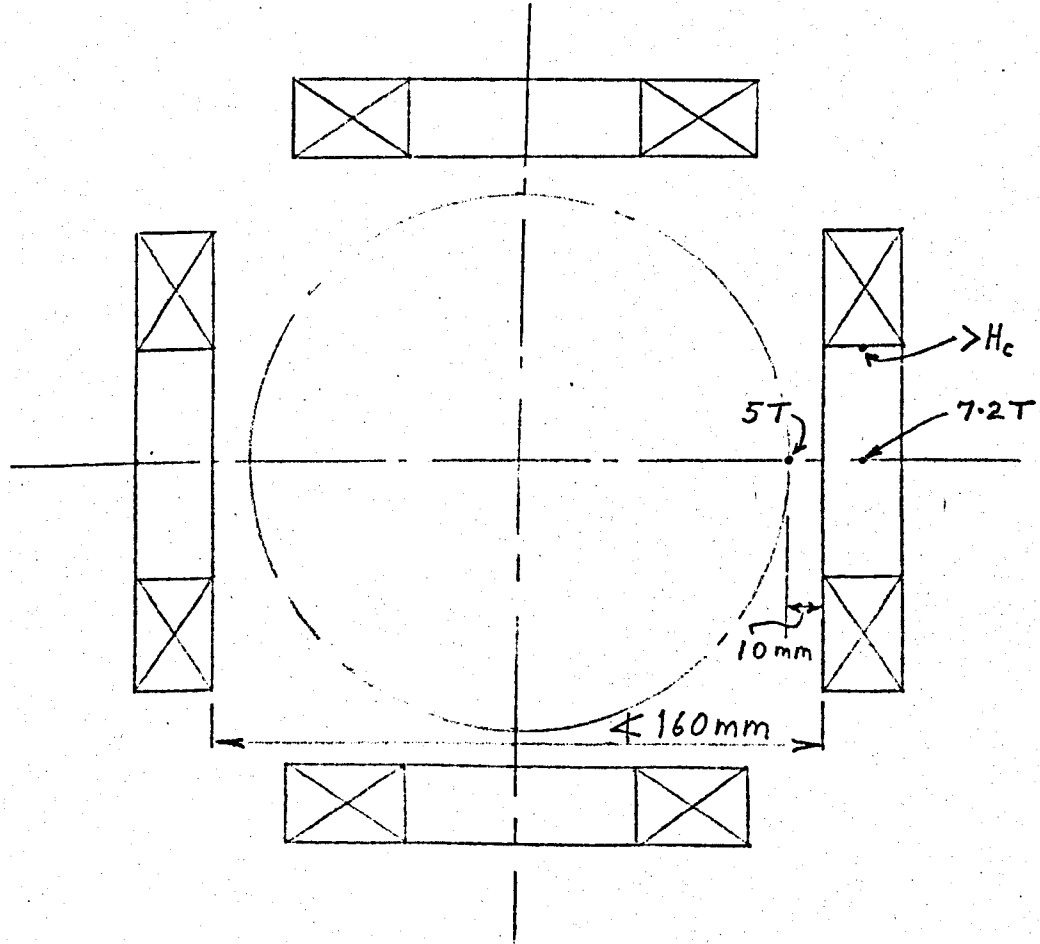


Fig. 64 Preliminary Estimates for Field Coil Arrangement

titanium and copper, but excluding the insulation.

TABLE III

Dimensions of 'Niomax-FM' Filamentary Superconducting Composite

Designation	Diameter Bare mm	Diameter Insulated mm	Filament Diameter mm	Weight/ Unit Length Bare kg/km
A61/33	0.33	0.355	0.028	0.66
A61/40	0.40	0.425	0.034	0.97
A61/50	0.50	0.525	0.042	1.52

As a stabilised superconducting magnet power supply capable of supplying up to 120A was available, it was decided to employ the largest of the three available sizes of wire, i.e. Niomix FM-A61/50 as this would result in coils with a better space factor and be easier to wind. Preliminary runs with computer programs indicated that the minimum distance between the inside faces of four symmetrically placed plane circular coils forming the field system (see fig. 64) could not be less than 160 mm for a maximum field of 5 tesla on the axes of the coils at 10 mm from the end of the coil, this distance being an initial estimate of the nearest the armature surface could possibly be to the field coils. The corresponding maximum field on the axis of the coils was approximately 7.2 tesla and the maximum field at the winding even higher. The current density required was slightly above the critical value given by the typical characteristic and therefore this arrangement was not a practical proposition.

Two alternatives were then considered. The first was to increase the scale of the dimensions so that a field of 5 tesla could be achieved at the armature surface without exceeding the critical values of the field or current of the superconductor and would involve increasing the coil spacing to 180 mm. This was discarded on account of the increased cost. (The balance remaining out of £4,000 of the first phase to purchase superconductor was not sufficient to acquire enough to make a viable machine.) It was therefore accepted that a compromise on the field at the armature would have to be made. By accepting a field of 4.5T at the armature surface, further programs of the field plot showed that this could be achieved with a coil spacing of 160 mm and an armature diameter of 140 mm without exceeding the values of critical field and current of the superconductor. It was realised that there would be very little margin, and practical considerations in the course of the design might mean a reduction in either the field generally available or a reduction in the armature diameter. The latter is particularly undesirable since a further reduction to say 120 mm would correspond to a field of less than 3.5T with a consequential reduction of 25% approximately of the output. This is an example of the contention made in Chapter 9 regarding the minimum viable rating of aircraft generators.

The decision to use plane circular field coils together with their geometry determined the field distribution, which in turn determined the active length of the armature conductors. Since the major cost was in the field system, this was designed first within the constraints discussed above, and optimised as far as practicable

to give the maximum field at the armature for minimum cost. The armature design depended on the diameter available for it, and this was determined by the separation of the field coils and the wall thickness of the cryostat. As the field fell off rapidly towards the centre along the armature radii, it was important to know the cryostat bore accurately before designing the armature. The order following the field design was thus that of the cryostat and then the electrical design of the armature. The objective here was to generate the rated voltage with as large a power output as the available space and cooling would permit. Finally the mechanical design of the armature and its associated parts was carried out.

11. Field Plotting and Design of Field System.

11.1 Approach to Field Design.

The design of the field system consists largely in choosing the size, proportions and dispositions of the field coils. Ideally, the designer of a synchronous generator would like to be able to specify the field form required at the armature surface, and from this be able to determine by analytical means the specification for the field coils to give the required field. Unfortunately, this is not possible for an air-cored machine as a general analytical solution has not been found.

For the experimental machine, the form of the field coils was decided on practical grounds as explained earlier. Their bore, proportions and spacing had to be decided and the method adopted was to make some initial estimates based on the fields along the axes and central planes of single coils which could be determined from very simple expressions and very small programs for computer evaluation. From the field due to the combination of four similar coils initial estimates were made for the bore (internal diameter), outside diameter, length and distance between the coils. A more exact determination of the field distribution was then made for these values of the coil dimensions and a suitable value of current estimated appropriate to the maximum field anticipated at any part of the windings. After several adjustments of dimensions and current, the final values were decided on.

11.2 Field Determination

The calculation of magnetic fields produced by various simple

electromagnetic configurations in air has been considered by the early classical physicists, but their treatments were confined to very simple cases such as circular loops, finite helical solenoids and infinite solenoids. For example, Maxwell⁽¹⁹⁶⁾ calculated the field at points off the axis of a simple current loop, but as Moullin implies in his book⁽¹⁹⁷⁾, the problem was not pursued enthusiastically because it was not of sufficient practical importance and in view of the intricate mathematics required. In the cases which were considered by them and some subsequent workers, such as the helical solenoid or the finite solenoid, the calculations were limited to the axis (e.g. 198 and 199). Derivations for off-axis positions were done by Foelsch⁽²⁰⁰⁾, but the solutions were obtained by means of a large number of approximate expressions which are valid over restricted ranges of size or position.

The great interest in plasmas either as a source of energy or as a propulsion system during the 1950's and 1960's lead to investigations of methods of plasma confinement of which the most promising was the use of magnetic fields. This caused interest to be renewed in the form of the magnetic fields produced by various configurations of conductors carrying current. Up to that time the major difficulty in the calculation of fields of nearly all configurations resulted from the fact that integral solutions could not be achieved without the use of various elliptic integrals. Although many of these were tabulated, the calculations involved were very laborious; however, with the advent of high-speed computers, it became possible to write programs for many of the elliptic functions, thus making it practicable to determine the field produced by many

conductor configurations with axial symmetry.

Snow (201) developed rather involved mathematical formulae in terms of elliptic integrals and legendre functions for the axial and radial components of the magnetic field produced by a cylindrical current sheet and a circular current sheet with circumferential flow of current, these cases being extended to that of a multilayer solenoid. Other elliptic integral formulae have been proposed, but usually they were developed for special applications and are of restricted application or of limited accuracy. In nearly all cases they are so difficult to use when precision is required over a wide range that the principal tables now available have been computed by methods of numerical integration. One very comprehensive set of such tables was produced by Alexander and Downing (202), and are for the field around the end of a semi-infinite current sheet; the coil in question is then built up from these current sheets by a method given in the introduction of the tables. On-axis and off-axis fields from any solenoid with any radial current distribution can be calculated by this means.

Where solutions of less accuracy are required over a restricted range of coil geometries and at either of two current-density distributions, the technical report of Brown, Flax et al (203) is useful, the data being presented in tables and sample graphs. The tabulation or graphical display of a function of four continuous variables, however, would require a very large amount of space for complete coverage of the range of variables of common interest. To reduce this difficulty, Brown and Flax (204, 205) have developed a method in which the magnetic field of any thick circular solenoid can be

treated as a superposition of the fields of four appropriately placed special semi-infinite solenoids with zero inner radius. The radial and axial field components of the special solenoids are expressed non-dimensionally in terms of non-dimensional field-point variables and are presented in both tabular and graphical form. The results are valid both on and off the axis, and inside as well as outside the solenoid winding. The method is intended for coils of uniform current density, but if tables were available for coils in which the current density is inversely proportional to distance from the axis, the method would be suitable for this type of coil as well.

An alternative approach employing spherical harmonics is propounded by Smythe ⁽²⁰⁶⁾ and developed by Garrett ⁽²⁰⁷⁾. It is restricted to systems with axial symmetry, and while having considerable advantages for certain design work and from the computational point of view, it suffers from a serious disadvantage for the field determination in an air-cored electrical machine. In the central zone of a thick solenoid within a sphere which does not reach the nearest corner of the coil, the field at any point is calculated from a power series expansion. An analogous power series, in inverse powers, is used for the field at points outside the sphere containing the remotest corner of the coil. In the shell between these two spheres, the power series fail to converge, and since this shell may form part of the volume in which the armature of a machine may rotate, it is therefore of considerable interest in this context. As the method breaks down in this region it will not be considered further, except to obtain some preliminary design data in the central

zone. Nevertheless, it is a very valuable method for the design of magnets producing fields of very high homogeneity.

In view of the limitations of the existing methods, it was decided to attempt to analyse the type of field used in the experimental machine, and possible in subsequent design studies also, from first principles in a way which avoided these limitations as far as possible. Since the machines would have pairs of symmetrically placed coils, the analysis is based on that of a pair of coils, or symmetrical dipole.

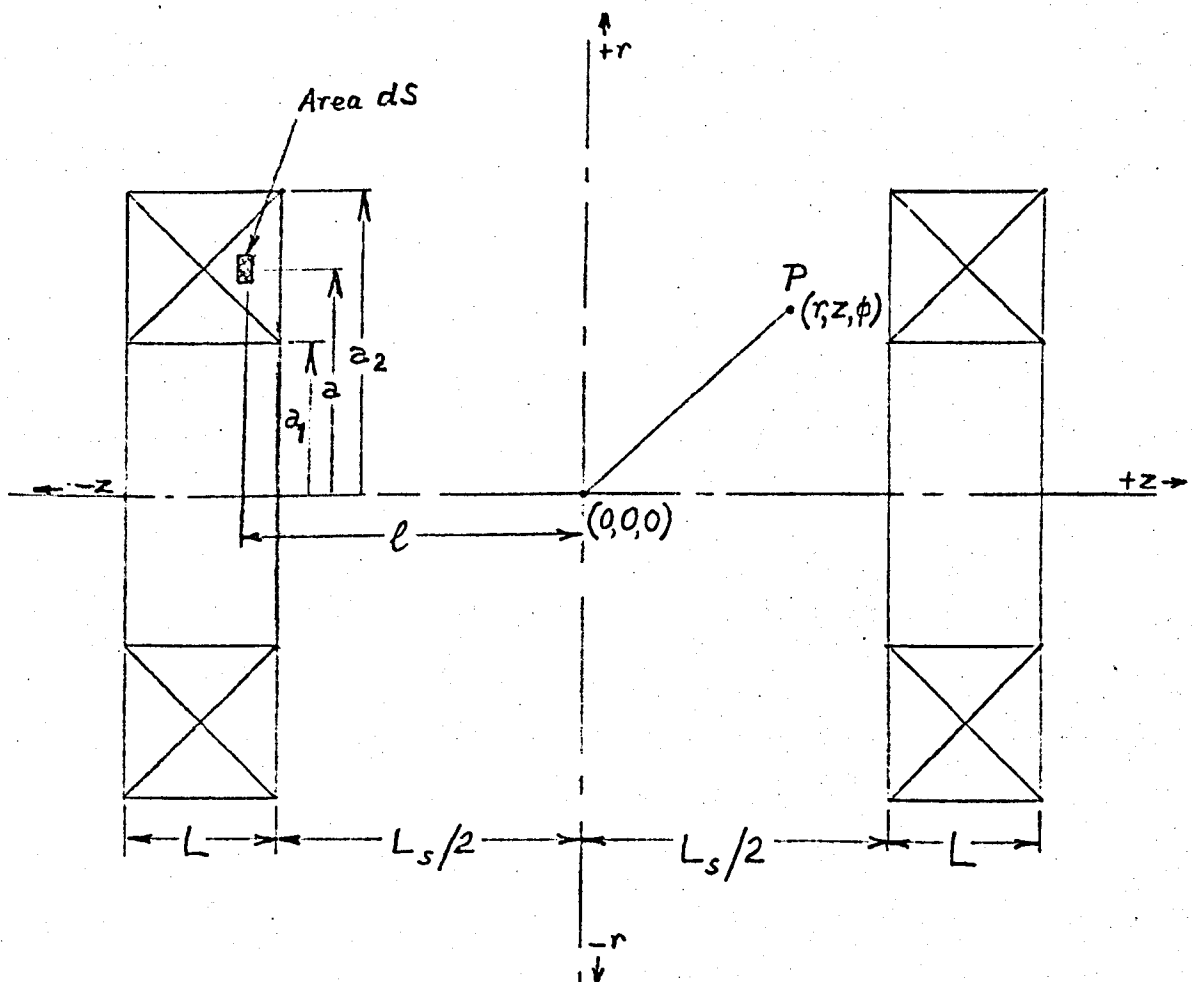


Fig. 65 Arrangement of Symmetrical Dipole Coils

11.3 Field due to symmetrical dipole coils

The dipole comprises two identical coils arranged symmetrically about the axes. The current in each coil is uniformly distributed and has the same value in each. The fields produced by the two coils may assist or oppose each other, as required by the number of pairs of poles in the rotating machine. If the number of pairs of poles is odd, the field distribution in the machine can be synthesized from the appropriate number of symmetrical dipole fields in each of which the fields assist: if the number of pairs of poles is even, the total field is synthesized from dipole fields in which the fields oppose.

The magnetic field due to a symmetrical pair of identical coils can be determined in terms of the vector potential \bar{A} . From cylindrical symmetry, the magnitude of \bar{A} is independent of ϕ . Thus for simplicity, the field point is chosen where $\phi = 0$. Further, it should be noted that equal elements of current equidistant from the axis of cylindrical symmetry (a axis) at $+\phi$ and $-\phi$ produce a resultant which is normal to the rz plane. Thus \bar{A} has only the single component A_ϕ whether each coil is considered separately, or as a pair acting together with either combination of polarities. (The value of A_ϕ will of course depend on which polarity combination exists). In terms of the vector potential, the radial component of flux density,

$$B_r = -\frac{\partial A_\phi}{\partial z}$$

and the axial component of flux density,

$$B_z = \frac{1}{r} \frac{\partial (rA_\phi)}{\partial r}$$

(since $\bar{B} = \nabla \times \bar{A}$).

For an element of a filamentary current loop of area dS with constant current density J :

$$dA_{\phi}(r, z, \phi) = \frac{\mu_0 dSJ}{4\pi} \oint \frac{a \cos \theta d\theta}{R} \quad (60)$$

where R is the distance between the element of the loop and the field point.

From the L.H. complete thick solenoid

$$A_{\phi} = \frac{\mu_0 J}{4\pi} \int_{-L_s/2}^{-(L_s/2 + L)} \int_{a_1}^{a_2} \int_0^{2\pi} \frac{a \cos \theta d\theta}{R} da dl$$

From the R.H. complete thick solenoid

$$A_{\phi} = \pm \frac{\mu_0 J}{4\pi} \int_{L_s/2}^{L_s/2 + L} \int_{a_1}^{a_2} \int_0^{2\pi} \frac{a \cos \theta d\theta}{R} da dl$$

where R is the distance from the local element of the filamentary current loop to the field point.

For the complete dipole, as shown in fig. 65:

$$A_{\phi} = \frac{\mu_0 J}{4\pi} \left(\int_{-L_s/2}^{-(L_s/2 + L)} \int_{a_1}^{a_2} \int_0^{2\pi} \frac{a \cos \theta d\theta}{R_L} da dl \pm \int_{L_s/2}^{L_s/2 + L} \int_{a_1}^{a_2} \int_0^{2\pi} \frac{a \cos \theta d\theta}{R_R} da dl \right)$$

Now $R = \sqrt{(\ell \mp z)^2 + a^2 + r^2 - 2ar \cos \theta}$, where ℓ is the axial distance from the origin to the filamentary current loop.

$$\text{Put } \zeta_L = \ell + z$$

$$\zeta_R = \ell - z$$

$$\zeta_1 = (\frac{1}{2}L_S + z)$$

$$\zeta_3 = (\frac{1}{2}L_S - z)$$

$$\zeta_2 = (\frac{1}{2}L_S + L + z)$$

$$\zeta_4 = (\frac{1}{2}L_S + L - z)$$

$$A_\phi = \frac{\mu_0 J}{4\pi} \left(\int_{-\zeta_1}^{-\zeta_2} \int_{a_1}^{a_2} \int_0^{2\pi} \frac{a \cos \theta \, d\theta}{\sqrt{\zeta_L^2 + a^2 + r^2 - 2ar \cos \theta}} \, da \, d\zeta_L \right. \\ \left. + \int_{\zeta_3}^{\zeta_4} \int_{a_1}^{a_2} \int_0^{2\pi} \frac{a \cos \theta \, d\theta}{\sqrt{\zeta_R^2 + a^2 + r^2 - 2ar \cos \theta}} \, da \, d\zeta_R \right) \quad (61)$$

Integrating with respect to ζ gives:

$$A_\phi = \frac{\mu_0 J}{4\pi} \left\{ \int_{a_1}^{a_2} \int_0^{2\pi} a \cos \theta \left[\ln (\zeta_L + \sqrt{\zeta_L^2 + a^2 + r^2 - 2ar \cos \theta}) \right]_{-\zeta_1}^{-\zeta_2} \, d\theta \, da \right. \\ \left. + \int_{a_1}^{a_2} \int_0^{2\pi} a \cos \theta \left[\ln (\zeta_R + \sqrt{\zeta_R^2 + a^2 + r^2 - 2ar \cos \theta}) \right]_{\zeta_3}^{\zeta_4} \, d\theta \, da \right\} \quad (62)$$

Integration of $I = \int_0^{2\pi} a \cos \theta \left[\ln(\zeta_L + \sqrt{\zeta_L^2 + a^2 + r^2 - 2ar \cos \theta}) \right]_{-\zeta_1}^{-\zeta_2} d\theta$

by parts w.r.t. θ gives

$$I = a \left[\sin \theta \left[\ln(\zeta_L + \sqrt{\zeta_L^2 + a^2 + r^2 - 2ar \cos \theta}) \right]_{-\zeta_1}^{-\zeta_2} \right]_{\theta=0}^{\theta=2\pi}$$

$$- \int_0^{2\pi} \left[\frac{a^2 r \sin^2 \theta}{(\zeta_L + \sqrt{\zeta_L^2 + a^2 + r^2 - 2ar \cos \theta}) \sqrt{\zeta_L^2 + a^2 + r^2 - 2ar \cos \theta}} \right]_{-\zeta_1}^{-\zeta_2} d\theta$$

The first term vanishes, so that

$$i = - \int_0^{2\pi} \left[\frac{a^2 r \sin^2 \theta (\sqrt{\zeta_L^2 + a^2 + r^2 - 2ar \cos \theta} - \zeta_L)}{(a^2 + r^2 - 2ar \cos \theta) \sqrt{\zeta_L^2 + a^2 + r^2 - 2ar \cos \theta}} \right]_{-\zeta_1}^{-\zeta_2} d\theta$$

$$= - \int_0^{2\pi} \frac{a^2 r \sin^2 \theta}{a^2 + r^2 - 2ar \cos \theta} d\theta$$

$$+ \int_0^{2\pi} \left[\frac{\zeta_L a^2 r \sin^2 \theta}{(a^2 + r^2 - 2ar \cos \theta) \sqrt{\zeta_L^2 + a^2 + r^2 - 2ar \cos \theta}} \right]_{-\zeta_1}^{-\zeta_2} d\theta$$

(63)

The first term is eliminated by the θ -limits, and hence:

$$A_{\phi} = \frac{\mu_0 J}{4\pi} \left\{ \int_{a_1}^{a_2} \int_0^{2\pi} \left[\frac{\zeta_L a^2 r \sin^2 \theta}{(a^2 + r^2 - 2ar \cos \theta) \sqrt{\zeta_L^2 + a^2 + r^2 - 2ar \cos \theta}} \right]_{-51}^{-52} d\theta da \right. \\ \left. \pm \int_{a_1}^{a_2} \int_0^{2\pi} \left[\frac{\zeta_R a^2 r \sin^2 \theta}{(a^2 + r^2 - 2ar \cos \theta) \sqrt{\zeta_R^2 + a^2 + r^2 - 2ar \cos \theta}} \right]_{53}^{54} d\theta da \right\} \quad (64)$$

For the radial component of flux density:

$$B_r = -\frac{\partial A_{\phi}}{\partial z} \text{ and from equ. (62),}$$

$$B_r = -\frac{\mu_0 J}{4\pi} \left\{ \int_{a_1}^{a_2} \int_0^{2\pi} \left[\frac{z \cos \theta}{\sqrt{\zeta_L^2 + a^2 + r^2 - 2ar \cos \theta}} \right]_{-51}^{-52} d\theta da \right.$$

$$\left. \pm \int_{a_1}^{a_2} \int_0^{2\pi} \left[\frac{z \cos \theta}{\sqrt{\zeta_R^2 + a^2 + r^2 - 2ar \cos \theta}} \right]_{53}^{54} d\theta da \right\}$$

(65)

Further reduction results in:

$$\begin{aligned}
 B_r = -\frac{\mu_0 J}{4\pi} & \left\{ \left[\int_0^{2\pi} \cos\theta \sqrt{\zeta_L^2 + a^2 + r^2 - 2ar \cos\theta} \, d\theta \right. \right. \\
 & + \int_0^{2\pi} r \cos^2\theta \ln \left\{ (a - r \cos\theta) + \sqrt{\zeta_L^2 + a^2 + r^2 - 2ar \cos\theta} \right\} d\theta \left. \right]^{-52} \\
 & \pm \left[\int_0^{2\pi} \cos\theta \sqrt{\zeta_R^2 + a^2 + r^2 - 2ar \cos\theta} \, d\theta \right. \\
 & \left. + \int_0^{2\pi} r \cos^2\theta \ln \left\{ (a - r \cos\theta) + \sqrt{\zeta_R^2 + a^2 + r^2 - 2ar \cos\theta} \right\} d\theta \right]^{-53} \left. \right\}^{a_2}_{a_1}
 \end{aligned}
 \tag{66}$$

Although equ.(66) is long, it can be solved numerically on a digital computer. The computer used was an ICL 1905A and the program was written in Fortran IV. It should be noted that equ.(66) is not valid for determining the radial component of flux density at the ends of the coils. Normally these values are not of interest in the synchronous machine, but if they were required, it should be possible to modify equ.(66) to make it valid for application at the ends of the coils.

The axial component of flux density is given by:

$$B_z = \frac{1}{r} A_\phi + \frac{\partial A_\phi}{\partial r}$$

Substitution from equ.(64) gives:

$$B_z = \frac{\mu_0 J}{4\pi} \left\{ \int_{a_1}^{a_2} \int_0^{2\pi} \left[\frac{\xi_L a^2 \sin^2 \theta}{(a^2 + r^2 - 2ar \cos \theta) \sqrt{\xi_L^2 + a^2 + r^2 - 2ar \cos \theta}} \right]_{-51}^{-52} d\theta da \right. \\ \left. \pm \int_{a_1}^{a_2} \int_0^{2\pi} \left[\frac{\xi_R a^2 \sin^2 \theta}{(a^2 + r^2 - 2ar \cos \theta) \sqrt{\xi_R^2 + a^2 + r^2 - 2ar \cos \theta}} \right]_{53}^{54} d\theta da \right\} \\ + \frac{\partial A_\phi}{\partial r} \quad (67)$$

From equ.(62):

$$\frac{\partial A_\phi}{\partial r} = \frac{\mu_0 J}{4\pi} \left\{ \int_{a_1}^{a_2} \int_0^{2\pi} \left[\frac{a \cos \theta (r - a \cos \theta)}{(\xi_L + \sqrt{\xi_L^2 + a^2 + r^2 - 2ar \cos \theta}) \sqrt{\xi_L^2 + a^2 + r^2 - 2ar \cos \theta}} \right]_{-51}^{-52} d\theta da \right. \\ \left. \pm \int_{a_1}^{a_2} \int_0^{2\pi} \left[\frac{a \cos \theta (r - a \cos \theta)}{(\xi_R + \sqrt{\xi_R^2 + a^2 + r^2 - 2ar \cos \theta}) \sqrt{\xi_R^2 + a^2 + r^2 - 2ar \cos \theta}} \right]_{53}^{54} d\theta da \right\} \\ = \frac{\mu_0 J}{4\pi} \left\{ I_1 + I_2 \right\} \quad (68)$$

$$I_1 = \int_{a_1}^{a_2} \int_0^{2\pi} \left[\frac{a \cos \theta (r - a \cos \theta) (\sqrt{\xi_L^2 + a^2 + r^2 - 2ar \cos \theta} - \xi_L)}{(a^2 + r^2 - 2ar \cos \theta) \sqrt{\xi_L^2 + a^2 + r^2 - 2ar \cos \theta}} \right]_{-51}^{-52} d\theta da$$

$$I_1 = \int_{a_1}^{a_2} \int_0^{2\pi} \left[\frac{a \cos \theta (r - a \cos \theta)}{(a^2 - r^2 - 2ar \cos \theta)} - \frac{\zeta_L a \cos \theta (r - a \cos \theta)}{(a^2 - r^2 - 2ar \cos \theta) \sqrt{\zeta_L^2 - a^2 - r^2 - 2ar \cos \theta}} \right]_{-\zeta_1}^{-\zeta_2} d\theta da$$

When the $-\zeta_1$ and $-\zeta_2$ limits are applied, the first term disappears.

$$\text{Hence } I_1 = - \int_{a_1}^{a_2} \int_0^{2\pi} \left[\frac{\zeta_L a \cos \theta (r - a \cos \theta)}{(a^2 + r^2 - 2ar \cos \theta) \sqrt{\zeta_L^2 + a^2 + r^2 - 2ar \cos \theta}} \right]_{-\zeta_1}^{-\zeta_2} d\theta da$$

$$\text{Similarly } I_2 = - \int_{a_1}^{a_2} \int_0^{2\pi} \left[\frac{\zeta_R a \cos \theta (r - a \cos \theta)}{(a^2 + r^2 - 2ar \cos \theta) \sqrt{\zeta_R^2 + a^2 + r^2 - 2ar \cos \theta}} \right]_{\zeta_3}^{\zeta_4} d\theta da \quad (69)$$

$$\begin{aligned} \text{Now } \zeta_L a^2 \sin^2 \theta - \zeta_L a \cos \theta (r - a \cos \theta) \\ = \zeta_L (a^2 \sin^2 \theta + a^2 \cos^2 \theta - ar \cos \theta) \\ = \zeta_L a (a - r \cos \theta) \end{aligned} \quad (70)$$

Combining equs. (67), (68), (69) and (70) gives

$$B_z = \frac{\mu_0 J}{4\pi} \left\{ \int_{a_1}^{a_2} \int_0^{2\pi} \left[\frac{\zeta_L a (a - r \cos \theta)}{(a^2 + r^2 - 2ar \cos \theta) \sqrt{\zeta_L^2 + a^2 + r^2 - 2ar \cos \theta}} \right]_{-\zeta_1}^{-\zeta_2} d\theta da \right.$$

$$\left. + \int_{a_1}^{a_2} \int_0^{2\pi} \left[\frac{\zeta_R a (a - r \cos \theta)}{(a^2 + r^2 - 2ar \cos \theta) \sqrt{\zeta_R^2 + a^2 + r^2 - 2ar \cos \theta}} \right]_{\zeta_3}^{\zeta_4} d\theta da \right.$$

$$= \frac{\mu_0 J}{4\pi} \left\{ I_3 \pm I_4 \right\}$$

$$I_3 = \int_{a_1}^{a_2} \int_0^{2\pi} \left[\frac{\zeta_L a (a - r \cos \theta)}{\{(a - r \cos \theta)^2 + r^2 (1 - \cos^2 \theta)\} \sqrt{\zeta_L^2 + (a - r \cos \theta)^2 + r^2 (1 - \cos^2 \theta)}} \right]_{-\zeta_1}^{-\zeta_2} d\theta da$$

Writing x for $(a - r \cos\theta)$ gives

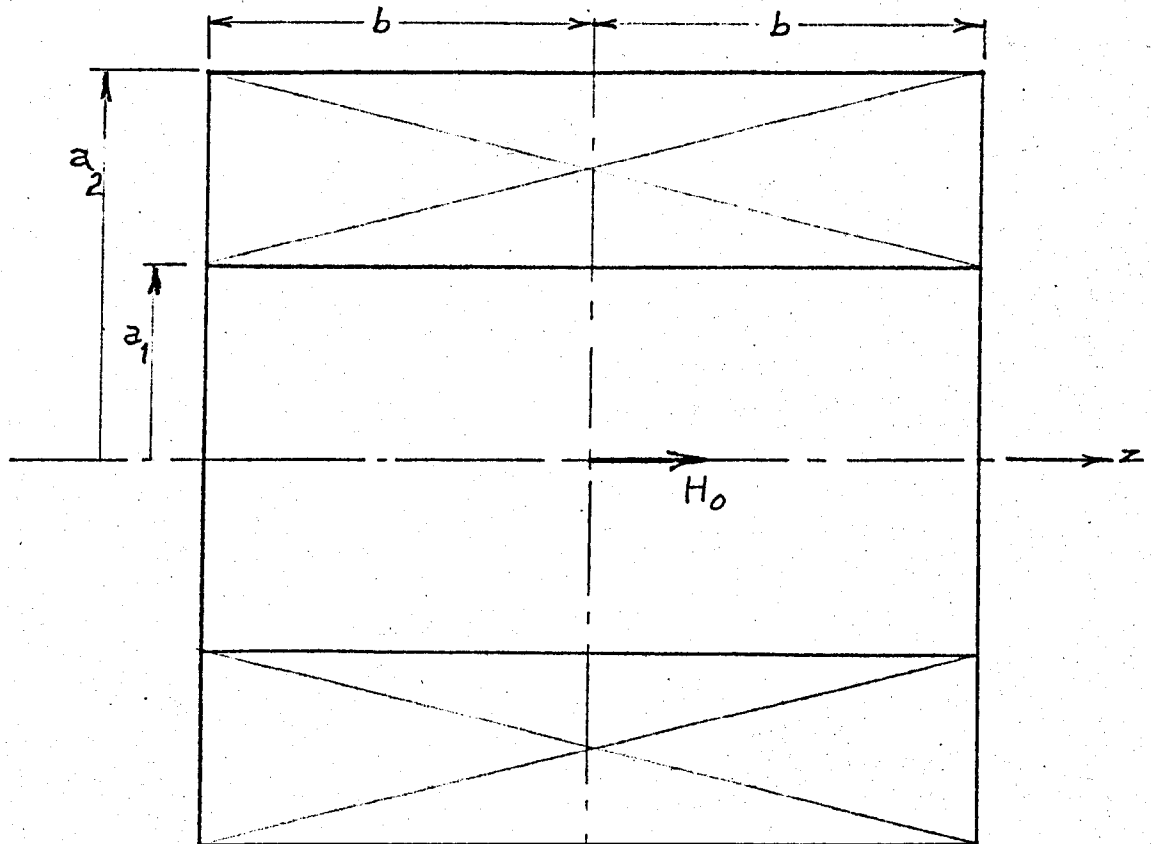
$$\begin{aligned}
 I_3 &= \int_{x_1}^{x_2} \int_0^{2\pi} \left[\frac{\zeta_L x(x + r \cos\theta)}{(x^2 + r^2 \sin^2\theta) \sqrt{\zeta_L^2 + x^2 + r^2 \sin^2\theta}} \right]_{-S_1}^{-S_2} d\theta dx \\
 &= \int_{x_1}^{x_2} \int_0^{2\pi} \left[\frac{\zeta_L (x^2 + r^2 \sin^2\theta)}{(x^2 + r^2 \sin^2\theta) \sqrt{\zeta_L^2 + x^2 + r^2 \sin^2\theta}} + \frac{\zeta_L x r \cos\theta}{(x^2 + r^2 \sin^2\theta) \sqrt{\zeta_L^2 + x^2 + r^2 \sin^2\theta}} \right. \\
 &\quad \left. - \frac{\zeta_L r^2 \sin^2\theta}{(x^2 + r^2 \sin^2\theta) \sqrt{\zeta_L^2 + x^2 + r^2 \sin^2\theta}} \right]_{-S_1}^{-S_2} d\theta dx \\
 &= \zeta_L \int_0^{2\pi} \left[\left[\ln \{ a - r \cos\theta + \sqrt{\zeta_L^2 + r^2 + a^2 - 2ar \cos\theta} \} \right]_{a_1}^{a_2} \right]_{-S_1}^{-S_2} d\theta \\
 &\quad + \frac{1}{2} \zeta_L \int_0^{2\pi} \left[\left[\frac{r \cos\theta}{|\zeta_L|} \ln \frac{\sqrt{\zeta_L^2 + r^2 + a^2 - 2ar \cos\theta} - |\zeta_L|}{\sqrt{\zeta_L^2 + r^2 + a^2 - 2ar \cos\theta} + |\zeta_L|} \right]_{a_1}^{a_2} \right]_{-S_1}^{-S_2} d\theta \\
 &\quad - \zeta_L \int_0^{2\pi} \left[\left[\frac{r \sin\theta}{|\zeta_L|} \tan^{-1} \frac{|\zeta_L| (a - r \cos\theta)}{(r \sin\theta) \sqrt{\zeta_L^2 + r^2 + a^2 - 2ar \cos\theta}} \right]_{a_1}^{a_2} \right]_{-S_1}^{-S_2} d\theta
 \end{aligned}$$

A similar expression can be deduced for I_4 . The second integral in these expressions can be simplified by integration by parts, and the final expression for the axial component of flux density is:

$$\begin{aligned}
 B_z = \frac{\mu_0 J}{4\pi} & \left\{ \left[\zeta_L \int_0^{2\pi} \ln \{ a - r \cos \theta + \sqrt{\zeta_L^2 + r^2 + a^2 - 2ar \cos \theta} \} d\theta \right. \right. \\
 & - \zeta_L ar^2 \int_0^{2\pi} \frac{\sin^2 \theta}{(a^2 + r^2 - 2ar \cos \theta) \sqrt{\zeta_L^2 + r^2 - a^2 - 2ar \cos \theta}} d\theta \\
 & - \frac{r\zeta_L}{|\zeta_L|} \int_0^{2\pi} \sin \theta \tan^{-1} \frac{|\zeta_L| (a - r \cos \theta)}{(r \sin \theta) \sqrt{\zeta_L^2 + r^2 + a^2 - 2ar \cos \theta}} d\theta \left. \right]_{-\zeta_1}^{-\zeta_2} \\
 & + \left[\zeta_R \int_0^{2\pi} \ln \{ a - r \cos \theta + \sqrt{\zeta_R^2 + r^2 + a^2 - 2ar \cos \theta} \} d\theta \right. \\
 & - \zeta_R ar^2 \int_0^{2\pi} \frac{\sin^2 \theta}{(a^2 + r^2 - 2ar \cos \theta) \sqrt{\zeta_R^2 + r^2 - a^2 - 2ar \cos \theta}} d\theta \\
 & \left. + \frac{r\zeta_R}{|\zeta_R|} \int_0^{2\pi} \sin \theta \tan^{-1} \frac{|\zeta_R| (a - r \cos \theta)}{(r \sin \theta) \sqrt{\zeta_R^2 + r^2 + a^2 - 2ar \cos \theta}} d\theta \right]_{\zeta_3}^{\zeta_4} \left. \right\}
 \end{aligned}$$

Although equ. (71) is even longer than equ.(66), it presents no particular problems in programming in Fortran IV, and is valid for all values of the parameters.

In order to provide a check on the programs written for B_r and B_z , the values obtained using these programs for specific examples were compared with those obtained from computations carried out with the MAGNAMOD program. This is a version of the Rutherford MAGNA program which we suitably modified for use on the ICL 1905A computer at Cranfield. Norris and Wilson described the program in ref. 208. Basically MAGNA is a computer program for calculating the magnetic field due to any arrangement of thick conductors in three dimensions, but does not include the use of iron. The calculation is based on the repeated application of a formula derived in ref.208 for the magnetic field due to a straight wire. The current system is divided into a large number of straight filaments, and the contribution of each to the total field is then calculated using the formula. The user approximates his coils and other conductors by a series of prisms of either triangular or parallelogram shaped cross-section. This procedure is very tedious and long even in the case of a simple plain solenoidal coil, but has the advantage of being very flexible. The program divides the end faces of the prisms and joins corresponding mesh points by straight lines, which form the filaments used to calculate the resultant field. An iterative procedure is incorporated which generates a mesh of half the size and the resultant field is again calculated. This process is continued with successively finer sub-division until the difference between the fields produced by two successive steps



$$\alpha = \frac{a_2}{a_1}, \quad \beta = \frac{b}{a_1}$$

J = Current density in conductors,

λ = Space factor.

Fig. 66 Definition of Parameters for a Finite Thickness
Coil with Uniform Overall Current Density, $J\lambda$

is less than some stipulated value.

11.4 Preliminary Estimates for Coils.

It is customary to express the field at the geometric centre of a coil, H_0 , in terms of the coil geometry and current density. The parameters are defined in fig. 66 and H_0 is given by:

$$H_0 = J\lambda a \beta \ln \frac{\alpha + (\alpha^2 + \beta^2)^{\frac{1}{2}}}{1 + (1 + \beta^2)^{\frac{1}{2}}} \quad (72)$$

$$\text{or } H_0 = J\lambda a_1 \beta \left(\sinh^{-1} \frac{\alpha}{\beta} - \sinh^{-1} \frac{1}{\beta} \right) \quad (73)$$

The right-hand parts of eqs.(72) and (73) are entirely geometry-dependent, and it is usual to define a "field factor", $F(\alpha, \beta)$, as:

$$F(\alpha, \beta) = \beta \ln \frac{\alpha + (\alpha^2 + \beta^2)^{\frac{1}{2}}}{1 + (1 + \beta^2)^{\frac{1}{2}}} \quad (74)$$

$$\text{or } F(\alpha, \beta) = \beta \left(\sinh^{-1} \frac{\alpha}{\beta} - \sinh^{-1} \frac{1}{\beta} \right) \quad (75)$$

The field $H_z(z, 0)$ along the axis of a coil with uniform current density is given by:

$$H_z \left(\frac{z}{a_1} \right) = H_0 \left[\frac{F(\alpha, \beta + z/a_1) + F(\alpha, \beta - z/a_1)}{2F(\alpha, \beta)} \right]$$

when the field point z is within the coil, and

$$H_z \left(\frac{z}{a_1} \right) = H_0 \left[\frac{F(\alpha, \beta + z/a_1) - F(\alpha, (z/a_1) - \beta)}{2F(\alpha, \beta)} \right]$$

when it is beyond the end of the coil. It was found more convenient to have the origin at the end of the coil, and with this change the equations are written:

$$H_z\left(\frac{z}{a_1}\right) = H_0 \left[\frac{F(\alpha, 2\beta + z/a_1) + F(\alpha, -z/a_1)}{2F(\alpha, 2\beta)} \right] \quad (76)$$

In order to estimate the maximum field at the windings, the field across the central plane, $H_z(r, \pi/2)$, was determined from an expression involving Legendre polynomials. Since the region of interest is within a sphere which does not reach the nearest corner of the coil, the series is convergent (207, 209) and if the origin is on the midplane of symmetry of the coil, the expansion will contain only even terms and is given by:

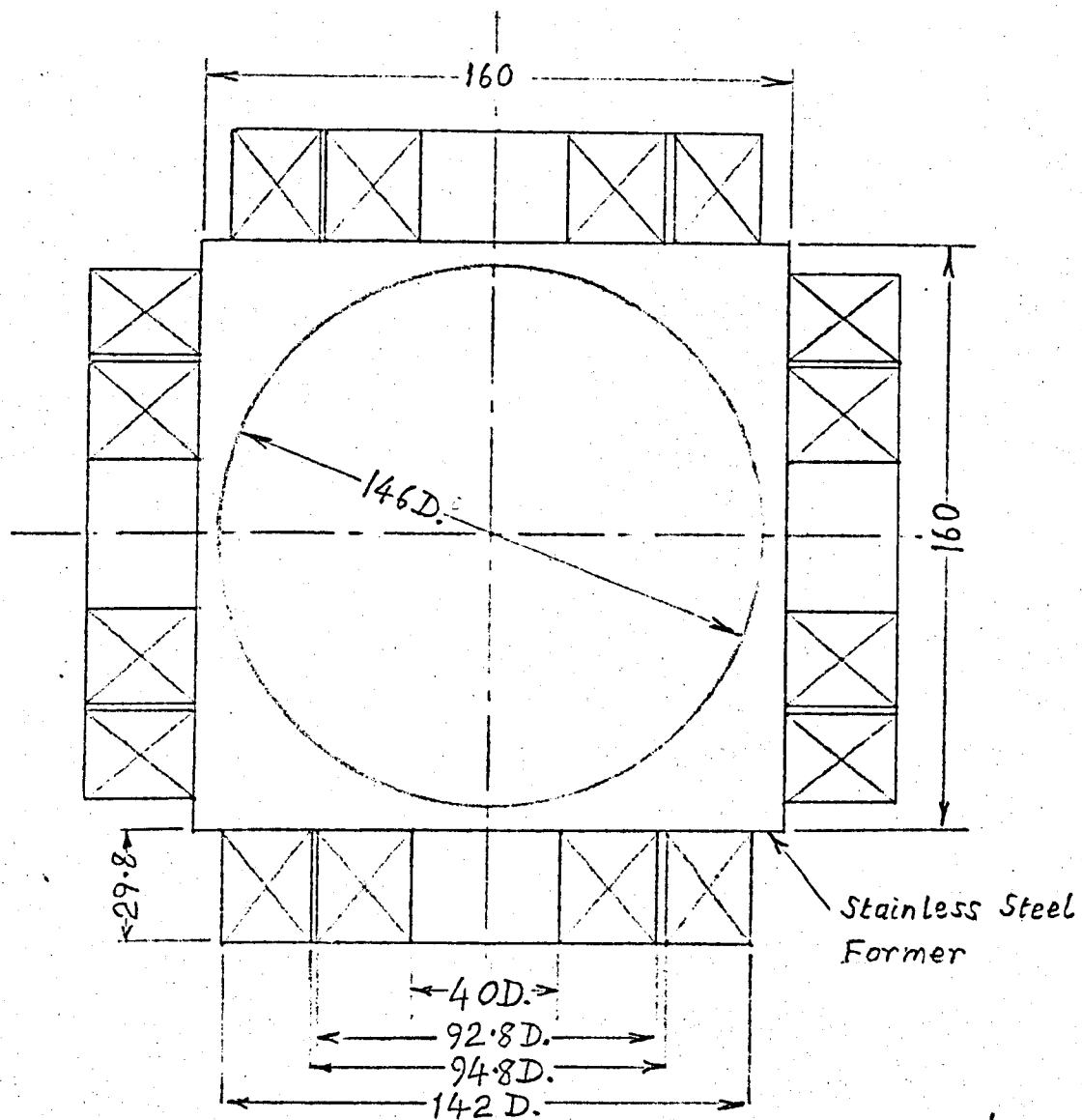
$$H_z(r, \pi/2) = H_0 \left[1 - \frac{1}{2} E_2 \left(\frac{r}{a_1}\right)^2 + \frac{3}{8} E_4 \left(\frac{r}{a_1}\right)^4 - \frac{15}{16} E_6 \left(\frac{r}{a_1}\right)^6 + \dots \right] \quad (77)$$

where the E_n coefficients are defined by:

$$E_{2n} = \frac{1}{H_0} \frac{1}{(2n)!} \left. \frac{d^{2n} H_z(z, 0)}{dz^{2n}} \right|_{z=0}$$

As E_2 for a solenoid is always negative, it is seen that the field increases from the axis in the radial direction.

Programs for eqs. (76) and (77) were written in Fortran IV, and these were used in the preliminary estimating of the coil dimensions.



All dimensions in mm.

SCALE: $\frac{1}{2}$ Full
Size

Four sets of coils are identical

Inner coil of each set only fitted in first stage

Fig. 67 Dimensions and dispositions of field coils for prototype machine

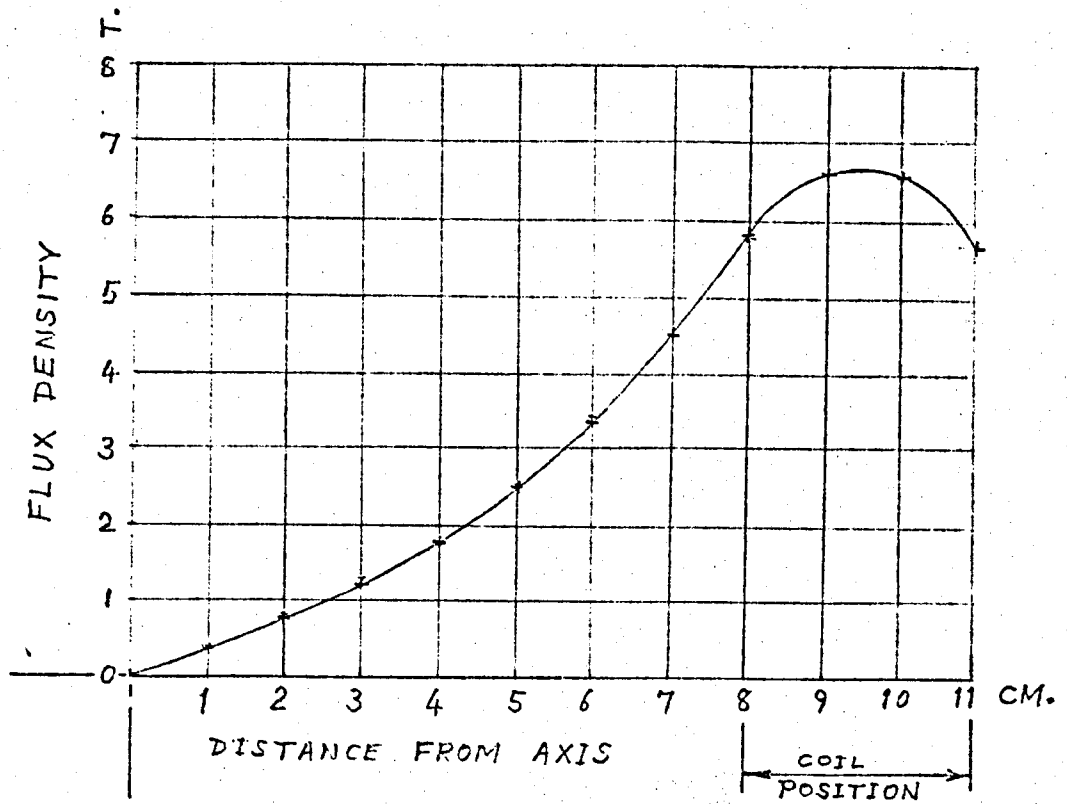
11.5 Final Design of Coils.

After several successive revisions, the final design of the field coils was arrived at. It was found to be advantageous and practical to use a single stage of current grading so that the final set of field coils for the second stage machine would operate with the outer sections at a high current density ($3.6 \times 10^4 \text{A/cm}^2$) while the inner sections would operate at a lower current density ($2.56 \times 10^4 \text{A/cm}^2$) since they experience a much higher field. In order to use a single current supply for the field, the grading is achieved by using a wire with smaller area of superconducting material for the outer sections than that in the inner sections, and connecting all the sections in series. IMI Niomax FM wire code A61/40 will be used for the outer sections when they are added at a future date, but the present inner sections which will be retained are wound with code A61/50.

The dimensions of the coils and a plot of the axis field are given in figs. 67 and 68. The design operating current for the field is 70A for the second stage, but when the inner sections operate on their own, a much higher current can be used because of the absence of the field due to the outer sections; a current of 90A for the inner coils only is considered a reasonable value.

11.6 Construction of Coils.

The coils were wound using facilities of the Oxford Instrument Company, and impregnated with epoxy resin. The numbers of turns on the coils as finally constructed are:



CURRENT DENSITIES : INNER COILS $2.56 \times 10^4 \text{ A/CM}^2$
 OUTER COILS $3.60 \times 10^4 \text{ A/CM}^2$

Fig. 68 Field along pole axis of experimental machine

2483

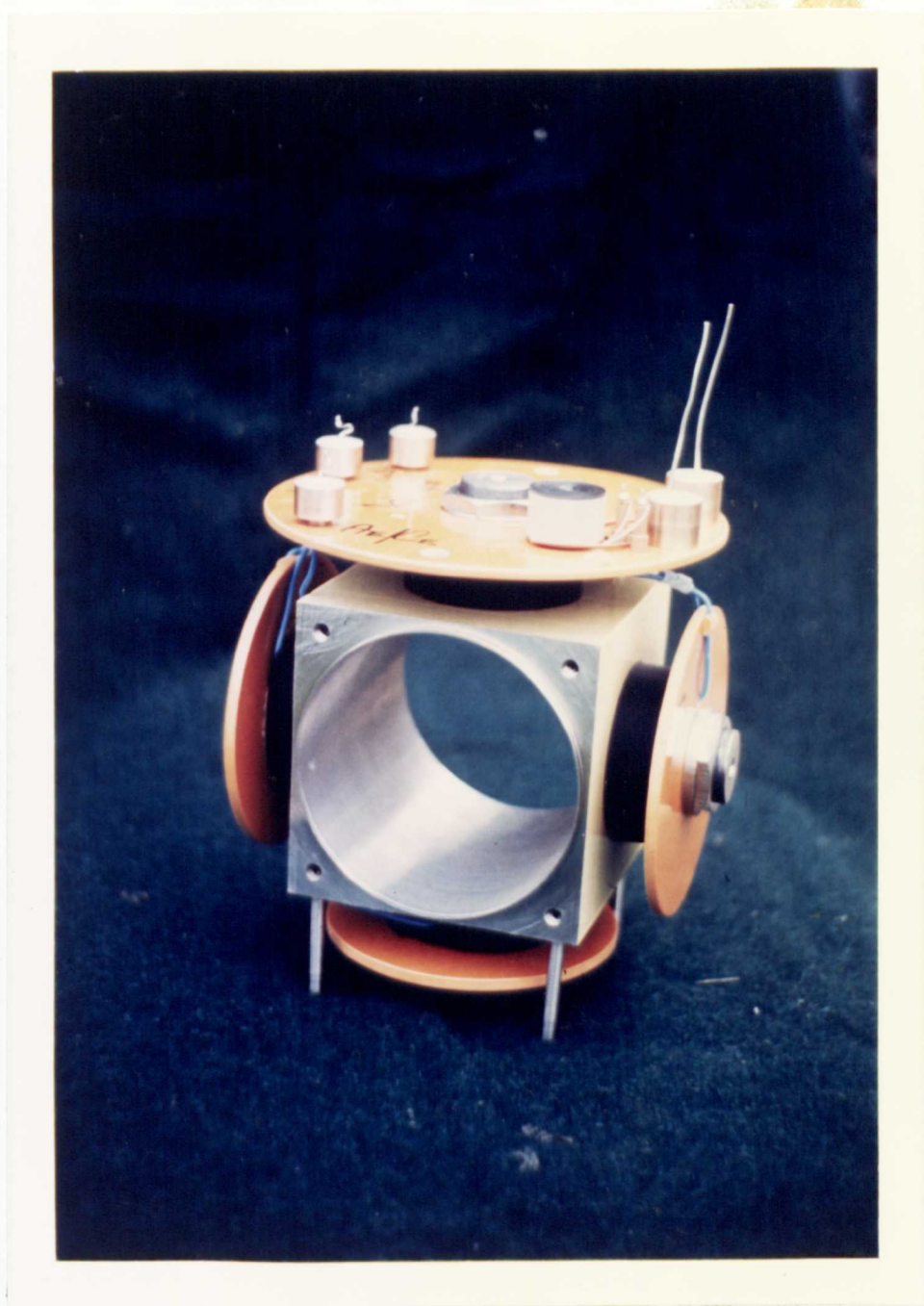
2483

2488

2487

Provision is made for operation of the coils in the persistent mode by the provision of a superconducting switch.

The coils are mounted in the cryostat on a stainless steel former machined from a solid block as shown in the cryostat drawings in the next chapter. This construction was adopted in order to provide rigidity for the field coils under the magnetic forces acting between them and to provide a means of transmitting the reaction torque from the armature to the inner vessel of the cryostat. A photograph of the completed field coil assembly appears on page 255.



Field Coil Assembly



Cryostat showing Room Temperature Aperture

12. Cryostat Design

12.1 General Features

The cryostat was designed in conjunction with the Oxford Instrument Company and manufactured by them. It consists basically of three concentric cylinders with their common axis vertical. The room temperature aperture in which the magnetic field is produced is a multiwalled horizontal cylinder symmetrically placed in relation to the vertical axis. The general arrangement is shown in fig. 69 and photographs of the completed cryostat appear on page 256 and in the view of the complete machine in the frontispiece.

The cryostat is designed to withstand the reaction torque on the field system when the armature is delivering 100 kW of power at 12,000 r.p.m., with a 25% margin to cater for excess torque under overload or fault conditions. Certain features of the construction (notably the main suspension tube for the helium container, and the torque transmission struts) are considerably stiffer than normal conditions would dictate in the absence of the reaction torque and consequently are the causes of higher heat leaks than would normally be accepted.

12.2 Main Construction.

The innermost vertical cylinder extends approximately halfway up the cryostat and forms the liquid helium container. It has an outside diameter of 324 mm with a wall thickness of 4 mm; the bottom is welded to it and formed from a 11 mm thick disc. The top is a 16 mm thick disc bolted to the cylindrical section with an indium seal so that the completed helium container is vacuum tight.

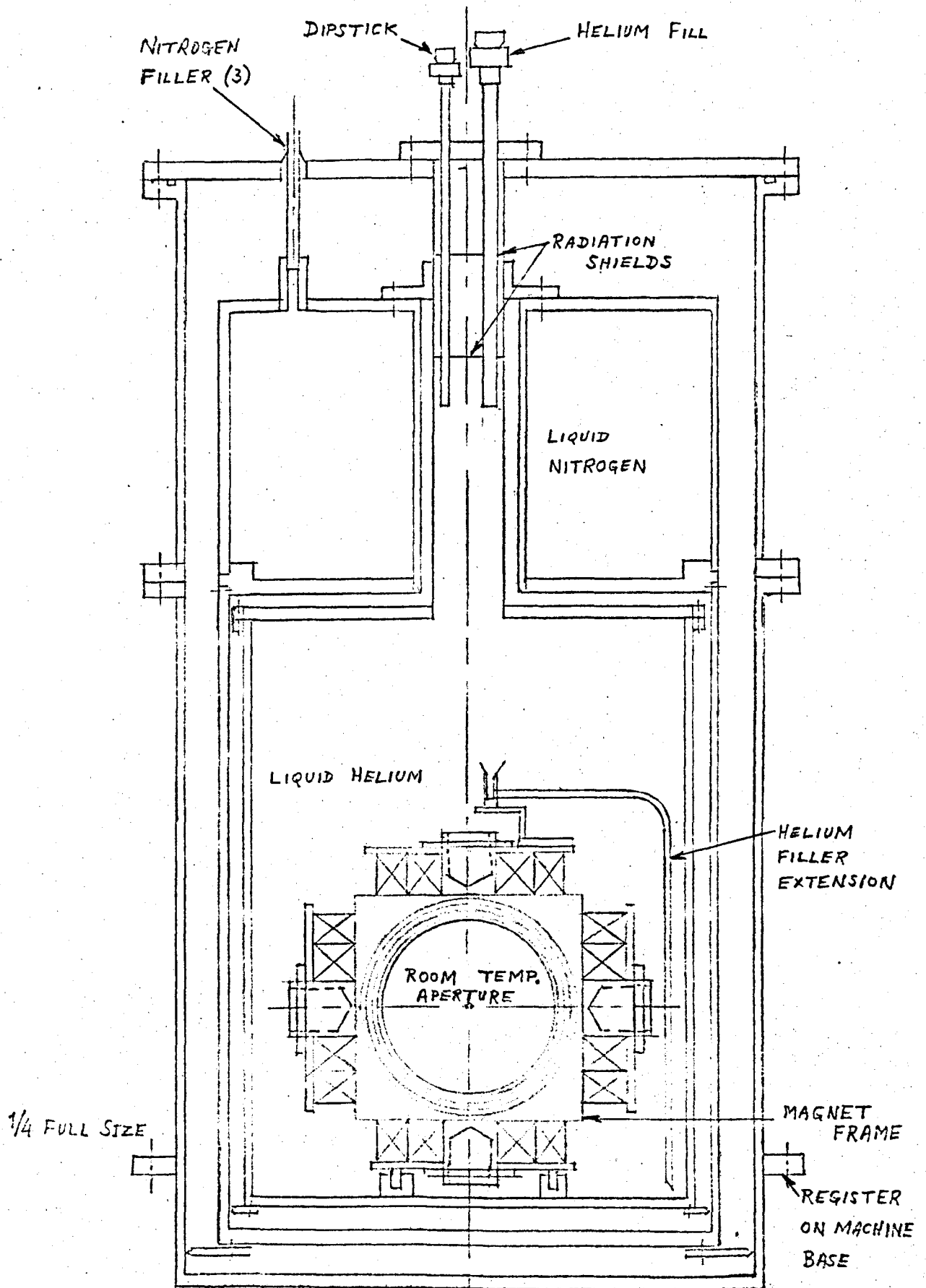


Fig. 69 Outline of Cryostat

The helium container is mounted from the outside top plate by a stainless steel suspension tube welded to it. It is made from cryogenic stainless steel and electro-polished externally to reduce radiation.

The middle vertical concentric cylinder of 3.3 mm walled aluminium forms two cylindrical cavities, the lower enclosing the helium container and forming the radiation shield and the upper forming the liquid nitrogen reservoir. The radiation shield continues under the base of the inner helium container with a 13 mm thick aluminium disc welded to the vertical cylinder. The radiation shield is cooled by conduction from liquid nitrogen in the upper cavity. The radiation shield is screwed to the 13 mm thick bottom plate of the liquid nitrogen reservoir so that it can be removed to give access to the helium container in the course of assembly. The liquid nitrogen reservoir has a 18 mm thick top plate carried on the same main suspension tube as the helium container, and from which it thus helps to remove heat inleaks from the external ambient.

The outer container is manufactured from aluminium and has cylindrical walls 4.8 mm thick with a 16mm base plate welded to it. It is screwed to the 13 mm thick top plate and sealed to it with an 'O'-ring joint. The top plate carries the usual accessories: vacuum connection and valve, liquid nitrogen and liquid helium filler tubes, helium boil-off connection, dipstick and lead-throughs for electrical connections. Vacuum insulation is used between the outer container and radiation shield and between the radiation shield and helium container. Both surfaces of the

radiation shield and the inside of the outer container are polished to minimise radiation in-leaks reaching the liquid helium. The helium transfer line (vacuum insulated) is fitted when required through the appropriate filler tube and connected to an extension tube on the top of the magnet assembly. This enables the liquid helium to be fed to the bottom of the helium container so that the enthalpy of the gas boil-off can be partly used to cool the magnet assembly.

The room temperature aperture for the rotating armature is formed from two cylinders. The inner cylinder at room temperature is made of brass and is needed to maintain the vacuum space between the outside air and the copper outer cylinder which form the radiation shield. The inner brass cylinder is mounted inside a bush at each end, these bushes being welded to the main outer container. A vacuum-tight joint is formed inside the bushes by double 'O'-rings. The radiation shield is similarly mounted inside bushes welded on to the main radiation shield, but in this case, a vacuum seal is not required but good thermal contact is essential. The radiation shield is made of ofhc copper to have a low electrical resistivity so that field variations due to armature currents are screened from the superconducting magnets and so that the eddy current heating thus caused will be predominantly dissipated in the liquid nitrogen rather than in the helium.

Liquid helium is prevented from reaching the radiation shield in the room-temperature aperture by using the inside cylindrical surface of the magnet assembly block, and sealing this to the main helium container by means of flexible corrugated bellows. By this

means, any stresses due to the thermal contractions, reaction torques, lack of alignment or other causes are transmitted via the main supports of the magnet assembly to the base of the helium container, thus avoiding unnecessary stresses on the comparatively thin cylinders forming the room-temperature aperture. These were made as thin as possible with minimum clearances so that the armature surface could be as close to the magnet coils as possible. It was hoped originally that this space would be only 10 mm, but in the final design it was found necessary to increase it to 12 mm to give a room temperature bore of 136 mm. Small spacers were included between the various cylindrical surfaces to maintain correct clearances; they consisted of 4 mm diameter pins with coned ends screwed into the radiation shield.

The torque reaction from the armature on the magnet coils is transmitted to the base of the helium container by the stainless steel support block and its support pillars. Part of the torque reaction is then taken directly by the main suspension tube to the main top plate and outer container, while the remainder is taken via six radial torque transmission struts to the radiation shield, and thence by six further torque transmission struts to the outer container.

The cryostat is mounted on the machine bed by a mounting ring welded on the outside of the outer container below the room temperature aperture. The mounting ring was accurately machined after it was welded in place so that its lower face would provide a register to ensure the accurate positioning and alignment of the cryostat on the machine bed in relation to the armature.

The cryostat is demountable to give easy access to the magnet assembly, and so that alternative cylinders can be fitted surrounding the room temperature aperture to enable the effects of different materials and thicknesses on the screening of time variant armature fields to be investigated subsequently.

13. Armature Design and Mechanical Features.

13.1 General Features.

The most unusual feature in the construction of the armature is the absence of ferro-magnetic material. The conventional iron teeth are not required, thus increasing the space available for armature conductors and obviating the need to insulate every conductor for the full voltage of the machine. The armature can be wound so that the conductors need be insulated only from neighbouring conductors, thus allowing a reduction in the amount of insulation required, or alternatively an increase in rated voltage. The absence of teeth means that the leakage inductance of individual conductors is much lower, and since they are exposed to the full intensity of the magnetic field, large eddy currents will be produced unless the basic conductors are sub-divided into insulated strands of sufficiently small diameter. With a large number of small strands per basic conductor, circulating current losses are potentially a serious problem, and twisting or transposition of the strands must be considered very carefully together with the method of terminating them.

The teeth and iron core form a major structural element in a conventional machine which takes all the reaction forces on the conductors. With the elimination of iron in the armature, some other method of supporting the conductors against the forces occurring under normal and fault conditions must be devised, and in order to keep the insulation requirements down, it is desirable that this structure is electrically non-conducting.

The increased space allowed for conductors by the absence of iron teeth makes the end turn geometry more difficult because conductors packed tightly together cannot easily be bent at the ends of the armature without a change in their geometry. The increased number of strands in the conductors may increase the complexity of the fabrication process. In any case, an armature with no iron will need to be constructed in a very different manner from a conventional armature.

13.2 Winding Scheme.

If the fundamental component of the flux distribution at the armature surface is considered, the r.m.s. value of the voltage generated in a single full-pitch turn on the armature is given by:

$$E_c = \sqrt{2\pi f \Phi} \quad (79)$$

where f is the frequency of the voltage generated, and Φ is the total fundamental component of the radial flux at the armature surface. For T_c turns connected in series in one phase of an armature winding, the voltage generated depends on the phase spread and the distribution of the winding, which can be taken into account by a distribution factor, k_d . For a winding distributed uniformly over a spread of 60° , k_d has a value of 0.955. Thus for a value of flux per pole of 3 mWb, corresponding to the field produced by the inner part of the field coils used in the first stage, 24 turns per phase are required; and for a flux per pole of 4.5 mWb (i.e. with the complete coils of the second stage) 16 turns per phase are needed in order for 120 V per phase to be generated.

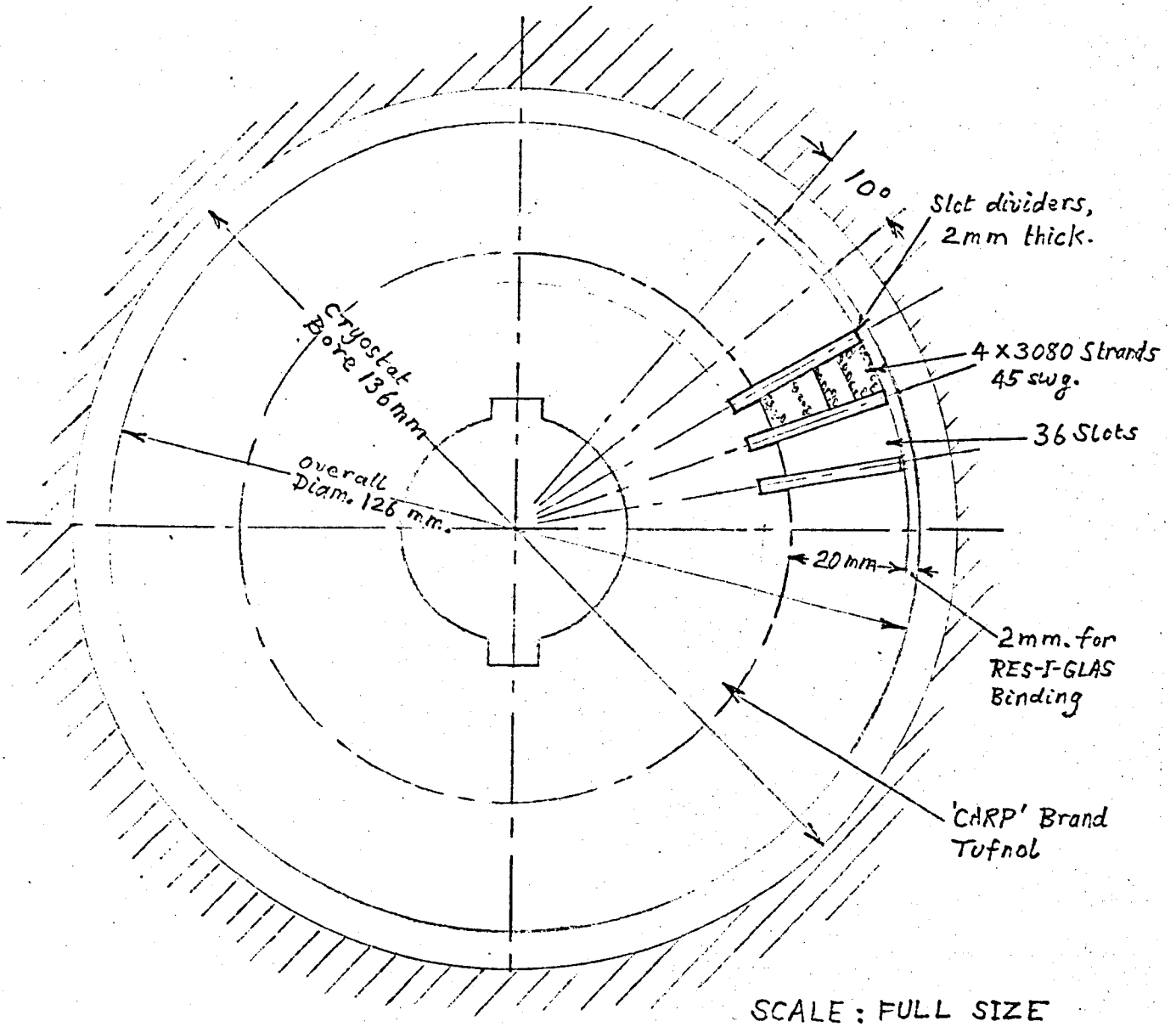


Fig. 70 Cross-section of armature

The room temperature bore of the cryostat is 136 mm and with a mechanical clearance of 5 mm between the cryostat and armature for cooling air, the outside diameter of the armature is 126 mm. It was decided to mount the armature conductors on a synthetic resin bonded fabric (SREF) cylinder of carp grade 'Tufnol' keyed to the armature shaft. The armature conductors would be located by radial fins of similar material 2 mm thick and held by axial slots machined in the core cylinder; these fins would also take the reaction forces on the armature conductors. It was intended originally to have three radial sets of conductors between each pair of fins, but it was found necessary to use a fin between each radial set of conductors to hold them in place during construction of the armature because the conductors were not sufficiently rigid to remain in place without individual support. This meant a reduction in the overall space factor and a corresponding reduction in current rating.

The conductors and end connections are held in place by circumferential banding with 12 mm wide woven glass tape wound on under a tension of 75 kg. The tape is supplied impregnated with epoxy resin and cured after assembly. The completed armature was impregnated with Araldite epoxy resin and then cured in an oven for 4 hours at 90°C followed by 12 hours at 150°C. After a final skimming cut on a centre lathe to remove irregularities on the hardened resin, the completed armature was dynamically balanced.

A cross-sectional view of the armature is shown in fig. 70 for the first stage. The axial length of the intense magnetic field is 55 mm (and increases to 80 mm with the outer sections of the field coils). In view of the uncertainty of some of the

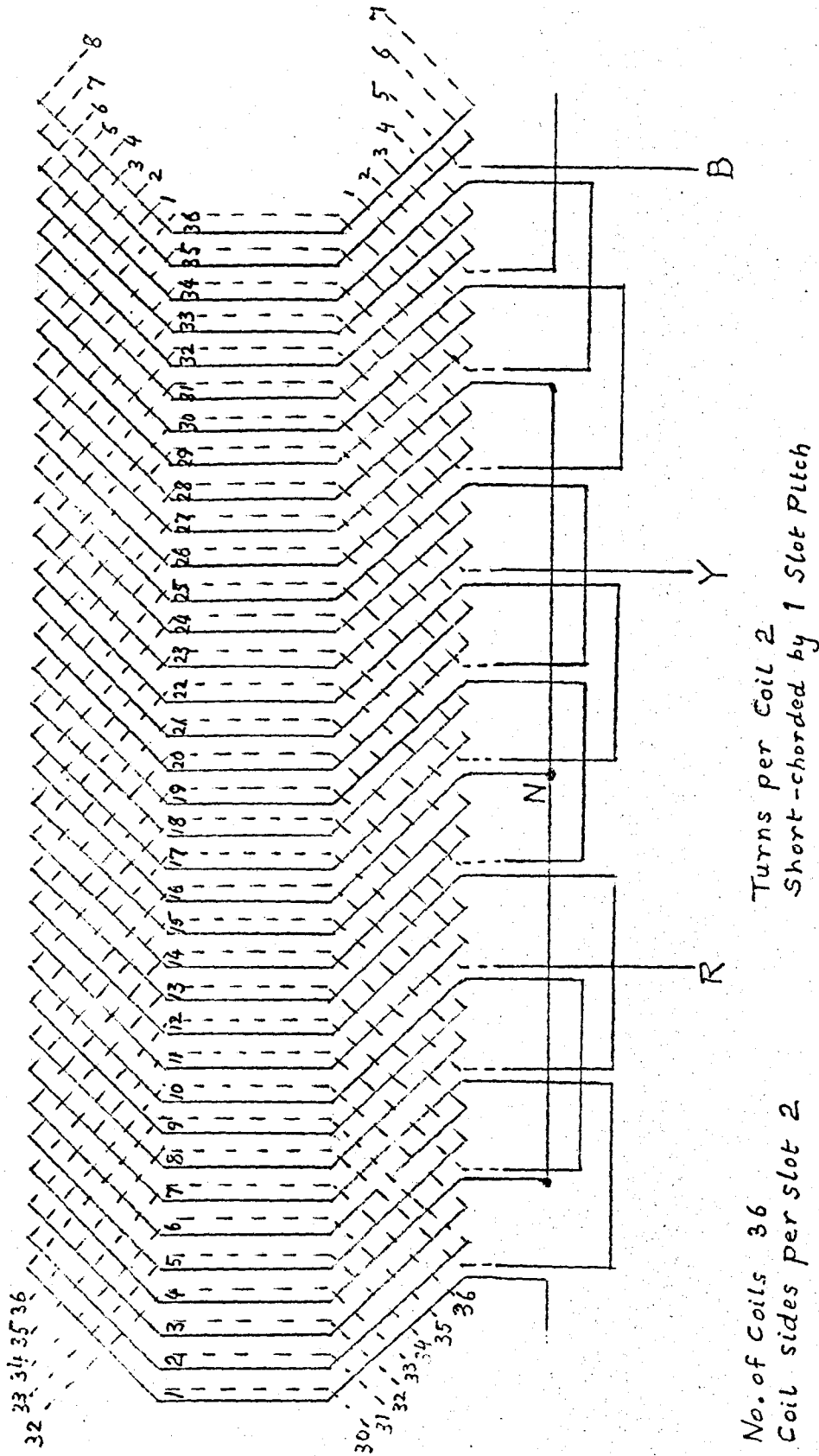


FIG. 71 Winding Diagram for Armature of Experimental Machine.

design parameters, the design of the first stage armature only was proceeded with, the design of the second stage being suspended until more reliable data became available.

For the first stage, single-turn coils with two coil sides per slot gave a very low overall space factor, and the most satisfactory arrangement appeared to be the use of double-turn coils with two coil sides per slot. The "slot" dimensions are 21 mm deep by 8 mm wide (mean), and allowing a current density in the conductors of $5A/mm^2$, a not too conservative figure based on a preliminary thermal analysis allowing for some forced cooling with air, and a space factor of 0.55 overall, the resulting phase current is 110 A with a corresponding machine rating of 40 kVA. The specific electric loading is 125,000 Ac/m, a high but not unreasonable value.

The winding selected is double-layer with lap-connected coils, as the constant pitch of this type enables the coils to be pre-formed on a single former. The coils are joined to each other by a soldered joint, thus ensuring that all the strands in the conductor are solidly connected together at the end of each coil. The need for this and stranding are explained in the next section. The phases are connected in star internally, and as there was no specific reason for using a 4-wire system, the star point is not brought out thereby saving one slipring. The winding diagram is given in fig. 71.

13.3 Electrical Losses.

A number of electrical losses can be identified in the armature winding due to various causes. Alternating currents and fluxes

have a tendency to confine themselves to the outer layers of a conductor, this phenomenon being called the skin effect. This results in a higher resistive loss than when the current is uniformly distributed. Secondly, the current-carrying conductors of the armature are located in the magnetic field produced by the poles of the machine which for the most part is transverse to the conductors, but in the end regions will traverse them in a most complicated manner. As the non-uniformly distributed flux changes spatially with respect to the conductors, eddy currents will be induced which cause the distribution of current across the section to become non-uniform and giving rise to eddy-current losses. Thirdly, the armature conductors are situated parallel to each other and consequently the distribution of the current across the cross-section of any one will be affected by the fields of neighbouring conductors. The non-uniform current distribution resulting from this proximity effect gives rise to further losses. Lastly, because various sections of any conductor will not be situated in fields of the same flux density due to the large radial gradient of the field produced by the poles, emf's of correspondingly different magnitudes will be generated and give rise to circulating currents within individual sections and a corresponding circulating current loss in the complete conductor.

Both skin effect and eddy current losses can be reduced to acceptable levels by stranding the armature conductors, and the circulating current loss drastically reduced by twisting or transposition of the strands within the conductors. In fact, it is the

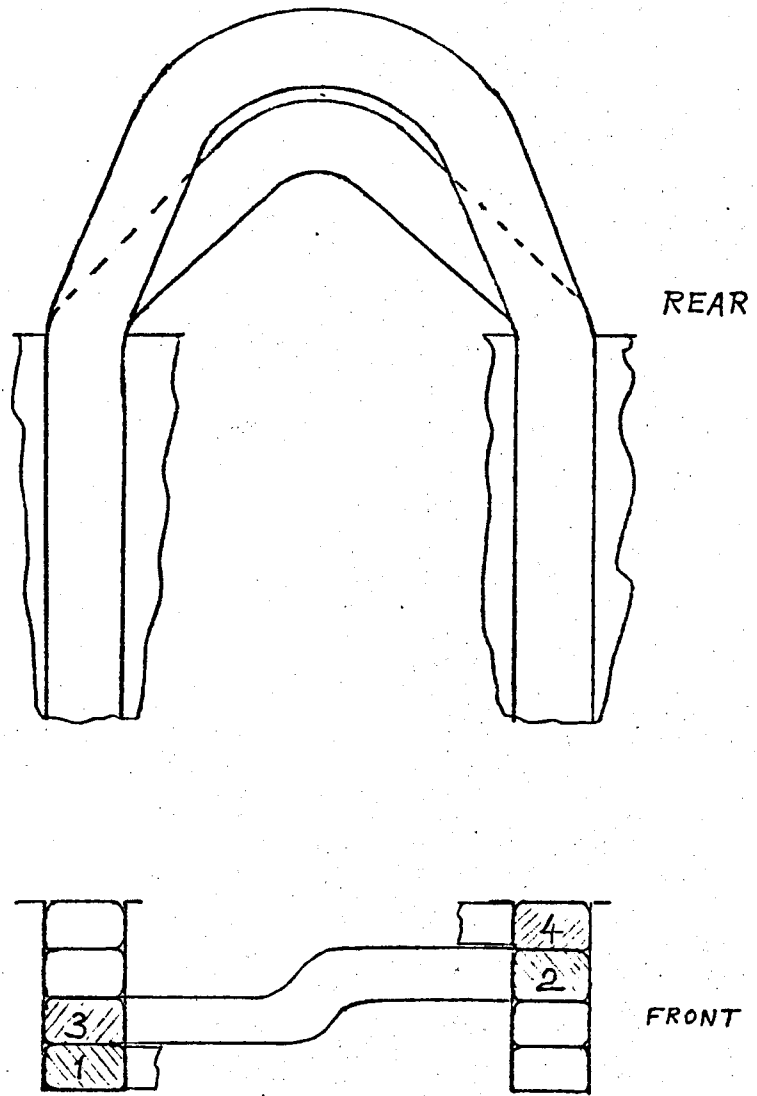


Fig. 72 Arrangement of coil sides and end connections.

eddy current loss which dictates the diameter of individual strands in the armature conductors and which results in a large number of very small strands. With a large number of small strands per conductor circulating current losses are potentially a serious problem and twisting and transposition of the strands must be considered carefully.

The design uses a double transposition. The group of strands in a single conductor has a twist pitch of approximately 25 mm throughout the length of a coil. Because of this short pitch in relation to the length of conductor in a double-turn coil, it is not necessary to consider the number of transpositions between the ends of a coil. The individual strands are all joined together at each end of a coil. The second transposition takes place within the coil, in that the overhang is arranged so that the conductor occupies one of the four possible positions in the slots once in each coil, as illustrated in fig. 72.

This pragmatic approach was taken because of the fundamental difficulty of determining an ideal transposition length for one coil. The problem is that circulating currents arise from different fluxes linking parallel strands. The flux linking parallel strands can arise from the field winding or the armature itself. The field patterns in the end turns are complex, and the field winding flux distribution will differ considerably from that of the armature self-flux. The total flux pattern will change with the relative magnitudes and positions of its two components, and a transposition length which is perfect for one particular load, might have significant circulating current losses at another load

of different magnitude or power factor. Because the field pattern is load dependent and is not accurately known in the end turns, and also for simplicity in construction, it was decided to adopt the above procedure with a constant twist pitch and transposition arrangement for all coils.

The loss due to proximity effect is likely to be considerably less than 8% of the transport current loss (210) with the stranding requirements due to eddy currents. Since the size, spacings and resistivity of the groups of conductors will not be known with high precision, and in view of the uncertainty of the circulating currents, the other losses are not likely to be known to an accuracy better than this value and so the loss due to proximity effect will not be considered further.

Carter (211) derives an expression for the loss in a conductor carrying alternating current in an alternating transverse field, located so that the field is at right angles to the axis of the conductor. Although the flux is assumed to be time-variant in the derivation given by Carter, it will be assumed to be also applicable in the case where a conductor moving at constant velocity crosses a stationary flux sinusoidally distributed in space, since the conductor appears to experience a flux changing sinusoidally in time. This is considered to be justified providing the width of the conductors is sufficiently small for the variation in field across an individual conductor strand to be negligibly small. Carter's expression for the eddy-current loss in a conductor with a circular cross-section is:

$$w_{ec} = \frac{\pi}{4} \cdot \frac{a_B^4 \omega^2}{\rho} \quad \text{watts per metre} \quad (80)$$

where a is the radius of the conductor,

B_0 is the maximum value of the flux density,

ω is the angular frequency, and

ρ is the resistivity.

The value of the skin effect can be determined from the expression given by McLachlan in reference 212, in conjunction with tables of Bessel functions. However, for the sizes of strands likely to be used based in equ. (80), the ratio of R_{ac}/R_{dc} differs very little from unity, and thus it is not necessary to consider skin effect any further.

13.4 Conductor Details.

As explained in the previous section, the size of strand required in the armature conductors is determined by eddy current loss considerations. Supposing that the optimum is obtained when the eddy current loss equals the normal resistance loss, equ. (80) gives a strand diameter of 0.016 mm for the current and flux density *and insulation thickness of the strands.* in the armature. This is an extremely fine wire, and apart from the difficulty in handling it in the course of manufacturing the armature, would result in an undue proportion of insulation and consequently a low space factor and a de-rating in overall current. It also presented the problem of terminating both ends of each strand in a satisfactory electrically conducting joint: the prospect of removing insulation from several thousand strands for each joint, even by chemical means, was a task likely to daunt the keenest enthusiast. Fortunately, an alternative was found which obviated this task. It was to use wire insulated with solderable

enamel. This wire is manufactured to British Standards 3188 and 4520 which cover dimensional and quality control requirements, but give no indications of acceptable operating conditions. Preliminary tests were, therefore, undertaken on samples of wire to determine the likely maximum operating temperature. For the type of duty which the laboratory machine would have to perform, a maximum operating temperature of 100°C was found to be acceptable, although this does not necessarily imply that this temperature would be suitable for a machine in continuous service. Other tests carried out were to check that the epoxy resin, hardener and accelerator did not attack the enamel chemically, or cause it to soften; also that the curing cycle required by the epoxy resin did not cause deterioration in the enamel. This was checked by voltage breakdown tests, but no reduction in breakdown voltage was found due to the effect of an extended curing cycle; there was only a very slight discolouration.

It was found that a braid of 28 strands of 45 SWG (0.71 mm) copper wire insulated with polyurethane base enamel with solderable properties was available commercially. It was considered that although this gauge was of larger diameter than that calculated earlier, it would be a more practical proposition to use in the construction, and since the space factor (and therefore current) was lower than originally intended, the difference between the wire proposed and the optimum based on the lower current would not be as marked as might appear.

The final choice of conductor, based on the number of strands which it was found could be introduced in the winding space was 110 braids, each braid consisting of 28 strands of 45 SWG insulated

copper wire. The use of such very fine strands made the conductor difficult to handle and it was found necessary to wrap the 110 x 28 strands with insulating tape after they were laid up and twisted. The resulting conductor was extremely flexible and quite unsuitable for pre-forming to a precise shape on a former. However, the flexibility enabled the end connections to be adjusted to shape after the coils have been put in place on the armature, and also enabled the unusual double-turn, double-layer lap winding to have a satisfactory arrangement of end connections, in some ways similar to those of a mush winding. The coils were formed to approximate shape and the two layers of conductor taped together prior to insertion in the armature. A carefully laid half-lap arrangement was used as this tape formed the insulation required between coils of different phases.

The tape used for this purpose and for wrapping the conductor was a thermosetting pressure sensitive adhesive polyester tape 0.064 mm thick and 25 mm wide. It had a voltage breakdown strength in excess of 1200 V and was suitable for continuous operation at 120°C. This tape was used also for wrapping the soldered joints between the coils in the armature winding.

13.5 Mechanical Details.

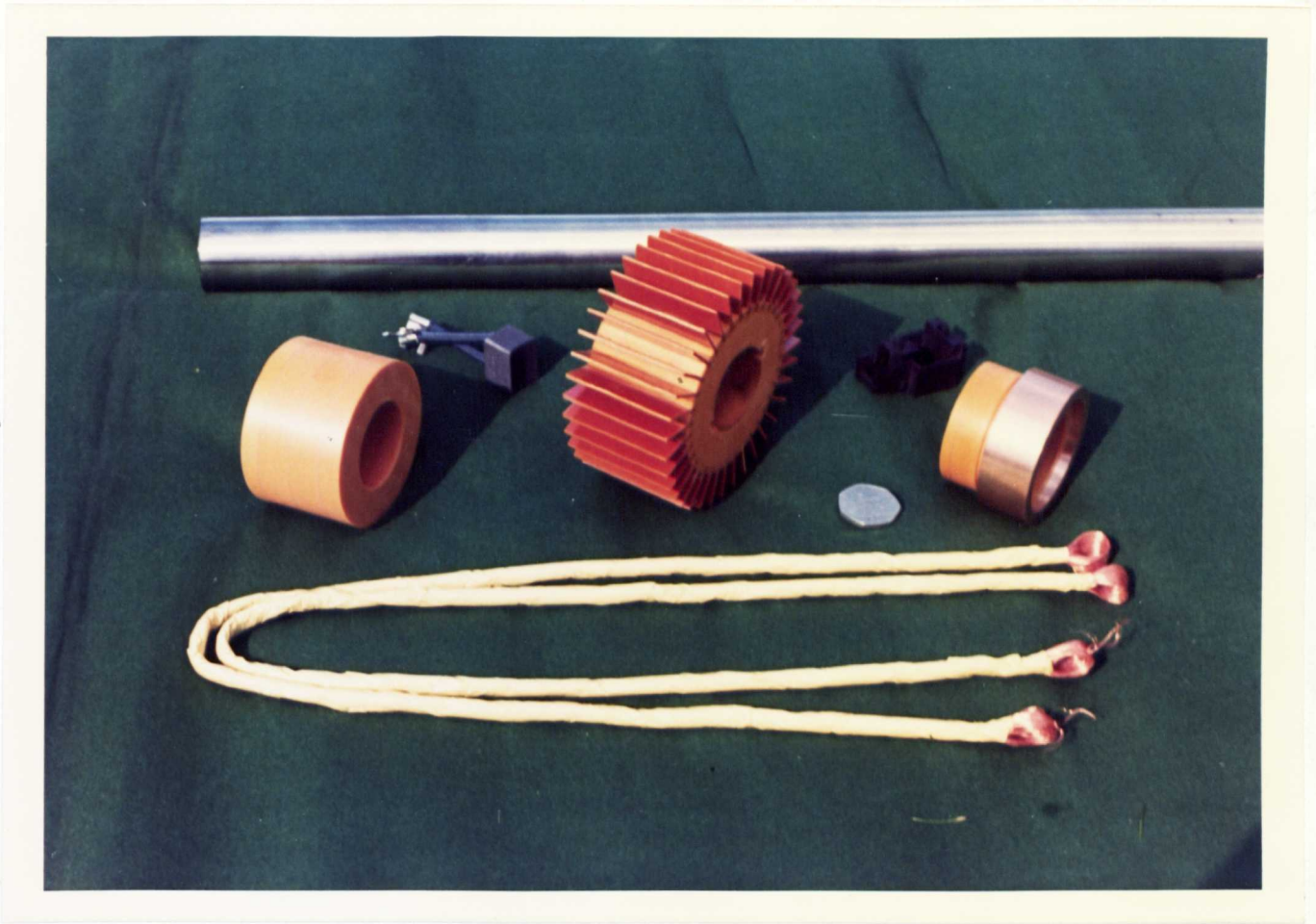
The armature assembly is carried on a stainless steel shaft 35 mm in diameter. This diameter was originally selected as being suitable for the second stage 100 kVA machine. It was retained at this diameter so that the bearings and similar details would be suitable for both stages. Calculation of the critical speed showed

this to be 260 Hz making allowance for the shaft and assuming the ends to be free to bend. The shaft is held in double ball bearings at each end, so the assumption of free ends is probably too severe, but to assume fixed ends for the shaft would not be justified. If it were, the critical speed would be 520 Hz. The condition of the shaft ends is between these extremes, and it is probable that the critical speed is above 260 Hz, corresponding to 15,600 r.p.m. and 30% above the normal speed of 12,000 r.p.m. However, it was considered unwise to reduce the shaft diameter below 35 mm as this would have reduced the critical speed.

Details of the completed machine and its components can be seen in the photographs on pages 277 and 278, and in the frontispiece.

13.6 Brushgear.

The three free ends of the star-connected winding are brought out via symmetrically arranged flat strips of copper to three slip rings. The diameter of the slip rings is 62.5 mm; they are 26 mm wide and made of phosphor bronze. There are 3 brushes on each slip ring of graphitic carbon, grade EGO. For higher current rating of the second stage machine, copper/carbon brushes are proposed, grade CMIS. The brushes are carried in commercial brush carriers suitably modified so that they can be mounted inside the room temperature aperture of the cryostat.



Group of Armature Components

Top: Stainless steel shaft

Middle (l. to r.): Support core for winding overhang

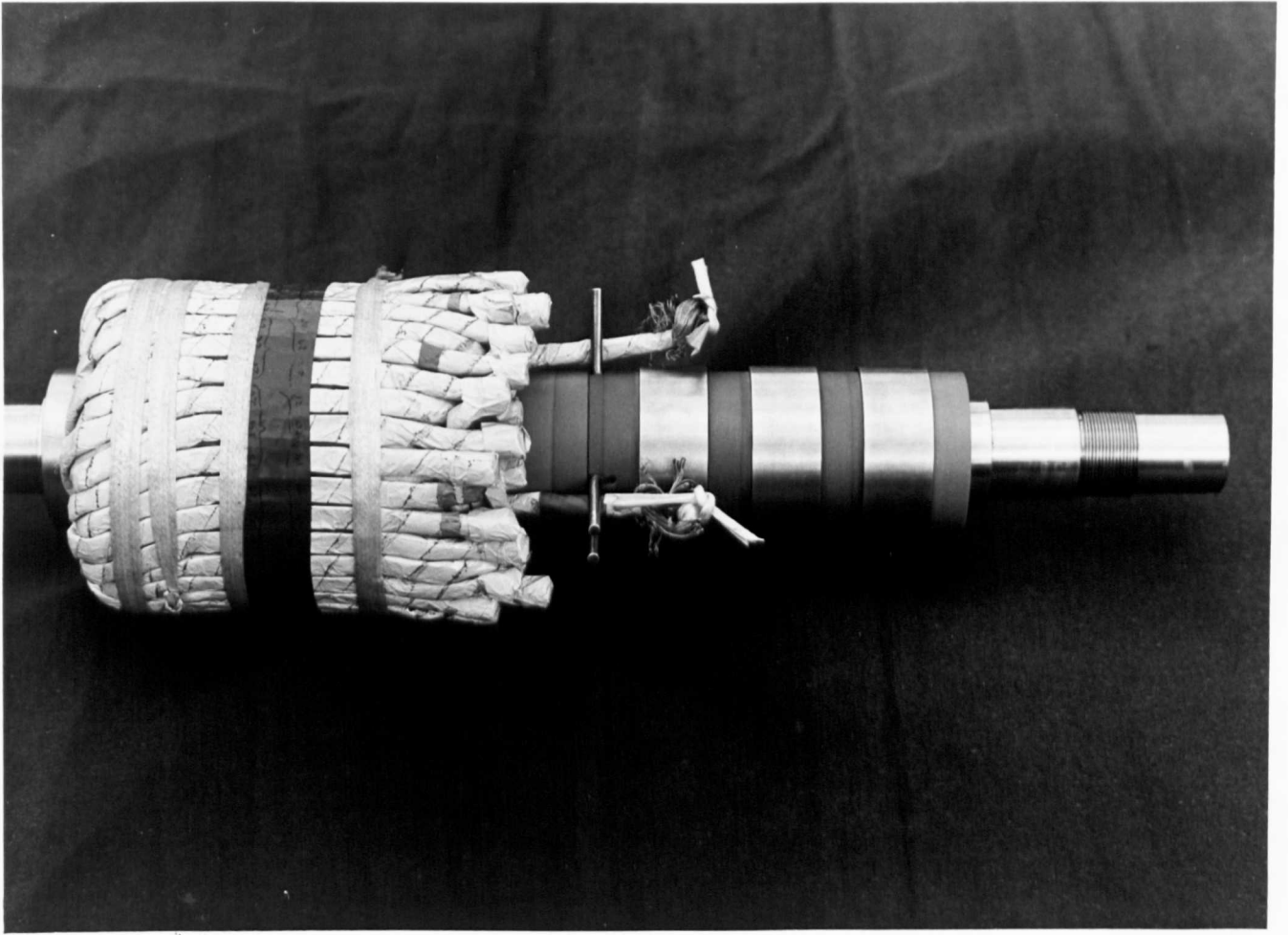
Graphitic carbon brush

Armature core with locating fins in position

Brush carrier

Phosphor-bronze slip ring with Tufnol spacer

Bottom: Laid-up and twisted armature conductors half-lap wrapped with polyester tape prior to forming into coils.



Completed Armature prior to Impregnation.

14. Electrical Performance Prediction and Testing of Prototype.

14.1 Cooldown and Helium Boil-Off.

The procedure adopted for cooling down the cryostat followed conventional practice although because of the large thermal mass of the stainless steel magnet support block and the internal extension of the helium transfer tube, some extra precautions were found necessary. The vacuum in the cryostat and the helium transfer line were checked and the nitrogen container filled with liquid nitrogen. The helium container was then also filled with liquid nitrogen and left until the nitrogen boil-off had reached a low rate; this was after about half an hour. A plain tube was then inserted in the cryostat and connected to the internal helium transfer tube and helium gas introduced at a pressure of 1 - 2 p.s.i. until all the nitrogen had been removed from the helium container. Liquid helium was then transferred to the cryostat from a 17-litre transport container. It was important to ensure that all the nitrogen was removed before attempting to introduce liquid helium, and also to make sure that the transfer line fitted properly into the internal extension tube.

It was found that approximately 20 litres of liquid helium were required to cool down the magnet and the helium container, and to fill the helium container to just below its top plate.

The helium boil-off after the initial stabilising period was 785 ml per hour of gas at 0°C; this increased to 965 ml per hour when the magnet coils were energised with a current of 9AA. The

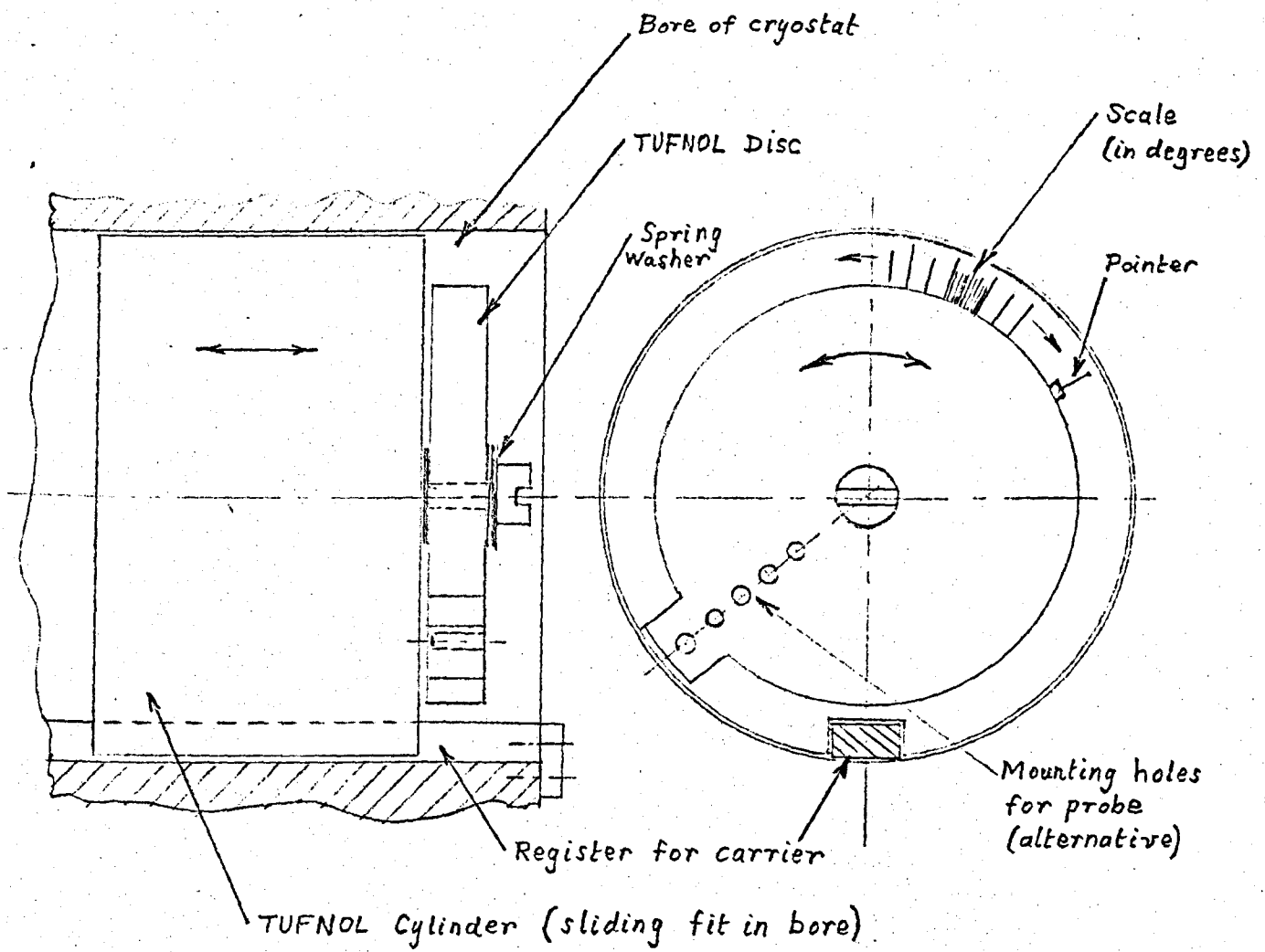


Fig. 73 Carrier for Hall-effect Probe

helium reservoir enabled the magnet to be operated for over six hours in the persistent mode.

14.2 Field Plot of Bore.

The field inside the room temperature aperture of the cryostat was explored with the aid of a Hall effect probe mounted in a special carrier so that it could be accurately positioned in the bore in both the radial and axial positions. The radius at which the measurements were taken could also be adjusted. A general arrangement of the carrier is shown in fig. 73. The probe was calibrated against a fluxmeter in a uniform magnetic field produced by an iron-cored electromagnet with 200 mm diameter pole pieces; for fields above that obtainable from this magnet, the linear calibration was assumed to hold true.

The radial component of the field along the bore at the armature surface is plotted in fig. 74,* and the radial component of the field across the central plane of the magnet along a pole axis is plotted in fig. 75. The radial component at the armature surface at various sections along the bore is given in fig. 76. From this the field distribution is seen to be far from ideal for an electrical machine, but of course this is the field from only the inner sections of the field windings, and it should be considerably improved with the addition of the outer section of the windings. There is good agreement with the predicted values, but there are minor discrepancies which indicate that the magnet system is slightly misaligned with the axis of the bore. This misalignment is not serious enough to interfere with the preliminary testing of the armature, and unlikely to interfere with the performance of the machine.

*Test results are given on page 285 et seq.

14.3 Resistance and Inductance Measurements.

On completion of the winding of the armature, the resistance of each phase was measured by the ammeter-voltmeter method, and the results compared for each phase and with the calculated value. The values are given in Table IV. The discrepancies are due to variations in the lengths of individual turns and due to the joint resistances.

The self-inductance of each phase was measured using a Marconi Inductor Analyser TF 2702 over a range of frequencies from 40 - 1200 Hz. The inductance was also determined from reactance measurements at 50 Hz and 400 Hz using currents in the region of 50A. These values are also given in Table IV from which it will be seen that there is remarkably close agreement between the values determined under the different measurement conditions. This is due primarily to the absence of iron, and partly due to the very fine stranding and twisting of the conductors.

14.4 Open Circuit Characteristic.

The armature was mounted in its bearings inside the cryostat after it had been dynamically balanced. The complete machine was mounted on the drive motor of a 150 hp Ward Leonard set and the various alignments carried out. The machine was run at various speeds up to its rated synchronous speed of 12,000 rpm and no abnormal conditions were observed in the behaviour of the rotating parts. The armature was run for a few hours to allow the brushes to bed down properly. The cryostat was then cooled down, and after the introduction of liquid helium the open circuit characteristic was taken at half synchronous and synchronous speeds. The superconducting

magnet was not operated in the persistent mode, and the magnet quenched well in excess of 100A. The open circuit characteristic (fig. 77) is linear with field current, and proportional to speed, as would be expected.

14.5 Load Test, Temperature Rise and Current Rating.

The machine was run at rated speed of 12,000 rpm and loaded with resistance balanced between the phases. The temperature rise in the steady state was measured as quickly as possible after the armature had been brought to rest using an electronic contact thermometer at several places on the armature surface which could be reached from the open ends of the cryostat aperture. These positions were mainly on the overhang parts of the winding, and did not include the central section immediately under the field coils. This was not an ideal way to determine the mean temperature rise of the winding accurately, but did serve to give a rapid indication of the rating which could reasonably be assigned to the machine. The results are plotted in fig. 78.

The terminal characteristic for unity power factor loads was taken at 12,000 rpm, and is plotted in fig. 79. The field current was kept constant at the value required to generate a line voltage of 208V on no load. The maximum current reached in the temperature rise test was used as a single-phase load between two slip rings. Apart from a slight increase in the nitrogen boil-off rate, the machine continued to operate satisfactorily indicating that the damper screen was effectively screening the superconducting windings from the adverse effects of the single-phase load.

It was not possible to carry out any further tests in the time available, and a much more extensive test programme is required in order to investigate the particular characteristics of superconducting generators under conditions of unbalanced loading, transient and sub-transient behaviour and under short-circuit and fault conditions including the action of the damper screen. However, the limited tests carried out do demonstrate the general feasibility of the design.

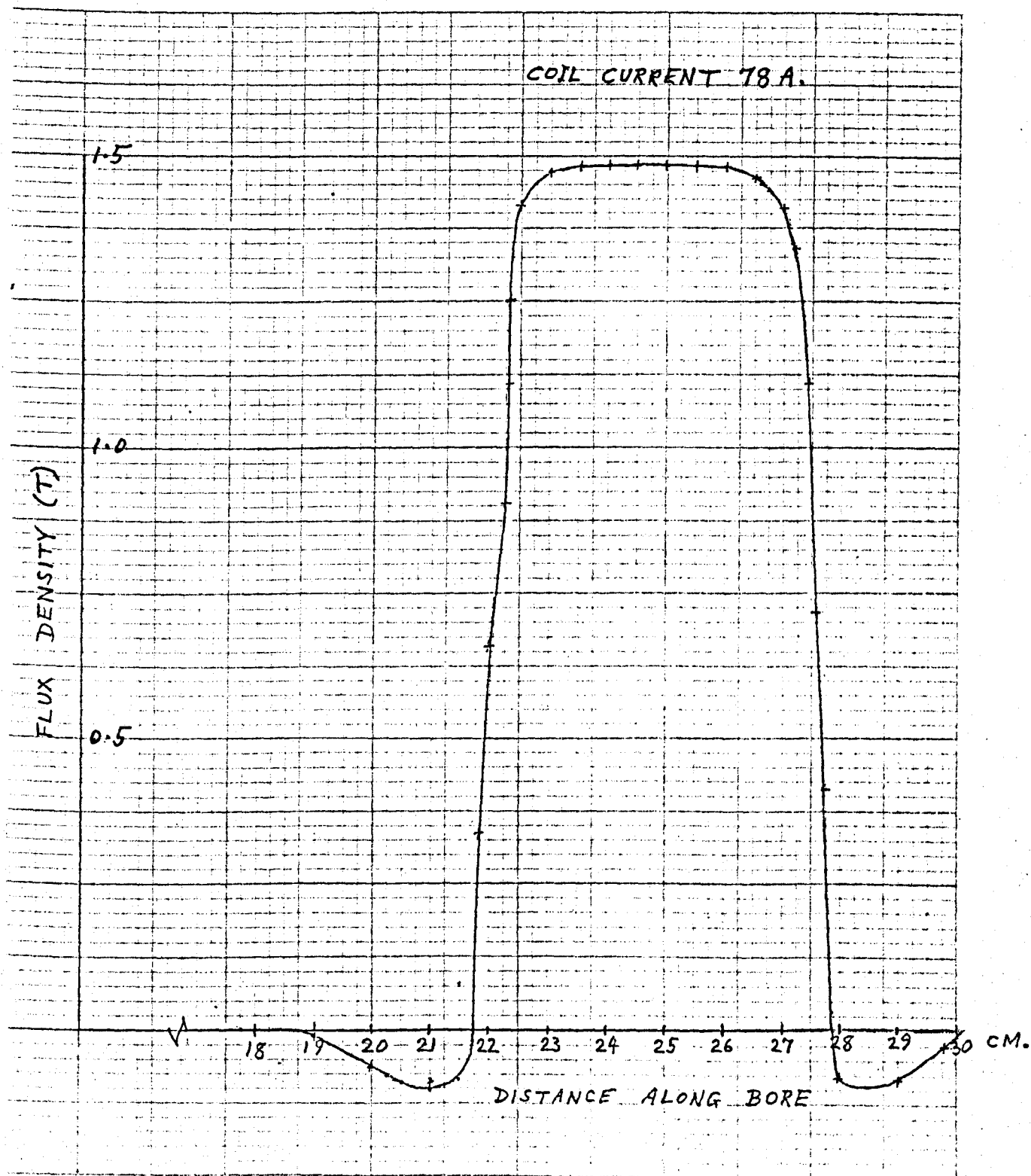


Fig. 74 Radial component of field at pole centre line along axial length of bore at armature surface.

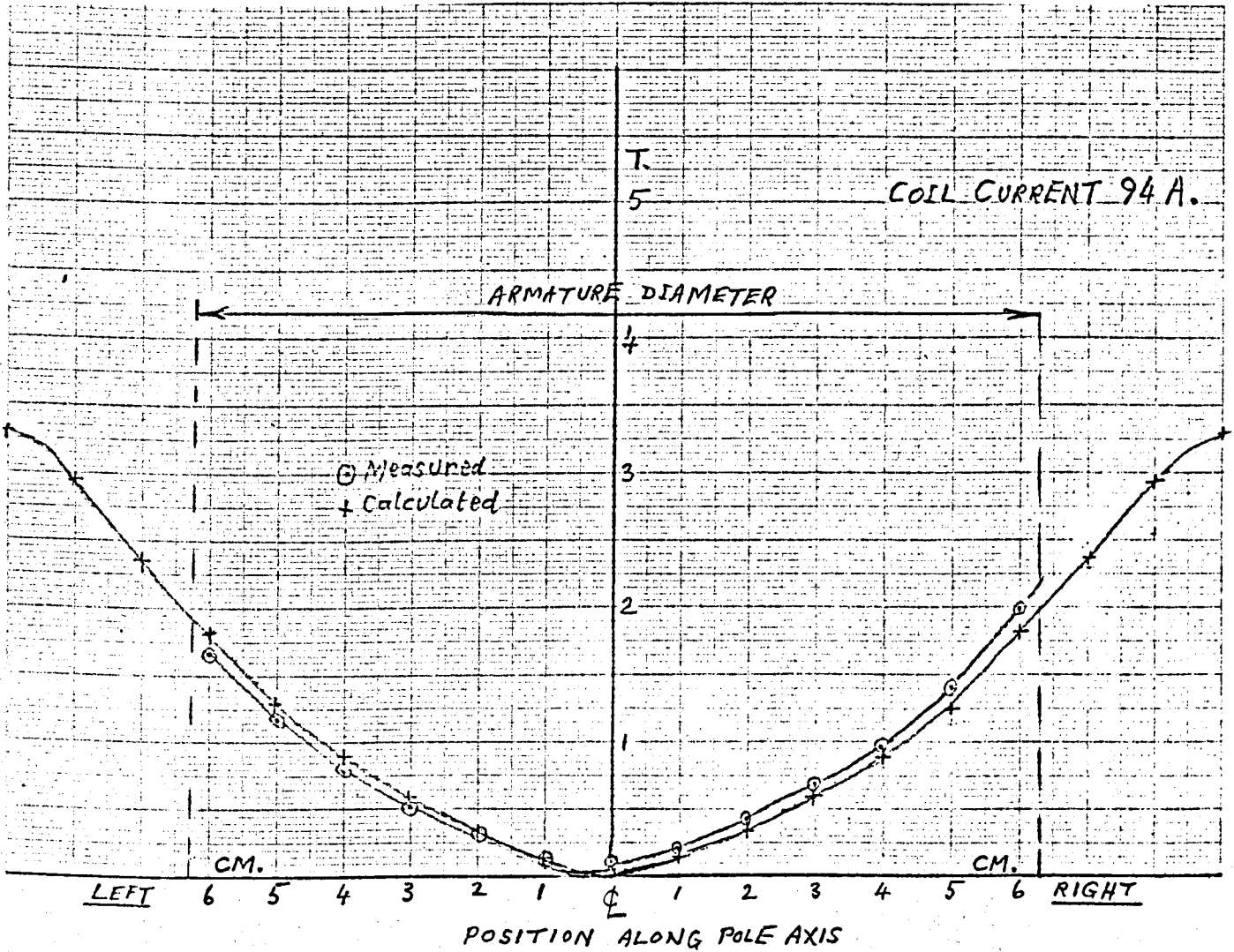


Fig. 75 Radial component of field across central plane of magnet along pole centre lines.

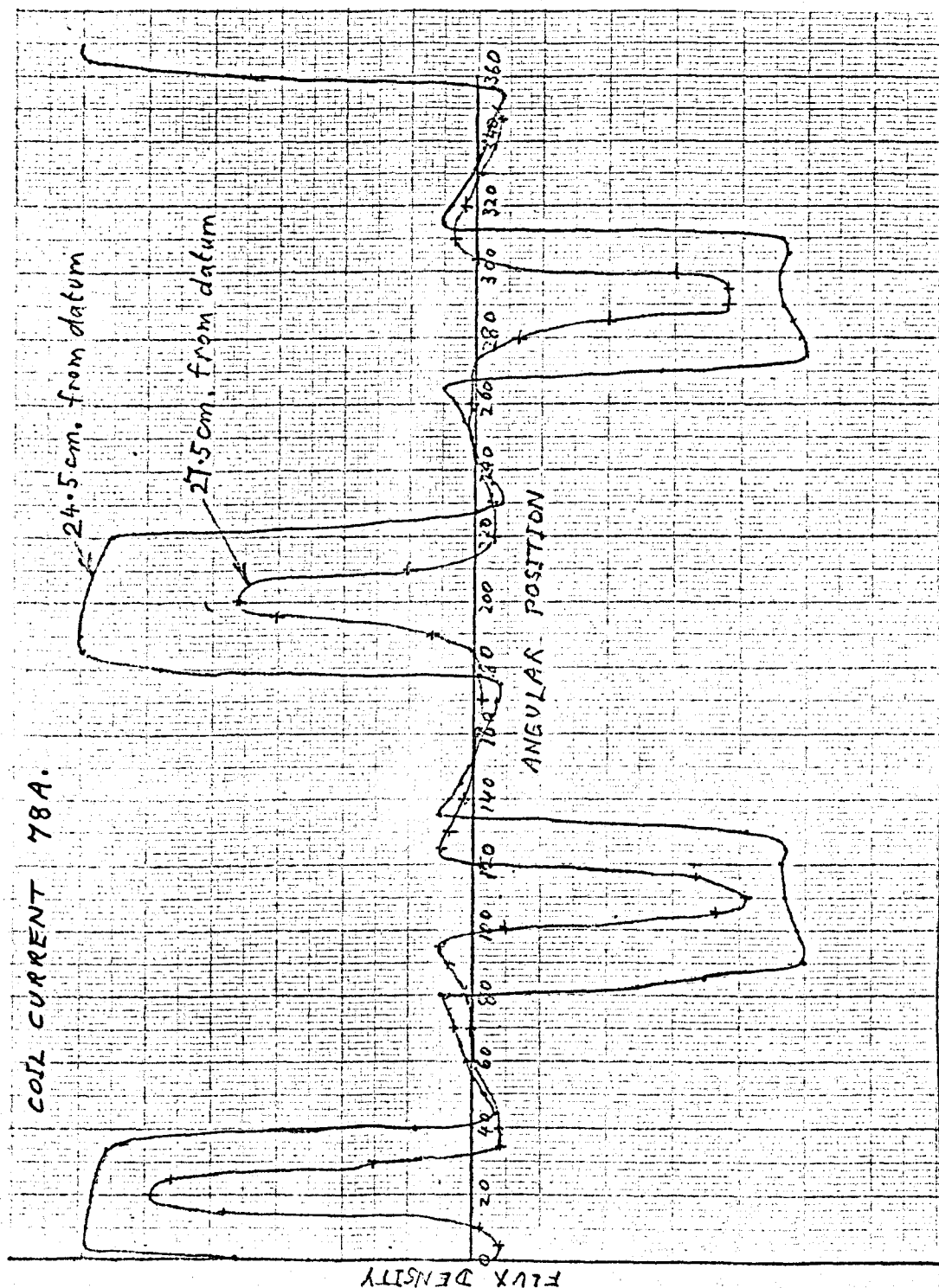


Fig. 76 Radial component of field at armature surface at various sections along bore.

TABLE IV

Resistances:	R phase	0.024 ohm
	Y phase	0.028 ohm
	B phase	0.022 ohm
	Calculated	0.0195 ohm

Self Inductance:	R phase	0.0062 mH)
	Y phase	0.0068 mH	
	B phase	0.0064 mH	

By Inductor Analyser
on ranges 40-1200 Hz.

R phase	0.0063 mH)
Y phase	0.0065 mH	
B phase	0.0064 mH	

By reactance measurements
at 50 Hz.

R phase	0.0063 mH)
Y phase	0.0068 mH	
B phase	0.0065 mH	

By reactance measurements
at 400 Hz

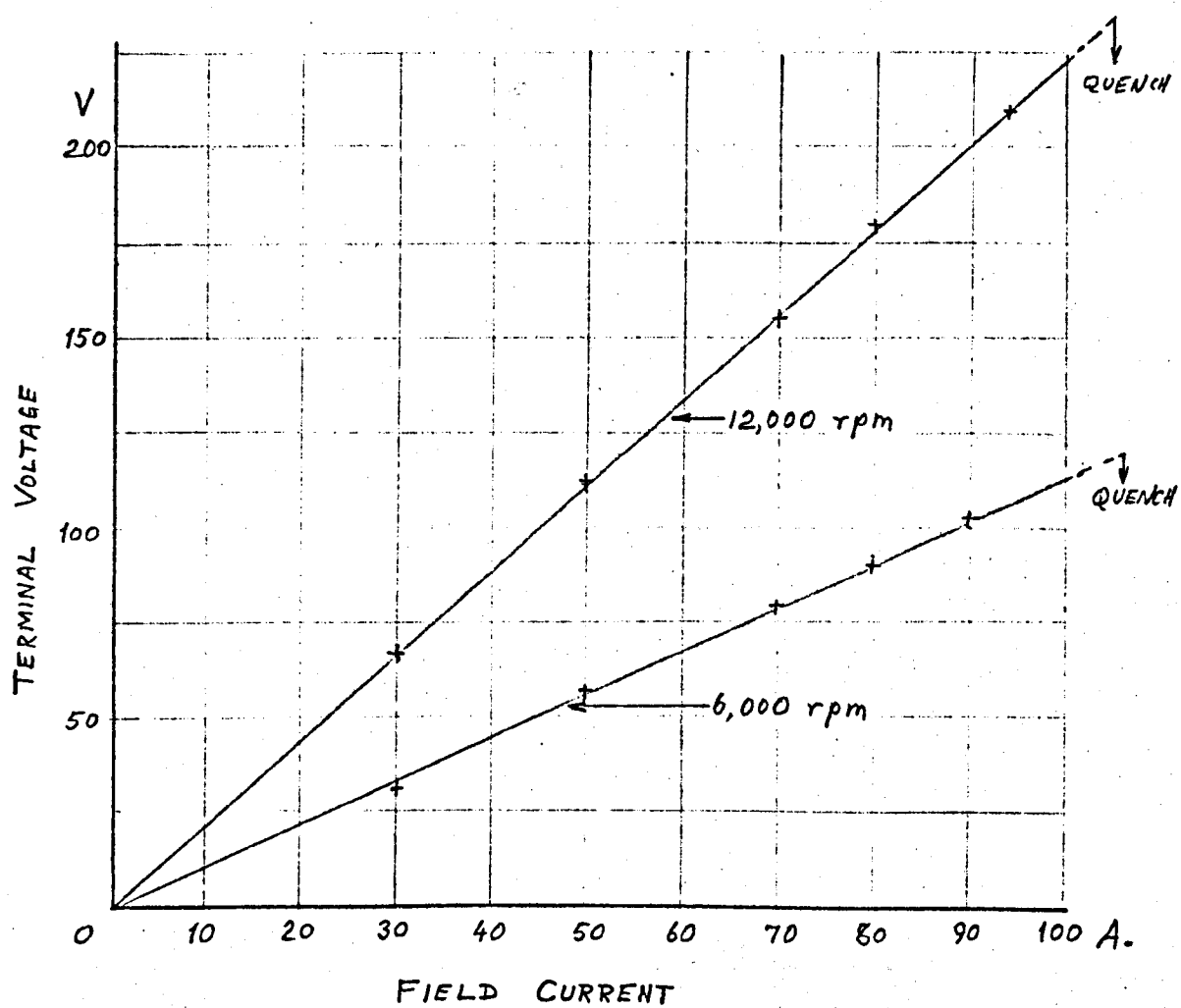


Fig. 77 Open-circuit Characteristics.

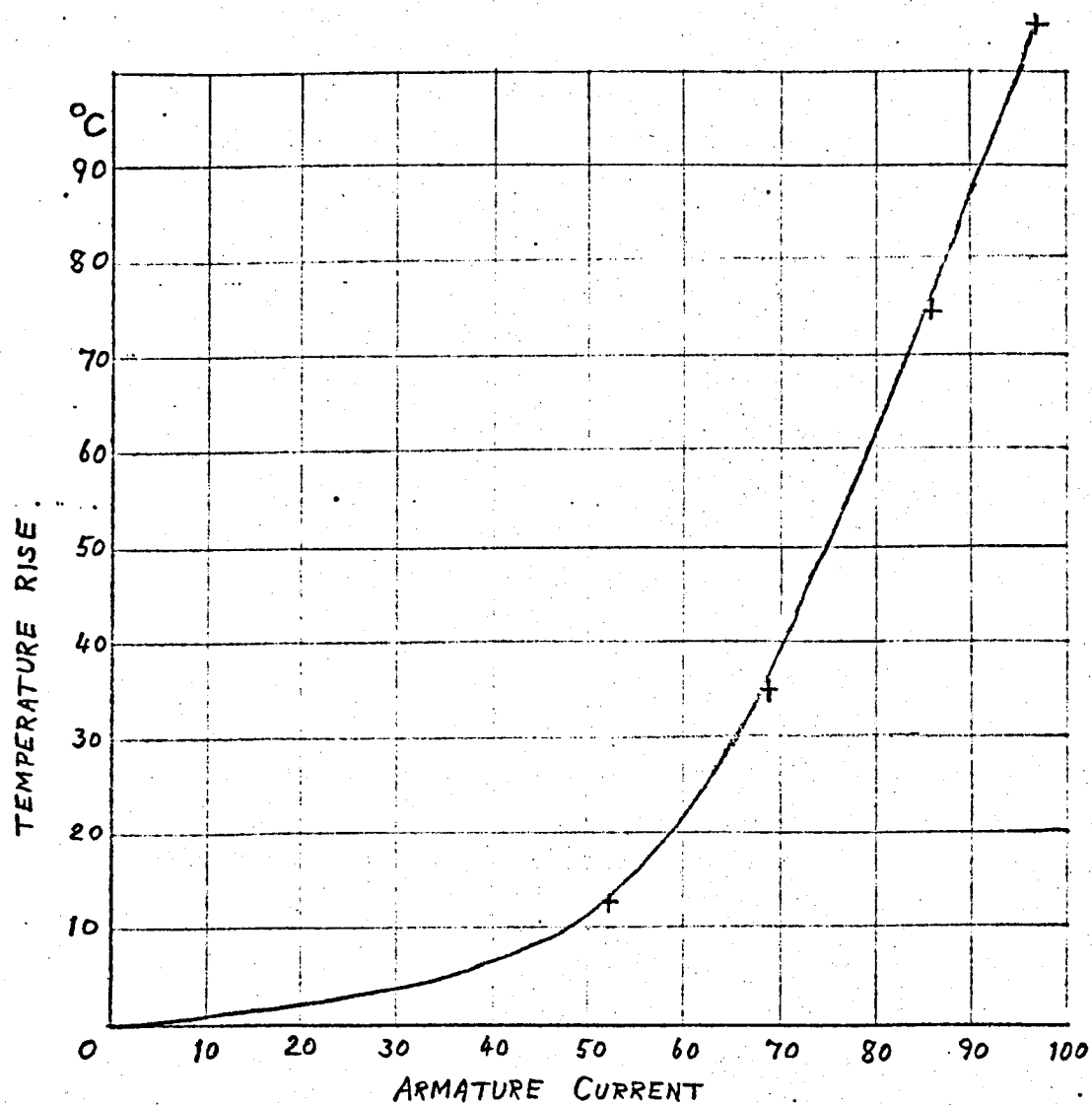


Fig. 78 Temperature rise on armature surface

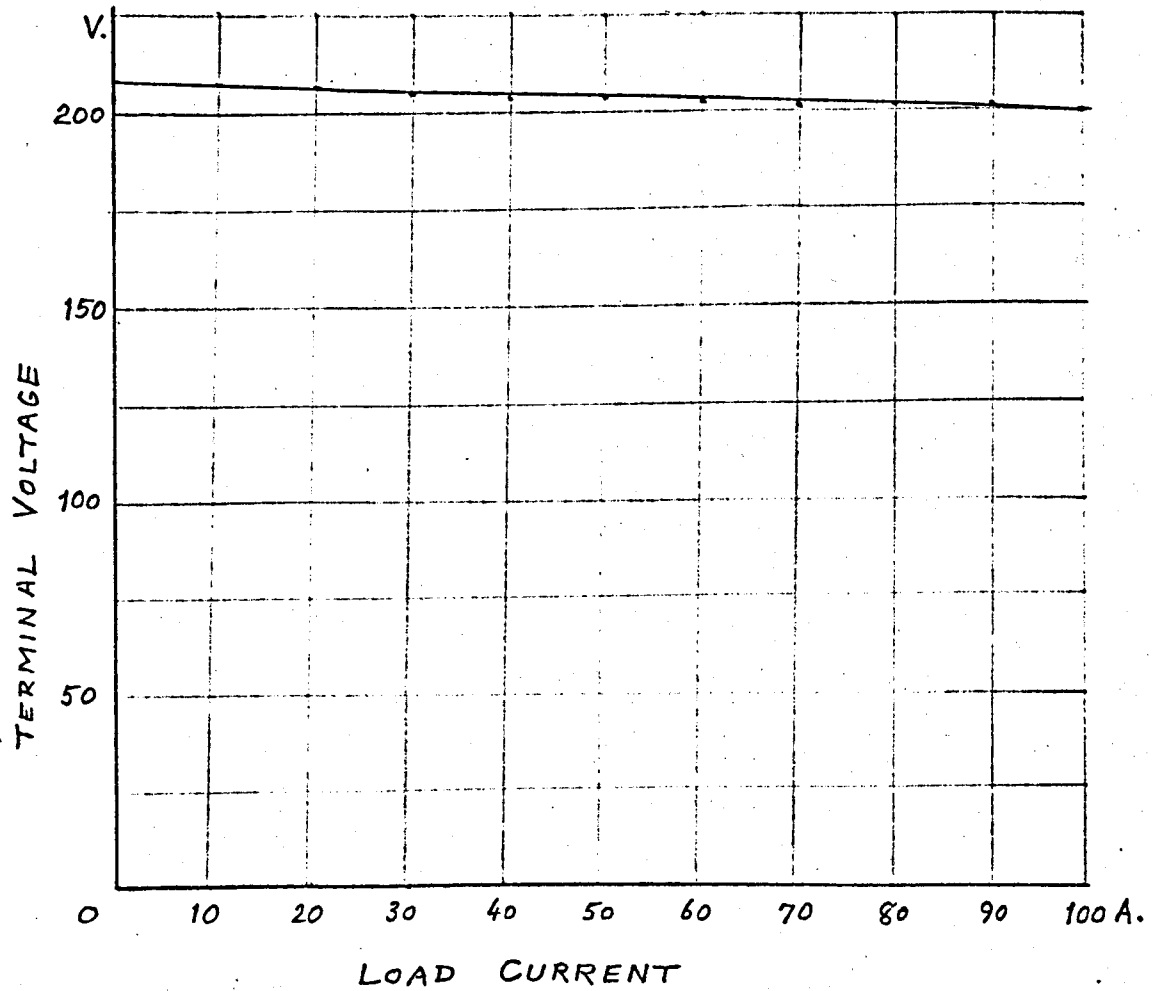


Fig. 79 Load characteristic with resistance loading and constant excitation at constant speed.

15. Theoretical Analysis of Superconducting Synchronous Machine

15.1 The two-Axis Lumped Parameter Model.

The conventional approach to analysing the performance of synchronous machines in recent years has been by so-called generalised machine theory in which the objective has been to represent all rotating electromagnetic machines with cylindrical symmetry by a single model with lumped parameters. Although this objective has not been completely met, it has been developed successfully to cover the majority of machines without saliency in the magnetic circuit, or where the saliency is restricted to either the rotating or stationary member but not both. An individual type of machine is then analysed by suitably constraining the general model so that it represents the required machine.

In the case of the three-phase synchronous machine this results in a network representation of the form given in fig.80 in which the machine is represented by three stationary and three rotating coils. By a suitable mathematical transformation, it can be represented by the network in fig.81 in which the five coils are stationary, but special properties are prescribed for those representing the armature to account for rotation; a further equation is needed so that the five coil representation can uniquely represent the original machine. The five coils are each associated with one of two orthogonal axes which correspond with the axes of magnetic saliency if these are present in the original machine. Solution of this network and the use of appropriate engineering approximations yields expressions

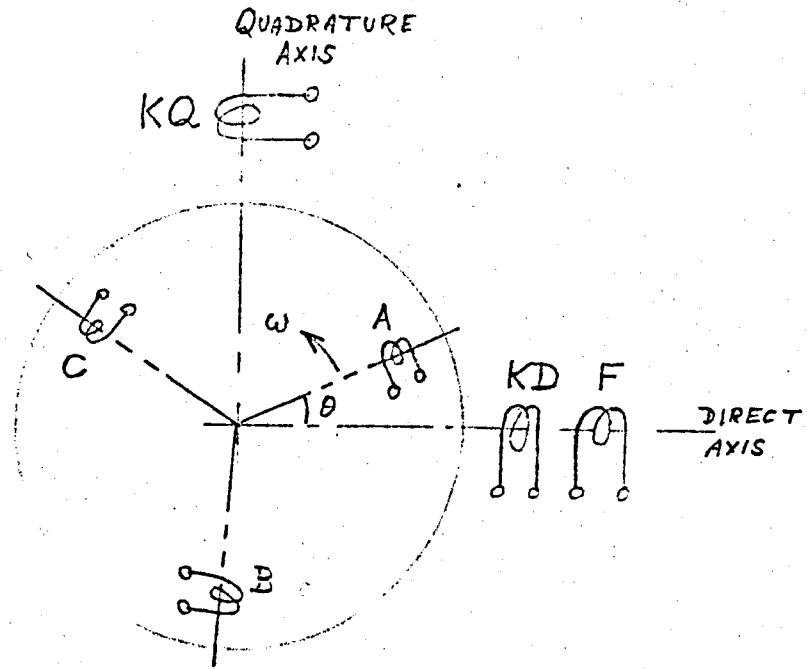


Fig. 80 Representation of synchronous machine with rotating armature axes.

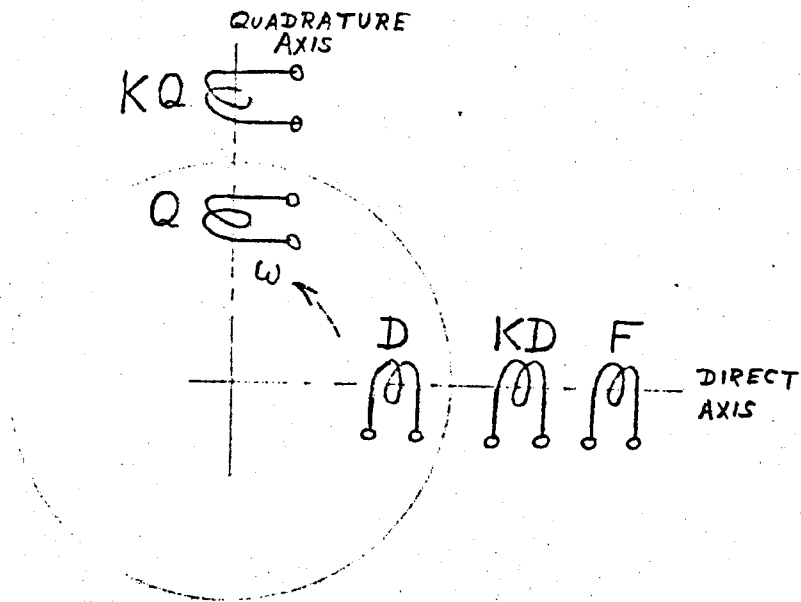


Fig. 81 Approximate representation of synchronous machine by five stationary coils.

for the machine performance under steady state, dynamic and transient conditions and expressed in terms of transient reactances and time constants.

The theory was largely developed by Kron (220) based on the earlier work of Doherty and Nickle (213-217), Parks (218,219) and others, and later expounded by Gibbs, Adkins and others. Thus it is by no means novel. However, its application to superconducting machines does not seem to have appeared in the literature as yet. There are three aspects which will now be dealt with, but it is not proposed to develop a fully comprehensive theory of superconducting synchronous machines, nor to provide experimental verification. The modest objective is to give an indication of the way such a theory might be developed and to leave its application to specific problems to other studies.

15.2 Application to Superconducting Machines.

It is customary in most treatments of generalised machine theory to assume that all windings on a common axis are magnetically coupled by a common mutual flux, and that windings on orthogonal axes are not coupled magnetically at all. The first assumption is made and is justified because of the presence of an iron core in the machine. In a superconducting machine which is essentially without an iron core, this assumption is obviously not true, and an alternative valid basis must be found. The second aspect to be dealt with is the evaluation of the inductance parameters, and the third involves the treatment needed to incorporate the effect of the damper screen.

The presence of the damper screen between the field and armature and its continuous nature enables a basic assumption to be made. This is that all the flux which links the armature phase windings and the field winding must pass through ^{the} damper screen. This enables the relationship between the various mutual and self inductances to be determined, as shown later, and makes an approximate solution of the machine equations possible.

15.3 Damper Screen.

The eddy current paths in the damper screen could be represented by two sets of coils, one set being associated with the direct-axis and the other with the quadrature-axis. Each set would require an infinite number of component coils each with its own appropriate values of resistance and inductances. By this means an exact representation of the continuous damper screen could be obtained, but clearly it would be impracticable, and a finite number of coils would have to be taken in order to achieve a practical representation. The number of coils would be restricted to that which gave the required degree of accuracy.

The usual assumption for an iron-cored machine that windings on orthogonal axes are not mutually coupled must be questioned for the case of an air-cored machine to see if there will now be mutual couplings not only between all coils on the same axis, but between all coils on orthogonal axes as well. In fact, of course, the validity of the assumption does not depend on the presence of an iron core, but on the symmetry of the windings with respect to the two axes. Since the windings and damper screen in a superconducting

machine will normally be symmetrical about the axes, the assumption of zero coupling between coils on different axes will still hold.

15.4 Simplified Representation.

The usual theoretical approach to conventional synchronous machines uses a representation of a simplified machine with one damper coil, KD, on the direct-axis and one damper coil on the quadrature axis, KQ. Although it is only an approximation, the results obtained are usually accurate enough for most purposes, and in fact the concepts usually used to describe the transient performance (i.e. the sub-transient reactances and transient reactances with the corresponding time constants) depend on this simplification. Even so, the calculation of a practical problem is still complicated, and further approximations may be introduced. Thus, as a first step in the investigation of the transient performance of a superconducting machine, its continuous damper screen corresponding to the damper windings in a conventional type will be represented by a single circuit on the direct-axis and by another on the quadrature-axis. If future studies show this to be an inadequate or too inaccurate representation, then multiple coils on each axis can be used instead. This simplified representation will enable the measure of the problem to be gained at an early stage in the development of superconducting machines, and although based on different assumptions from the theory for conventional types results in equations which have similarities to those obtained from this theory.

Thus the superconducting synchronous machine is represented by

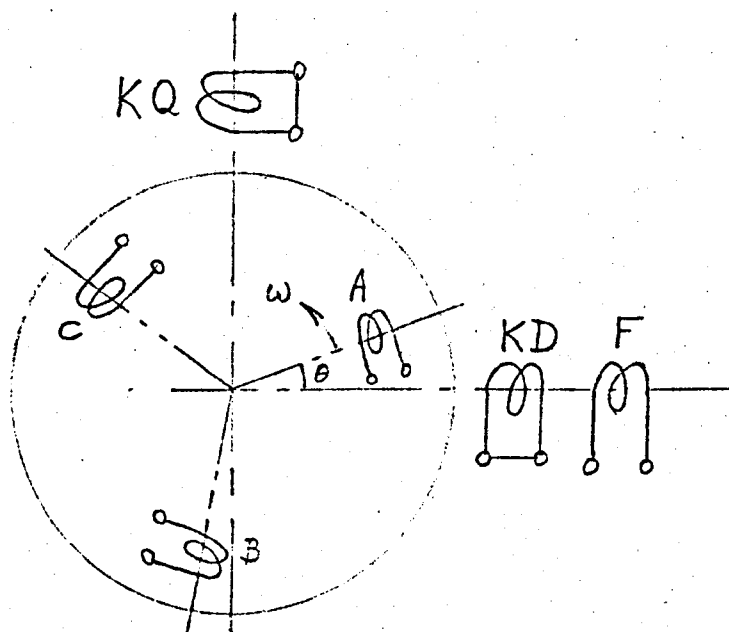


Fig. 82 Representation of superconducting synchronous machine with rotating armature axes.

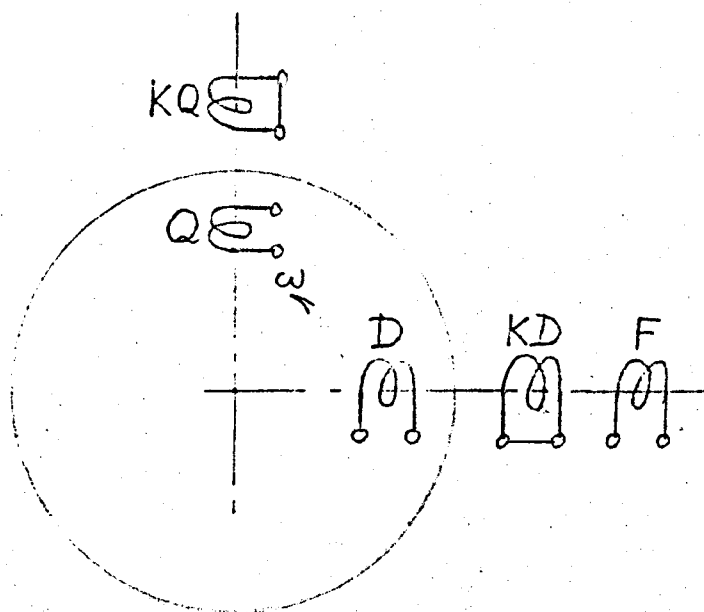


Fig. 83 Approximate representation of superconducting synchronous machine by five stationary coils.

the simplified network shown in fig.82 where the superconducting field is represented by coil F, the continuous damping screen by KD on the direct-axis and KQ on the quadrature-axis, and the three-phase armature by coils A, B and C associated with the rotating system of axes. The relationships between the fluxes linked by the windings and currents are expressed by equ. 83.

$$\begin{bmatrix} \Psi_f \\ \Psi_{kd} \\ \Psi_{kq} \\ \Psi_a \\ \Psi_b \\ \Psi_c \end{bmatrix} = \begin{bmatrix} L_f & M_{fkd} & 0 & M_{fa} & M_{fb} & M_{fc} \\ M_{kdf} & L_{kd} & 0 & M_{kda} & M_{kdb} & M_{kdc} \\ 0 & 0 & L_{kq} & M_{kqa} & M_{kqb} & M_{kqc} \\ M_{af} & M_{ekd} & M_{akq} & L_{aa} & M_{ab} & M_{ac} \\ M_{bf} & M_{ekd} & M_{bkq} & M_{ba} & L_{bb} & M_{bc} \\ M_{cf} & M_{ekd} & M_{ckq} & M_{ca} & M_{cb} & L_{cc} \end{bmatrix} \begin{bmatrix} i_f \\ i_{kd} \\ i_{kq} \\ i_a \\ i_b \\ i_c \end{bmatrix}$$

(83)

Since the machine possesses no magnetic saliency the self inductances of the armature windings and the mutual inductances between them will be constant, and by their physical symmetry the magnitudes of the self inductances will be equal, as will the magnitudes of the mutual inductances. As the machine is air-cored and thus linear, reciprocity applies and the matrix must be symmetrical about the diagonal so that $|M_{ab}| = |M_{ba}|$ etc. Self and mutual inductances associated with the stationary direct- and quadrature-axes are constant, and because the damper screen is continuous its inductance parameters will be equal for each axis.

Thus by symmetry and reciprocity:

Armature

$$L_{aa} = L_{bb} = L_{cc} \quad (= L_a \text{ say})$$

$$M_{ab} = M_{bc} = M_{ca} = M_{ba} = M_{cb} = M_{ac} \quad (= L_{ab} \text{ say})$$

Field to Armature

$$|M_{af}| = |M_{bf}| = |M_{cf}| = |M_{fa}| = |M_{fb}| = |M_{fc}|$$

$$(\quad = L_{af}, \text{ say})$$

M_{af} , etc. are functions of rotor angle, θ .

Damper Screen to Armature

$$|M_{akd}| = |M_{bkd}| = |M_{ckd}| = |M_{kda}| = |M_{kdb}| = |M_{kdc}|$$

$$|M_{akq}| = |M_{bkq}| = |M_{ckq}| = |M_{kqa}| = |M_{kqb}| = |M_{kqc}|$$

$$(\quad = M_{ka}, \text{ say})$$

M_{akd} , etc. are functions of rotor angle, θ .

Damper Screen to Field

$$M_{fkd} = M_{kdf} \quad (= M_{kf}, \text{ say})$$

Damper Screen

$$L_{kd} = L_{kq} \quad (= L_k, \text{ say})$$

Substitution of these values in equ. (83) gives:

$$\begin{bmatrix} \psi_f \\ \psi_{kd} \\ \psi_{kq} \\ \psi_a \\ \psi_b \\ \psi_c \end{bmatrix} = \begin{bmatrix} L_f & M_{kf} & 0 & L_{af} & L_{af} & L_{af} \\ M_{kf} & L_k & 0 & M_{ka} & M_{ka} & M_{ka} \\ 0 & 0 & L_k & M_{ka} & M_{ka} & M_{ka} \\ L_{af} & M_{ka} & M_{ka} & L_a & L_{ab} & L_{ab} \\ L_{af} & M_{ka} & M_{ka} & L_{ab} & L_a & L_{ab} \\ L_{af} & M_{ka} & M_{ka} & L_{ab} & L_{ab} & L_a \end{bmatrix} \begin{bmatrix} i_f \\ i_{kd} \\ i_{kq} \\ i_a \\ i_b \\ i_c \end{bmatrix} \quad (84)$$

In order to simplify the equations, the actual phase voltages and currents, $e_a, e_b, e_c, i_a, i_b, i_c$ are replaced by another set of variables $e_d, e_q, e_o, i_d, i_q, i_o$ using a transformation in the form originally proposed by Park ⁽²¹⁸⁾. The three phase coils A, B, C associated with a rotating set of axes are replaced by two fictitious stationary coils D and Q associated respectively with the direct- and quadrature-axes, and another stationary coil not directly associated with the main coil configuration representing the zero sequence network. The transformation involves an arbitrary choice which is exercised in the following equations defining the new variables in terms of the original:

$$\begin{bmatrix} i_d \\ i_q \\ i_o \end{bmatrix} = \frac{2}{3} \begin{bmatrix} \cos \theta & \cos(\theta - 2\pi/3) & \cos(\theta - 4\pi/3) \\ \sin \theta & \sin(\theta - 2\pi/3) & \sin(\theta - 4\pi/3) \\ 1/2 & 1/2 & 1/2 \end{bmatrix} \begin{bmatrix} i_a \\ i_b \\ i_c \end{bmatrix} \quad (85)$$

* See fig. 83, page 297.

$$\begin{bmatrix} e_d \\ e_q \\ e_o \end{bmatrix} = \frac{2}{3} \begin{bmatrix} \cos \theta & \cos(\theta - 2\pi/3) & \cos(\theta - 4\pi/3) \\ \sin \theta & \sin(\theta - 2\pi/3) & \sin(\theta - 4\pi/3) \\ 1/2 & 1/2 & 1/2 \end{bmatrix} \begin{bmatrix} e_a \\ e_b \\ e_c \end{bmatrix} \quad (86)$$

The equations of the inverse transformations are:

$$\begin{bmatrix} i_a \\ i_b \\ i_c \end{bmatrix} = \begin{bmatrix} \cos \theta & \sin \theta & 1 \\ \cos(\theta - 2\pi/3) & \sin(\theta - 2\pi/3) & 1 \\ \cos(\theta - 4\pi/3) & \sin(\theta - 4\pi/3) & 1 \end{bmatrix} \begin{bmatrix} i_d \\ i_q \\ i_o \end{bmatrix} \quad (87)$$

$$\begin{bmatrix} e_a \\ e_b \\ e_c \end{bmatrix} = \begin{bmatrix} \cos \theta & \sin \theta & 1 \\ \cos(\theta - 2\pi/3) & \sin(\theta - 2\pi/3) & 1 \\ \cos(\theta - 4\pi/3) & \sin(\theta - 4\pi/3) & 1 \end{bmatrix} \begin{bmatrix} e_d \\ e_q \\ e_o \end{bmatrix} \quad (88)$$

Several advantages have been found to accrue from working in terms of per unit (p.u.) values and it is usual to employ such a system in electrical machine theory in which actual quantities are normalised in terms of some base values, usually the rated or full-load values. The p.u. system employed here follows that used by Adkins (Bibliography 1) in which unit current in the armature is the full-load rms current, and unit current in another winding is the current which produces the same mmf as unit current in the armature. Unit voltage in the armature is the nominal rms phase voltage and unit flux linkage Ψ is such that the induced voltage

is equal to the time derivative of the p.u. flux linkage, $d\psi/dt$. Unit voltage in another winding is that due to $d\psi/dt$ providing that the axes are coincident. Unit power is taken as the power corresponding to unit voltage and unit current in a main circuit, and in order that this definition can remain the same for the machines represented by the two systems of axes, the unit current in the axis coils (i_d, i_q) is made 1.5 times the p.u. value in the phase coils (i_a, i_b, i_c). Thus p.u. power input for the three-phase armature winding is:

$$P = \frac{1}{3}(e_a i_a + e_b i_b + e_c i_c) \quad (89)$$

and the p.u. power input for the machine with stationary axes represented by the transformed equations is:

$$P = \frac{1}{2}(e_d i_d + e_q i_q) + e_o i_o \quad (90)$$

When the transformation of equ.(85) is applied to equ.(84) and reduced to a per unit basis, the following expression for the flux linkages results:

$$\begin{bmatrix} \psi_f \\ \psi_{kd} \\ \psi_d \\ \psi_q \\ \psi_{kq} \\ \psi_o \end{bmatrix} = \begin{bmatrix} L_f & M_{kf} & M_{fd} & 0 & 0 & 0 \\ M_{kf} & L_k & M_{kd} & 0 & 0 & 0 \\ M_{fd} & M_{kd} & L_d & 0 & 0 & 0 \\ 0 & 0 & 0 & L_d & M_{kd} & 0 \\ 0 & 0 & 0 & M_{kd} & L_k & 0 \\ 0 & 0 & 0 & 0 & 0 & L_o \end{bmatrix} \begin{bmatrix} i_f \\ i_{kd} \\ i_d \\ i_q \\ i_{kq} \\ i_o \end{bmatrix}$$

(91)

$$\begin{aligned}
 \text{where } L_d &= L_a \\
 M_{fd} &= |L_{af}| \\
 M_{kd} &= |M_{ka}| \\
 L_o &= L_a - 2L_{ab}
 \end{aligned}$$

The equations for the corresponding voltages can be written down in the usual form as follows using p for the derivative operator, d/dt :

$$\begin{aligned}
 e_f &= r_f i_f + p\psi_f \\
 e_{kd} &= r_{kd} i_{kd} + p\psi_{kd} = 0 \\
 e_d &= r_a i_d + p\psi_d + \nu\psi_q \\
 e_q &= r_a i_q - \nu\psi_d + p\psi_q \\
 e_{kq} &= r_{kq} i_{kq} + p\psi_{kq} = 0 \\
 e_o &= r_a i_o + p\psi_o \tag{92}
 \end{aligned}$$

It should be noted that these equations do not introduce any special assumptions regarding the distribution of the stationary windings, except that they are symmetrical about the axis. The flux distribution in a superconducting machine will not be sinusoidal and the values of self and mutual inductance must allow for this. In the case of the armature windings, the distribution factors of the windings in respect of harmonics will usually be arranged so that they are zero or negligible, so that although the field distribution may contain harmonics, the resulting emf induced in the armature is approximately sinusoidal. The assumption of zero or negligible harmonic distribution factors will be assumed here and corresponds to Park's assumption of a 'sinusoidally distributed winding'.

15.5 Operational Impedances.

It has become usual to express the terminal performance of conventional synchronous machines in terms of operational impedances. If the currents in the field and damper windings are eliminated from the equations for such a machine, a single operational relation between ψ_d , i_d and e_f may be obtained of the form:

$$\psi_d = \frac{x_d(p)}{\omega} i_d + \frac{G(p)}{\omega} e_f \quad (93)$$

The factor ω is introduced in the denominator so that $x_d(p)$ has the dimensions of an operational impedance ($\omega = 2\pi f$, where f is the synchronous frequency).

Before the network analysis of synchronous machines provided by generalised machine theory became developed, transients were studied on a phenomenological basis in terms of subtransient and transient reactances. These are the reactances of the armature in the periods in which the conventional damper windings and the field winding respectively are regarded as maintaining constant flux linkage after a short circuit at the armature terminals. Associated with the subtransient and transient reactances are the time constants of the relevant circuits.

By making appropriate approximations, the functions $x_d(p)$ and $G(p)$ can be expressed in terms of the subtransient and transient reactances and time constants. We now propose to develop equs.(91) and (92) for the superconducting machine on similar lines to this in order to develop the operational impedances for the superconducting machine.

By eliminating i_f and i_{kd} from the expressions for e_f , e_{kd} and e_d in eqs. (91) and (92), ψ_d may be expressed in the form of equ. (93). The value of i_d is given by Cramer's rule by the quotient of two determinants as follows:

$$i_d = \frac{D_1}{D_2} \quad (94)$$

$$\text{where } D_1 = \begin{vmatrix} e_f & r_f + L_f p & M_{kf} p \\ 0 & M_{kf} p & r_k + L_k p \\ \psi_d & M_{fd} & M_{kd} \end{vmatrix}$$

$$= r_f r_k \left[1 + (T_1 + T_2)p + T_1 T_3 p^2 \right] \psi_d + \left[-M_{fd} r_k - p(M_{fd} L_k - M_{kd} M_{kf}) \right] e_f \quad (95)$$

$$D_2 = \begin{vmatrix} r_f + L_f p & M_{kf} p & M_{fd} p \\ M_{kf} p & r_k + L_k p & M_{kd} p \\ M_{fd} & M_{kd} & L_d \end{vmatrix}$$

$$= r_f r_k L_d \left[1 + (T_4 + T_5)p + \left(T_4 T_6 + \frac{M_{fd}}{L_d r_f r_k} (M_{kf} M_{kd} - L_k M_{fd}) \right) p^2 \right] \quad (96)$$

The values of the time constants in the expressions for D_1 and D_2 we define as:

$$T_1 = \frac{L_f}{r_f}$$

$$T_2 = \frac{L_r}{r_k}$$

$$T_3 = \frac{L_k}{r_k} \left(1 - \frac{M_{kf}^2}{L_k L_f} \right)$$

$$T_4 = \frac{L_f}{r_f} \left(1 - \frac{M_{fd}^2}{L_d L_f} \right)$$

$$T_5 = \frac{L_k}{r_k} \left(1 - \frac{M_{kd}^2}{L_d L_k} \right)$$

$$T_6 = \frac{L_k}{r_k} \left\{ \frac{1 - \frac{M_{kd}^2 L_f - M_{kf} M_{kd} M_{fd} + M_{kf}^2 L_d}{L_d L_f L_k}}{1 - \frac{M_{fd}^2}{L_d L_f}} \right\} \quad (97)$$

Before proceeding to solve for Ψ_d , we will examine the implication of the basic assumption that all the flux which links the armature phase windings and the field winding must pass through the damper screen. The windings concerned are the three on the direct axis: F, KD and D. With a current i_d flowing in D, the flux linkage produced by i_d is:

$$\Psi_d = L_d i_d$$

Only part of this flux links with KD, viz.

$$\Psi_k = M_{kd} i_d$$

so that $\frac{\Psi_k}{\Psi_d} = \frac{M_{kd}}{L_d}$

Similarly considering coil F in relation to flux linking coil KD,

$$\frac{\Psi_f}{\Psi_k} = \frac{M_{kf}}{L_k}$$

Now if Ψ_f is part of Ψ_k which in turn is produced by i_d in coil D, and Ψ_f is the only flux produced by i_d in coil D which does link with F, then $\Psi_f = M_{fd} i_d$, by definition of M_{fd} .

Hence substituting for Ψ_f and Ψ_k gives:

$$\frac{M_{fd} i_d}{M_{kd} i_d} = \frac{M_{kf}}{L_k}$$

$$\text{or } M_{fd} L_k = M_{kd} M_{kf} \quad (98)$$

By using equ.(98), we simplify eqs.(95) and (96) to:

$$D_1 = r_f r_k \left[1 + (T_1 + T_2)p + T_1 T_3 p^2 \right] \Psi_d - M_{fd} r_k e_f \quad (99)$$

$$D_2 = r_f r_k L_d \left[1 + (T_4 + T_5)p + T_4 T_6 p^2 \right] \quad (100)$$

This leads to the value of Ψ_d as:

$$\Psi_d = \left[\frac{1 + (T_4 + T_5)p + T_4 T_6 p^2}{1 + (T_1 + T_2)p + T_1 T_3 p^2} \right] L_d i_d + \left[\frac{1}{1 + (T_1 + T_2)p + T_1 T_3 p^2} \right] \frac{M_{fd}}{r_f} e_f \quad (101)$$

Comparing the expressions for Ψ_d given in equs. (93) and (101) and equating coefficients, we obtain:

$$x_d(p) = \left[\frac{1 + (T_4 + T_5)p + T_4 T_6 p^2}{1 + (T_1 + T_2)p + T_1 T_3 p^2} \right] x_d \quad (102)$$

$$\text{and } G(p) = \left[\frac{1}{1 + (T_1 + T_2)p + T_1 T_3 p^2} \right] \frac{x_{fd}}{r_f} \quad (103)$$

where x_d and x_{fd} are reactances corresponding to the inductances L_d and M_{fd} respectively.

It is customary to express $x_d(p)$ and $G(p)$ in the form:

$$x_d(p) = \frac{(1 + T_d' p)(1 + T_d'' p)}{(1 + T_{do}' p)(1 + T_{do}'' p)} x_d \quad (104)$$

$$G(p) = \frac{1 + T_{kd} p}{(1 + T_{do}' p)(1 + T_{do}'' p)} \frac{x_{fd}}{r_f} \quad (105)$$

where the constants T_{do}' , T_{do}'' , T_d' , T_d'' are the four principal time constants of the conventional synchronous machine. Because of the similarity between the resulting expressions for the performance of the conventional and superconducting synchronous machines (albeit not an exact identity between the two), we propose to apply the usually accepted terminology for the former to the latter. Since the basic assumptions for the two machines are different, the resulting expressions differ in detail but the same general form

can be recognised.

Thus we define four principal time constants for the superconducting machine by the following identities obtained from equs. (102) - (105).

$$(1 + T_{do}^I p) (1 + T_{do}^{II} p) \equiv 1 + (T_1 + T_2)p + T_1 T_3 p^2 \quad (106)$$

$$(1 + T_d^I p) (1 + T_d^{II} p) \equiv 1 + (T_4 + T_5)p + T_4 T_6 p^2 \quad (107)$$

The values of the time constants can be calculated accurately from equs. (106) and (107), but simpler expressions can be obtained by making a further approximation that the time constant of the field circuit will be much longer than that of the damper screen. Thus $T_2 \ll T_1$ and $T_3 \ll T_1$; also $T_5 \ll T_4$ and $T_6 \ll T_4$. Hence T_{do}^I and T_{do}^{II} are approximately equal to T_1 and T_3 respectively. Similarly T_d^I and T_d^{II} are approximately equal to T_4 and T_6 .

Expressions for the quadrature axis can be developed in a similar way by eliminating i_{kq} from the expressions for e_{kq} and Ψ_q in equs. (91) and (92). They are simpler because there is no quadrature field winding. The operational expression corresponding to equ. (93) is:

$$\Psi_q = \frac{x_q(p)}{\omega} i_q \quad (108)$$

and the quadrature-axis operational reactance, $x_q(p)$ is given for the conventional machine by:

$$x_q(p) = \frac{1 + T_{qo}^{II} p}{1 + T_{qo}^I p} x_q \quad (109)$$

Assuming equ. (109) is also appropriate for the superconducting machine, we find that:

$$T''_{q0} = \frac{L_k}{r_k}$$

$$T''_q = \frac{L_k}{r_k} \left(1 - \frac{M_{kd}^2}{L_d L_k} \right)$$

The derived reactances for the superconducting machine in terms of the usually accepted terminology are as follows:

Direct-axis synchronous reactance, $x_d = \omega L_d$

Direct-axis transient reactance, $x'_d = x_d \frac{T'_d}{T'_{do}} = x_d \left(1 - \frac{M_{fd}^2}{L_d L_f} \right)$

Direct-axis subtransient reactance, $x''_d = x_d \frac{T'_d T''_d}{T'_{do} T''_{do}}$

$$= x_d \left[\frac{1 - \frac{M_{kd}^2 L_f - M_{kf} M_{kd} M_{fd} + M_{kf}^2 L_d}{L_d L_f L_k}}{1 - \frac{M_{fd}^2}{L_d L_f}} \right]$$

Quadrature-axis synchronous reactance, $x_q = \omega L_d$

Quadrature-axis subtransient reactance, $x''_q = x_q \frac{T''_q}{T''_{q0}}$

$$= x_q \left(1 - \frac{M_{kd}^2}{L_d L_k} \right)$$

It has thus been demonstrated that the five-coil representation of the generalised electrical rotating machine can be made to apply to the synchronous machine with a superconducting field winding and continuous damper screen between the armature and field by applying appropriate constraints. The resulting equations are similar, but not identical to those for the conventional synchronous machine. The theory can be applied to determine the steady operation of the superconducting machine at synchronous speed, during run-up and synchronisation and under balanced and unbalanced loading conditions. Performance under transient conditions such as short circuit, the switching of large loads, forced and free mechanical oscillations and the stability of the superconducting machine connected to a power system can all be investigated following the techniques already existing for conventional machines. The solution of problems peculiar to the superconducting machine, such as the current, torque and thermal conditions of the field winding and damper screen under transient and fault conditions can also be attempted. However, it is not intended to pursue such detailed studies here, but the evaluation of the basic inductance parameters will be introduced.

15.6 Parameter Evaluation

In the evaluation of the parameters required for the application of the theory given in the preceding section, two main problems present themselves: the evaluation of the self and mutual inductances of the concentrated and distributed windings of discrete conductors and the time constant of the continuous damper screen (see Section 15.8).

Woodson et al (187) have presented formulae for calculating the self and mutual inductance parameters for the field and armature of an air-cored synchronous machine with a superconducting field winding. They assume two-dimensional configurations and a three-phase armature winding with a 60° phase spread; the field winding space is assumed to be filled uniformly with superconducting wire. The calculation of the magnetic fields caused by current flow in the different windings is then treated as a linear problem in magnetostatics, and the field resulting from each winding is calculated separately and the results superimposed. The effective current densities in the field winding and an armature phase are defined and the magnetizing force for each obtained in terms of cylindrical harmonics for a p -pole-pair armature. The fundamental components of these field quantities are then used to calculate the inductance parameters required; the expressions are somewhat cumbersome but would present no problems for computer calculation. Although it would be very tedious, the method could be extended to include all the space harmonics of both the armature and field if any particular problem required it. The method could also be applied to windings with other phase spreads.

15.7 Effect of Ferromagnetic Shield.

The expressions derived by Woodson et al (187) are for machines without magnetic shielding. It is now proposed to deal with the case of a ferro-magnetic shield surrounding the armature, using the method of electromagnetic images described by Hague in Bibliography 4. The problem will be treated in two dimensions using cylindrical co-ordinates and it will be assumed that the permeability of the shield is constant and equal to μ_s . The arrangement of the superconducting winding and the ferromagnetic shield are as shown in fig. 84.

The magnetizing force in air at any point P inside the space enclosed by the shield is that due to the currents in the field winding with that due to the image currents in the shield superimposed. Thus the radial component of the magnetizing force at $P(r_p, \phi_p)$ is:

$$H_{rs} = H_r + H'_r$$

where H_r is the magnetizing force due to the field winding currents and H'_r is that due to the image currents. Similarly

$$H_{\phi s} = H_{\phi} + H'_{\phi}$$

The image current at a point Q' in the ferromagnetic shield corresponding to the real current at a point $Q(r, \phi)$ in the field winding is situated so that Q' is the point (r', ϕ') where $r' = R_s^2 / r$ and $\phi' = \phi$; (R_s is the inner radius of the ferromagnetic boundary).

The magnitude of the image current i'_Q at Q' is given in terms of the current i_Q at Q by:

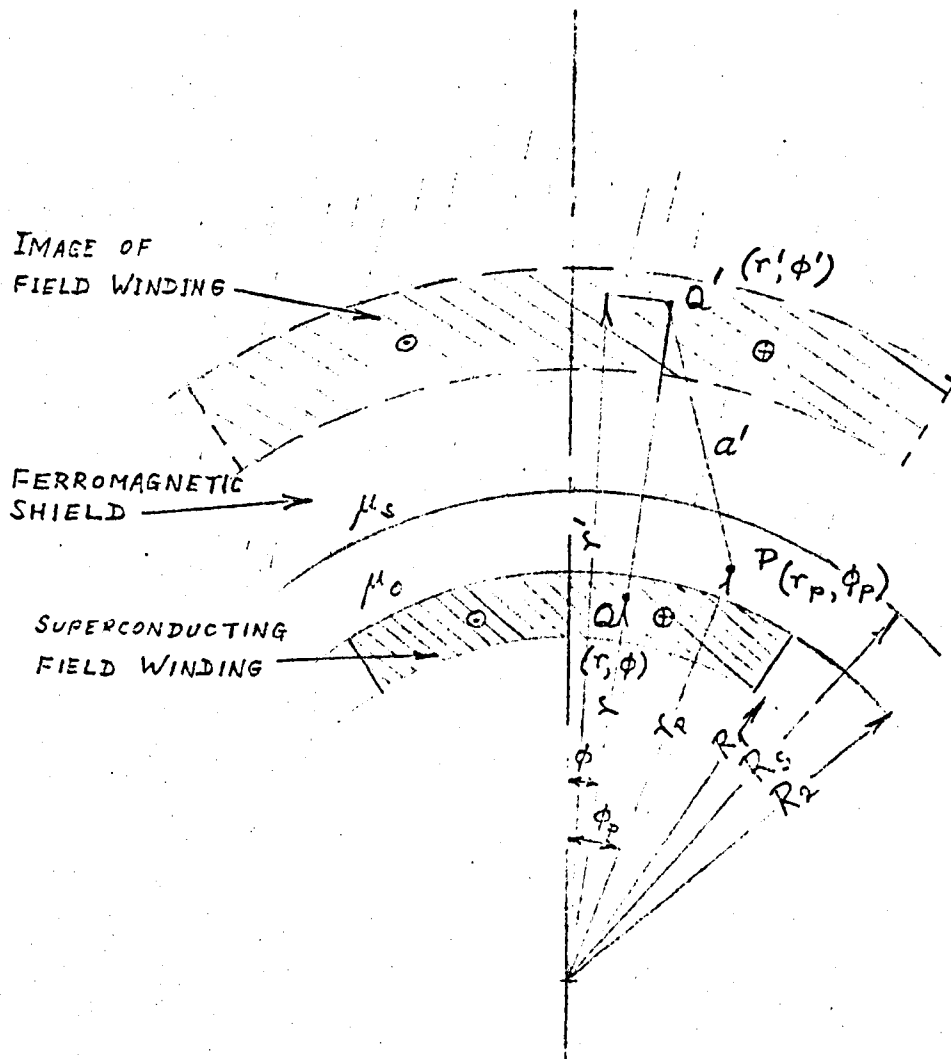


Fig. 84. Arrangement of superconducting winding and ferromagnetic shield.

$$i_q' = \frac{1 - (\mu_o/\mu_s)}{1 + \mu_o} i_q$$

If J and J' are the values of the corresponding current densities for the real and image currents, then;

$$J' = \left\{ \frac{1 - (\mu_o/\mu_s)}{1 + \mu_o} \right\} \left(\frac{r_s}{r'} \right)^4 \cdot J \quad (110)$$

The components of the magnetizing force in the radial and tangential directions due to the image currents can be determined from the vector potential \bar{A} , since

$$H_r' = \frac{1}{\mu_o r'} \cdot \frac{\partial A'}{\partial \phi}$$

$$\text{and } H_\phi' = -\frac{1}{\mu_o} \cdot \frac{\partial A'}{\partial r} \quad (111)$$

The axial component of \bar{A} at P is given by:

$$A' = \frac{\mu_o}{2\pi} \int_{S'} J' r' dr' d\phi \ln a'$$

where S' is the area occupied by the shield with the image current,

$$\text{and } a' = \sqrt{r_p^2 + r'^2 - 2r_p r' \cos(\phi_p - \phi)}$$

Expressing the vector potential in terms of a Fourier series gives:

$$A' = \frac{\mu_o}{2\pi} \int_S J' r' dr' d\phi \sum_{n=1}^{\infty} \frac{1}{n} \left(\frac{r_p}{r'} \right)^{np} \cos np(\phi_p - \phi) \quad (112)$$

Integration over the whole area occupied by the image current, and substitution in eqs.(111) with further reduction gives:

$$H_r' = J' \frac{R_2}{4\pi} \left[\frac{1 - (\mu_o/\mu_s)}{1 + \mu_o} \right] K_r' \cos np\phi \quad (113)$$

$$H_\phi' = -J' \frac{R_2}{4\pi} \left[\frac{1 - (\mu_o/\mu_s)}{1 + \mu_o} \right] K_\phi' \sin np\phi \quad (114)$$

$$\text{where } K_r' = K_\phi' = \sum_{n=1}^{\infty} \frac{8}{n(np+2)} \cdot \frac{1 - r_1^{np+2}}{r_s^{2np}} \cdot r^{np-1} \quad (115)$$

The radii have been normalised in terms of the outer radius of the field winding as follows:

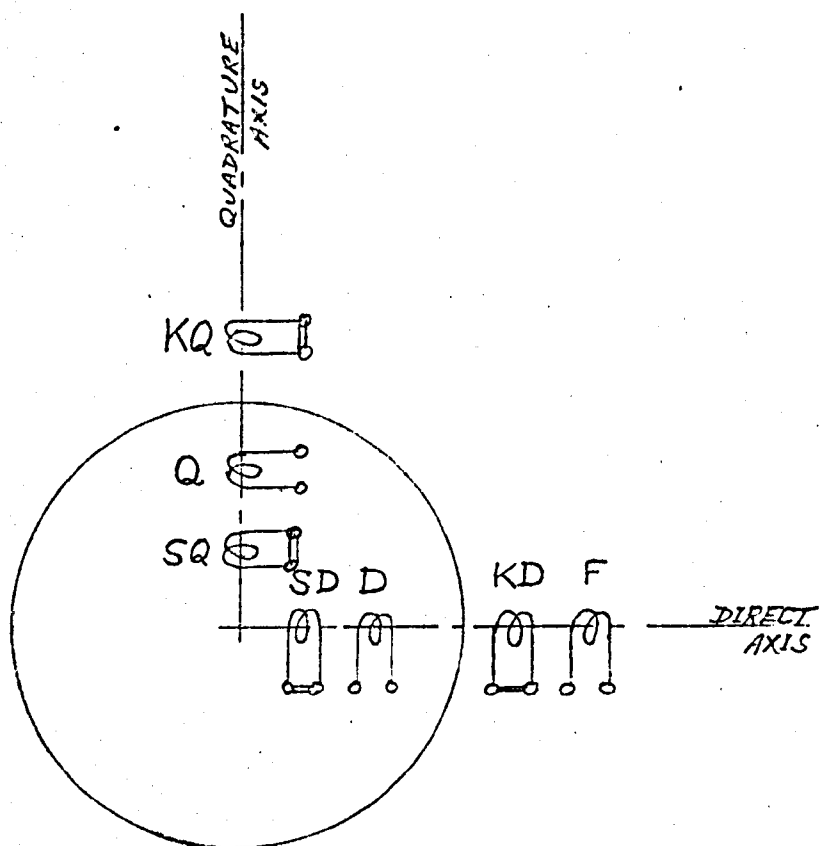
$$r_1 = R_1/R_2, \quad r = R/R_2 \quad \text{and} \quad r_s = R_s/R_2$$

In a machine with a ferromagnetic shield round the outside of the armature, the values of the radial and tangential magnetizing force can be obtained by multiplying the values given by Woodson et al (187) by equs. (113) and (114) respectively. The values of inductance follow from the modified values of magnetizing force.

15.8 Effect of Eddy Current Shield.

The value of the time constant for the damper screen can be obtained from the work of Jaeger in reference 221.

The analysis of the performance of a synchronous machine with an eddy current shield would need a more complicated model than the five-coil simplified representation we have presented in Section 15.4. It is suggested that a seven-coil model illustrated in fig.85 could form one approach. The eddy current shield is primarily associated with the armature and therefore it would be necessary to transform the rotating coils representing the eddy current shield by a trans-



Coil F represents the superconducting field coil
 Coils D and Q (pseudo-stationary) represent the armature
 Coils KD and KQ represent the damper screen
 Coils SD and SQ (pseudo-stationary) represent the eddy-current shield.

Fig. 85 Representation proposed for superconducting synchronous machine with eddy-current screen.

formation similar to that of Parks for the armature coils. The principal time constants for these coils could be evaluated from Jaeger (221), but the damper screen constraint of equ.(98) would not be applicable. The resulting equations for the performance of such a machine would thus be considerably more complicated, and it is not proposed to pursue the topic further here.

In the case of the ferromagnetically shielded machine, the effect of the shield is taken into account by modifying the inductance parameters as proposed above. Any currents induced in the ferromagnetic shield would be small by virtue of its design, e.g. by laminating the shield, and by comparison with the other currents in the machine could probably be neglected. This is another area of speculation requiring detailed investigation.

16. Conclusions and Recommendations.

16.1 Possible Applications.

The purpose of this study was to examine the phenomenon of superconductivity and to explore the possibilities of utilizing it in rotating energy converters.

Of the three properties unique to superconductors, (the Meissner effect, zero resistivity and the transition between the normal and superconducting states), none seemed to offer the possibility of incorporation into a machine which would offer technological advantages, with the possible exception of a very few specialised uses, such as inertial gyros and a positioning device at very low cryogenic temperatures.

The high field property of superconductors was then examined in relation to existing conventional types of machines to see in which of these it might be feasible to incorporate superconducting windings. The advantages, technical and economic, were then assessed of using such windings. It was concluded from this section of the study that only the d.c. homopolar machine, the Harrowell toroidal reciprocating generator and the synchronous machine offered any scope for having superconducting windings incorporated in them.

16.2 The Harrowell Generator.

Apart from the basic objection raised by some to this machine which is that it reciprocates, it does offer certain advantages by way of reduced weight, cost and losses, better operational characteristics and a greater potential for scaling to large powers than conventional rotary machines. A design procedure for establishing

the leading dimensions was delineated and some preliminary conclusions drawn regarding the design of these machines. A detailed parametric design study is now required to examine the potential of this type of machine and an experimental study needed to obtain technological data and limiting values for the various parameters. Finally a costing exercise would be needed to complete the technological and economic assessment, in order to show whether or not it would be worthwhile to develop this type of machine.

16.3 D.C. Homopolar Machines.

That d.c. homopolar machines of ratings of a few thousand horsepower with superconducting field windings are technically feasible, is without question and has been demonstrated by the IRD Company. It was shown that, neglecting development expenditure, the break-even capital cost of this type of machine compared with a conventional d.c. tandem-armature machine is not well-defined and detailed cost analyses would be required for individual machine specifications in order to assess which type had the lower capital cost. However, the main cost benefit seemed to accrue, not from lower capital cost of the superconducting machine, but rather from its lower losses, lighter weight and smaller volume.

Although several applications for superconducting homopolar machines were suggested, developments in other technologies and the general lack of sufficient market opportunities for machines in the 1 - 10 MW range, would not provide much incentive for their continued development on any scale.

16.4 Large Synchronous Machines.

From a review of the expected requirements for large scale power generation and the characteristics anticipated from superconducting synchronous generators, it would appear that they offer the most promising and economical means of meeting the demand anticipated in the next decade. Although many formidable problems present themselves, none would appear to be intrinsically incapable of solution.

The choice of damper screen location, material and proportions requires detailed analysis and experimental verification. The type of magnetic screening, whether by iron or eddy current high conductivity cylinder, needs considerable investigation in order to select the more appropriate for a given machine; the influence of the screen on the terminal characteristics and economics needs a major investigation. In our study, an introduction to the magnetic effects of these screens has been presented which could serve as an introduction to such an investigation.

A considerable number of other problems connected with the liquid helium, cryogenics, mechanical construction, cooling and refrigeration and control of the field need to be investigated but we have concentrated on the electromagnetic aspects. The overriding consideration at least as far as the U.K. is concerned is the need for an overall policy regarding the funding of such development. However, given that the necessary development effort is forthcoming, the indications are that superconducting synchronous generators for large-scale power generation are both technically feasible and likely to be economically viable.

16.5 Aircraft Generators.

Although aerospace was one of the regions in which generators utilizing superconductors were first contemplated, the results of our detailed studies show that the early optimism for this application has no basis in fact. In summary, we showed that only in ratings above 1 MVA did the 400 Hz aircraft superconducting generator and its liquid helium refrigeration system become competitive on a weight basis with conventional machines, and only then if some cryogen was already on board and available for cooling intermediate thermal radiation shields. Thus there is no incentive to develop superconducting generators for civil aircraft where ratings of less than 90 kVA are required, and the case for use in military applications is marginal with currently available superconducting materials and helium refrigerators unless extremely large powers are required.

16.6 Experimental Study.

The feasibility of synchronous machines with superconducting field windings has been demonstrated by previous workers, and the object in constructing our machine was to investigate its electrical performance in an endeavour to verify the theory we had developed in the course of its design and subsequently. The effect of a damper screen in shielding time-variant armature-produced fields was shown together with the successful operation of filamentary niobium-titanium superconducting wire very close to its transition condition of field and current. Although only the first (inner) sections of the field coils were available during this study, several features of superconducting machines were successfully demonstrated and within

reasonable limits, provide verification of some of the theoretical and design studies. Much more experimental work needs to be done to form a complete and comprehensive study.

16.7 Synchronous Machine Analysis.

Although a fully comprehensive analysis of superconducting synchronous machines has not been presented, nevertheless we have indicated a suitable basis for such a theory and how it could be subsequently developed and applied in the solution of transient problems, fault conditions and in the study of stability and power system performance. Some specific problems requiring investigation are the adjustment of the reactance parameters and their relation to the survival of the machine under fault conditions, the role played by the damper screen and the extent to which the mechanical torques under fault conditions act on it, the selection of the superconductor operating point in relation to the rise in field current during a fault, and the thermal conditions pertaining to the damper screen during fault conditions. Further work is also needed to determine the transposition requirements in a large scale machine, and in particular the magnetic fields in the winding end-connection sections need to be known with more exactitude to enable more accurate determination of the winding inductances to be made.

16.8 General Conclusions.

In some respects the conclusions drawn from this study are disappointing, since the application in rotating electrical machines of the superconductors now currently available is ruled out in the

majority of instances on technical grounds. Where the application is technically feasible, as in the d.c. homopolar machine, the case is marginal on economic grounds. However, the optimism referred to in Chapter 1 (1, 2) in relation to large superconducting synchronous generators seems wholly justified.

Bibliography

1. Adkins, B. : The General Theory of Electrical Machines. (Chapman and Hall)
2. Brosan, G.S. and Hayden, J.T. : Advanced Electrical Power and Machines. (Pitman)
3. Carter, G.W.: The Electromagnetic field in its Engineering Aspects. (Longmans)
4. Hague, B.: The Principles of Electromagnetism applied to Electrical Machines. (Dover)
5. Hoare, F.E., Jackson, L.C. and Kurti, N.(Eds.): Experimental Cryophysics. (Butterworth)
6. Kolm, H., Lax. B., Eitter, F. and Mills, R. (Eds.): High Magnetic Fields. (MIT/Wiley)
7. Kuper, C.G.: An Introduction to the Theory of Superconductivity. (Oxford)
8. Lynton, E.A.: Superconductivity. (Methuen)
9. McLachlin, N.W.: Bessel Functions for Engineers. (Oxford)
10. Montgomery, D.B.: Solenoid Magnet Design. (Wiley)
11. Parkinson, D.H. and Mulhall, B.E.: The Generation of high magnetic Fields. (Heywood).
12. Say, M.G.: The Performance and Design of a.c. Machines. (Pitman)
13. Smythe, W.R.: Static and Dynamic Electricity. (McGraw-Hill)

References

1. Anon.: IEE News, 17 May, 1971, p.2.
2. Anon.: Business Week, 13 May 1972, pp. 150, 154.
3. ERA Technological Planning Unit: Report No. 60/01/1021.
4. Livingston, J.D. and Schadler, H.W.: Progress in Mat. Sci., 12 pp. 183-287, 1964.
5. Dew-Hughes, D.: Maths. Sci. and Eng., 1, pp. 2-29, 1966.
6. Catterall, J.A.: Metal. Reviews No. 102, 1966.
7. Lowell, J.: Cryogenics, 5, pp. 185-93, 1965.
8. Goodman, B.B.: Rep. Progr. Phys., 29 pt II, pp.445-87, 1966.
9. Quinn, D.J. and Ittner, W.B.: J. App.Phys., 33 p.748, 1962.
10. Abrikosov, A.A.: Sov. Phys. JETP, 5, pp.1174-82, 1957.
11. Matricon, J.: Phys. Lett., 9 , pp. 289-91, 1964.
12. Kleiner, W.H., Roth, L.M. and Autler, S.H.: Phys. Rev., 133 , pp. A1226-7, 1964.
13. Cribier, D., Jacrot, J., Madhav Rao, L. and Farnoux, B.: Phys. Lett., 9 , pp.106-7, 1964.
14. St. James, D. and de Gennes, P.G.: Phys. Lett., 7 , pp.306-7, 1963.
15. Hempstead, C.F. and Kim, Y.B.: Phys. Rev. Lett., 12 , pp.145-7, 1963.
16. Tomasch, W.J. and Joseph, A.S.: *ibid.* pp. 148-50.
17. Anderson, P.W.; Phys. Rev. Lett., 9(7), pp.309-11, 1962.
18. Anderson, P.W., and Kim, Y.B.: Rev. Mod. Phys., 36 , pp.39-43, 1964.
19. Kim, Y.B., Hempstead, C.F. and Strnad, A.R.: Phys. Rev., 129, pp. 528-35, 1963.
20. Kim, Y.B., Hempstead, C.F. and Strnad, A.R.: Phys. Rev. Lett., 9 (7), pp.306-8, 1962.
21. Friedel, J., de Gennes, P.G. and Matricon, J.: Appl. Phys. Lett., 2 , pp.119-21, 1963.

22. Evetts, J.E. and Campbell, A.M.: Proc. of LT10, pp.32-7, Moscow, 1966.
23. Kim, Y.B., Hempstead, C.F. and Strnad, A.R.: Phys. Rev., 131, pp.2486-95, 1963.
24. Strnad, A.R., Hempstead, C.F. and Kim, Y.B.: Phys. Rev. Lett., 13, p.794, 1964.
25. Kim, Y.B., Hempstead, C.F. and Strnad, A.R.: Phys. Rev., 139 No.: 4A, pp.A1163-72, 1965.
26. Tinkham, M.: Phys. Rev. Lett., 13, p.804, 1964.
27. Stephen, M.J. and Bardeen, J.: Phys. Rev.Lett., 14, p.112, 1965.
28. Dowley, M.W.: Appl. Phys. Lett., 4, pp.41-3, 1963.
29. Lubell, M.S., Mallick, G.T. and Chandrasekhar, B.S.: J.Appl.Phys., 35, pp.956-8, 1964.
30. Leblanc, M.A.R. and Vernon, F.L.: Phys. Lett., 13, pp.291-3, 1964.
31. Leblanc, M.A.R.: Phys. Rev., 124, pp.1423-5, 1961.
32. Lubell, M.S. and Mallick, G.T.; Appl. Phys. Lett., 4, pp.206-7, 1964.
33. Laverick, C.: Cryogenics, 5, pp.152-8, 1965.
34. Evetts, J.E., Campbell, A.M. and Dew-Hughes, D.: Phil. Mag., 10, pp.339-43, 1964.
35. Wertheimer, M.R. and Gilchrist, J. Le G.: J. Phys. Chem. Solid., 28, pp.2509-2524, 1967.
36. Wertheimer, M.R. and Gilchrist, J. Le G.: Proc. LT11, pp.865-8, St. Andrews, 1968.
37. Bean, C.P.: Phys. Rev. Lett., 8 (6), pp.250-3, 1962.
38. Bean, C.P.: Rev. Mod. Phys., 36, pp.31-9, 1964.
39. Silcox, J. and Rollins, R.W.: *ibid.* pp.52-54.
40. Irie, F. and Yamafuji, K.: J. Phys. Soc. Jap., 23, pp.255-268, 1967.
41. Urban, E.W.: J. Appl. Phys., 42, pp.115-27, 1971.
42. Riemersma, H., Hulm, J.K. and Chandrasekhar, B.S.: Adv. in Cryo. Eng., 2, pp.329-337, 1964.

43. Schrader, E.R. and Freedman, N.S.: Appl. Phys. Lett., 4 , pp.105-6, 1964.
44. London, H.: Phys. Lett., 6 , pp.162-5, 1963.
45. Hancox, R.: Pr.IEE, 113 , pp.1221-8, 1966.
46. Voigt, H.: Phys. Lett., 20 , p.262, 1966.
47. Green, I.M. and Hlawiczka, P.: Pr.IEE, 114 , pp.1329-33, 1967.
48. Dunn, W.I. and Hlawiczka, P.: Brit. J. Appl. Phys., Ser. 2, 1 , pp.1469-76, 1968.
49. Linford, R.M.F.: Ph.D.Thesis, University of Warwick, 1968.
50. Linford, R.M.F. and Rhodes, R.G.: J. Appl. Phys., 42 , pp.10-15, 1971.
51. Chant, M.J., Halse, M.R. and Lorch, H.O.: Proc.IEE, 117, pp.1441-7, 1970.
52. Kamper, R.A.: Phys. Lett., 2 , p.290, 1962.
53. Rhodes, R.G., Rogers, E.C. and Seebold, R.: Cryogenics, 4 , pp. 206-8, 1964.
54. Easson, R.M. and Hlawiczka, P.: Brit. J. Appl. Phys., 18 , pp. 1237-49, 1967.
55. Easson, R.M. and Hlawiczka, P.: Brit. J. Appl. Phys., Ser. 2, 1 , pp.1477-85, 1968.
56. Slaughter, R.J., Rogers, E.C. and Grigsby, R.: Phys. Letts., 23, p.214, 1966.
57. Dahl, P.F., Morgan, G.H. and Sampson, W.B.: J. Appl. Phys., 40, pp.2083-5, 1969.
58. Ulmaier, H.A. and Gauster, W.F.: J. Appl. Phys., 37 , pp.4519-21, 1966.
59. Wipf, S.L.: Proc. of the Brookhaven Summer Study, 1968.
60. Autler, S.H.: "High Magnetic Fields" (Eds. Kolm, Lax, Bitter, Mills), Chapter 34, 1961.
61. Laverick, C.: Int. Adv. In Cryo. Eng., 10 (M-V), pp105-12, 1965.
62. Hulm, J.K., Chandrasekhar, B.S. and Riemersma, H.: Adv. in Cryo. Eng., 8 , pp.17-29, 1963.
63. Stekly, Z.J.J.: Adv. in Cryo. Eng., 8b , pp.585-600, 1963.

64. Kantrowitz, A.R. and Stekly, Z.J.J.: Appl. Phys. Lett., 6 , pp.56-7, 1965.
65. Shimamoto, S. and Ohtsuki, S.: Jap. J. Appl. Phys., 5 , pp.184-5, 1966.
66. Schrader, E.R. and Kolondra, F.: RCA Rev., 25 , pp.582-95, 1964.
67. Coffey, H.T., Hulm, J.K., Reynolds, E.T. et al.: J. Appl. Phys., 36 , pp.128-36, 1965.
68. Kunzler, J.E.: "High Magnetic Fields", Chapter 68, 1961.
69. Boom, R.W., Roberts, L.D. and Livingston, R.S.: Nucl. Instrum., 20, pp.495-502, 1963.
70. Hancox, R.: Phys. Lett., 16, pp.208-9, 1965.
71. Hancox, R.: Appl. Phys. Lett., 7 , pp.138-9, 1965.
72. Hancox, R.: Proc. LT10, pp.43-46, Moscow 1966.
73. Swartz, P.S. and Bean, C.P.: Bull. Am. Phys. Soc., 10 , p.359, 1965.
74. Irie, F. and Yamafuji, K.: Proc. ICEC 1, pp.177-80, 1967.
75. Kim, Y.B.: ibid. pp.168-74.
76. Wipf, S.L.: Phys. Rev., 161 , pp.404-16, 1967.
77. Wipf, S.L. and Lubell, M.S.: Phys. Lett., 16 , pp.103-5, 1965.
78. Swartz, P.S. and Bean, C.P.: J. Appl. Phys., 39 , pp.4991-8, 1968.
79. Iwasa, Y. and Montgomery, D.B.: Appl. Phys. Lett., 7 , pp.231-3, 1965.
80. Gauster, W.F. and Ullmaier, H.A.: J. Appl. Phys., 37 , p.1014, 1966.
81. Lubell, M.S. and Wipf, S.L.: ibid, pp.1012-4.
82. Yamafuji, K., Takeo, M. et al.: J. Phys. Soc. Jap., 26 , pp.315-30, 1969.
83. Neuringer, L.J. and Shapira, Y.: Phys. Rev., 148 , pp.231-46, 1966.
84. Kantrowitz, A.R. and Stekly, Z.J.J.: Appl. Phys. Lett., 6 , pp.56-7, 1965.

85. Stekly, Z.J.J. and Zar, J.L.: Tr.IEEE, NS-12, pp.367-72, 1965.
86. Montgomery, D.B.: Proc. ICEC 1, pp.81-87, 1967.
87. Williams, J.E.C.: Phys. Lett., 19 , pp.96-97, 1965.
88. Cornish, D.N.: J. Sci. Instrum., 43 , pp.16-20, 1966.
- 89.
90. Keilin, V.E., Klimenko, E.Yu., Kremlov, M.G., and Samoilov, B.N.:
Proc. of Conf. on Intense Magnetic Fields,
Grenoble, 1966, pp.231-6.
91. Williams, J.E.C.: ibid, pp.281-8.
92. Stekly, Z.J.J.:Proc.LT 10,pp.25-42, Moscow, 1966.
93. Stekly, Z.J.J.:Proc.ICEC 1, pp.112-8, 1967.
94. Kremlev, M.G.: Cryogenics, 7 , pp.267-70, 1967.
95. Gauster, W.F.: Cryogenics, 9 , pp.136-7, 1969.
96. Whetstone, C.N. and Boom, R.W.: Adv. in Cryo. Eng., 13 ,
pp.68-79, 1968.
97. Gauster, W.F. and Hendricks, J.B.: J. Appl. Phys., 39 ,
pp.2572-8, 1968.
98. Gauster, W.F. and Hendricks, J.B.: Tr.IEEE, MAG-4 , pp.489-92,
1968.
99. Purdy, V., Frederking, T.H.K., Boom, R.W. et al.: Adv. in
Cryo. Eng., 14 , pp.146-58, 1969.
100. Kremlev M.G., Zenkevitch, V.E., and Al'tov, V.A.: Cryogenics,
8 , pp.173-4, 1968.
101. Gauster, M.F., Efferson, K.R., Hendricks, J.B., Ullmaier, H.A.
and Wilkes, W.R.: Cryogenics, 8 , pp.13-7, 1968.
102. El Bindari, A.: J. Appl. Phys., 40 , pp.2070-5, 1969.
103. El. Bindari, A: and Bernert, R.E.: J. Appl. Phys., 39 ,
pp.2529-32, 1968.
104. Maddock, B.J., James, G.B., and Norris, W.T.: ibid, 9 , pp.261-73,
1969.
105. Jackson, J. and Fruin, A.S.: Proc. Int. Conf. on Mag. Tech., Oxford,
1967, pp.494-5.

106. Eutler, A.P., James, G.B., Maddock, B.J. and Norris, W.T.:
Int. J. Heat Mass Transf., 13 , pp.105-14, 1970.
107. El Hindari, A.: AGARD Conf.Proc. No.104, 1972.
108. Taylor, M.T.: Proc. Int. Conf.on Mag. Tech., Oxford, 1967,
pp.529-32.
109. Brechna, H.: SLAC-PUB-528, December 1968.
110. Laverick, C.: Adv. in Cryo. Eng., 11 , pp.659-67, 1966.
111. Bronca, G.: Minutes of Royal Society - CERN Study Conference,
Geneva, October 1968, p.3.
112. Carruthers, R., Cornish, D.N., and Hancox, R.: Proc.ICEC 1,
pp.107-9, 1967.
113. Williams, J.E.C.: Rev. Sci. Instr., 37 , pp.1030-1, 1966.
114. Montgomery, D.B. and Rinderer, L.: Cryogenics, 8 , pp.221-4,
1968.
115. Hancox, R.: Cryogenics, 7 , p.242, 1967.
116. Hale, J.R. and Williams, J.E.C.: Superconductivity Conf.,
Austin, Texas, 1967.
117. Stevenson, R.: Can. J. Phys., 47 , pp.1401-7, 1969.
118. Iwasa, Y., Weggel, C. et al.: J. Appl. Phys., 40 , pp.2006-9,
1969.
119. Smith, P.F., Spurway, A.H. and Lewin, J.D.: Brit. J. Appl. Phys.,
pp.947-56, 1965.
120. Iwasa, Y. and Montgomery, D.B.: Adv. in Cryo. Eng., 14, pp.114-22,
1969.
121. Jackson, J.: Cryogenics, 9 , pp.103-5, 1969.
122. Chester, P.F.: Proc.ICEC 1, pp.147-9, 1967.
123. Hancox, R.: Tr.IEEE, MAG-4, pp.486-8, 1968.
124. Vetrano, J.B. and Boom, R.W.: J. Appl. Phys., 36 , pp.1179-80,
1965.
125. Lange, F. and Verges, P.: Cryogenics, 9 , pp.373-5, 1969.
126. Sekula, S.T., Boom, R.W. and Bergeron, C.J.: Appl. Phys. Lett.,
2 , pp.102-4, 1963.
127. Heaton, J.W. and Rose-Innes, A.C.: Phys. Lett., 9 , pp.112-3,
1964.

128. Sugahara, M.: J. Appl. Phys., 41 , p.3668-72, 1970.
129. Lynton, E.A.: "Superconductivity", Chapter VII.
130. De Gennes, P.G.: "Superconductivity of metals and alloys", pp. 85-7.
131. A Series of five papers by Smith, P.F., Wilson, M.N., Walters, C.R., Lewin, J.D. and Spurway, A.H.: Rutherford Laboratory Preprint RPP/A 73, 1969.
132. Salmon, D.R. and Catterall, J.A.: J. Phys. D.: Appl. Phys., 3 , pp.1023-32, 1970.
133. McInturff, A.D.: J. Appl. Phys., 40 , pp.2080-2, 1969.
134. Morgan, G.H.: *ibid.*, 41 , pp.3673-8, 1970.
135. Critchlow, P.R. and Zeitlin, B.: *ibid.*, 41 , pp.4860-5, 1970.
136. Eastham, A.R. and Rhodes, R.G.: AGARD Conference Proc. No.104, Paper 3, 1972.
137. Volger, J. and Admiraal, P.S.: Phys. Lett., 2 , pp.257-9, 1962.
138. Felici, N.: Compt. rend., 206 , pp.242-4, 1938.
139. van Houwelingen, D., Admiraal, P.S. and van Suchtelen, J.: Phys. Lett., 8 , pp.310-1, 1964.
140. van Beelen, H., Arnold, Miss A.J.P.T., De Bruyn Cuboter, R., Eenakker, J.J.M. and Taconis, K.W.: Phys. Lett., 4 , pp.310-3, 1963.
141. van Suchtelen, J., Volger, J. and van Houwelingen, D.: Cryogenics, 5 , pp.256-66, 1965.
142. Wipf, S.L.: Adv. in Cryo, Eng., 2 , pp.342-8, 1964.
143. Sass, A.R.: Tr.IEEE, AS-2 , pp.822-5, 1964.
144. van Beelen, H., Arnold, Miss A.J.P.T., Sypkens, H.A. et al.: Physica, 31 , pp.413-43, 1965.
145. Atherton, D.L.: IEEE Spectrum, pp.67-71, 1964.
146. Buchhold, T.A.: Sci. Am., 202 , pp.74-82, 1960.
147. Pierro, J.J. and Unnewehr, L.E.: Tr.IEEE, AS-1 , pp.838-46, 1963.
148. McFee, R.: Elec. Eng., pp.122-9, 1962.
149. Schoch, K.F.: Adv. in Cryo. Eng., 6 , pp.65-72, 1961.

150. Jones, J.D. and Matthews, P.W.: Rev. Sci. Instr., 35 , pp.630-3, 1964.
151. Williams, J.E.C:"Superconductivity and Its Applications", p.151.
152. Huret, J. and Mailfert, A.: Bull.de la Soc. Francaise des Elec., 8^e série, V , pp.654-5, 1964.
153. Harrowell, R.V.: Nature, 222 , p.598, 1969.
154. Harrowell, R.V.: Cryogenics, 12 , pp.109-114, 1972.
155. Appleton, A.D.: ibid. 9 , pp.147-157, 1969.
156. Appleton, A.D.: Private communication.
157. Appleton, A.D. and MacNab, R.B.: Proc. LTEP Conference, pp.112-9, 1969.
158. Private Communication.
159. Appleton, A.D.: Proc.ICEC4, pp.256-62, 1972.
160. Anon: Electronics and Power, 14 , p.114, 1968.
161. Morton, P.: Private Communication.
162. Wormald, G.A.: Private communication.
163. Goodman, B.B.: Private communication.
164. BEAMA: Private communication.
165. Various authors: Brown-Boveri Review, 57 , pp.96-133, 1970.
166. Yamamoto,M.: Proc.LTEP Conference, pp.55-60, 1969.
167. Mole, C.J., Parker, J.H. and Lowry, L.R.: AGARD Conf. Proc. No.104, 1972.
168. Robert, J.: Entropie, pp.63-9, 1967.
169. Chabrerie, J.P., Fournet, G. and Mailfert, A.: AGARD Conf.Proc. No. 104, 1972.
170. Arnold, J.J.: The Chartered Mechanical Engineer, pp.478-85, 1970.
171. Anon.: Power Progress 8, (published by CEGB, 1966).
172. Krick, N.: Brown Boveri Review, pp.368-79, 1969.
173. Thullen, P. and Smith, J.L.: Adv. in Cryo. Eng., 15, pp.132-40,1970.

174. Sabrie, J.L.: Proc.ICEC3, pp.433-7, 1970.
175. Mole, C.J., Haller, H.E. and Litz, D.C.: Paper M-4, Applied Superconductivity Conf. 1972.
176. Stekly, Z.J.J. and Woodson, H.H.: AGARD Conf.Proc. No.104, 1972.
177. Smith, J.L., Kirtley, J.L., Thullen, P. and Woodson, H.H., Paper M-3, Applied Superconductivity Conf. 1972.
178. Woodson, H.H., Smith, J.L., Thullen, P. and Kirtley, J.L.: Tr.IEEE, PAS-90, pp.620-7, 1971.
179. EEI Bulletin, pp.140-3, May, 1970.
180. Stekly, Z.J.J., Woodson, H.H. et al.: Tr.IEEE, PAS-85, pp.274-80, 1966.
181. Oberhauser, C.J. and Kinner, H.R.: Adv. in Cryo. Eng., 13 , pp.161-7, 1968.
182. Thullen, P., Dudley, J.C., Greene, D.L., Smith, J.L. and Woodson, H.H.: Tr.IEEE, PAS-90 , pp.611-9, 1971.
183. Mole, C.J.: Private communication.
184. Smith, R.J.: Wright-Patterson Air Force Base, Ohio, Report No. ASD-TDR-62-811, 1962.
185. Stekly, Z.J.J. and Woodson, H.H.: Tr.IEEE, AS-2 , pp.826-42, 1964.
186. Mueller, P.M.: ibid, pp.843-50.
187. Woodson, H.H., Stekly, Z.J.J. and Halas, E.: Tr.IEEE, PAS-85 , pp.264-74, 1966.
188. Hayden, J.T.: Cranfield Memo. No.11, 1968.
189. Howe, D.: Private communication.
190. Khan, G.K.M. and Reece, A.B.J.: Proc. of Conf. on the Design of Electric Machines by Computer, Queen Mary College, London, 1969.
191. Fanthome, R.: RAE Tech. Report 69144, 1969.
192. Wakefield, G.G.: Private communication.
193. Bainbridge, A: Private communication.
194. Daunt, J.G. and Goree, W.S.: U.S. Office of Naval Research Report Nonr.-263(70) and N00014-67-C-0393.

195. Hayden, J.T.: AGARD Conf. Proc. No.104, 1972.
196. Maxwell, J.C.: "A Treatise on Electricity and Magnetism", 2 , Chapter 14.
197. Moullin, E.B.: "Principles of Electromagnetism", p.30.
198. Mapother, D.E. and Snyder, J.N.: Univ. of Illinois, Dept. Phys., Tech. Rept. 5, 1954.
199. Morris, D.E. and Kilgore, R.A.: NASA Tech. Note D-1013, 1962.
200. Foelsch, K.: Archiv. f.Elek.XXX, pp.139-57, 1936.
201. Snow, C.: NES Appl. Maths. Series No.38, 1953.
202. Alexander, N.B. and Downing, A.C.: ORNL Report No.2828, 1959.
203. Brown, G.V., Flax, L., Itean, E.C. and Laurence, J.C.: NASA Tech. Report R-170, 1963.
204. Brown, G.V. and Flax, L.: NASA Tech. Note D-2494, 1964.
205. Brown, G.V. and Flax, L.: J. Appl. Phys., 35 , pp.1764-67, 1964.
206. Smythe, W.R.: "Static and Dynamic Electricity", p.127 et seq.
207. Garrett, M.W.: "High Magnetic Fields", Chapter 2, 1961.
208. Norris, W.T. and Wilson, M.N.: Rutherford Lab. Memo. RHEL/M172, 1969.
209. Garrett, M.W.: J. Appl. Phys., 22 , pp.1091-1107, 1951.
210. Carter, G.W.: "The E.M. Field in its Engineering Aspects", p.256.
211. *ibid.*, pp.254-6.
212. McLachlan, N.W.: "Bessel Functions for Engineers", pp.156-60.
213. Doherty, R.E. and Nickle, C.A.: Tr.AIEE, 45 , pp.912-26, 1926.
214. Doherty, R.E. and Nickle, C.A.: *ibid.*, pp.927-42, 1926.
215. Doherty, R.E. and Nickle, C.A.: *ibid.*, 46 , pp.1-14, 1927.
216. Doherty, R.E. and Nickle, C.A.: *ibid.*, 47 , pp.457-87, 1928.
217. Doherty, R.E. and Nickle, C.A.: *ibid.*, 49 , pp.700-14, 1930.
218. Park, R.H.: *ibid.*, 48 , pp.716-27, 1929.

219. Park, R.H.: *ibid.*, 52 , pp.352-54, 1933.
220. Kron, G.: *GE Review*, 36 , 1935.
221. Jaeger, J.C.: *Phil. Mag.*, 29 , pp.18 - 31, 1940.
222. Lorch, H.O.: *Proc.IEE*, 120, pp. 221-7, 1973.

AppendixPublications by the Author

Over a dozen reports and papers have been written on various subjects in electrical engineering as a result of the author's previous research work on aircraft electrical power systems, liquid-filled fuses, calculation of reactance parameters and pole-shoe optimisation by means of a digital computer and thyristor drives. Other papers on possible applications of superconductivity in transport and a lecture on this subject to the Institution of Electrical Engineers, London, have been presented. A textbook on electrical engineering (see bibliography) has been published as joint author.

Half a dozen papers on the subject of this thesis have been published, including references 188 and 195, and two parts are to be submitted for publication in the near future.

No reprints are submitted, as the salient features of the above papers are included in the text of the thesis, or are not relevant to it.